

# Feasibility Analysis of Internally Fired s-CO<sub>2</sub> Cycle for Energy Transition

Kaushal Dave

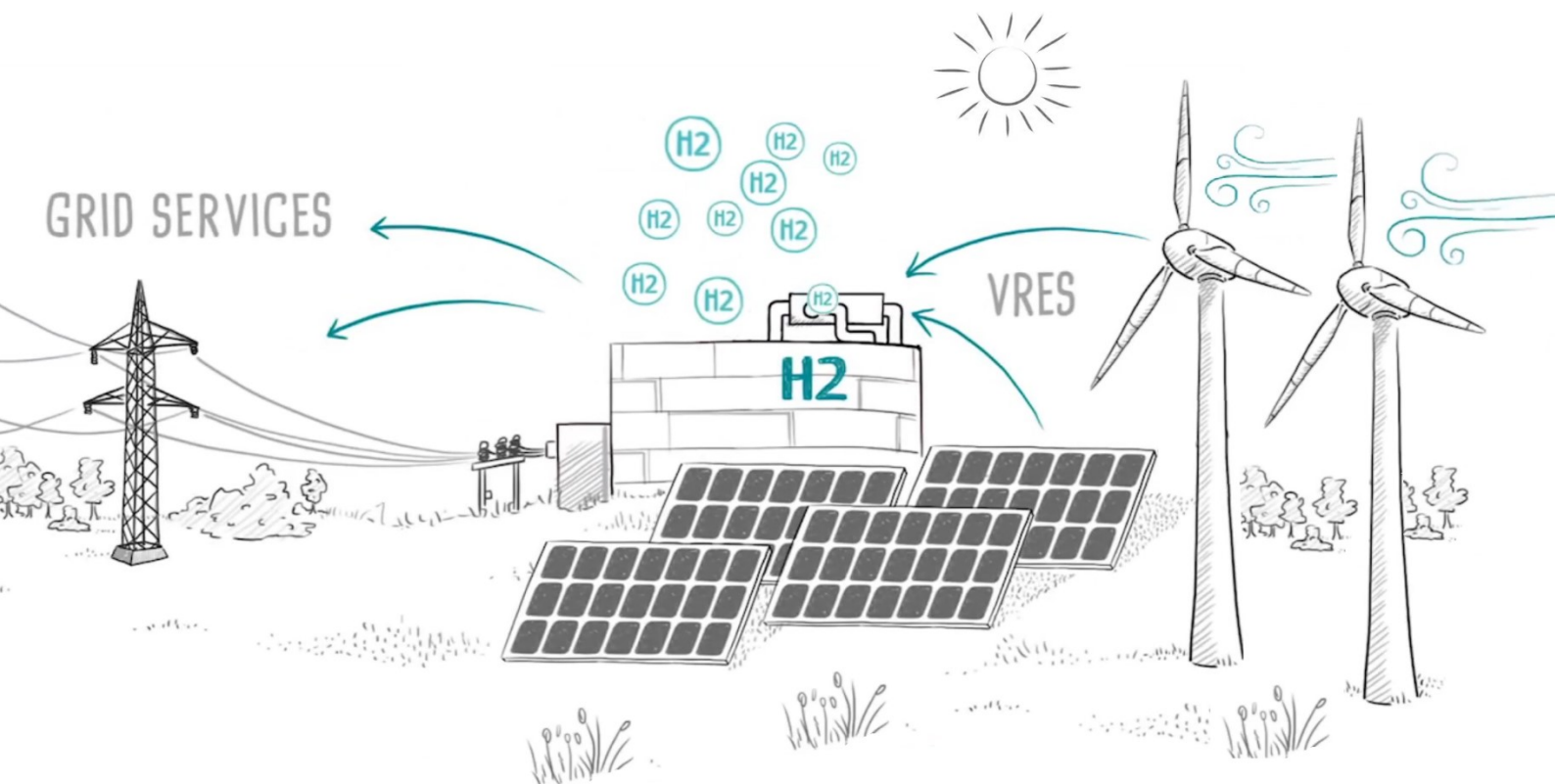


Image credit: H2FUTURE project - VERBUND



# Feasibility Analysis of Internally Fired s-CO<sub>2</sub> Cycle for Energy Transition

By

Kaushal Dave

in partial fulfilment of the requirements for the degree of

**Master of Science  
in Aerospace Engineering**

at the Delft University of Technology,  
to be defended publicly on Friday September 18, 2020 at 09:00 hours.

Student Number: 4826906

Project duration: December 8, 2019 – August 31, 2020

Supervisor: Dr. Arvind Gangoli Rao

Thesis committee: Dr. Arvind Gangoli Rao, TU Delft, Chair

Dr.ir. Matteo Pini, TU Delft, Examiner

Dr.ir. Rene Pecnik, TU Delft, Examiner

Prof.dr.ir. Georg Eitelberg, TU Delft, Examiner

Prof.dr.ir. Sikke Klein, TU Delft, Examiner

*This thesis is confidential and cannot be made public until September 1, 2023.*

An electronic version of this thesis is available at <http://repository.tudelft.nl/>



# Acknowledgement

The successful completion of this project was only made possible by the assistance, unwavering support and encouragement that I received from several people. I would like to take this opportunity to express my sincere gratitude to some of them and acknowledge their contribution.

First of all, I would like to thank Prof. Arvind Gangoli Rao for giving me an opportunity to work on this exciting project. Our long conversations (that, thankfully, you never restricted to the thesis topic) not only enabled me to explore the depth of the subject, but also considerably broadened my viewpoint on a gamut of topics ranging from science and technology to matters of global politics. I am grateful for your contribution to my personal and professional growth over the last two years.

Secondly, I would like to express my gratitude to Prof. Matteo Pini for providing critical feedback on this project. Your valuable inputs aided me to make this project more robust and opened my mind to new possibilities that could be explored in this topic during future research work. Also, the assistance provided by Mr. Teus van der Stelt with the FluidProp software is greatly appreciated. Lastly, I would also like to thank my friends and fellow students Aditi Ahuja and Chaitanya Boppana for all the help and support they provided during this project.

A successful completion of this project marks the end of the journey I started two years back with the goal to attain a master's degree in Aerospace Engineering. I would not have been able to pursue a master's degree much less complete one successfully, but for the grit and patience instilled in me by my parents. I can never thank them enough for their love and sacrifices, so instead I opt to say that I am forever indebted to them. It is they who deserve the credit of all my achievements including this one. My sincere thanks to all my family members and friends back in India for keeping faith in me, motivating me and enabling me throughout this journey. I hope to have kept your faith and made you all proud.

Thank you all.  
Kaushal Dave



# Table of Contents

<b>ACKNOWLEDGEMENT .....</b>	<b>I</b>
<b>TABLE OF CONTENTS.....</b>	<b>III</b>
<b>LIST OF FIGURES .....</b>	<b>V</b>
<b>LIST OF TABLES .....</b>	<b>VII</b>
<b>LIST OF ABBREVIATIONS.....</b>	<b>IX</b>
<b>LIST OF SYMBOLS.....</b>	<b>XI</b>
<b>ABSTRACT .....</b>	<b>XIII</b>
<b>1. INTRODUCTION.....</b>	<b>1</b>
1.1 PROJECT CONTEXT .....	1
1.2 RESEARCH TOPIC MOTIVATION.....	2
1.3 RESEARCH OBJECTIVE.....	5
1.4 REPORT STRUCTURE .....	6
<b>2. EXISTING ENERGY INFRASTRUCTURE .....</b>	<b>9</b>
2.1 THE “LEGACY” PROBLEM OF THE ENERGY SECTOR.....	9
2.2 VARIABLE RENEWABLE ENERGY SOURCES.....	11
2.3 ENERGY STORAGE SOLUTIONS.....	18
2.4 HYDROGEN – THE BEDROCK OF FUTURE LOW-CARBON ENERGY MARKETS .....	22
<b>3. HYDROGEN –THE FUTURE ENERGY CARRIER.....</b>	<b>27</b>
3.1 HYDROGEN PRODUCTION .....	28
3.2 HYDROGEN STORAGE .....	30
3.3 HYDROGEN UTILISATION.....	32
3.4 EXISTING H <sub>2</sub> BASED POWER GENERATION TECHNOLOGIES .....	33
3.5 ADVANCED POWER CYCLES WITH ZEP .....	36
<b>4. S-CO<sub>2</sub> POWER CYCLE .....</b>	<b>41</b>
4.1 INTRODUCTION TO S-CO <sub>2</sub> POWER CYCLES.....	41
4.2 VARIATIONS OF THE S-CO <sub>2</sub> CYCLE.....	44
4.3 THERMODYNAMIC MODEL DEVELOPMENT PROCESS.....	46
4.4 MODEL VALIDATION.....	57

<b>5. THERMODYNAMIC ANALYSIS .....</b>	<b>67</b>
5.1 DESIGN POINT SELECTION .....	67
5.2 SELECTION OF FINAL CONFIGURATION OF THE PROPOSED CYCLE .....	68
5.3 PARAMETRIC ANALYSIS .....	72
5.4 PERFORMANCE MAP.....	82
5.5 SUMMARY .....	83
<b>6. COMBUSTION ANALYSIS .....</b>	<b>87</b>
6.1 FRAMEWORK OF THE PROPOSED COMBUSTION ANALYSIS.....	87
6.2 LITERATURE REVIEWED ON H <sub>2</sub> /O <sub>2</sub> COMBUSTION.....	89
6.3 COMBUSTION MODEL DEVELOPMENT .....	94
6.4 COMBUSTION STUDIES .....	100
6.5 SUMMARY .....	113
<b>7. CONCLUSIONS &amp; RECOMMENDATIONS.....</b>	<b>117</b>
7.1 PROJECT SUMMARY .....	117
7.2 CONCLUSIONS .....	118
7.3 RECOMMENDATIONS FOR FUTURE WORK .....	122
<b>BIBLIOGRAPHY.....</b>	<b>123</b>

# List of Figures

Fig. 1 Breakdown of global energy-related CO <sub>2</sub> emissions by sector in 2015 [5] .....	3
Fig. 2 Comparison of efficiency vs power output of several power plant concepts [8].....	4
Fig. 3 Different phases of this research project and a list of key objectives each phase.....	6
Fig. 4 Electricity production by source in 2017 [13] .....	10
Fig. 5 Operational status of global coal-fired capacity [14].....	11
Fig. 6 Selected countries by integration phase and share of VRES, 2017 [21].....	13
Fig. 7 Expected integration challenges with increasing VRE penetration level [23].....	14
Fig. 8 Categorisation of challenges caused by VRES [24] .....	14
Fig. 9 Categorisation of challenges caused by VRES [24] .....	15
Fig. 10 Energy storage technology categorised based on type of energy stored [29] .....	19
Fig. 11 Role of energy storage systems & comparison of several energy storage technologies [67] ...	21
Fig. 12 Hydrogen production pathways and its conversion to other useful end products [26].....	28
Fig. 13 Hydrogen production costs per technology – Expected scenario in 2030 [26].....	29
Fig. 14 Hydrogen costs from hybrid solar PV and onshore wind systems in the long term [26].....	30
Fig. 15 Hydrogen storage options[29].....	31
Fig. 16 VRES integration pathways by means of hydrogen [30].....	32
Fig. 17 Highly efficient s-CO <sub>2</sub> cycle configurations – Schematic Layouts [49].....	45
Fig. 18 Schematic representation of the configurations to be included in thermodynamic model [49]	49
Fig. 19 Software architecture .....	56
Fig. 20 Plot showing the effect of flue gas mixture on recuperator performance .....	58
Fig. 21 Specific heat capacity of flue gas mixture at 34 bar estimated using different models .....	60
Fig. 22 Specific volume of flue gas mixture at 34 bar estimated using different mixture models.....	63
Fig. 23 Schematic representation of the proposed layout of NET Power cycle [53] .....	65
Fig. 24 Schematic representation of the SFC and IC configurations .....	69
Fig. 25 Schematic representation of the IC-RH and IC-SE cycle configurations. ....	70
Fig. 26 Schematic layout and T-s chart representation of the proposed s-CO <sub>2</sub> power cycle .....	71
Fig. 27 Effect of varying turbine inlet pressure on cycle efficiency .....	73
Fig. 28 Effect of varying turbine outlet pressure on cycle efficiency .....	74
Fig. 29 T-s diagram of the compression process illustrating they effect of varying TOP.....	74
Fig. 30 Design pressure & temperature capabilities of PCHE .....	75
Fig. 31 Effect of varying turbine outlet temperature on cycle parameters .....	76
Fig. 32 Effect of varying compressor inlet temperature on cycle parameters.....	77
Fig. 33 Effect of pressure drop on cycle performance .....	78

Fig. 34 Effect of varying isentropic efficiency of compression & expansion process .....	79
Fig. 35 Effect of heating the turbine cooling flow cycle parameters.....	80
Fig. 36 T-s chart showing effect of coolant temperature on expansion process at design point TOT ..	80
Fig. 37 Effect of varying isentropic efficiency of compressor and turbine .....	81
Fig. 38 Heat exchange process in the recuperator at design point.....	82
Fig. 39 Performance map .....	83
Fig. 40 Sensitivity analysis of ignition time delays as a function of pressure at 1000 K [56].....	92
Fig. 41 Temperature profile changing with N <sub>2</sub> thermodynamic and kinetic properties[65].....	93
Fig. 42 Flue gas temperature at outlet of PSR predicted using shortlisted mechanisms .....	95
Fig. 43 Concentration of the main products of H <sub>2</sub> /O <sub>2</sub> /CO <sub>2</sub> combustion at 300bar & ~1450K.....	96
Fig. 44 Experimental data [65] vis-à-vis simulated results from shortlisted mechanisms .....	99
Fig. 45 Flow distribution (shown as % of total flow) in the base case of combustion simulation .....	101
Fig. 46 Reactor network used for design point combustion analysis .....	101
Fig. 47 Evolution of flue gas mixture composition during combustion .....	102
Fig. 48 Temperature profile and evolution of O <sub>2</sub> /CO concentration profile at design point .....	103
Fig. 49 Reactor network used for parametric study of the combustion process .....	104
Fig. 50 Effect of combustor residence time on the flue gas properties .....	105
Fig. 51 Effect of combustor inlet pressure on the flue gas properties .....	106
Fig. 52 Effect of combustor inlet temperature on the flue gas properties .....	108
Fig. 53 Effect of dilution rate on the flue gas properties .....	109
Fig. 54 Effect of equivalence ratio on the flue gas properties .....	111

# List of Tables

Table 1 Several VRES integration challenges correlated with available/proposed solutions [24] .....	16
Table 2 Evaluation matrix for the advance power cycles .....	39
Table 3 Various thermodynamic features with the associated labels & role in the s-CO <sub>2</sub> cycle .....	44
Table 4 Highly efficient s-CO <sub>2</sub> cycle configurations – Performance Parameters [49].....	45
Table 5 Model input parameters.....	47
Table 6 Cycle configuration parameters .....	48
Table 7 Effect of mixture model on recuperator .....	59
Table 8 Effect of mixture model on combustor performance .....	62
Table 9 Effect of mixture model on turbine performance.....	62
Table 10 Comparison of NET Power cycle performance parameters for model validation .....	65
Table 11 List of parameters analysed during parametric study.....	68
Table 12 Net cycle efficiency obtained with SFC configuration and IC configuration at design point	69
Table 13 Key cycle parameters of IC-RH vs IC-SE cycle configurations at design point.....	70
Table 14 Recent hydrogen combustion mechanisms compared by Olm et. al. [55] .....	90
Table 15 Experimental data used to compare the shortlisted combustion mechanisms [65].....	98
Table 16 Combustor inlet parameters at design point.....	101
Table 17 Reactor parameters used during base case simulation. ....	102
Table 18 Estimation of deviation in flue gas properties caused by ignoring minor species. ....	103
Table 19 Mixture composition at different equivalence ratios.....	112



# List of Abbreviations

AEC	Alkaline electrolytic cell
ASU	Air separation unit
BES	Battery energy storage
BoP	Balance of plant
CAES	Compressed air energy storage
CAGR	Compound annual growth rate
CAPEX	Capital expenditure
CCS	Carbon capture and storage
CCUS	Carbon capture, utilisation and storage
CHP	Combined heat and power
CPOC	Cryogenic pressurized oxy-combustion cycle
CSP	Concentrated solar power
DPC	Dense phase compression
EoS	Equation of state
EPR	Expansion pressure ratio
ERCOT	Electricity Reliability Council of Texas
FBES	Flow battery energy storage
FES	Flywheel energy storage
FG	Flue gas
FSR	Flow split ratio
GERG	Groupe Europeen de Recherches de Gazieres (The European Gas Research Group)
GHG	Greenhouse gas
HES	Hydrogen energy storage
HEX	Heat exchanger
HP	High pressure
HTR	High temperature recuperator
IC	Intercooled compression
IC-RH	Intercooled reheated
IC-SE	Intercooled simple expansion
IEA	International energy agency
IHC	Inter-stage heating and cooling
JRC	Joint research centre
JSR	Jet stirred reactor
LCOE	Levelized cost of energy
LCOH	Levelized cost of hydrogen
LHV	Lower heating value
LNG	Liquified natural gas
LP	Low pressure
LTR	Low temperature recuperator
MCFC	Molten carbonate fuel cell
NG	Natural gas
NTP	Normal temperature and pressure

O&M	Operation and maintenance
OECD	Organisation for Economic Co-operation and Development
OPEX	Operating expenditure
P2G	Power-to-gas
P2G2P	Power-to-gas-to-power
PAFC	Phosphoric acid fuel cell
PCHE	Printed circuit heat exchanger
PCP-SAFT	Perturbed-chain polar statistical associating fluid theory
PEM	Proton exchanging membrane
PEMEC	Proton exchange membrane electrolytic cell
PEMFC	Proton exchange membrane fuel cell
PHS	Pumped hydroelectric storage
PSR	Perfectly stirred reactor
PV	Photovoltaic
R&D	Research and development
RF	Radiative forcing
RH	Reheated expansion
RSQ	Research sub-questions
SDG	Sustainable development goals
SFC	Split-flow before compression
SFE	Split-flow before expansion
SFH	Split-flow before heating
SFHE	Split-flow before heating & expansion
SMES	Superconducting magnet energy storage
SOEC	Solid oxide electrolytic cell
SOFC	Solid oxide fuel cell
TIP	Turbine inlet pressure
TIT	Turbine inlet temperature
TOP	Turbine outlet pressure
TOT	Turbine outlet temperature
TRL	Technology readiness level
UN	United Nations
VPC	Vapor phase compression
VRES	Variable renewable energy sources
WACC	Weighted average cost of capital
WHR	Waste heat recovery
ZEP	Zero-emission potential

# List of Symbols

## Roman Symbols

$DR$	Dilution rate	[-]
$H$	Enthalpy	[J]
$h$	Specific enthalpy	[J/kg]
$h^*$	Enthalpy of a pure component	[J/kg]
$\dot{m}$	Mass flow rate	[kg/s]
$n$	Total number of moles in a mixture	[-]
$P$	Pressure	[bar]
$R$	Universal gas constant	[J/kg]
$s$	Entropy	[J/kg.K]
$s^*$	Entropy of a pure component	[J/kg.K]
$T$	Temperature	[K]
$w$	Arbitrary thermodynamic property of mixture	[-]
$w^*$	Arbitrary thermodynamic property of a pure component	[-]
$x$	Mole fraction	[-]
$y$	Mass fraction	[-]

## Greek Symbols

$\beta$	Coefficient based on type of cooling	[-]
$\Delta$	Change in a property	[-]
$\eta$	Efficiency	[%]
$\mu$	Flow rate correction factor	[-]
$\Phi$	Cooling effectiveness	[-]
$\Phi_\infty$	Asymptotic value of maximum cooling effectiveness	[-]
$\varphi$	Equivalence ratio	[-]
$\sigma$	Sensitivity coefficient	[-]

## Subscripts

$b$	Blade
$c$	Coolant
$comb$	Combustion
$comp$	Compression
$exp$	Expansion
$f$	Fuel
$in$	Inlet
$is$	Isentropic
$mix$	Mixture
$out$	Outlet
$ref$	Reference



# Abstract

Decarbonisation of the energy sector by switching to low-carbon renewables is inevitable for a sustainable future. However, the intermittent and variable nature of low-carbon renewables, like wind and solar, poses several challenges when integrated into the existing energy grids. This is one of the main factors slowing down the transition to a more sustainable energy model. Long-term energy storage solutions are expected to alleviate these issues. The technologies currently available for this application (PHS and CAES) have a limited sustainable deployment potential which makes power-to-gas (P2G) technology, the only long-term strategy that can ensure decarbonisation of the future global economy. Green hydrogen, a fundamental part of this concept, is the critical energy technology that can catalyse a paradigm shift in the existing energy markets. Yet, a widescale deployment of this technology is currently limited by several factors including low overall conversion efficiency, poor scalability and operational unreliability of fuel cell technology, high overall costs, absence of necessary infrastructure etc. This research project aims to propose a highly efficient combustion-based power cycle that can address several issues commonly associated with H<sub>2</sub>-based power generation application of the fuel-cell technology. Preliminary analysis identified that the s-CO<sub>2</sub> Brayton cycle was the most suitable candidate for this application and thus, a thermodynamic analysis was conducted to determine the feasibility for this solution. This report documents the work completed in this project and proposes a novel oxy-combustion based green H<sub>2</sub> fuelled s-CO<sub>2</sub> power cycle concept as an alternative to the existing H<sub>2</sub>-based distributed power generation systems.



# Chapter 1

## Introduction

### Overview

This chapter aims to provide a comprehensive overview of the project. The first section of the chapter outlines the broad context in which this project is envisaged, while the second section discusses the motivation behind the selection of this particular research topic and its larger scientific significance. Subsequently, the scope of the current project is demarcated in the third section of the chapter by defining the main research objective and a set of research questions. Lastly, the organisation of this report is outlined in the fourth section, including the gist of the content of the subsequent chapters.

### 1.1 Project context

Decarbonisation of the present-day energy sector – the single largest emitter of anthropogenic CO<sub>2</sub> – by transitioning to low-carbon renewable energy sources is inevitable for a sustainable future. However, low-carbon renewables like wind and solar, aptly referred to as Variable Renewable Energy Sources (VRES), are inherently variable, distributed, and stochastic sources of energy. VRES are in stark contrast with conventional fossilized energy sources which are more predictable and concentrated. This difference results in several integration challenges with the existing energy grids, that are primarily designed around reliable and centralized power generation models. Energy storage technologies are expected to address a number of these integration challenges but to support a large share of VRES in the electrical grids long-term seasonal energy storage solutions are essential. Lately battery energy storage technology has gathered a lot of attention, but it is not suitable for long-term seasonal storage applications. Technologies found to be having the most promising prospects for seasonal energy storage applications are pumped-storage hydropower (PSH), compressed air energy storage (CAES) systems

and hydrogen energy storage (HES) system. PSH and CAES are both mature technologies but have a limited sustainable deployment potential compared to HES technology. Currently, HES technologies lack a wide-scale application due to the various operational/technological challenges that riddle the associated sub-systems. Amongst these, converting the stored energy back to power using existing technologies is a key challenge. The goal of this research project is to explore a potential solution that in principle, can help address several of these issues. Supercritical CO<sub>2</sub> (s-CO<sub>2</sub>) Brayton cycle is a highly efficient power cycle which when deployed with an oxy-combustion system can be a zero-emission potential (ZEP) power cycle. This project aims to evaluate the feasibility of an internally fired, H<sub>2</sub>/O<sub>2</sub> fuelled s-CO<sub>2</sub> power cycle as an energy transition technology. Thermodynamic evaluation and parametric study of this cycle is proposed to that effect. If found feasible, this concept will have the potential to drastically transform the energy sector in the coming years.

Irrespective of the outcome of this research project, this investigation is expected to add valuable findings to the larger body of science. Sustainable and sensible development is no longer a choice but a necessity in today's time. Energy sector desperately needs technologies that can enable a wide-scale adoption of low-carbon technologies. Therefore, if the outcome of this study is positive and the concept is proved feasible, it will open a new avenue of research in energy transition powered by this concept. Even if the study cannot conclusively prove the concept to be feasible, it will surely bring to light, the technological and knowledge gaps in the fields of s-CO<sub>2</sub> power cycle concept and HES systems. Even in the unlikely event that this study conclusively proves the concept to be unfeasible, it will contribute towards identification of the main problems and engineering challenges in the proposed concept and serve as a useful reference case for deciding the direction of future research effort. Therefore, it can be said with a good amount of certainty that this project is quite relevant in a larger context of striving for sustainability.

## 1.2 Research topic motivation

Climate change and its mitigation are one of the most important global issues of this generation. Climate change is a multifaceted and a complex problem with several hurdles spread across a broad spectrum. The challenges and concerns raised by climate change seem to be unending, while the solutions seem inadequate to even make a dent. Anthropogenic emissions of greenhouse gases (GHGs) are at the heart of the current climate change phenomenon. Climate change is partly a natural phenomenon with cycles of global warming and cooling occurring in a periodic manner. The time periods over which this occurs naturally, however, typically vary from a few thousand years to a few hundred thousand years and produces an average temperature change of ~2-3 °C [1]. But rapid use of fossil fuels, triggered by industrialisation in the second half of the 19th century, has accelerated this phenomenon to an unprecedented rate. The global mean temperature is ~1°C higher than in 1850 and this global temperature rise is expected to be between 1.5-2°C by end of the century. Therefore, a process that would naturally take a few thousand years at the least, was accelerated to take place in 200-250 years due to human activities. Studies show that several species have not be able to adapt to this rapid change in their ecosystems and are threatened with global extinction. The global rate of species extinction is already at least tens to hundreds of times higher than the average rate over the past 10 million years and is accelerating [2]. This marked shift in Earth's state over the past few centuries has prompted geologists to define a new human-dominated geological epoch called Anthropocene.

The present atmospheric concentration of greenhouse gases is more than it has ever been in the last few hundred thousand years. CO<sub>2</sub> which is the worst offender amongst the GHGs, merely due to the proportions in which it is emitted (over 75% of global GHGs emission is in the form CO<sub>2</sub>), has an

atmospheric concentration of ~407.4 ppm in 2018, which is significantly higher than the pre-industrial levels of 180-280 ppm [3]. Anthropogenic CO<sub>2</sub> emissions have been the main culprit causing an increase in the effective radiative forcing<sup>1</sup> (RF) since the start of industrialisation [4]. Also, as can be seen from Fig. 1, the power sector is the single largest source of CO<sub>2</sub> emissions, accounting for about 38% of total energy-related CO<sub>2</sub> emission in the year 2015 [5]. Therefore, if the impacts of climate change must be mitigated and global warming effect must be stabilized, annual CO<sub>2</sub> emissions will have to be cut down drastically in the coming years. To achieve any meaningful reduction in CO<sub>2</sub> emissions in the coming decades, transitioning to clean energy technology remains the cornerstone of all global decarbonisation strategies.

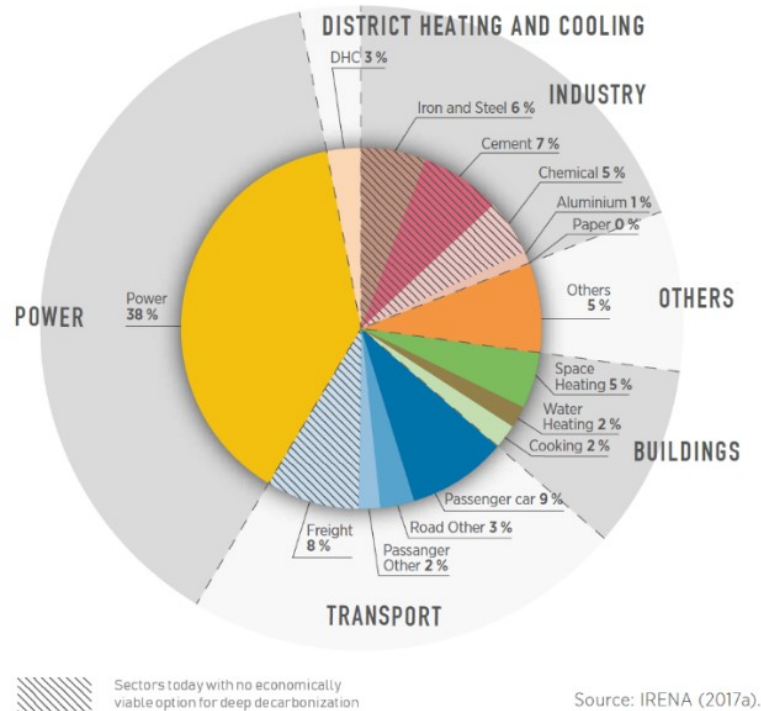


Fig. 1 Breakdown of global energy-related CO<sub>2</sub> emissions by sector in 2015 [5]

Taking cognizance of the gravity of the current situation, two landmark inter-governmental agreements were signed in 2015, namely, UN’s 2030 Agenda for Sustainable Development (September 2015) and the Paris Agreement on Climate Change (December 2015). Both these agreements focus on limiting the temperature rise below 2°C while pursuing efforts to limit it to 1.5°C. To achieve this, it is essential that, not only the future growth in energy demand but also the demand created by the retirement of existing energy assets be fulfilled by low-carbon sources. Last two decades have seen rapid growth in wind and solar power installation, but their share in the present energy mix is relatively low. The share of wind and solar-based generation in 2017 stood at to 4.4% and 1.8%, respectively, putting the total non-hydro low-carbon generation at ~6.2% [6]. This share is expected to increase by over 50% by 2040 [7]. However, this level of deployment also depends on how rapidly energy storage cost will decline and whether a viable seasonal storage solution with widespread deployment potential becomes available during this time.

Hydrogen produced by water electrolysis using renewable energy is termed as green hydrogen and is widely considered to be a potent solution for decarbonising the future energy markets. However, there

<sup>1</sup> Radiative forcing is a measure of the net increase in absorption of radiative flux induced by external drivers of climate change

are several challenges that remain to be addressed before which its large-scale deployment seems unlikely. Hydrogen based energy storage systems currently have a low overall conversion efficiency, high technological uncertainty, lack of operational know-how of the fuel-cell technology, high initial and maintenance costs etc. Some of these challenges are because of the lack of necessary infrastructure, given the developmental stage of the technology, while few others stem from the challenges posed by the processes and sub-systems involved. The current project focuses on the process of converting green hydrogen back to electricity.

Most proposed systems for converting green hydrogen back to electrical power are either based on hydrogen-fuelled conventional gas-turbine power plants or involve fuel-cells or a combination of these two technologies. The energy markets in future are predicted to be based on a distributed generation model and the role of conventional generators is expected to change from baseload generation to grid balancing operation. Modern gas-turbine power plants operating in combined cycle mode are highly efficient energy generation systems but are more suitable for medium to large scale operations since they derive several of their advantages from the economies of scale. This makes it a less attractive option for future distributed generation scenarios because of their downscaling problems. Fuel-cells technology, on the other hand, faces several challenges while scaling-up and most applications at present are smaller than 1 MW. Theoretically, fuel-cells provide better conversion efficiencies compared to conventional gas-turbine based power plants since they do not need to combust fuel – a process that results in maximum exergy destruction in conventional thermal power cycles. However, use of fuel-cells in commercial-scale power generation application faces a host of problems like scalability, reliability of operation, high rate of degradation leading to the high cost of operation and limited stack life, safety concerns, poor load following capability etc. Therefore, as can be seen from Fig. 2, there is a clear need for a combustion based power cycle that is not only easily scalable in mid-generation range (10-50 MWe) but has cycle efficiencies comparable to fuel-cell technology, while having the favourable operational characteristic of a gas turbine power plant. The novel cycle proposed in this project is specifically targeted for this market space.

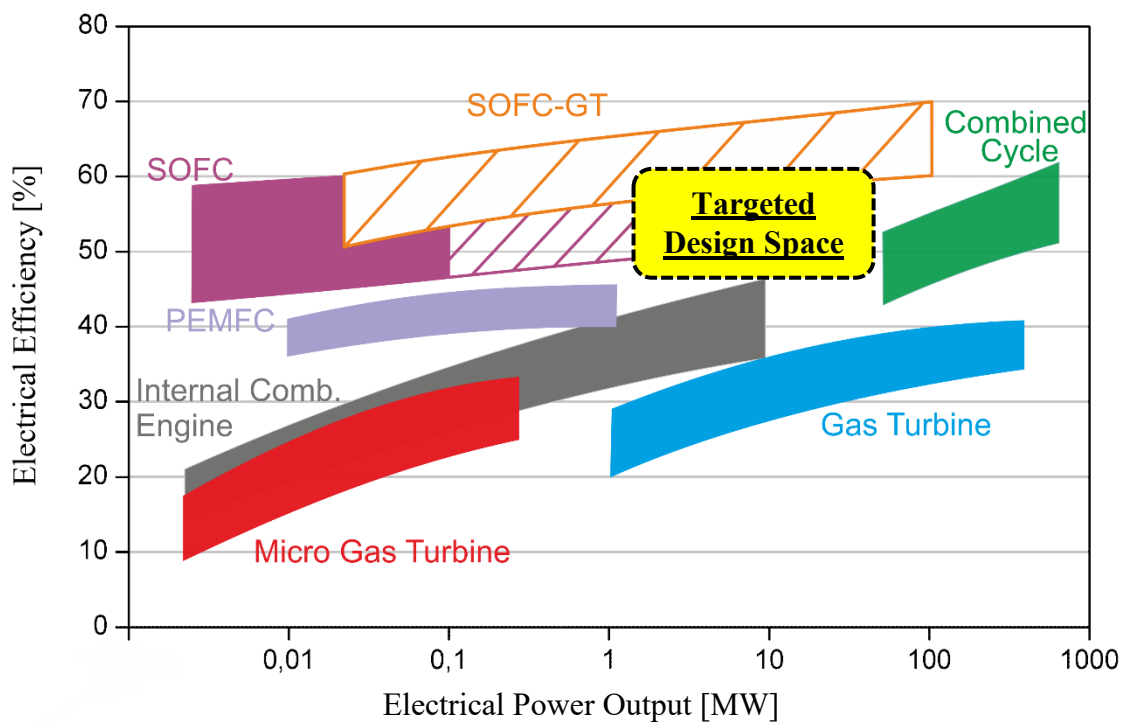


Fig. 2 Comparison of efficiency vs power output of several power plant concepts [8]

Internally fired s-CO<sub>2</sub> Brayton cycle was found to be a suitable candidate for this application. This project aims to analyse its performance and compare it to the existing technologies for converting green hydrogen back to power. The objective is to evaluate the feasibility of an internally fired, H<sub>2</sub>/O<sub>2</sub> fuelled s-CO<sub>2</sub> power cycle as an energy transition technology and an alternative to the fuel-cell based power cycle that is generally envisaged with a HES system. The potential benefits that can be expected with the use of the proposed power cycle include increased scalability, reliability of operations, a reduced plant footprint, better load following characteristics and enhanced operational safety. Given that the technologies under consideration are still in an early phase of development, a cost comparison is most likely to include a high degree of uncertainty. Hence, a detailed economic evaluation is not included in the present scope of this study.

### 1.3 Research Objective

The broad objective of this project, as mentioned in the previous section, is to assess the feasibility of an internally fired H<sub>2</sub>/O<sub>2</sub> fuelled s-CO<sub>2</sub> power cycle as an energy transition technology by carrying out a thermodynamic evaluation on the s-CO<sub>2</sub> cycle. Although defining the objective provides a general overview of the project scope, it fails to provide more specific information about the project. To address this shortcoming, a set of research questions is developed which will serve as a tool to provide direction and control to the project. In addition to this, the research questions will also serve as a progress monitoring tool during implementation.

Research questions have two main functional requirements, efficiency (the measure of the extent to which they contribute towards achieving the research objective) and steering capacity (how well they give direction to the project). To ensure both the functions are met, the central research question is broken down into a set of sub-questions. The sub-questions when fully answered will answer the central question as well as fulfil the research objective of the project.

#### Central research question

The central question that this research project aims to answer is, “*What is the feasibility of an internally fired H<sub>2</sub>/O<sub>2</sub> fuelled s-CO<sub>2</sub> power cycle as an energy transition technology?*” The associated set of sub-questions are as follows.

#### Research sub-questions (RSQ)

- RSQ#1. What are the main design constraints that restrict the operating envelope of the proposed cycle? In terms of cycle pressures and temperatures, what is the operating envelope and the design point?
- RSQ#2. What configurations of the s-CO<sub>2</sub> power cycle are relevant in the context of the proposed application? What is the final configuration selected for this internally fired H<sub>2</sub>/O<sub>2</sub> fuelled s-CO<sub>2</sub> power cycle?
- RSQ#3. What is the variation seen in the overall cycle performance within the imposed operating envelope? How is the cycle performance affected by variation in the critical design parameters?

- RSQ#4. What is the feasibility of the combustion of  $H_2/O_2$  mixture in an  $s-CO_2$  environment at elevated pressure levels? Can the proposed power cycle be categorised as a zero-emission cycle?
- RSQ#5. What is the effect of varying combustion parameters like residence time, combustor inlet temperature and pressure, and relative concentration of the fuel/oxidizer/diluent species etc., on the kinetics of the combustion reactions? Is the thermodynamic performance of the cycle substantially affected by the composition of flue gas generated during combustion?
- RSQ#6. Based on the thermodynamic and combustion analysis, what can be predicted about the operating characteristics of the proposed  $s-CO_2$  power cycle? How does it compare with existing hydrogen-based power generation technologies?
- RSQ#7. What can be concluded about the technical feasibility of the proposed  $H_2/O_2$  fuelled  $s-CO_2$  power cycle concept? Should more research effort be dedicated in future towards developing this concept?

## 1.4 Report structure

In the previous sections of this chapter, the context, motivation and the essentials of the project set-up were briefly laid out for the reader. In this section, a gist of the subsequent chapters is described to apprise the reader of the overall flow of information in the report. The set-up of this project and the structure of this report is schematically shown in the Fig.3 while a brief summary of the subsequent chapters of this report is described in the paragraphs that follow.

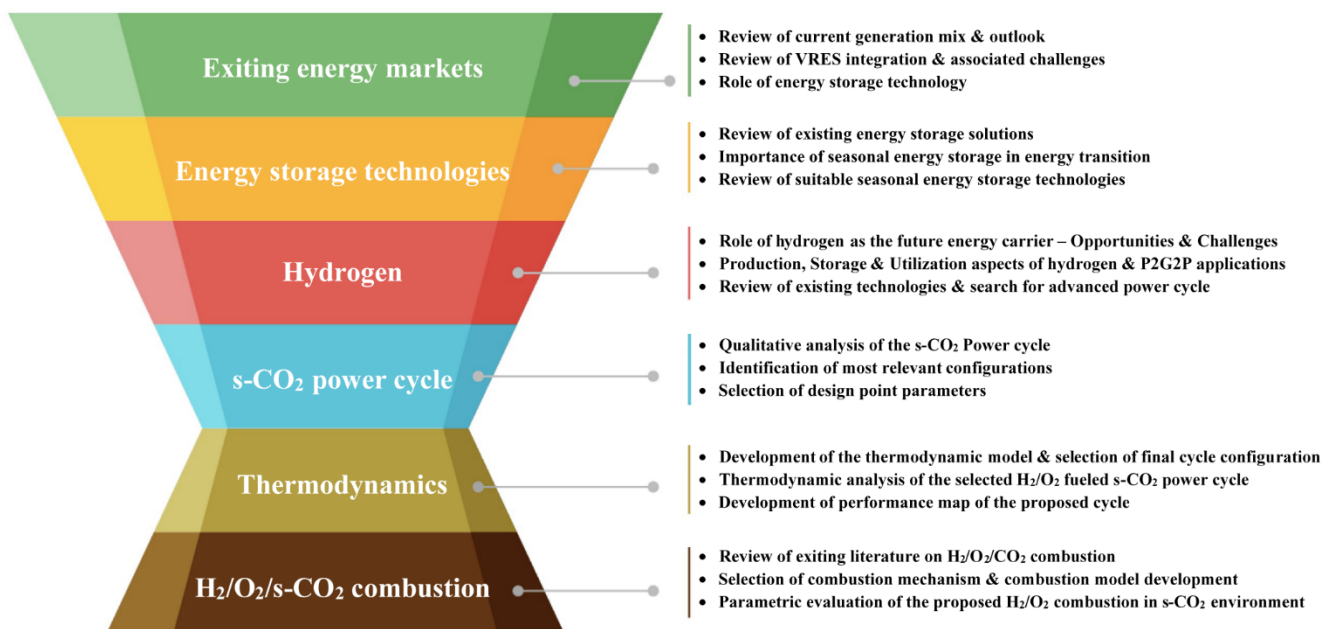


Fig. 3 Different phases of this research project and a list of key objectives each phase

The second chapter outlines the main findings of an extensive review of the trends in existing energy markets. The emphasis of this review was on identifying the key challenges that are impeding the pace of the transition process to a low-carbon, more sustainable energy model. It also included an evaluation of the existing energy storage technologies. The main outcome of this review was the identification of hydrogen as the critical energy technology that can catalyse a paradigm shift in existing energy markets.

The third chapter of the report briefly introduces the different aspects of hydrogen technologies that currently being developed. However, it is not possible to comprehensively cover all aspects under this project, and thus, it was decided to focus on hydrogen-based power generation application. A preliminary review of existing technologies available for this application highlighted the market gap between fuel-cell based solutions and conventional gas-turbine based solutions. This prompted a search for a power cycle that can combine the strengths of these two systems (i.e. the high operating efficiencies of fuel-cells based systems and the favourable operational characteristics of the gas-turbine based systems) and bridge this gap between these two technologies. This search ended with the identification of the s-CO<sub>2</sub> Brayton cycle as the most suitable candidate for this application.

The fourth chapter explores the concept of the s-CO<sub>2</sub> Brayton cycle in greater details. Although this technology is yet to be proven feasible for commercial-scale power generation applications, it was conceptualised decades ago with the first reference dating back to the late 1940s. The research interest waxed and waned several times over these years mainly driven by forces in the energy markets such as the variation in fuel prices and a global push for de-carbonisation of the energy sector. However, significant developments were made since 2010 when Allam cycle was first proposed [12]. Since then, a 50 MW<sub>th</sub> installation has been set-up by NET Power LLC in Texas, USA, to test and demonstrate various aspects of the Allam cycle. This is only one of the several variations of the s-CO<sub>2</sub> power cycle reviewed under this project to identify the key thermodynamic features that enable these cycles to deliver exceptionally high thermal efficiencies (>50%). This analysis is also discussed in the fourth chapter. After identifying the most relevant configurations in the context of the current project, a thermodynamic evaluation model is developed to analyse the proposed power cycle. The fourth chapter concludes with the discussion on the process of developing this model and its validation.

The fifth chapter of the report discusses the thermodynamic evaluation of the proposed H<sub>2</sub>/O<sub>2</sub> fuelled s-CO<sub>2</sub> power cycle. The main topics covered in this chapter are the selection of the design point parameters and the final configuration of the proposed cycle, a parametric analysis of the effect of design parameters on the overall performance of the cycle, and the development of a performance map for the proposed cycle. This chapter is concluded by summarising the most important findings of the thermodynamic analysis.

The sixth chapter is dedicated to the combustion analysis of the proposed cycle. After outlining the main goals of the combustion analysis, the important findings on the topic hydrogen combustion gained from the review of existing literature is summarised in this chapter. The focus of the literature review performed in this phase of the project was to identify the most suitable combustion reaction mechanism that could be used to simulate H<sub>2</sub>/O<sub>2</sub> combustion in an s-CO<sub>2</sub> environment. Although this combustion process at elevated pressures is not an extensively researched topic, several studies on combustion of H<sub>2</sub> in high CO<sub>2</sub> environment at lower pressure levels have been performed because of the relevance of this process in applications like the exhaust gas recirculation in combustors and syngas combustion. Many valuable insights were gained from the review of these studies which proved to be useful while analysing the combustion process of the proposed power cycle. The main outcome of this literature review process was the list of four combustion reactions mechanisms that were generally considered to be suitable for

studying H<sub>2</sub>/O<sub>2</sub> combustion in a high CO<sub>2</sub> environment. Out of these four mechanisms, Kéromnès-2013 [56] was ultimately selected for use in the combustion analysis performed under this project. After this, several different combustion simulations were set-up to study the proposed combustion process and these are discussed at length in the sixth chapter of the report. This chapter is concluded by summarising the most important findings of the combustion analysis.

Lastly, the seventh chapter of the report presents the final conclusions and recommendations of this project. The research question laid out in the previous section of this chapter are answered and the feasibility of the proposed power cycle concept is discussed. In addition to this, the recommendations for future research work in this area is also briefly discussed.

# Chapter 2

## Existing Energy Infrastructure

### Overview

This chapter summarizes the findings of an extensive review of existing energy infrastructure and gives an overview of the challenges and the opportunities in the current energy markets. In the initial stage of the project, a funnel approach was adopted, and the review process was started at a very broad level. Then based on the findings at each step of the process, the area of focus was consciously narrowed down to a selected number of topics. Therefore, the summary provided in this chapter presents a similar flow of information. The first section of the chapter outlines the main challenges in the energy sector that are slowing the pace of its transition to low-carbon sustainable future. After this, the second section of the report outlines the current progress in deployment of variable renewable energy sources. The integration challenges associated with VRES deployment and the role of energy storage systems in mitigating these issues are also identified in this section. The third section of this chapter explores various energy storage systems that are currently available or are being developed and technologies that are considered crucial in the long term are shortlisted for further analysis. Lastly, the fourth section focuses on the discussion about the role of green hydrogen in the future energy markets, the drivers that are promoting its rapid growth and also the challenges that are yet to be addressed.

### 2.1 The “Legacy” problem of the energy sector

Global electricity production in 2017 increased by 2.5% to reach 25 721 TWh [4]. In terms of global production shares, carbonaceous fuels accounted for about 2/3 of total world electricity production that year [13], thus emitting significant amount carbon dioxide in the process. This fraction varies quite a bit from country to country depending their national priorities, economic development and commitment to

sustainability. For Organisation for Economic Co-operation and Development (OECD) countries this fraction stood at 59% which is lower than the global average. As can be anticipated, for the other less economically developed countries this fraction was slightly more than 72%. From Fig. 4, one can easily understand the global power sector scenario and its strong dependence on combustible fuels especially, on coal.

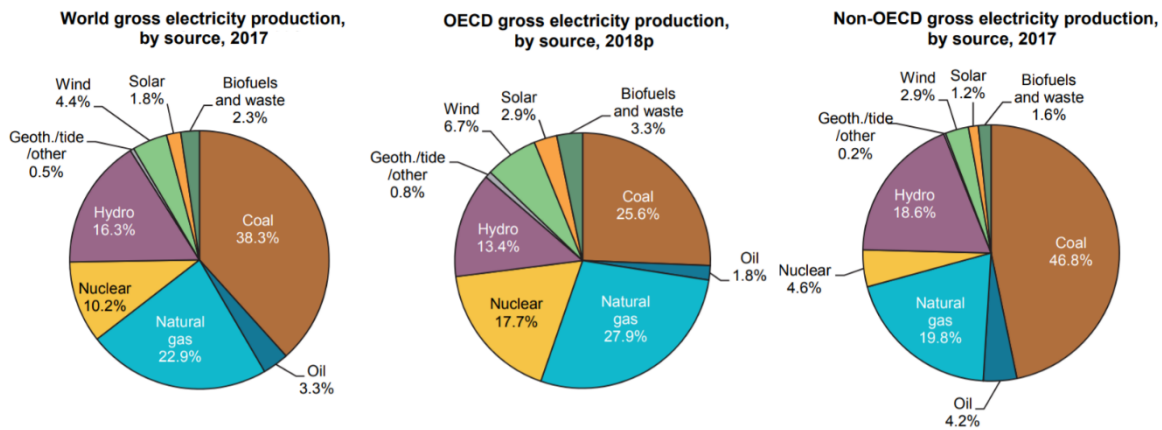


Fig. 4 Electricity production by source in 2017<sup>2</sup> [13]

The long-term effects of GHG emissions is a complex geo-political issue that has been a point of contention between the developed and the developing part world for many years. And therefore, the two landmark inter-governmental agreements mentioned earlier, are of monumental importance. Under UN's Sustainable Development framework for the year 2030, 3 Sustainable Development Goals (SDG) were related with the energy sector. SDG 3 (to reduce the severe health impacts of air pollution), SDG 7 (affordable and clean energy for all) and SDG 13 (to be in line with the goal of limiting temperature rise by 2°C and pursuing efforts to limit it to 1.5°C). The Paris Agreement on Climate Change, [ratified by 189 countries as of July 2020](#), amongst other goals this agreement strives to limit the long-term temperature rise well below 2°C while pursuing efforts to limit it to 1.5°C. In order to achieve these targets, global GHG emissions will have to be drastically cut in the coming decades and this requires implementation of some disruptive solutions. However, implementing fundamental change in the energy sector is not easy and this aspect is probed further using the case of coal-fired power plants.

Coal-fired power plants are the worst culprits for GHGs emission within the power sector. This is true even for places where the progressive governments follow a strict regulatory guideline on fugitive emissions, and therefore, the less said the better, about the situations in other places where environmental concerns are not the top priority of the regulators/governments. In order to achieve the set emission reduction targets, the existing coal-based power generation capacity will have to be replaced with low-carbon alternatives in the coming years. However, this doesn't seem likely when one looks at the statistics about the existing global fleet of coal power plants. Fig. 5 shows age profile of the existing global coal-fired assets as per the assessment done for IEA's world energy outlook 2019 report [14].

IEA's study shows that 60-65% of the total coal-fired capacity is located in Asia and other developing parts of the world. The average age of these plants is close to 12 years and hence, these plants, which are typically designed to last 35-40 years, have a long service life left before retirement.

<sup>2</sup> Data for OECD countries is preliminary data for 2018

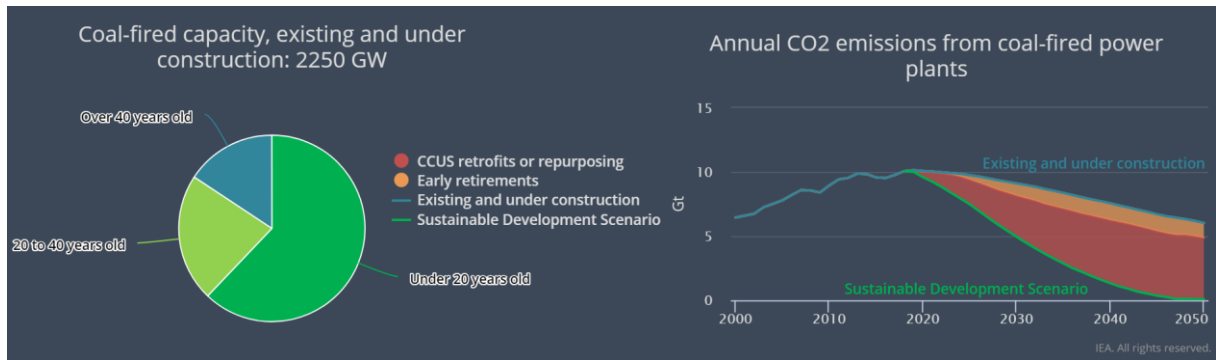


Fig. 5 Operational status of global coal-fired capacity [14]

As shown in the graph (right) in Fig.5, to meet the long-term sustainable development goals, virtually all the emissions from coal power plants must reduce to zero by the year 2050. But if the trend based on existing and planned projects is considered, the projected emission does not even reduce by 50%. This is because there is a substantial amount of “locked-in” emission due to the existing and under construction coal power plants. The options to tackle this issue and reduce the gap between the two scenarios is early retirements and retrofitting existing coal power plants with CCS/CCUS technologies. However, since many of new plants in the fleet are located in economically developing countries, it is unlikely that they will be retired before the end of their service life which is typically around 35-40 years. Also, retrofitting of existing plants with CCS/CCUS technology is unlikely in absence of strong policy push as this too shall need a considerable capital investment into these assets which may affect financial viability of these projects. Hence, in absence of a strong regulatory changes, these mitigation measures are unlikely to be implemented on wide-scale.

The key point to note is that the established paradigm in the energy sector supports legacy technologies based on fossil fuels. In many energy markets around the world there exists an institutional architecture that imposes regulatory hurdles or other policy disadvantages favouring existing technology or discouraging new entrants. Such systems are backed by huge corporations and market forces and therefore not easily changed. And at times the situation is only bolstered by strong and deeply felt public expectations of cheap energy and support to infrastructure adapted to the requirements of existing technologies. Thus, enabling a transition in the energy sector does not only require innovation and progress on the technological front, but also requires fundamental and structural reform in the policy/regulatory framework.

## 2.2 Variable Renewable Energy Sources

### 2.2.1 Role of VRES in coming decades

The share of renewables in our energy grid has increased very rapidly over the last two decades. Amongst the various renewable energy technologies, Wind Energy and Solar PV technologies have seen the largest growth during this period. The installed capacities of wind and solar power plants were estimated to be 17.3 GW and 1.23 GW, respectively in the year 2000 [15]. By the end of year 2019, these had increased to be more than 622.7 GW and 580.2 GW, respectively [16]. This results in a compound annual growth rate (CAGR) of ~20% for wind energy installations and ~36% for solar energy installations. These trends are expected to continue even in the coming year with IEA forecasting the wind installations to grow by 324 GW between 2018-2023 while the solar installations are expected to

more than double over this same period. It is expected that ~320 GW of utility scale solar PV plants will be added between 2018-2023 while the distributed solar installations are expected to add ~250 GW of generation capacity [17]. This rapid deployment is enabled by several factors including, government subsidies, rapidly declining investment cost, energy security concerns, and growing global consensus around the climate change. Multiple integrated assessment models (IAMs) [18 & 19] have suggested a key role for VRES over the next century. These models predict that, the share of wind and solar energy in the world energy mix can vary between 35-63% by 2050 and between 47-86% by 2100, if policies that limit warming in 2100 to 2° Celsius above pre-industrial levels are introduced. The projected range is quite large, because the models make several assumptions such as, cost of storage solutions and normalized capital cost of the project. Pessimistic assumptions result in deployment represented by the lower limit of the range, while if optimistic trends are assumed the upper limits of the reported range are obtained.

### 2.2.2 Associated Integration challenges

Deployment of VRE plants in the electrical grid in such proportions will give rise to several implementation challenges. There is not a fixed VRES penetration level at which integration challenges being to show in the grid and this is rather dependent on the characteristics and flexibility of individual grid systems. For an instance, we look at the two interesting cases mentioned in an IEA article on the subject of grid integration challenges [20]. The authorities in Ireland had to impose a moratorium on development of new wind farms back in 2003 in view of security and stability of the country's power system. The share of wind energy in the annual energy generation at the time stood at as low as 2%, yet a limit had to be imposed for stable operation of the system. In the following years, the challenges were analysed, and the system was re-designed and revamped to allow for higher wind energy share in the generation mix which stood at 25% as of 2017 and is planned to be ramped to about 39% by 2023. Similar challenge was faced in case Electricity Reliability Council of Texas (ERCOT) in 2009 when the development of wind energy plants outpaced the development of necessary grid infrastructure causing the curtailment levels to be as high as 20%. Since then, the grid has been strengthened and the curtailment was now below 2%.

IEA analysis [21] categorizes the integration of VRES into local energy grids in six distinct phases. This categorisation is useful because regulators/grid operators can be use it to priorities different steps to support system flexibility, identify relevant challenges and implement appropriate measures to support the integration of VRES. The six phases are as follows. Phase 1 captures very early stages where VRES deployment (often no more than a few percent of annual energy demand) has no immediate impact on power system operation. Phase 2 flexibility issues emerge but the system is able to cope with them through minor operational modifications. Phases 3 through 6 respectively indicate greater influence of VRES in determining system operations; starting from the need for additional investments in flexibility; structural surpluses of VRE generation leading to curtailment; and structural imbalances in energy supply at seasonal and inter-year periods requiring sector coupling. Fig. 6 shows list of selected energy markets categorized across these categories along with their respective levels of VRES deployment.

Although Fig. 6 shows VRES deployment only up to phase 4, is possible to deploy VRES beyond this level but has not yet been witnessed in the world. Integrating very high levels of VRES in existing grids poses a technical challenge because electrical grids have traditionally been designed to handle demand side variability and VRES introduces considerable variability on the generation side as well. Maintaining a reliable supply of electricity requires that supply and demand be balanced continuously across all timescales, from sub-seconds to years and thus when the variability in the grid increases, it is

necessary to take measure to increase the flexibility of the grid proportionally. Therefore, VRES deployment in phase 5 & 6 requires many more measures such as electrification, integration and diversification of different end-use sectors, deployment of seasonal energy storage systems and use of synthetic fuels such as hydrogen. Many of these measures are currently under development and hence further deployment of VRES depends on the success of these research initiative.

- Phase 1: No relevant impact on system integration
- Phase 2: Drawing on existing system flexibility
- Phase 3: Investing in flexibility
- Phase 4: Requiring advanced technologies to ensure reliability

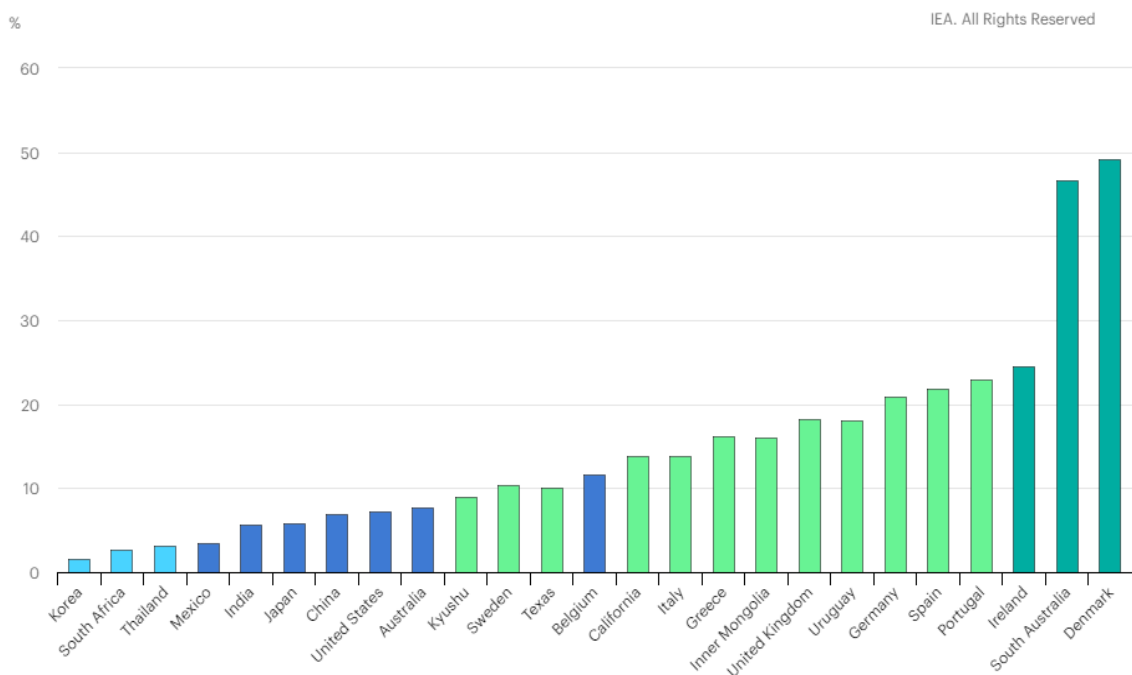


Fig. 6 Selected countries by integration phase and share of VRES, 2017 [21]

In addition to having a low carbon footprint in comparison to conventional power generation methods, VRES based generation methods such as wind and solar plants also have other benefits such as shorter implementation time frames, faster debt payment cycles, lower operational cost etc. Although this make them economically attractive, they have a disadvantage compared to conventional energy sources because of the following reasons [22];

1. Variable output due to primary resource variability
2. Unpredictable over longer durations
3. Modular and generally small installed capacity
4. Location constrained
5. VRE generators usually of are non-synchronous type

Due to these factors VRE power plants, upon integration, create several technical challenges in the existing power systems. Based on the data gathered from operation of several grids with various levels of VRES deployment, many of these challenges can generally be anticipated with increasing share of renewable energy in the generation mix. Fig. 7 shows various technical issues that can be expected at different levels of VRES in the energy grid as reported by Mararakanye et. al. in their analysis. [23].

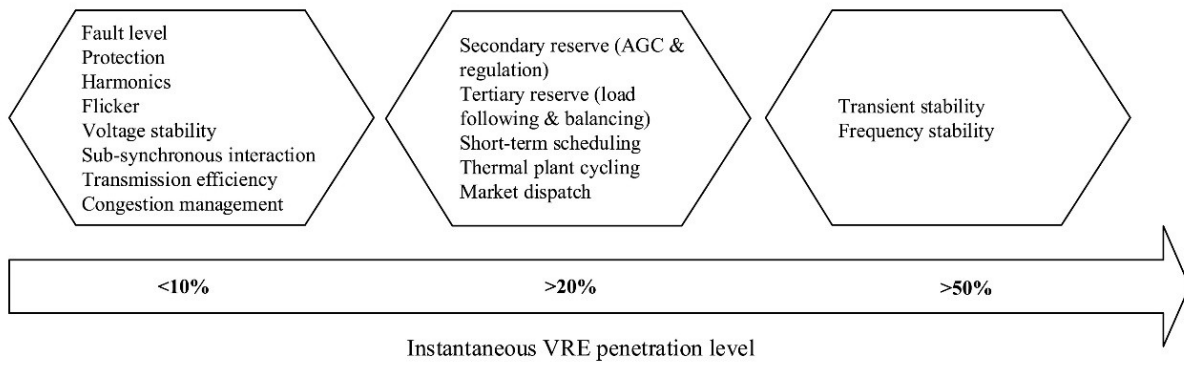


Fig. 7 Expected integration challenges with increasing VRE penetration level [23]

Another study by Sinsel et. al [24] goes a step further in this direction and segregates the various challenges caused by VRES into 4 main categories namely, quality, flow, stability, and balance issues. Fig. 8 shows this categorisation of several technical challenges caused by VRES integration in existing energy grids.

Category	Symptoms
Quality	- local trips, shorter lifetime or damage to equipment at end consumer - safety hazards
Flow	- regional trips, shorter lifetime or damage to transmission and distribution equipment - loop flows, redispatch or curtailment due to congestion - increased losses
Stability	- increased dynamic stability violations, redispatch or curtailment due to stability concerns - controllability or resonance issues
Balance	- increasing mismatches between supply & demand

Fig. 8 Categorisation of challenges caused by VRES [24]

The power quality category comprises of the issues encountered while maintaining an uninterrupted supply of power at stable conditions of voltage and current at the consumer's end, as well as maintaining safe conditions in case of outages. The main VRE characteristics responsible for introducing these challenges at the grid level are modularity of VRE generators and the fact that most of them are non-synchronous type generators. These two characteristics are also mainly responsible for the issues under the stability category which mainly includes the challenges associated with the frequency and voltage control in the power grids and system recovery post blackouts. The issues in the flow category, as the name suggests, are mainly related efficient transmission and distribution of power. There are several factors associated with VRES that lead to the flow challenges, the most important ones are variability, modularity and location constraints of VRES. Lastly, the problems under the balance category are mainly related to short – to – long term balance of active power supply and demand. This mainly includes the co-ordination of loading/off-loading rates of all the power plants connected to the grid to counteract the variability introduced in the grid by VRE power plants while maintaining the necessary minimum generation level of different power plants in the grid. Load balancing challenges are mainly cause by the variability and uncertainty of VRES.

### 2.2.3 Potential solutions

In view of the fact that, transitioning to low-carbon renewable energy is the only long term solution that can make the energy sector more sustainable in the long run, considerable amount of research effort in the last decade has been dedicated towards solving the integration challenges. Sinsel et. al [24] categorized several of these integration technologies based on their scale and their function in the power system. Based on the scale of application, the technologies are classified under distributed and centralized solutions. Based on their function in the power system, they can be classified as flexibility technologies (that improve the power generation aspect) and grid technologies (that improve the transmission and distribution aspects). Fig. 9 shows some technologies categorized under this system of classification.

Role \ Scale	<i>Distributed Technologies</i>	<i>Centralized Technologies</i>
<i>Flexibility Technologies</i>	<ol style="list-style-type: none"> <li>1. Reciprocating engines</li> <li>2. Battery energy storage(BES)</li> <li>3. Demand management</li> <li>4. Modification of VRE generators</li> </ol>	<ol style="list-style-type: none"> <li>1. GTs. reciprocating engines</li> <li>2. PHS/Grid scale BES/HES</li> <li>3. Demand management</li> <li>4. Modification of VRE generators</li> </ol>
<i>Grid Technologies</i>	<ol style="list-style-type: none"> <li>1. Adapted Equipment Protection</li> <li>2. Voltage management</li> <li>3. Current limiters</li> <li>4. Real time grid (local) management</li> </ol>	<ol style="list-style-type: none"> <li>1. Forecasting</li> <li>2. Active/reactive power controller</li> <li>3. Inertia/short ckt power provider</li> <li>4. VRE curtailment</li> </ol>

Fig. 9 Categorisation of challenges caused by VRES [24]

Table 1 also adapted from the Sinsel et. al study [24] correlates various implementation challenges and the technological solutions available to address them in a qualitative way. Two additional terms are introduced during the discussion namely, solution potential and solution space. The first term, ‘**solution potential**’, refers to the ability of a solution to address a variety of integration challenges. Technologies with a higher solution potential can address a higher number of different integration problems while those with a smaller solution potential typically are designed to specifically solve a particular integration problem. The second term, ‘**solution space**’, relates to the stiffness of the integration problem being discussed. A problem with a large solution space is usually less stiff since it can be solved by implementing a number different solution, while a stiff problem will have a small solution space and demand a more tailored solution.

On a broad level, the data presented in Table 1 indicates that if the various categories of VRE integration issues ranked in a decreasing order of stiffness, the list would be quality, flow, stability and balance issues. In order words, it can be said that the stability and balance issues can be alleviated by a number of technologies, but the power quality and flow category problems require more tailored and specific solutions. From the solution category perspective, flexibility solutions (both at centralized and distributed levels) can help with alleviate many of the stability and grid balance issues. Grid technologies are more suitable for solving the power quality and flow issues since many of the solutions in this category are customized solutions for instance power flow controllers and harmonic filters.

Table 1 Several VRES integration challenges correlated with available/proposed solutions [24]

	Integration technology (Refer Table 1-b)	#1	#2	#3	#4	#5	#6	#7	#8	#9	#10	#11	#12	#13	#14	#15	#16	#17	#18	#19	#20	#21	Solution Space		
Quality Issues	Increasing flicker	•																						1	
	Increasing harmonic distortions	•									•													2	
	Unreliable shut-down during blackouts	•					•																	2	
	Increasing local voltage excursions	•				•	•																	3	
Stability Issues	Insufficient reactive power provision	•	•									•		•				•		•	•			7	
	Decreasing level of short-circuit power											•	•	•								•		4	
	Decreasing level of inertia											•		•			•					•		4	
	Inadequate coordination of frequency trip limits	•	•	•	•							•	•	•	•							•	•	10	
	Inadequate coordination of voltage trip limits	•	•									•		•							•	•			6
	Decreasing frequency control reserves	•	•	•	•							•	•	•	•										8
	Increasing control interactions											•								•					2
Flow Issues	Increasing regional voltage excursions	•	•	•	•	•	•	•	•												•		•	10	
	Missing distribution grid capacity	•	•	•	•	•		•															•	7	
	Increasingly volatile flow patterns from lower grid levels	•	•	•	•	•			•								•	•					•	9	
	Inadequate protection design						•		•	•														3	
	Increasing short-circuit currents	•				•	•				•														4
	Missing controllability of VRE generation			•	•				•														•	4	
	Missing visibility of VRE generation	•				•			•								•	•							5
	Narrow voltage trip limits	•	•					•					•												4
	Missing transmission grid capacity		•	•										•	•			•	•	•					7
	Increasing transmission distances																	•	•						2
Balance Issues	Insufficient short-term generation adequacy	•	•	•	•							•	•	•	•	•								9	
	Insufficient long-term generation adequacy		•	•									•	•										4	
	Insufficient firmness of VRE generators	•	•	•	•							•	•	•	•	•								9	
	Insufficient forecasting of VRE generators		•	•	•							•	•	•	•	•								8	
	Restricted dispatchability of VRE generators	•	•	•	•							•	•	•	•	•								9	
<b>Solution Potential</b>		<b>17</b>	<b>14</b>	<b>12</b>	<b>10</b>	<b>6</b>	<b>5</b>	<b>3</b>	<b>5</b>	<b>2</b>	<b>1</b>	<b>12</b>	<b>8</b>	<b>12</b>	<b>7</b>	<b>6</b>	<b>5</b>	<b>3</b>	<b>2</b>	<b>3</b>	<b>5</b>	<b>5</b>			

Table 1-b List of integration technologies considered in Table 1-a [24]

Distributed Technologies	Flexibility Technologies	Modification to distributed VRE generators	#1
		Distribution conventional generators	#2
		Distributed Storage	#3
		Distributed demand response	#4
	Grid Technologies	Distribution grid reinforcement / expansion	#5
		Adapted equipment protection strategies	#6
		Voltage management solutions for distribution grids	#7
		State estimation solutions for distribution grids	#8
		Current limiter devices	#9
		Harmonic filters	#10
Centralised Technologies	Flexibility Technologies	Modifications to large VRE generators	#11
		New or modified large conventional generators	#12
		Centralized storage	#13
		Centralized demand response	#14
	Grid Technologies	VRE forecasting technology	#15
		Transmission grid reinforcement/ expansion	#16
		HVDC transmission systems	#17
		Power flow controller	#18
		Reactive power controller	#19
		Inertia or short-circuit power providers	#20
		Central feed-in monitoring & control	#21

Considering the ongoing discussion, it is important to take note that Table 1 correlates the solution technologies with the problems only in a qualitative manner. The extent to which different solutions/technology will solve a particular issue is not factored in this discussion, So the terms, solution potential and solution space, only provide a high-level correlation and should not be used as a metric to judge one technology better over others or to conclude particular issue more problematic than other issues. The main takeaway in the context of this report is the role storage solutions can be expected to play with increasing penetration of VRES in the world energy mix. Energy storage solutions provide the much-needed grid flexibility and primarily contribute to solving grid stability and balancing issues. Distributed storage solutions can also help in addressing the some of the challenges in the flow category as can be seen from Table 1. The next section, therefore, focuses on several aspects of energy storage solutions.

## 2.3 Energy Storage Solutions

### 2.3.1 Role of energy storage solutions

The modern electrical grid, from a simplistic perspective, can be imagined to be similar to a series of water pipes connecting a certain number of households in a town to the town central water source, say a pumping station situated on a nearby lake. In absence of any water storage options in the network, the central pumping station will have to start pumping water each time demand for water arises. This system may work fine if the number of the consumers is not large and the total instantaneous demand for water is always less than the total pumping capacity of the system. However, as the number of consumers increases, the system becomes more prone to overload and failure. A simple way to alleviate this issue and better match the demand and supply of water would be include adequate number of water storage facility at several points in the town. The main pumping station can then feed these storage tanks which can cater to the local demand. Inclusion of storage tanks in this case allows the system operator to decouple the demand and supply cycles.

Modern electrical grids, in principle, operate like this simple water supply network albeit are several times more complicated. The complication not only arises from the fact that there are millions and millions of end-consumers but also from the fact that the grid operators are bound to supply power within tightly constrained power quality parameters. A sudden increase/decrease in the grid load can cause dip/increase in grid frequency or voltage which can result in a grid failure and blackouts. With introduction of VRES in our existing grid infrastructure, the complexity of grid operations has only increased. Renewable energy plants introduce variability of supply at various time scales, be it from sub-second level caused by a cloud cover passing over a solar farm, to seasonal variation in solar insolation or wind patterns. This variability makes it difficult for grid operators to match the demand and supply curves. Another problem especially with solar power plants is the offset between demand and supply peaks. In case of solar power plants, the peak generation on a clear day occurs around noon but the peak demand for electricity occurs during the evening hours when household consumers are returning home from work.

Energy storage systems, theoretically, plays the same role as that played by the water storage tanks in the earlier example of the town's water supply network. It supplies energy during demand peaks and stores it during times of low demand. Energy storage systems can help us decouples the generation of electricity from its consumption and, in so doing, can help to better manage the grid, optimize the use of existing resources, and integrate large-scale renewables. Imagine the possibility of generating renewable energy from an offshore wind/solar farm, storing it in form of hydrogen and using it as and when needed. Progress in development of seasonal energy storage systems is making this possibility more and more real with each passing day.

The cost of storing energy, however, is a major factor that needs to be considered when analysing different energy storage systems. The study by M. McPherson et al. [\[18\]](#) has shown that the trend of cost of storage technologies will have significant impact the VRES penetration levels in future world energy markets, especially if the energy markets develop without imposition of tax on carbon emission (baseline scenario). VRES penetration levels reduced by ~14% when the assumption for cost of energy storage systems is changed from the optimistic level to the pessimistic level in the baseline scenario. However, this is not the case when the baseline scenario is changed to Tax30 scenario. In this case the VRES share only reduces by 3% when all storage cost assumptions are changed from optimistic to pessimistic. This study suggests that in the absence of a strong climate policy taxing carbon emission in

the future, the main driver for integration of renewable in the energy mix will purely be the economic considerations and these are highly sensitive to the development of viable low-cost large-scale seasonal energy storage solutions. Investments to reduce the cost of power-to-gas (P2G) technologies appears particularly important for facilitating VRE shares above 40% where seasonal curtailment becomes an issue. In case climate policies are implemented over the next decade to curb CO<sub>2</sub> emissions from the energy sector, costs of storage technologies don't have a significant impact on VRES deployment, Yet, R&D investments that lower the costs of storage technologies will reduce the cost of the low-carbon energy transition required to mitigate climate change.

### 2.3.2 Categorisation of Energy Storage Solutions

Several energy storage technologies are commercially available or being developed for future applications. These can be categorized based on various technical characteristics like the nominal storage capacity, scale of application, type of energy stored etc. The last approach of classifying the storage technologies based on the form of energy stored is most widely used in literature. Fig. 10 shows the main technologies that are currently being studied/considered for deployment in high VRES scenarios in the coming decades. Some of these technologies such as PHS, FES, BES etc. have been commercially mature while others are relatively new or not operationally mature.

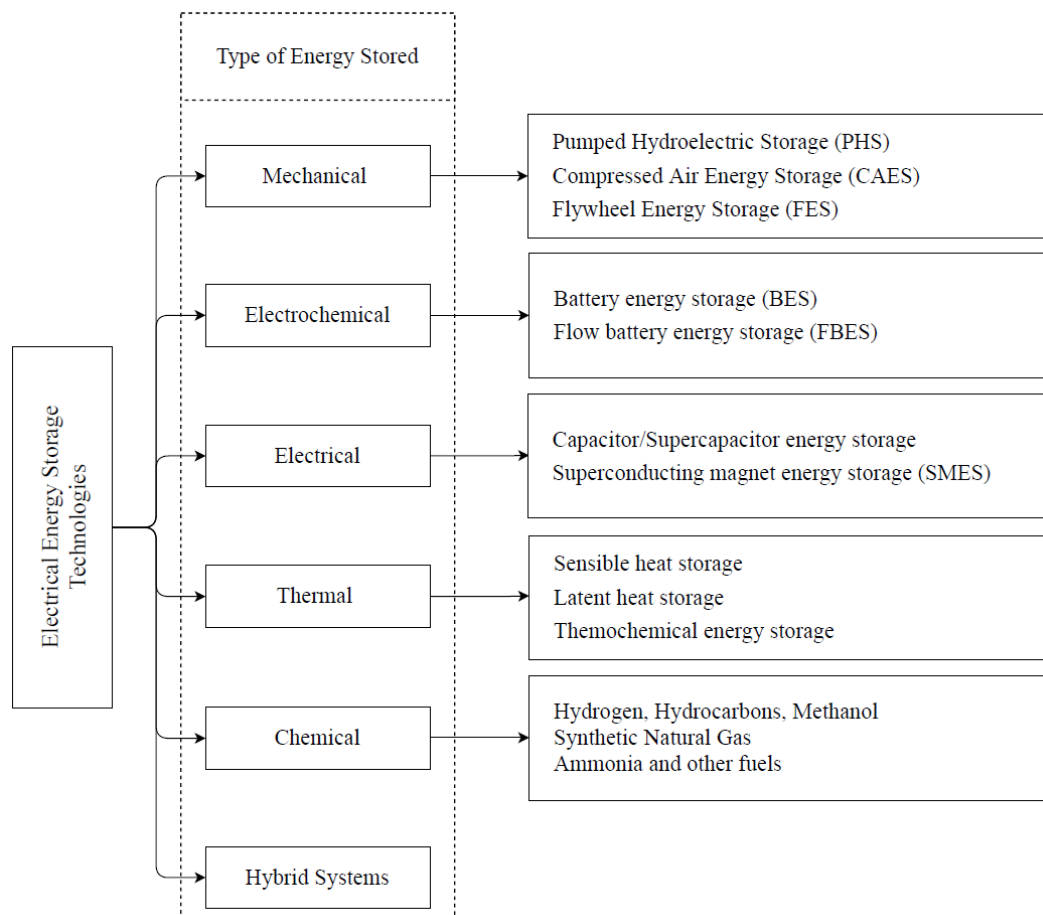


Fig. 10 Energy storage technology categorised based on type of energy stored [29]

The concept of energy storage systems isn't a recent one but the need for its wide-scale deployment only rose when share of renewables increased. This is the main reason none of the technologies mentioned have seen a wide-scale application yet. Amongst all the solutions listed, pumped storage hydropower

plants see the largest application with a total install capacity of about ~170 GW. The world largest energy storage plant is also a PHS system with a storage capacity of ~24 GWh and power capacity of 3GW. However, site suitable for building these plants is limited and this limits its deployment potential besides the fact that it has a very high initial investment cost which makes it less attractive. CAES is other large-scale energy storage solution that has been on the energy markets for a while and has a total installed capacity of 640 MW worldwide. It is often installed in tandem with a natural gas fired power plant.

In recent years a spike in deployment of grid scale battery storage systems is seen mainly deployed in conjunction with wind farms/solar parks. It is an attractive option for short term energy storage solution (typically a few hours) but is not suitable for long-term seasonal energy storage solution because of its high self-discharge rate. Flow battery energy storage systems overcome this problem by storing the electrolytes separately. This increases the storage duration considerably making them partly suitable for seasonal energy storage applications, but they still have a limited storage capacity.

Other solutions like flywheel energy storage, capacitor/supercapacitor energy storage, superconducting magnet energy storage have a very energy discharge rate but are very limited in their overall energy storage ability and hence mostly suited for alleviating power quality problems such as frequency regulation, voltage support etc. Lastly, chemical based energy storage systems are amongst the most promising technologies for seasonal storage application mainly because of its versatility and the ability to integrate several end-use sectors. For instance, chemical energy stored in green hydrogen can directly be used to replace use of fossil fuels in industry or can be used as fuel in fuel-cell vehicles or converted back to power during times of peak demand.

### **2.3.3 Shortlisting of relevant seasonal energy storage solutions**

During the literature review phase of the project, the energy storage technologies listed in Fig. 10 were analysed in detail followed by a preliminary comparison based on a set technical parameters, potential environmental impacts and potential areas of application. To keep the present discussion concise, these details are not included explicitly in this report. A reader interested in these details may refer the literature survey report prepared during the first phase of this project [25]. Only the most relevant findings of this comparison are summarized in this section.

In line with the findings of the study done by McPherson et al. [18], deployment of seasonal energy storage systems was found to be imperative to support renewable energy share of more than ~40% in the global energy mix. Therefore, future deployment of low-carbon energy systems is critically linked with development of a viable seasonal energy storage option. Assuming this to be one of the key drivers of the long-term transition to sustainable energy grids, technologies compatible for seasonal energy storage application were shortlisted. These mainly included PHS, CAES, HES. Fig. 11 shows a comparison of several energy storage technologies and their role in energy grids based on their discharge time and rated power capacity.

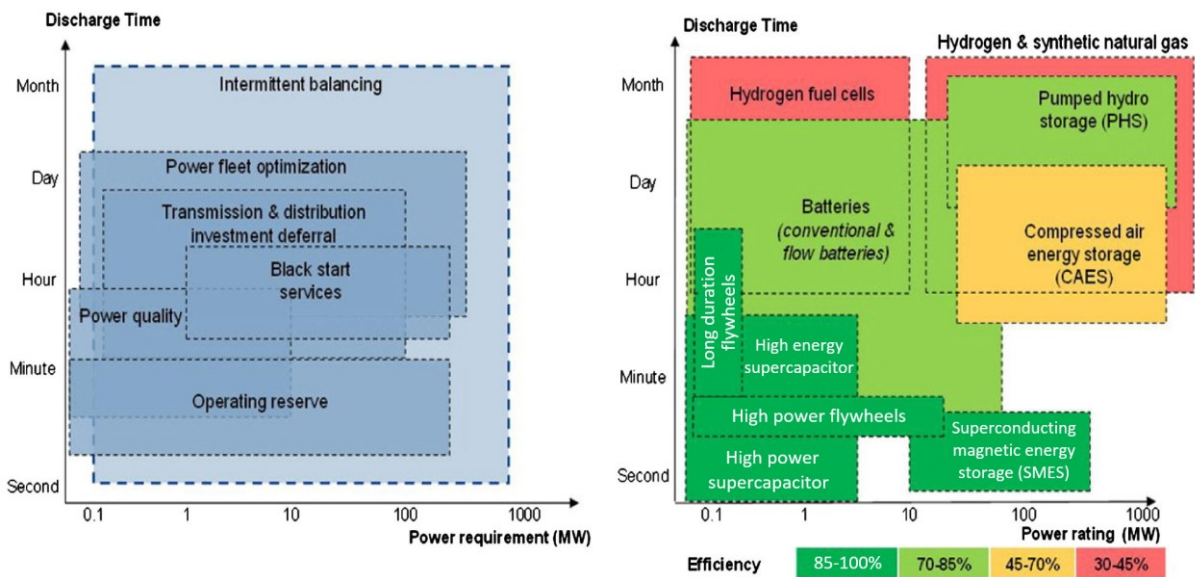


Fig. 11 Role of energy storage systems & comparison of several energy storage technologies [67]

PHS is the most mature long-term energy storage technology and has the highest level of deployment compared to all other energy storage options. The global energy storage landscape in terms for total installed capacity is dominated at present by PHS systems occupying over 95% of all installed capacity. Despite having some favourable characteristics such as low energy storage cost and a long operational lifetime, the main disadvantage of PHS include that its deployment potential is limited by availability of suitable sites, the associated negative impact on ecosystems in the catchment areas, rehabilitation challenges typical of large hydropower project, high initial costs etc. Many of these challenges can be addressed if the underground PHS systems are considered, but this only further escalate the initial cost required. Overall, it was concluded that although PHS systems will see a growth in future and have a role to play in the future energy scenarios, it is unlikely to be the critical technology/solution that will enable large-scale integration of VRES into our energy mix given its limited deployment potential.

Similarly, CAES solutions have been commercially available for a number of years but is yet to see a wide-scale deployment. It shares many similarities with PHS in terms of its low energy storage cost, high storage efficiency, and long operational life. In addition to this it also has some advantages over PHS system with lower initial investment and less stringent site requirements. However, the disadvantages come in the form of higher operational cost, and a high downstream emission potential since they are usually deployed in conjunction with natural gas fired power plants. This particular problem maybe overcome in future if natural gas is replaced with green hydrogen in future. Yet, just like PSH plants, CAES has a low energy storage density which makes availability suitable sites large enough for a grid scale energy storage system scarce. Hence as was concluded with PHS technology, CAES systems will see a growth in its deployment in coming years, but it the authors opinion that even CAES isn't the one technology that will be critical in bringing about a paradigm shift in the energy sector.

HES technology, in contrast with PHS and CAES, was found to be a highly scalable energy storage solution with an enormous implementation potential and therefore critical for enabling a transition in the energy sector. It has many favourable characteristics such as high energy density, environmentally sustainable, compatibility with various end-use sectors etc. The disadvantages include moderately high

implementation cost, limited life of electrolysis cells, lower cycle efficiency, lack of supporting infrastructure etc.

Despite these challenges, the recent surge in research interest in this area is promising and many of the existing challenges can be expected to be addressed in the coming years. Firstly, the cost of implementation is expected to reduce as the technology sees a wider implementation. Secondly, investment commitments for developing the necessary infrastructure has been seen in past few years with Japan and South Australia being at the forefront of this effort. Several projects/policies for integration of green hydrogen in the existing energy markets have been announced/implemented by several European countries as well. Lastly, although the power-to-power round-trip efficiency of HES system may not increase up to the levels offered by other storage options such as battery energy storage solution, this point is somewhat less relevant since the role expected to be played by HES solutions is quite different from BES systems. Batteries, for example, are expected to store energy for a period of few hours when there is a peak in generation and supply this energy at the highest possible efficiency when the demand peaks. Green hydrogen, on the other hand, is a convenient energy carrier and is expected to integrate several different sectors and directly replace the fossil fuel consumption in hard-to-abate sectors as well. These and some more key aspects of the HES technology are discussed in detail in the following sections of this report.

## **2.4 Hydrogen – The bedrock of future low-carbon energy markets**

The main challenges in implementation of seasonal energy storage solutions identified in the previous discussion are availability of suitable sites (mainly with PHS), associated environmental impacts (PHS, CAES), limited energy storage potential and limited service life (FBES) and high costs involved (Initial cost in PHS and CAES and operational cost in FBES). Hydrogen based energy storage can potentially overcome many of these limitations. Unlike PHS, there is no technical limitation on availability of suitable site for setting-up electrolysis based H<sub>2</sub> production plant. H<sub>2</sub> has a high specific energy and therefore, it will result in a smaller area requirement for the energy storage facility compared to CAES and FBES. Also because of the high volumetric and mass specific energy and power density of HES, theoretically, the plant capacities are only limited by the availability of excess energy.

Hydrogen has a long-shared history with the energy sector from being the fuel that powered the first internal combustion engine back in 1806 to becoming an integral part of the modern refining industry. The global demand for hydrogen is seeing a robust growth phase and more than tripled since 1975, to the extent that supplying pure hydrogen to industries is a major business around the world – almost entirely produced using fossil fuels. To give a sense of scale, hydrogen production accounts for 6% of global natural gas consumption and 2% of global coal consumption. The CO<sub>2</sub> emissions arising from hydrogen production is around 830 MtCO<sub>2</sub>/year – equivalent the annual CO<sub>2</sub> emission of Indonesia and the United Kingdom combined. In energy terms, the global demand for hydrogen is around 330 mtoe which is equal to the annual primary energy consumption of Germany [26]. This demand for hydrogen is despite the fact that it is almost completely absent from the energy mix in sectors such as transport, buildings and power generation. Therefore, hydrogen can make a significant contribution to clean energy transitions by way of strategic policy implementation paving way VRE based hydrogen production and its widespread adaptation in sectors where it has been traditionally absent. The following sections systematically discuss the various opportunities and challenges related to wide-scale adoption of hydrogen as an energy carrier, not just in the context of energy storage but from a broader policy and clean energy strategy perspective.

### 2.4.1 Opportunities

In addition to the advantages it offers as an energy storage solution, hydrogen has the potential to play a much more central role in the low-carbon future scenarios. It can play the role of an energy carrier that is flexible and complements clean electrical energy in the future. It is important to take note that hydrogen, much like electricity, is an energy carrier and not an energy source. If deployed in a sustainable manner (produced from low-carbon sources), both hydrogen and electricity have the potential to substantially reduced the anthropogenic GHG emissions and significantly contribute to the transition process to a low carbon future – the keyword being sustainable deployment. Currently, almost entire hydrogen production and ~70% of electricity generation in the world is based on fossil fuels. To reduce CO<sub>2</sub> emissions and meet the goals set in Paris Agreement on Climate Change, it is important to reduce reliance on hydrocarbon fuels and the combination of renewable energy and hydrogen gives a perfect opportunity to do this. The future of hydrogen technologies looks very promising primarily because of the following reasons [26].

#### 1. Hydrogen can enable deep emission reductions, even in the hard-to-abate sectors

Green hydrogen can be instrumental in reducing emission from sectors that are considered as hard-to-abate emission sources (because of their low electrification). These include sectors such as aviation, international shipping, iron and steel manufacturing, chemical manufacturing, high-temperature industrial heat applications, long haul road transport etc. About 80% of the world's total primary energy demand is met by carbon-containing fuels. In order to meet our long-term emission targets, considerable reduction in emissions from all fossil fuel dependent sectors is crucial. Hydrogen currently, is the best poised synthetic fuel to replace the share of fossil fuels. Thus, a huge market opportunity already exists for industrial scale hydrogen production using renewable energy making the outlook positive for this technology.

#### 2. Hydrogen can help in achieving a wider range of policy objectives

Renewable energy based hydrogen production also has the potential to fulfil other policy objectives such as energy security, local air pollution, economic development and universal clean energy access. Energy security is often a considered to be a key part of national security and independence of a country. The current geopolitical situation is that majority of world nations are dependent on a small group of nations (exporters of primary energy resources, mainly, oil and gas) for meeting their energy needs which is not ideal for these economies. Hence, they can leverage the booming growth of renewable energy sources and the development of hydrogen technologies to enhance their energy security. Secondly, air pollution is a major problem that is prevalent in big cities throughout the world. Replacing fossil fuels with hydrogen can help to greatly alleviate this problem. Hydrogen also presents a good opportunity for economic development. Nations with ample VRES potential can explore commercial production and export of hydrogen and other hydrogen-based chemicals like ammonia, synthetic methane and methanol. Hydrogen projects in South Australia are amongst the first major projects in the world exploring this business opportunity. Lastly, the viability of distributed renewable energy production makes distributed hydrogen production possible thus increasing the chances of meeting the target of universal access to affordable and clean energy by 2030 (Sustainable Development Goal #7). Thus, hydrogen technologies can enable achieving a host of policy objectives in future.

### 3. Hydrogen and VRES can mutually support and enable/ensure a rapid growth.

One of the main drivers of the unprecedented momentum that hydrogen technologies are currently enjoying is the rapidly declining cost of renewable energy. As wind and solar cost decline, their expected share in future energy mix rise. Several countries and regions now have ambitious targets for the share of electricity coming from low-carbon sources [26], with South Australia aiming for 100% by 2025, Fukushima Prefecture by 2040, Sweden by 2040, California by 2045 and Denmark by 2050. Many other countries have emissions reduction targets that indicate similar future scenarios. The EU objective of reducing emissions by 80–95% by 2050 compared to 1990 levels, for example, implies almost complete decarbonisation of power generation and high levels of variable renewables. At high levels of VRES, variability of supply will have to be adequately managed. As discussed above hydrogen can be stored or used in a variety of sectors. Hence, converting electricity to hydrogen, in combination with other storage technologies, can help with the matching of variable energy supply and demand, both temporally and geographically. Growth of VRES and hydrogen technologies is a mutually dependent. Increased share of VRES and declining cost of energy enables development and deployment of hydrogen technologies. Development in hydrogen technologies improves the feasibility of seasonal storage technologies which in turn enables higher share of VRES.

#### 2.4.2 Challenges

Although the current outlook of hydrogen technologies looks promising, significant challenges remain that are yet to be addressed. The challenges can be grouped into three broad categories;

##### 1. Policy and technology uncertainty

Climate change mitigation is still the single most crucial factor driving the widespread interest in clean hydrogen. The speed at which governments will push for transition policies for low-carbon energy sources in different countries and sector remains a major uncertainty. In absence of a strong, and ideally – binding, policy push for transition to low-carbon future, the major hydrogen technologies and infrastructure projects become financially less attractive.

There are also some uncertainties on the technology front. These become apparent from the extensive discussion regarding production, storage, transportation and utilisation of hydrogen, A clear consensus is yet to be reached mostly because of lack of operational experience making it difficult for governments and companies to make significant and long lasting decisions and financial commitments. The suitability of available technology options can be expected to become clearer with continued R&D effort and with learnings from the pilot projects around the world.

##### 2. Value chain complexity and infrastructure requirements

Hydrogen, as discussed previously, is a versatile energy carrier. Its production, storage, handling, transportation and utilisation can be done in many different ways. Therefore, the most cost-effective combination of production technology, handling & storage, and utilisation methods can be different for different regions and sectors. This fact makes the hydrogen value chain highly linked and complicated which requires the policies and the investment in technology development to be synchronized in scale and time. In many cases, governments and companies will have to develop new cross-sectoral dynamics to make the most of the business opportunity.

Missing infrastructure support is another hurdle that is slowing the pace at which hydrogen technologies are adopted. Although distributed production of hydrogen is technically possible, its storage and distribution can gain benefit from economies of scale. The investment requirement for widespread development of infrastructure to support a hydrogen-based economy is estimated to be substantial and the ability of the governments to commit infrastructure investments at these scales is limited in many countries and regions. Public private partnership in this sector can be a solution but that adds another layer of complication. Many of these infrastructure development projects will require co-operation at international level that is not yet seen for hydrogen.

### 3. Regulations, standards, and framework

The regulations and standards related to hydrogen that are currently in place around the world, limit utilisation of hydrogen and do not allow to fully exploit the benefits hydrogen can provide. They deal with a range of technical but important questions surrounding handling, storage, safety and utilisation of hydrogen in the current markets. These need to be updated from the perspective of future energy markets if hydrogen is to have the opportunity to fulfil its potential.

Many essential standards are yet to be agreed upon, including standards related with hydrogen vehicle refuelling, safety measures, composition of gas from cross-border sales, materials and how to assess lifecycle environmental impacts. This issue of lifecycle impact assessment is particularly important here because hydrogen molecules can be produced and combined from source that have different CO<sub>2</sub> intensities. Accounting standards for diverse sources of hydrogen along the supply chain may be fundamental to creating a market for low-carbon hydrogen and need to be developed on an internationally agreed basis.

Lastly, hydrogen comes with some safety risks, high upfront infrastructure costs and some of the industrial dynamics of fossil fuel supply and distribution. It is not yet clear how end-users will react to these aspects of hydrogen, or how they will weigh them alongside the convenience and environmental benefits of some hydrogen applications, as well as the potential importance of hydrogen to long-term sustainability.

#### **2.4.3 Final remarks**

Currently, there is an unprecedented momentum for R&D of hydrogen-based energy solutions even when other storage solutions like batteries are proving their commercial success. The growing global consensus around climate change is expected to further bolster financial commitments towards R&D of hydrogen technologies. It can therefore be said that there is willingness on the part of stakeholders and a space in the energy markets for a largescale implementation of hydrogen energy storage solutions. Hydrogen based storage / distribution of renewable energy looks particularly promising because of its ability to make a multi-sectoral impact. Thus, despite the implementation challenges, there are strong indications that hydrogen technologies will have a significant role in the low-carbon economy of the future. At a broad level, rapid development of hydrogen technologies is vital for achieving our long-term sustainable development targets and for enabling the impending transition in the existing energy markets.



# Chapter 3

## Hydrogen –The Future Energy Carrier

### Overview

This chapter briefly discusses various aspects of the hydrogen supply chain. The review of existing energy storage options led to the conclusion that hydrogen technologies may well be the missing link between the contemporary and the low-carbon energy markets of the future. However, there are several factors that require consideration when discussing the hydrogen-based energy solutions. These can be sub-divided to broadly fall under the production, storage and utilisation categories. Since these topics are too extensive to study comprehensively under this thesis project, only some key points are discussed in this chapter. The first section focusses on discussing the production aspects of the hydrogen value chain. This discussion is divided into two parts, the first focusing on the technological considerations while the second focusses on the economic considerations of hydrogen production. After this, the second section briefly outlines many promising hydrogen storage technologies that are either commercially available or are being developed at present. After briefly mentioning various sectors in which hydrogen can promote VRES integration in the third section, the discussion in the fourth section quickly shifts to focus on the power-to-gas-to-power (P2G2P) applications of green hydrogen. Existing solution for hydrogen based power generation are discussed and their benefits and drawback are analysed. The fifth and the last section of this chapter outlines the analysis of several advanced power cycles that led to the selection of the s-CO<sub>2</sub> power cycle proposed under this project. A preliminary investigation showed that an internally fired H<sub>2</sub>/O<sub>2</sub> fuelled s-CO<sub>2</sub> power cycle coupled with HES system was a very promising concept and had the potential to be the much needed transition technology that can enable the shift from present fossil fuel dominated energy market to a low-carbon more sustainable energy market of the future.

### 3.1 Hydrogen Production

Although statistically hydrogen is the most abundant element in the universe, its rarely available in its elemental form. To be able to use hydrogen in industrial processes and other applications, it first needs to be extracted from its compounds. Therefore, hydrogen, much like electricity, should be treated as an energy carrier and not as an energy source. The technological and economic factors that must be considered in the context of hydrogen production are outlined in this sub-section.

#### 3.1.1 Technological considerations

At present we have 3 main sources to extract hydrogen – fossil fuels, biomass, and water. The efficiency, cost and emissions associated with hydrogen production is dictated by the choice of production method. As mentioned earlier in this chapter, most of the hydrogen demand at present is being met by directly using fossil fuels. Interestingly, this was not the case in 1960s when the production by way of water electrolysis was the most favoured choice. However, given that the electricity generation in that period was completely based on fossil fuels, hydrogen production was therefore still dependent on fossil fuel albeit indirectly. Fig. 12 shows the different pathways/processes that can be employed to extract hydrogen from its compounds.

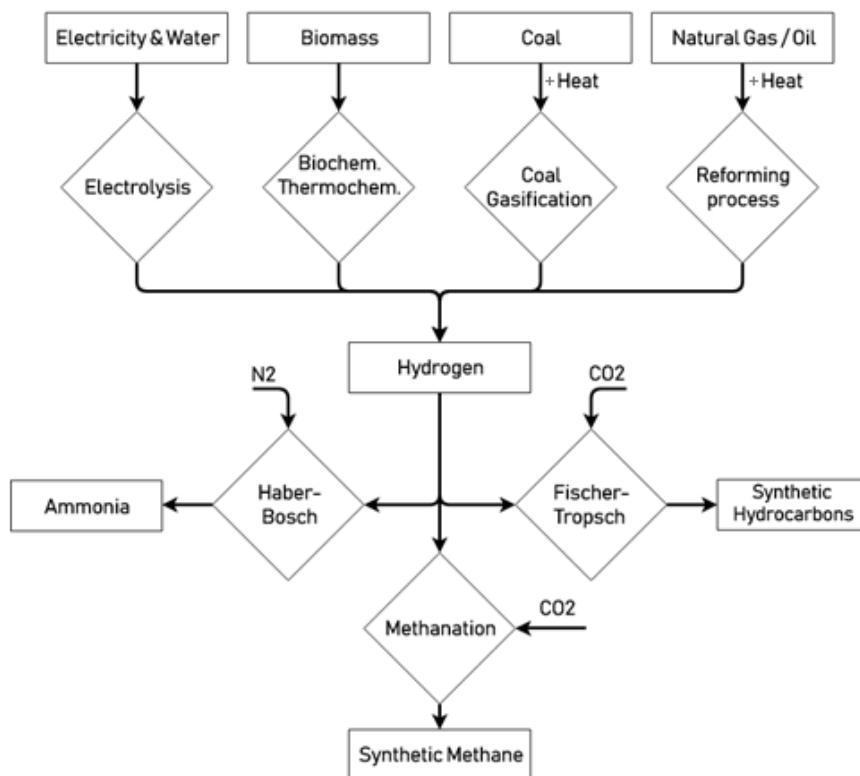


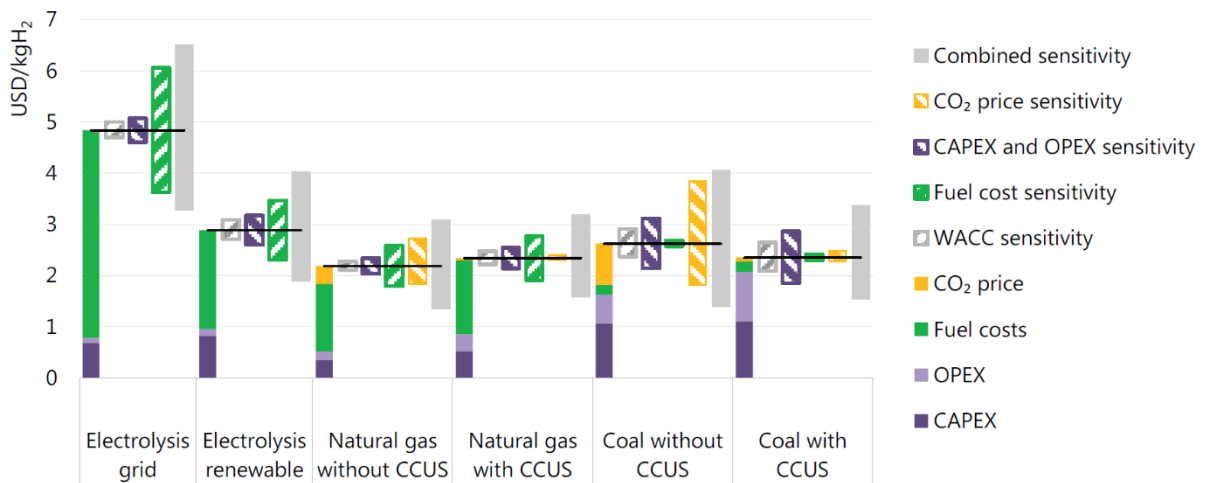
Fig. 12 Hydrogen production pathways and its conversion to other useful end products [26]

Each of these processes are discussed in greater detail in literature review report, with main emphasis on production of green hydrogen using water electrolysis. The three main electrolysis technologies at present are alkaline electrolysis, polymer electrolyte membrane or proton exchanging membrane (PEM) electrolysis and solid oxide electrolysis. Of these, the first two, alkaline electrolytic cell (AEC) and PEM electrolytic cell (PEMEC), are commercially mature technology. Based on a preliminary techno-economic comparison of these technologies, it was observed that parity between AEC and PEMEC technologies can be reached in the next couple of years. Most of the new addition of electrolyzer capacity

is based on PEMEC technology. Solid oxide electrolytic cell (SOEC) technology has promising prospects but is largely a lab scale/demonstration technology (TRL6 ~ TRL7 as found in EU Horizon 2020 annexes) and many important operational issues are yet to be addressed. The present-day efficiency of hydrogen production using renewable energy was found to be in the range 60% to 65% and the target for the next decade is to increase it up to 75% to 80% level.

### 3.1.2 Economic considerations

The current choice of fossil fuels over other sources for production of hydrogen is ruled by the favourable economics of reforming process in comparison to electrolysis and gasification. A quick look at the economics of hydrogen production shows that the cost of fuel is the single largest determinant of levelized cost of hydrogen (LCOH) for all production methods except for gasification where the CAPEX and OPEX were found to be the most important factor. Therefore, the future movement of the hydrogen production market is mainly dependent on the cost of electricity/natural gas. Fig. 13 below is taken from the IEA report on future of hydrogen technologies and it very concisely conveys the most pertinent information about the costs of hydrogen production.



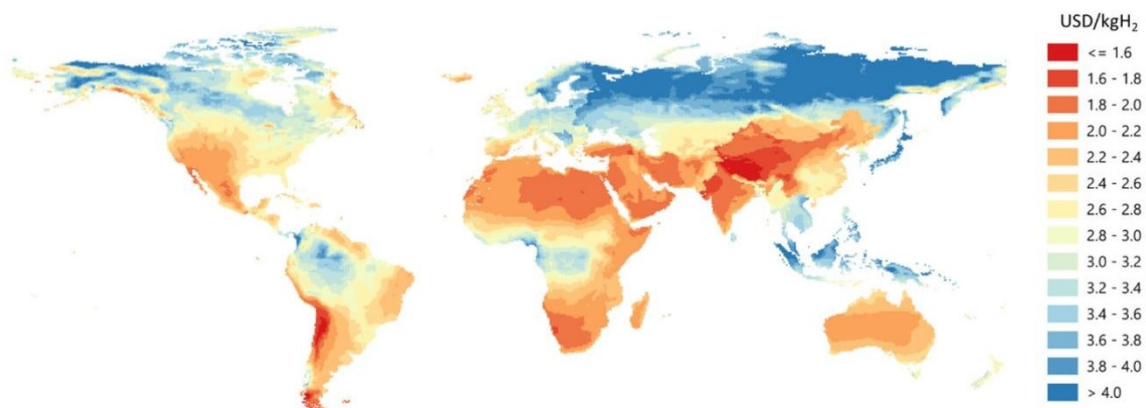
Notes: WACC = weighted average cost of capital. Assumptions refer to Europe in 2030. Renewable electricity price = USD 40/MWh at 4 000 full load hours at best locations; sensitivity analysis based on +/-30% variation in CAPEX, OPEX and fuel costs; +/-3% change in default WACC of 8% and a variation in default CO<sub>2</sub> price of USD 40/tCO<sub>2</sub> to USD 0/tCO<sub>2</sub> and USD 100/tCO<sub>2</sub>. More information on the underlying [assumptions](http://www.iea.org/hydrogen2019) is available at [www.iea.org/hydrogen2019](http://www.iea.org/hydrogen2019)  
 Source: IEA 2019. All rights reserved.

Fig. 13 Hydrogen production costs per technology – Expected scenario in 2030 [26]

As can be seen from Fig. 13, it is expected that fossil fuel-based production especially from natural gas will continue to have an edge economically and therefore dominate the hydrogen production market in the present decade. However, all hope is not lost for the business case of green hydrogen. If renewable energy assumed to be available at the lowest cost considered in the sensitivity analysis, i.e. 28 USD/MWh, the cost of electrolytic hydrogen then becomes competitive with that produced using natural gas reforming. This price assumption, although ambitious, is not outside the realm of possibility given the expected trends in the cost electricity from VRES. As per projections made by IRENA, by 2030, onshore wind is expected to reach LCOE levels in the range of 30-50 USD/MWh [27] while LCOE from solar PV plants is expected to range between 20-80 USD/MWh [28]. Installing dedicated electricity

generation from renewables as an alternative to the use of grid electricity for hydrogen production is another possibility that may become viable with falling cost of generation of renewable energy.

On the whole, it can be said that by 2030s, electrolytic production of hydrogen will achieve a partial cost parity with the reforming process in regions where the levelized cost of renewable energy reduces to a level between 20-30 USD/MWh. With declining costs for solar PV and wind generation, building electrolyzers at locations with excellent renewable resource conditions could become a low-cost supply option for hydrogen, even after taking into account the transmission and distribution costs of transporting hydrogen from these locations (often remote) with abundant low-cost renewable energy potential to the end users. IEA’s report on hydrogen [26] found that several promising regions exist where these projects maybe feasible, for example, in Patagonia, New Zealand, Northern Africa, the Middle East, Mongolia, most of Australia, and parts of China and the United States (see Fig. 14). The Asian Renewable Energy Hub project site in Western Australia aims to build 7.5 GW of wind generation and 3.5 GW of solar generation, with around 8 GW of the generation being dedicated to hydrogen production for domestic use and for export (Asian Renewable Energy Hub, 2019). Several other projects to produce hydrogen from dedicated renewable resources in various parts of the world are in preparation or have been announced. In areas where both resources are excellent, combining solar PV and onshore wind in a hybrid plant has the potential to lower costs further.



Notes: This map is without prejudice to the status of or sovereignty over any territory, to the delimitation of international frontiers and boundaries and to the name of any territory, city or area.

Electrolyser CAPEX = USD 450/kWe, efficiency (LHV) = 74%; solar PV CAPEX = between USD 400–1 000/kW and onshore wind CAPEX = between USD 900–2 500/kW depending on the region; discount rate = 8%.

Sources: IEA analysis based on wind data from Rife et al. (2014), NCAR Global Climate Four- dimensional Data Assimilation (CFDDA) Hourly 40 km Reanalysis and solar data from renewables.ninja (2019).

Fig. 14 Hydrogen costs from hybrid solar PV and onshore wind systems in the long term [26]

### 3.2 Hydrogen Storage

In this section we briefly discuss the various hydrogen storage options. The main factors considered while evaluation of storage technologies for mass storage applications are economic viability, environmental impacts, and sustainability. Although, hydrogen has a very a high energy density (LHV of 120 MJ/kg) when compared other fuels like methane (LHV of 50 MJ/kg) or fossil fuels (LHV of 40 MJ/kg), the main challenge in storing it arises due to its extremely low mass density at ambient

conditions. At NTP, tank with a volume of ~12 m<sup>3</sup> is required to store 1 kg of hydrogen which is just too large to be practically viable for most applications and rules out the option of storage at ambient conditions. The volumetric energy density of hydrogen needs to be increased to make its storage practical. This can be achieved by several ways like compressing it to high pressures before storage, cooling it to very low temperatures, using sorption processes or by converting it to other chemicals, which are easier to handle like methanol/ammonia. The main technology options for hydrogen storage are summarized in Fig. 15 [29].

Compressed gas storage is the most commonly used option at present due to ease of operation and vast experience of operating gas compression plants. Depending on the pressure at which the product gases are produced and stored, the parasitic load of compression plants can range up to 15-20% of total stored energy. Liquefaction is a very energy intensive process, needing about 35% of the total energy that is stored, thus is not attractive for large-scale deployment in energy storage applications at present. Although this option is interesting when hydrogen has to be transported over long distances (e.g. intercontinental export which would in principle be similar to LNG transport). The expected trend hydrogen storage in liquefied form is that the energy fraction required for liquefaction can reduce up to 20% of total stored energy in future, at which point it may become competitive with compressed gas storage option.

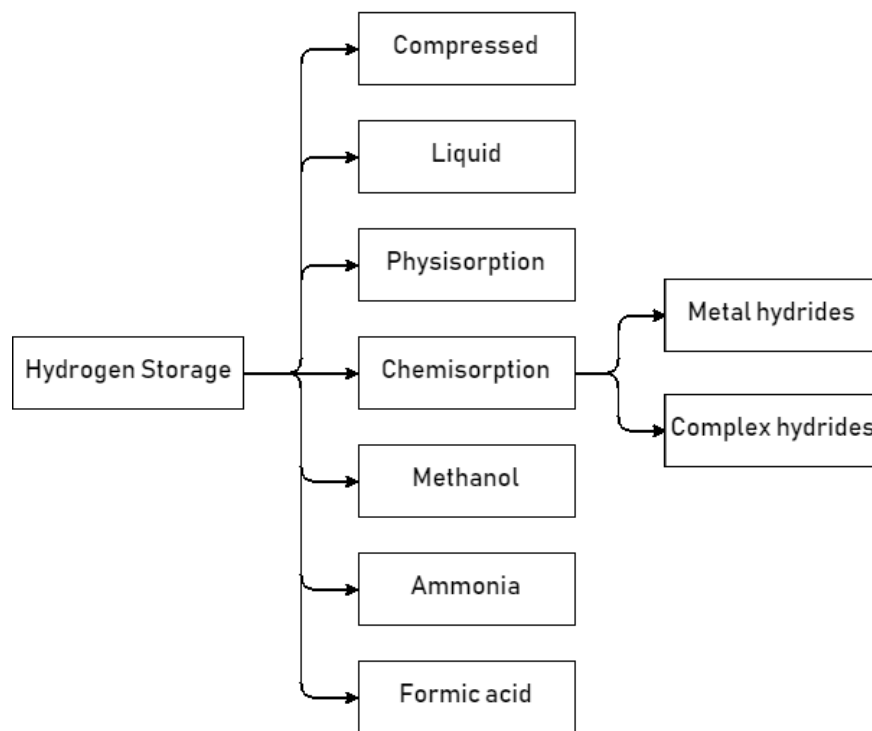


Fig. 15 Hydrogen storage options[29]

Other storage technologies like physisorption and chemisorption look promising at this point but are at nascent stage of development. In most cases, a breakthrough is required in the regeneration (hydrogenation) method to make them economically viable. Another choice for storage and handling of hydrogen is its conversion into organic and inorganic compounds –like methanol, ammonia and formic acid – that can either act as hydrogen carriers or hydrogen substitutes in some industrial

processes. There already exists demand for these chemicals for industrial processes and these are presently being bulk produced from natural gas. Therefore, this method is not only serving as a hydrogen storage technology but also as a means of promoting usage of VRES (thus decarbonising) hard-to-abate sector of industrial manufacturing. But since the focus is on seasonal energy storage, this aspect is not pursued further.

The purpose of this discussion on hydrogen storage is not to be comprehensive but only bring to light the various storage options that are available or are being studied. Most of these technologies are still riddled with several implementation/operational challenges. Amongst the various storage options mentioned, it makes most sense to consider compressed gas storage as the preferred option in all calculations/models because other options at present have a high energy requirement and /or high cost of implementation and are not technologically ready for wide-scale implementation. Cost is still a primary concern for hydrogen storage because the processes either need to use expensive catalysts for hydrogenation/dehydrogenation reactions or are highly energy intensive and therefore have a low hydrogen-to-hydrogen efficiency. Albeit, looking at the current research momentum and investment commitments that green hydrogen technologies are enjoying, it seems clear that at least some of these storage technologies will reach economically viable levels for wide-scale implementation in next 8-10 years.

### 3.3 Hydrogen Utilisation

Storing renewable energy in form of hydrogen not only makes large-scale seasonal storage of VRES possible, but also promotes introduction of renewable energy resources in several industrial sectors where conventionally they have been absent – such as sectors with low electrification levels. The Fig. 16 below shows various pathways of integrating VRES to different end uses via hydrogen [30].

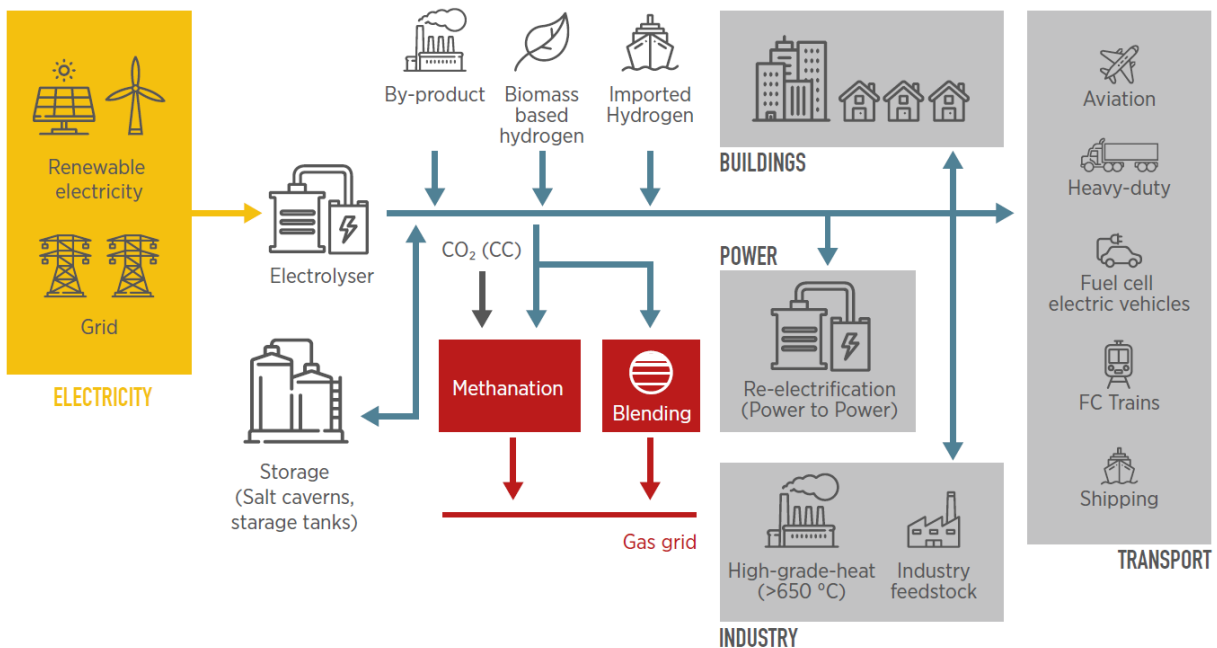


Fig. 16 VRES integration pathways by means of hydrogen [30]

Although, the potential to decarbonize hard-to-abate sectors like international transport, manufacturing processes etc. is one of the main advantages of hydrogen-based energy transition systems over all other solutions, this aspect is beyond the scope of this report. The core focus of this report is to discuss P2G2P application of the hydrogen energy storage technology. In the medium to long term, hydrogen could become a primary energy carrier to transport and distribute VRES over long distances, especially in those cases where the electricity grid has insufficient capacity or when it is too impractical or expensive to build. For example, in the case of offshore wind projects, hydrogen could be produced offshore and then be distributed (via existing natural gas pipelines) reducing the investment required for such projects. This hydrogen can be converted back to power or directly used in industry depending on the regional demand. However, the catch here is that there are substantial energy losses during hydrogen production and storage. Based on the data reviewed during literature review, the median value LHV efficiency of hydrogen production can be assumed to be ~ 60-65% and a further ~ 15-20% energy is used in compression or other hydrogen storage processes. Therefore, usable fraction of VRES when converted to hydrogen is ~50-55% at present. Continued R&D efforts on various technological fronts are trying to increase this fraction and 65%-70% by 2030 seems to be an achievable target based on the current trends.

In cases where green hydrogen is used as feedstock for manufacturing sector, these conversion ratios are not very prohibitive as far as its levelized cost is competitive with blue hydrogen<sup>3</sup>. However, when it comes to converting green hydrogen back to power, the conversion efficiencies of the processes involved become more prohibitive. Therefore, to make power production from green hydrogen a viable option in future, the process/cycle used for hydrogen-to-power conversion will have to be highly efficient. In addition to a high cycle efficiency requirement, the power cycle will have to be suitable for few more operational requirements. Unlike the present centralized generation model, the future energy markets are expected to be much more distributed due to a high VRES share. VRE plants along with nuclear power plants are expected to replace coal power plants as baseload plants and all other assets including storage systems and gas-fired plants will have the primary function of maintaining adequate flexibility in the system. Therefore, in contrast with conventional power cycles, a power cycle for future markets will need to be efficient even at small to medium scale installations and have excellent performance characteristics at part load operations. This is where fuel-cell based power plants become relevant as explained in the next sub-section.

### 3.4 Existing H<sub>2</sub> based power generation technologies

Since the oil crises in the 1970s, hydrogen has recurrently been touted as the viable alternative to fossil-fuel based energy model. However, the interest in hydrogen waxed and waned several times over this period owing to disruptive growth in other contemporary technologies like wind, solar and most recently batteries. Although leading energy experts [31] still view hydrogen as a low impact, highly uncertain energy issue of 2019 on a global level, they see strong trends many countries including Germany, Japan, Iceland and New Zealand which are seen as the early movers in this field. A strong policy-driven push in these countries has led to the development of niche markets that are driving the global research effort in hydrogen technologies. This has given rise to a movement in the technology market that was previously unseen.

As mentioned earlier in this report, green hydrogen-based power generation systems are typically envisaged along with conventional gas-turbine based generation or with fuel-cell based power generation solutions. All the leading turbine manufacturers are targeting to achieving 100% hydrogen

---

<sup>3</sup> The term blue hydrogen is used to refer to conventional hydrogen production methods but with CCS technology.

firing capability by 2030 while fuel-cell based power systems, especially the based on PAFC, SOFC and MCFC, are witnessing an unforeseen surge in demand. Most modern gas turbines can use fuels blended with hydrogen, although the maximum allowable hydrogen fraction in the mixture varies over a wide range (30-80%) from one system to another. If hydrogen indeed becomes the primary energy carrier of choice over the next decade, there is an enormous market opportunity for replacing/retrofitting existing gas-turbine fleet with new combustion technology capable of using pure hydrogen. This is the main motivation that driving current research into hydrogen turbines. This scenario is being viewed as the sustainable version of 'business as usual' that will perhaps cause the least possible disruption to existing energy markets and power infrastructure. Other factors that favour gas-turbine based power generation systems in future over fuel-cell based systems include high flexibility, reliability and the overall compactness they offer. The stark contrast between these two solutions can be contextualized by comparing a mobile power unit based on open cycle gas turbine supplied by Siemens (SGT – A45 TR [32]) and a Molten Carbonate fuel-cell based unit sold by FuelCell Energy (Sure Source 1500 [33]). Both these are highly modular power units running on natural gas and require approximately the same area for installation (~2200 sq. ft.). However, the gas-turbine based unit is rated to nominally produce about 44 MW of electrical power while the MCFC based system is rated generate 1.5 MW electrical power. This comparison accentuates the difference in energy density and overall compactness of the two systems.

Albeit, fuel-cells do have a clear advantage over gas-turbines when it comes to net cycle efficiency. The combustion process (responsible for largest exergy destruction) is completely avoided in a fuel-cell. This gives a substantial boost to its overall performance making it possible to achieve efficiencies (LHV % efficiency ranging from 50 – low 60s) that are comparable to best large-scale conventional power generation units, at power generation scale ranging from a few kW to a few hundred kW. This advantage makes fuel-cell based systems an ideal choice in distributed power generation models. Although these efficiencies are often achieved with existing gas-turbines solutions (operating in combined cycle mode) at an energy production level of several MW, it is extremely difficult to replicate them at distributed generation levels since the benefits of economies of scale are lost.

Fuel-cell technology has been quite successfully adopted in niche applications such as uninterruptable power supplies for data centres, small scale domestic CHP application and transportation sector, especially in countries like Japan, US and South Korea. However, it is yet to make substantial inroads in large-scale commercial power generation applications. The most prominent fuel-cell technologies that are presently being deployed include Proton Exchange Membrane Fuel Cell (PEMFC), Phosphoric Acid Fuel Cells (PAFC), Molten Carbonate Fuel Cells (MCFC) and Solid Oxide Fuel Cells (SOFC). These technologies are briefly discussed below and their respective applications, advantages, drawbacks and future research outlooks are outlined based on recent technology review reports published by the European Commission's Joint Research Centre (JRC) [34] & US government's Department of Energy [35].

- **PEMFC:** Currently, these are mostly used in transportation and small scale residential applications. Several large-scale stationary application demonstration projects are being set-up around the world but PEMFCs are yet to see the breakthrough observed in other fuel-cell technologies included in the list. The main advantages of PEMFCs included faster start-up/shut-down times and superior load following capabilities. On the other hand, the key issues that need further R&D include very low tolerance for impurities in fuel resulting in a high cost of operation, low stack life, lower efficiencies compared to MCFC/SOFC technologies. In addition to addressing these issues, the current research effort is focused on developing PEMFCs with higher operating temperatures which are expected to

yield better performance, higher tolerance to impurities in fuel stream and an overall reduction in cost. 1 MWe PEMFC unit sold by Hydrogenics Corporation is an interesting example of large-scale power generation application.

- **PAFC:** These systems are proven to be the most resilient fuel cell technology with stack life exceeding 80,000 hours of operation at 400kW level. There are several MW scale installations of PAFCs units and most of these installations are supplied by Doosan Corporation. The main advantage these systems offer is improved tolerance to fuel impurities that greatly reduce the cost operation. Also, they operate at 400 – 500 K level, and therefore, are useful for CHP applications. The main drawbacks of PAFC include low efficiency (~40%), Long start-up/shut-down times, limited load following capabilities, use of expensive catalyst.
- **MCFC:** This technology has the highest share amongst all fuel-cell systems in large-scale power generation application (rated over 200kW) [30] and is generally operated on biogas taking advantage of its high fuel flexibility. It is generally operated at a temperature ranging from 850 – 1000K and therefore offers high electrical efficiencies (often over 50%). However, the drawbacks caused by high temperature operation include high cost of BoP, reliability issues related to the mechanical performance of the cell, long start-up/shut-down times and poor load following characteristics (they are most suited baseload operation). Similar to trend seen with PAFC, most of the large-scale MCFC installation around the world are supplied by one company, FuelCell Energy, and are located in South Korea which the major market for these systems.
- **SOFC:** Large-scale SOFC installations are almost exclusively found in the US and its demand mainly is driven by large tech companies using it as uninterruptable power supply at their data centres. Like MCFCs, these are also operated at a high temperature typically ranging from about 800 – 1200 K and offer exceptional electrical conversion efficiencies of over 60%. The main challenges faced with this technology include high cost of BoP, reliability issues, long start-up/shut-down times, limited thermal cycling capability of the cell (which necessitates to keep it on hot standby), high rate of performance degradation, high-temperature corrosion, limited stack life (< 20000 hours). Although currently, many companies are actively investing in research and development of large-scale SOFC systems, like all other fuel-cell technologies discussed, the supply chain of large-scale SOFC system is dominated by single company i.e. Bloom Energy.

Based on this brief discussion it can be summarized that the main issues impeding successfully deployment of the fuel-cell technology in power generation application include;

1. High O&M costs due to the following technical issues
  - High temperature corrosion and breakdown of cell components (MCFC/SOFC)
  - Need of expensive catalysts (PEMFC/PAFC)
  - Need for contaminant removal from fuel streams (all fuel-cell technologies)
2. Limited stack lifetime (PEMFC/ SOFC)
3. Long start-up/shut-down times and poor load following capabilities (MCFC/ SOFC)
4. Challenges in scaling-up to 10-50 MW levels due to low power density (all fuel-cell technologies in general but SOFC/PEMFC in particular)
5. Challenges related to performance stability and unreliable operational characteristic at high operating temperatures (MCFC/ SOFC)

The preceding discussion shows that both the technologies (gas-turbines and fuel-cells) typically proposed to generate electricity from green-hydrogen have their relative pros and cons. Existing research efforts may marginally reduce the gap between these systems however, it can be said with a high level of certainty that a large gap in operational characteristics of these two technologies will persist. In absence of new generation techniques, engineers designing hydrogen-based power generation systems, especially at distributed generation levels, will have to choose between exceptional efficiencies offered by fuel-cell technology and the superior operational characteristics offered by gas-turbine based power systems. This dichotomy is one of the several issues slowing down the wide-scale adoption of the HES based P2G2P systems. A viable gas-turbine based thermal power cycle that can operate at efficiencies comparable to that of fuel-cells while maintaining the operational characteristics of a conventional gas-turbine engine can help address this issue and improve the odds of HES based P2G2P systems getting deployed in future. Several advanced power cycles found during the literature review phase can satisfy this requirement. Such a power cycle will bridge the gap between exiting hydrogen-based power generation technologies. A more detailed analysis of these power cycles is discussed in more details in the next sub-section of this chapter.

### 3.5 Advanced power cycles with ZEP

The theoretical performance of thermal power cycles is influenced by several parameters, one of the crucial factors being turbine inlet temperature. The reason for this is that heat addition accounts for the largest loss of exergy in the entire cycle and can be reduced by increasing the temperature of flue gases at end of heat addition process. Indirectly fired power cycles are typically limited in the maximum allowable TIT due to the prohibitive cost of high-temperature piping material. Much higher TIT values can be achieved in directly fired gas turbine units since length of hot section is generally not large. Nonetheless, by employing superheating and supercritical operating conditions, steam power plants running on modified Rankine cycle manage to achieve LHV conversion efficiencies up to 46-49% at present, whereas combined cycle power plants can achieve up to 63% conversion efficiency on LHV basis in power generation mode while its efficiency can reach up to 80% in cogeneration mode.

The main shortcoming of these cycle is that it performs exceptionally well at large-scale but not so well at small to medium scale installations. Component efficiencies are adversely affected at lower power levels reducing the overall conversion efficiency and making its application economically less attractive. The main assumption while analysing advanced power cycles for hydrogen-power conversion was that the hydrogen production facility is in close vicinity of the power plant and hence, both product gases of electrolysis ( $H_2$  and  $O_2$ ) are available for use during combustion. However, since little literature was available on performance of  $H_2$  fuelled oxy-combustion power cycle, the data used in this preliminary stage is based on values found for natural gas fuelled oxy-combustion cycles. The following is the list of desirable characteristics in a future green hydrogen-fuelled advanced thermal power cycle.

1. High cycle LHV efficiency (ideally more than 50%).
2. Sustained performance at distributed generation levels typically less than 50 MW<sub>el</sub> and during part load operation.
3. Flexibility of generation and fast ramp up time to accommodate fluctuation in local grids caused by increasing number of energy prosumers and demand supply gap.
4. Cycle complexities should be minimum, and it should be suitable for application over a wide range of output power level.
5. Potential for Net-zero emission of GHGs for long-term sustainability.
6. Favourable cost economic characteristics for its wide-scale implementation.

Climate change concerns have triggered many studies in the recent years to investigate power cycles that are suitable for use with CCUS technology. These plants are usually conceptualized based on oxy-combustion of natural gas and post-combustion carbon capture [36, 37, 38]. These studies also had high thermodynamic efficiency as a criterion since implementing CCUS systems imposes a penalty on overall system performance. The inherent cycle efficiency must then be higher (in comparison to conventional power systems without CCS) so that the performance penalty associated with CCUS systems are mitigated to some extent. Many of the cycles were identified in these studies which can be also be suitable for to our case of hydrogen-fuelled oxy-combustion cycle. The main cycles shortlisted and briefly explained below. In this list, a cycle based on combination of solid oxide fuel-cells (SOFC) and gas turbine is also included for comparison.

1. **s-CO<sub>2</sub> Brayton cycle:** These are typically closed/semi-closed Brayton cycle operating with super-critical CO<sub>2</sub> as the working fluid. Allam cycle is a semi-closed variation of this cycle based on oxy-fuelled combustion of NG. Since oxy combustion is used, the main product of combustion is CO<sub>2</sub> and water which at the end of the cycle can be separated from the flue gas stream. The maximum operating pressure usually ranges from 20 – 40 MPa while the max temperature at turbine inlet is typically limited to ~1250 °C. The reported LHV efficiency of this cycle is more than 55%.
2. **Modified S-Graz cycle:** Amongst the several variation of Graz cycle that have been proposed over the years, the Modified S-Graz cycle is the most promising variant from efficiency perspective and therefore has been considered in this study. This cycle uses H<sub>2</sub>O as the primary working fluid and typically includes a set of 2 gas turbines and 1 steam turbine. Similar to s-CO<sub>2</sub> cycle, this is also a semi-closed cycle proposed with oxy-fuelled combustion of NG. The cycle operates with maximum cycle pressure in the range of 40 bars with the peak temperature in the cycle reaching ~1400 °C. The reported LHV efficiency of the cycle was close to ~50%.
3. **CES cycle:** CES cycle is a zero-emission power cycle concept that is similar to S-Graz cycle in the way that it recirculates H<sub>2</sub>O stream as the working fluid but is based on a simpler architecture. It can be thought of to be similar to a direct fired Rankine cycle where the fuel (NG) is fired using oxygen with steam as the bath gas. The peak pressure and temperature of this cycle were found to of the order of 30 MPa and 1150 °C. The reported LHV efficiency of the cycle was close to but less than ~50%.
4. **Helium Brayton cycle:** This is variation of closed loop Brayton cycle originally proposed to be used with high temperature nuclear reactors. Many variations are proposed for this cycle but the inter-stage heating and cooling (IHC) –an intercooled-recuperated variant of the cycle– appears to be most efficient cycle. It was proposed with medium operating conditions with peak pressure in the range of ~8MPa and the maximum temperature of the order of 880 °C. Reported LHV efficiencies are of the order of ~52%. It enjoyed the tag of having superior performance amongst Brayton cycle variations until s-CO<sub>2</sub> Brayton cycles operating at much higher pressure gained prominence in recent years. For the same turbine inlet temperature, s-CO<sub>2</sub> cycle outperforms Helium Brayton cycle mainly because of its reduced compression work requirement.
5. **SOFC/GT hybrid cycle:** As discussed in the previous subsection, fuel-cell based power generation solutions are widely being studied for converting green hydrogen to power in by systems that are operationally reversible. An extension of this concept is the SOFC-GT hybrid cycle. Since SOFC usually operate at medium-high temperatures (650-1000 °C) and pressures (up to 15 bar), the

products i.e. steam when operating with hydrogen as fuel are formed at high temperature and can be expanded in a turbine. The benefit of using gas turbine here is that the unused/additional fuel can be fired in the combustion chamber of the turbine to modulate the TIT as desired level. This concept in theory is very efficient and can have LHV efficiency in excess of 65% when operating in power generation mode and much higher in co-generation mode. It is because of this reason it is included in this comparison even though it is not entirely a thermal power cycle we are looking for. This cycle is expected to be main competitor of other power generation methods in future when SOFC have reached operational maturity. Another promising configuration that was identified during this analysis was the hybrid concept of Molten Carbonate Fuel-cell (MCFC) with s-CO<sub>2</sub> Brayton cycle [39 & 40]. However, the capacity considered in these studies was less than 1 MWe suggesting this cycle is still only being studied at lab-scales. Therefore, although we do not consider this cycle in the present analysis, it is a very promising concept for future power generation projects.

Following a brief discussion of the shortlisted power cycles, they were compared based on the operational/performance parameters, operational benefits and drawbacks of each cycle. Given that all the power cycles discussed in this section are at an early stage in their development lifecycle and are yet to prove their performance and reliability in commercial operation, each of them has some degree of associated development risk. To take this into account, each cycle was assigned a novel equipment development index. This system of indexing was adopted from IEAGHG's assessment report oxy-turbine cycle [36]. In this method of assessment, all major components of the cycle are assigned risk level based on the deviation between the desired operating condition and that of the state-of-the-art equipment currently operating/commercially available. This system included four levels of development risks where Index 1 represent the least risk and index 4 stands for the highest risk. The evaluation matrix comparing all the shortlisted cycles is shown in Table 2.

Based on the data shown in Table 2, it was concluded that SOFC-GT hybrid cycle and s-CO<sub>2</sub> Brayton cycle are the two most promising cycle for future power generation applications. This conclusion is also supported by the technology development trends emerging from the energy markets (research effort directed towards commercial deployment was seen only for these two concepts). Therefore, s-CO<sub>2</sub> Brayton cycle appears to be the only thermal cycle that can compete with fuel-cells cycles in hydrogen-based power generation application. Even though s-CO<sub>2</sub> Brayton cycle is yet to be proven a viable solution in commercial power generation application, several demonstration and pilot projects based on s-CO<sub>2</sub> cycle have successfully been implemented. The most promising of these projects is the Allam cycle based 50 MWth (~25 MWe) natural gas fired power plant in Texas, USA setup by NET Power LLC. They plan to start operation of a second, commercial scale 300 MWe plant by 2021. Thus, power plants based on s-CO<sub>2</sub> Brayton cycle can be expected to begin commercial operations over next 5-10 years. In view of these points, it decided to assess the feasibility of an internally fired H<sub>2</sub>/O<sub>2</sub> fuelled s-CO<sub>2</sub> power cycle as an alternative to fuel-cell based solutions for hydrogen based power generation applications.

Table 2 Evaluation matrix for the advance power cycles

Cycles	Novel Equipment Development Index*	Cumulative Development Index Penalty <sup>#</sup>	Potential LHV efficiency %	Cycle efficiency score	Final Score
s-CO <sub>2</sub> cycle	Turbine: 2 Combustor: 2 Recuperator: 2	3	56–63%	9	6
Modified S-Graz Cycle	HT Turbine: 2 Compressor: 2	2	49–53%	7	5
Supercritical CES Cycle	Turbine: 3 Combustor: 2	3	49–53%	7	4
Helium Brayton cycle	Turbine: 2 Combustor: 2 Recuperator: 2	3	51–55%	8	5
SOFC/GT hybrid cycle	SOFC: 3 BOP: 2	3	62–71%	10	7

<sup>#</sup>Cumulative Development Index Penalty is calculated by adding the right penalty (see the Table below) for each component in accordance with its development index.

\*Legend for Novel Equipment Development Index & associated development index penalty (adopted from [36])

Novel Equipment Development Index	Description of Development stage	Development Index Penalty
1	Commercial component or technology very close to the state-of-the-art can be used. Modifications to existing components or new design activities are moderate and relatively low-cost	0
2	The component requires dedicated design, but component development seems feasible in short-midterm with current knowledge. Limited modifications to the process parameters are possible, considering techno-economic limitations on component design	1
3	The component requires dedicated design and operates at conditions far from current commercial components. Significant modifications to the process parameters might be needed because of possible techno-economic limitations on component design	2
4	The component requires a technology breakthrough and the successful techno-economic development is quite uncertain at this point	3



# Chapter 4

## s-CO<sub>2</sub> Power Cycle

### Overview

This chapter documents the review of the s-CO<sub>2</sub> power cycle and the development of the thermodynamic evaluation model for this project. The historical development of this cycle is outlined in the first section of the chapter. A short discussion on the consequences of choosing supercritical CO<sub>2</sub> as the working fluid is also included in this section. Given its long history of conceptual development, several variations of this cycle were found in the literature reviewed. The process of categorising, reviewing, and shortlisting the most relevant configurations/thermodynamic features of this cycle for this project is discussed in the second section of the chapter. A thermodynamic evaluation model was required to study the shortlisted configurations and to identify the most suitable configuration for the application proposed in this project. The process of developing this model is discussed in the third section while its validation is covered in the fourth section of the chapter.

### 4.1 Introduction to s-CO<sub>2</sub> power cycles

The s-CO<sub>2</sub> Brayton cycles have a very long history with the oldest reference dating back to 1948 when Sulzer Bros patented a partial condensation CO<sub>2</sub> Brayton cycle. The seminal work on the concept was carried out in the 1960s by Angelino [41, 42] and Feher [43, 44]. However, given the limited advancement in material technology at the time, no practical applications of this concept could be implemented and slowly the research interest in the topic decayed. This concept saw a resurgence in the late 1990s and early 2000s when the concept of clean energy generation started gaining traction on a global stage. COOPERATE-DEMO cycle [45] and MATIAINT cycle [46] proposed in the 1990s were both based on a similar concept. It relied on a multistage expansion process where, the first expansion

was performed at pressures and temperatures prevailing in contemporary steam turbines, while the second expansion at a lower pressure was done at a much higher temperature typical of the contemporary gas turbines. However, both these cycles have been abandoned at the theoretical development stage mainly because of their complex layouts.

Around this same period, several studies were also investigating the use of s-CO<sub>2</sub> power cycle for applications featuring indirect/external heat addition process. The work of Dostal [47] (2004) triggered a spike in research focused on the application of the s-CO<sub>2</sub> cycle for new-generation nuclear power plants, waste heat recovery applications and use in solar thermal power plants. The main reason of this research interest, to use s-CO<sub>2</sub> cycle for an indirectly/externally heated power generation application, was found to be the exceptionally high cycle efficiencies that could be achieved at moderate temperatures prevalent in these applications. This trend is also seen in the case of internally fired power cycles and will be discussed in detail at a later point in this chapter. One of the more recent developments of s-CO<sub>2</sub> Brayton cycle is called the Allam cycle [48]. It is a semi-closed, internally fired, oxy-combustion based natural gas fuelled s-CO<sub>2</sub> power cycle with post-combustion capture of CO<sub>2</sub>. It is one of the most promising ZEP power cycles expected to enter commercial operation over the next few years. It is also the most developed variation of the directly/internally fired s-CO<sub>2</sub> power cycle and thus, will be the basis of the proposed cycle for hydrogen-based power generation application.

After briefly outlining the historical development of the s-CO<sub>2</sub> power cycle, it is also worthwhile to consider the choice of s-CO<sub>2</sub> as a working fluid. It is fascinating to note the irony in the fact that carbon dioxide, the gas which is the very cause of global climate change problems, maybe an integral part of the solutions that can address these problems. CO<sub>2</sub> as a GHG emission from present-day power plants is terrible, but it makes an excellent choice of working fluid for future power cycles. This is mainly because it has many favourable chemical and physical properties, most importantly a critical temperature that is very close to ambient temperature. Also, it is cheap because it is abundant, chemically stable, non-poisonous and operationally safe when used as a working fluid in Brayton power cycle.

The benefits of using supercritical working fluids in thermal power cycles are known for several decades. The first supercritical Rankine cycle power plant entered commercial operation in the late 1950s and with advancements in material technology since then, it has now become a norm in the power sector. Beyond the critical point, there is no distinction between liquid and vapor phases of fluid and this behaviour can be exploited to optimise the heat addition process in supercritical Rankine cycle. On the other hand, a supercritical Brayton cycle can take advantage of the high fluid densities and optimize the compression work requirement of the cycle which can substantially boost its net cycle efficiency. Conventional Brayton cycles operating with air as the working fluid, however, can derive no such advantage because they are typically operated in regions characterized by a low density of air. Any thermal power cycle is essentially a heat engine converting thermal energy to mechanical work operating between a high-temperature source and a low-temperature sink. To operate conventional Brayton cycle in supercritical regime, it would require a sink at cryogenic temperature to cool the air at inlet of compressor to a sufficiently low temperatures to reach high fluid densities. The need for a cryogenic sink makes the supercritical operation of conventional Brayton cycle infeasible for most applications. This is where the choice of CO<sub>2</sub> as a working fluid for Brayton cycle makes all the difference.

CO<sub>2</sub>, with its critical temperature (~31°C) close to global ambient temperature, enables transcritical/supercritical operation of the Brayton power cycle, while using the “surroundings” as the low-temperature sink. In other words, to operate a supercritical power cycle using CO<sub>2</sub> as working fluid, no additional/special arrangements, such as a cryogenic sink, are required. This makes CO<sub>2</sub> an excellent

choice as the working fluid for advanced power cycles. The density of CO<sub>2</sub> at its critical point is 467.2 kg/m<sup>3</sup> which is several times higher than that of air at the same pressure and temperature which considerably reduces the compressor work requirement. In addition to this, a higher density of working fluid also reduces the overall size of power cycle components, making the plant compact in comparison to existing power plant installations. This will be an engineering challenge in itself, but the expected positive impacts are likely to outweigh the initial development challenges.

After mentioning the positive aspects of supercritical CO<sub>2</sub> as the working fluid, it is important to note that drastic variation of physical properties seen in supercritical working fluids is not always beneficial and may even lead to some design complications. Therefore, it is necessary to closely analyse variations in all important properties and their impact on the design and performance of the power cycle components. Since the component level design is not included in the scope at present, only a preliminary discussion on the expected impacts of physical property variation is included here, to highlight the type of challenges that may arise while designing the power cycle components. Following a brief reflection of various component design/working principles, the property variations that are considered most important include, variation in specific heat capacity, density, speed of sound, viscosity, thermal conductivity, solubility, and diffusivity.

Variation in specific heat capacity is expected to reduce the compressor work requirement but is likely to make the design of low temperature recuperator more challenging. The recycle stream at lower temperature has a much larger specific heat capacity in comparison to the low-pressure exhaust gas stream. This may cause the pinch point to shift inside the heat exchanger making its design trickier than usual. Although a carefully designed heat exchanger can avoid the heat integration problems caused by the pinch temperature, this variation in specific heat inherently limits/affects the recuperation problem and may even require special heat exchanger arrangements to avoid large heat recuperation losses. This aspect will be discussed in more detail while evaluating the performance of the heat exchanger during the thermodynamic analysis. High flow density and its variation at various points in the cycle is expected to make design of components more challenging by reducing the overall size of the components (since it is generally difficult to design compact components without making a large compromise its performance). Variation in the speed of sound (a function of specific heat) and viscosity will have an impact on the design of turbomachines, especially the compressor, while the variation in thermal conductivity is expected to impact the recuperator design.

The last two properties listed above namely, solubility and diffusivity are expected to affect the overall operational characteristics of the cycle. Solubility will impact the tendency of working fluid contamination, while diffusivity of CO<sub>2</sub> into metal surfaces at high pressure may cause rapid corrosion and structural damage that may reduce the operational life of the power cycle components. However, at present, not enough is known about these effects since experimental data is not available. Hence, these aspects are being actively researched to understand the effects of using supercritical CO<sub>2</sub> as the working fluid on the operation and the lifecycle of the power cycle components.

The key takeaway from this discussion is that variation of fluid properties can substantially affect the s-CO<sub>2</sub> power cycle operation and therefore, will have to be carefully analysed during the design process. From all the properties mentioned earlier, variation in specific heat and density are expected to have the largest impact on cycle thermodynamics and therefore, they will be duly considered during thermodynamic analysis. Other property variations, although important from an individual component design perspective, do not explicitly affect the thermodynamics and therefore, are not specifically analysed in this investigation.

## 4.2 Variations of the s-CO<sub>2</sub> cycle

Over a prolonged period spanning a few decades since the inception of the s-CO<sub>2</sub> power cycle, several authors have proposed configurations/variation of this cycle suitable for different applications like waste heat recovery, nuclear power plants, CSP plants, and oxy-combustion power cycles. Crespi et. al. [49] have systematically categorized a collection of 80 configurations of the s-CO<sub>2</sub> cycle (42 stand-alone cycles and 38 combined cycles) along with references to their original works and the reported performance parameters. This extensive review was used as a coarse filter to identify the most relevant configurations that may be of interest for the current project. The assumptions made by Crespi et. al. in [49] are applicable in this project as well and are only stated here. Detailed explanation about these assumptions can be found in the indicated review paper.

1. Fundamental division between simple and combined cycles.
2. No discrimination between purely supercritical and transcritical cycles
3. No discrimination between cycles with or without condensation
4. No discrimination based on the type of heat source
5. Cycles are labelled with a code based on thermodynamic features, excluding condensation (see Table 3)

Table 3 Various thermodynamic features with the associated labels & role in the s-CO<sub>2</sub> cycle

Thermodynamic feature	Label	Thermodynamic role
Regeneration	R	Recovery of heat from turbine exhaust
Intercooled compression	IC	Reduction of compressor work requirement
Reheated expansion	RH	Improvement of specific work output Alleviation of temperature induced design challenges
Split-flow before compression	SFC	Improvement in heat integration
Split-flow before expansion	SFE	Improvement of specific work output
Split-flow before heating	SFH	Improvement in heat integration
Split-flow before heating & expansion	SFHE	Improvement in heat integration

The data reported in this study includes 8 internally fired configurations, while the rest of the stand-alone cycles are for applications featuring external heating. Overall, it is observed that the average thermal efficiency of all the proposed standalone s-CO<sub>2</sub> cycles was ~41%, which would be considered low for the present application but when this efficiency is put in perspective of low/moderate temperature applications such as WHR and CSTP it serves as evidence of the superior performance that s-CO<sub>2</sub> Brayton cycles offer. That said, most oxy-combustion power cycles with high TIT are reported to have much higher efficiencies, ranging between 50-65% and these are the configurations that are of interest in this project. Table 4 enlists these standalone s-CO<sub>2</sub> cycle configurations along with reported performance parameters, while Fig. 17 shows their schematic representation. The first two configurations with efficiency greater than 60% are proposed with cryogenic fuels like LNG/LH<sub>2</sub>. The cold energy of these fuels is proposed to be used as the low temperature sink. This option, although, is not commercially viable as of yet, but may become competitive in future if the liquefaction process is optimized and liquified storage of hydrogen becomes commercially viable.

Table 4 Highly efficient s-CO<sub>2</sub> cycle configurations – Performance Parameters [49]

No.	Cycle name	Category label	P <sub>min</sub> [MPa]	P <sub>max</sub> [MPa]	T <sub>min</sub> [°C]	T <sub>max</sub> [°C]	η <sub>th</sub> [%]	Application
1	Quasi-combined	R3 – IC – RH – SFC – SFHE	0.1	15.6	–70	1300	65.6	Oxy-combustion
2	Recuperated CPOC	R2 – IC	0.1	17.5	–62	1200	63	Oxy-combustion
3	Allam + RH	R1 – IC – RH	0.1	30	20	1150	60	Oxy-combustion
4	Allam	R1 – IC	3	30	20	1150	59	Oxy-combustion
5	Double reheated recompression	R2 – RH – SFC	7.5	30	32	620	52.4	Fossil fuel (Coal)
6	DEMO	R1 – IC – RH	0.4	24	20	1250	52	Oxy-combustion

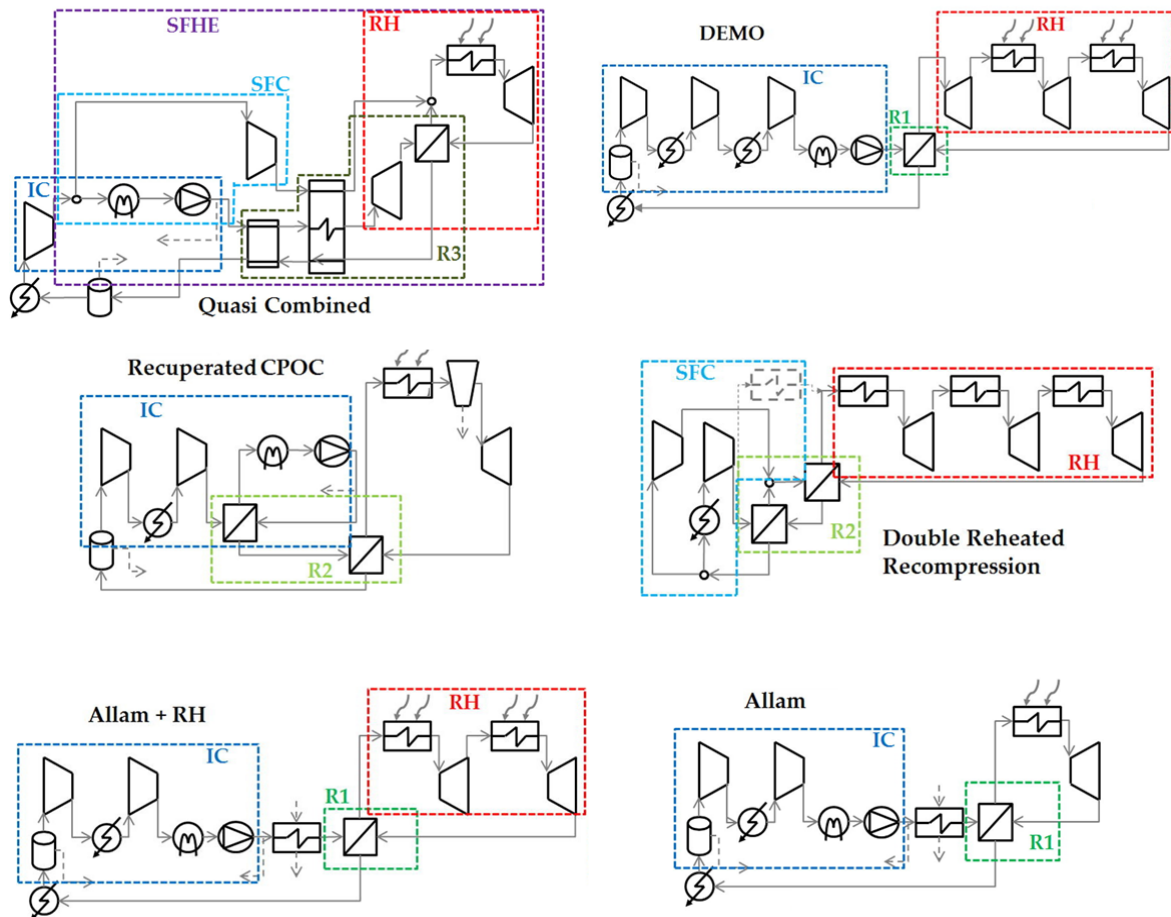


Fig. 17 Highly efficient s-CO<sub>2</sub> cycle configurations – Schematic Layouts [49]

The key takeaway is that different thermodynamic features will have to be included in the model and evaluated during the thermodynamic analysis of the s-CO<sub>2</sub> cycle for the proposed application. As can be seen from Table 4, the main features included in previously proposed high-efficiency s-CO<sub>2</sub> cycle configurations are recuperator(s), intercooled compressors, split flow compressors, and reheated

expansion process. These features will be included in the thermodynamic tool and analysed while proposing the final configuration for the internally fired H<sub>2</sub>/O<sub>2</sub> fuelled s-CO<sub>2</sub> power cycle.

For the sake of completeness of the discussion, it is worth mentioning that several combined cycle configurations with high efficiencies were also reported in [49]. These configurations include the s-CO<sub>2</sub> cycle in both the topping as well as the bottoming roles. When proposed as the topping cycle, the highest cycle temperatures reported are significantly lower than the firing temperatures of present-day gas turbine-based combined cycle power plants although the efficiencies obtained are comparable. This is indicative of the superior performance of the s-CO<sub>2</sub> Brayton cycle in comparison to conventional air Brayton cycle. The aim of this project, however, is to assess the feasibility of s-CO<sub>2</sub> power cycle for small to medium scale applications and thus, combined cycle configurations are not included in this analysis, as they are generally more suitable for large-scale power generation applications.

### 4.3 Thermodynamic Model development process

In the previous section of the report, the s-CO<sub>2</sub> cycle configurations that may be of interest for hydrogen-based power generation application were shortlisted. The thermodynamic features identified to be most pertinent for the current project include, multistep recuperation, intercooled compression, split flow compression, and reheated expansion. These features will be modelled in the thermodynamic evaluation tool. The process adopted with developing this tool is outlined in this section and can be organized in three parts, conceptual design, mathematical design, and numerical design. Firstly, the overall process is explained where the various steps performed during each design stage are briefly described. After this, the method is applied to the present case of development of a thermodynamic tool required to assess the feasibility of s-CO<sub>2</sub> power cycle for H<sub>2</sub> based power generation applications.

#### 4.3.1 Process Description

##### Conceptual design

The conceptual design stage starts by defining of the purpose of model development. It is important to have a clear idea about the end goal and the requirements of the model to keep the modelling process as efficient as possible by avoiding unnecessary iterations. This is followed by identifying/defining a set of system variables that will be used to control the model and extract information from it. Once the scope of the model is defined, the next important step is to list all the relevant phenomena occurring in the system in an orderly manner. However, while doing this, the purpose of the model development should be clear and only the necessary phenomena/process should be included. From a modelling perspective, all the processes occurring in nature can be infinitely complex and therefore, a designer will need to make certain simplifying assumptions and hypotheses. The crucial point here is to methodically document these assumptions and hypotheses such that it allows the user to adequately qualify the results/data obtained from the model. The goal should always be to keep the model as simple as possible without compromising on the details/complexity needed to fulfil the purpose of model development. The last step in the conceptual design stage is to break large and complex models into smaller sub-models, if required. The designer may then choose to repeat the conceptual design process of these sub-models either implicitly or explicitly depending on the complexity of the problem at hand.

## **Mathematical design**

After developing the conceptual design of the model, the next step of the development process is to build the mathematical model. The first step in this process is to identify all the relevant conservation laws and constitutive equations. Some of the equations may, however, be unnecessarily complicated to implement in the software code and should be adequately simplified. When all the processes of interest are fully defined by appropriate equations, the mathematical model is complete and can be implemented in the software of choice.

## **Numerical design**

The first step in this stage of modelling is to select the software in which the mathematical model would be implemented. The decision is guided by many factors that include not only technical aspects such as, the purpose of developing the model, the capabilities offered by the software, technical support available for troubleshooting etc., but also the designer's comfort level with the chosen platform. Having selected the software, the mathematical model can then be converted to actual code and be implemented. Upon completing implementation, the model can be used for simulation, but it should be validated and verified before using it for analysis.

### **4.3.2 Implementation**

#### **1. Purpose:**

The purpose of developing this thermodynamic model is to determine a first level estimate of the performance that an s-CO<sub>2</sub> power cycle can deliver when used in oxy-combustion power generation application using H<sub>2</sub> as the fuel. In addition to this, the model will also be used to perform a parametric study to understand the impact of various cycle parameters on the performance. A "Static – on-design" model is envisaged to be developed for this purpose. In addition to the fundamental processes of a power cycle, the model is expected to incorporate the following thermodynamic features: a two-stage recuperation process, a multistage intercooled compression process, split compression process where a part of the FG stream can directly be compressed without heat rejection in the condenser, and reheating /inter-turbine burner.

#### **2. Model input parameters:**

The list of input parameters required by the model is specified in Table 5 and Table 6.

Table 5 Model input parameters

<b>Sr. No.</b>	<b>Input Parameter</b>	<b>Units</b>	<b>Base Value</b>
1	Combustor pressure recovery ratio	[-]	0.9900
2	HEX pressure recovery ratio	[-]	0.9750
3	LP side pressure recovery ratio	[-]	0.9825
4	HP side pressure recovery ratio	[-]	0.9973
5	Flow split ratio	[-]	1
6	#Steps in vapor phase compression [VPC] process	[-]	2
7	#Steps in dense phase compression [DPC] process	[-]	2

Sr. No.	Input Parameter	Units	Base Value
8	Density at start of DPC	[kg/m <sup>3</sup> ]	800
9	Isentropic efficiency of VPC process	[%]	80.00%
10	Isentropic efficiency of DPC process	[%]	80.00%
11	Isentropic efficiency of the expansion process	[%]	83.00%
12	Effectiveness of low temperature recuperator [LTR]	[%]	88.10%
13	Effectiveness of high temperature recuperator [HTR]	[%]	93.10%
14	Combustion efficiency	[%]	99.00%
15	Pressure at turbine inlet	[bar]	300
16	Pressure at turbine outlet	[bar]	34
17	Compressor inlet temperature	[K]	302.15
18	Maximum temperature at recuperator inlet	[K]	1073.15
19	Maximum allowable blade temperature	[K]	1073.15
20	Hot end terminal temperature difference for TCH	[K]	15.00
21	Turbine cooling model constant $\mu_c$	[-]	0.08
22	Turbine cooling model constant $\beta$	[-]	0.90
23	Turbine cooling model constant $\Phi_\infty$	[-]	0.90

Table 6 Cycle configuration parameters

Sr. No.	Input Parameter	Optional states
1	Mixture Modelling Status	0 = Off   1 = On
2	Compression Configuration	0 = Simple Compression   1 = Intercooled Compression [IC] 2 = Split Flow Compression [SFC]   3 = IC-SFC
3	Expansion Configuration	0 = Simple expansion 1 = Reheated expansion
4	Turbine Cooling	0 = Off   1 = On
5	Turbine Coolant Heating Configuration	0 = Off   1 = On
6	Turbine Cooling Model	0 = Fixed   1 = Variable

### 3. Relevant Phenomena to be modelled:

To be able to evaluate the performance of the s-CO<sub>2</sub> cycle, the four basic processes of the cycle, i.e. compression, regeneration, combustion, and expansion, will have to be modelled. Also, the thermodynamic variation of the compression and expansion process, namely, intercooled compression, split flow compression and reheated expansion, shortlisted in the previous section, will be included. The various configurations desired to be analysed using this model are schematically represented in the Fig. 18.

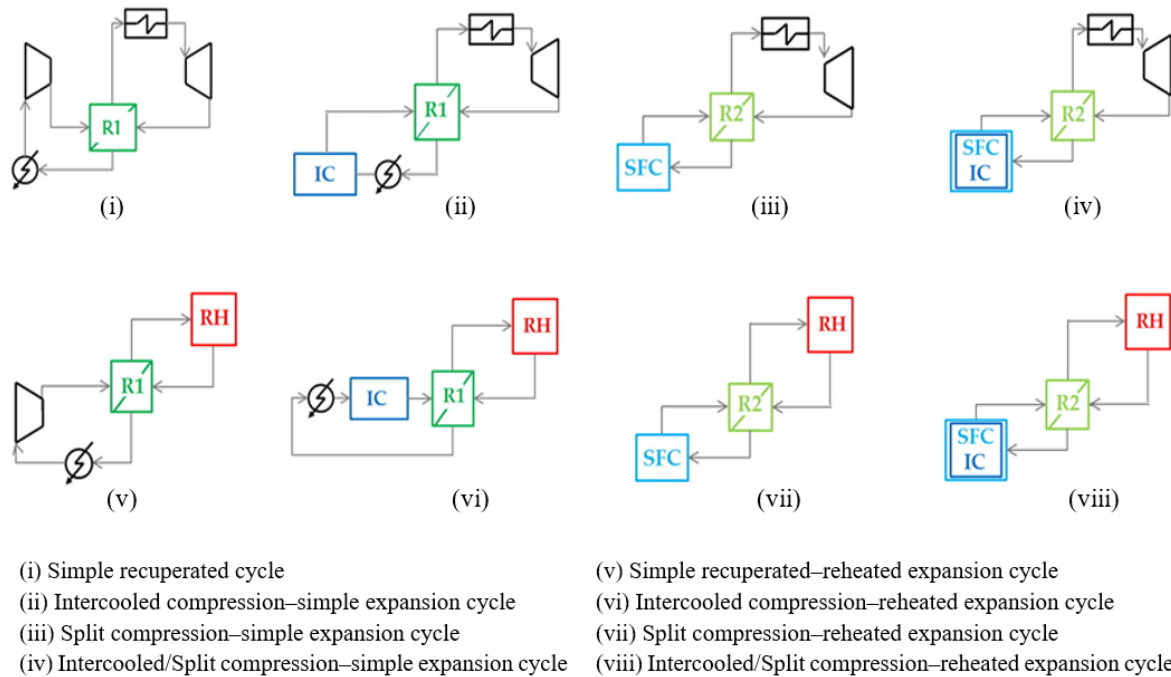


Fig. 18 Schematic representation of the configurations to be included in thermodynamic model [49]

In addition to these processes, the model will also include the three important effects that are explained in the paragraphs below.

- Property variations of the supercritical working fluid:

The general approach while building a low-fidelity, thermodynamic model for Brayton cycle would be to model the working fluid with two distinct sets of properties, one applicable before combustion (pure fluid) and one applicable post-combustion (flue gases). This approach would give a fairly decent estimate in case of air Brayton cycle but is expected to induce a large error while estimating the performance of s-CO<sub>2</sub> Brayton cycle. This is because of the large variation in properties of the working fluid discussed in the first section of this chapter. Therefore, while modelling s-CO<sub>2</sub> cycle it is important to account for these variations in the thermodynamic evaluation. This could be done either by directly implementing a suitable Equation of State (EoS) to model the fluid behaviour or by including a property database to evaluate thermodynamic properties at desired conditions. The second option was opted in this model and CoolProp [12] is included to provide the properties of the working fluid at the required thermodynamic state. It was preferred over other property databases mainly because it is an open-source database that does not require a proprietary software license. It uses the Span and Wagner EoS [50] to model carbon dioxide while water is modelled based on Wagner and Pruß EoS [51].

- Effect of modelling flue gas as mixture:

Heat addition by direct combustion of H<sub>2</sub>/O<sub>2</sub> can add a substantial amount of water in the working fluid after the combustion process. Preliminary analysis showed that it was essential to account for the effect of mixture to get fairly decent estimates of the cycle performance. Ignoring this effect and treating flue gas as a pure component (CO<sub>2</sub>) resulted in substantial underestimation of the cycle efficiency caused by a mismatch between the heat capacities of the hot and cold line. Considering water in the flue gas mixture increases the hot side heat capacity. In addition to the fact that H<sub>2</sub>O

has a higher specific heat capacity than CO<sub>2</sub>, its presence in the flue gas mixture results in the heat exchange process partially taking place in the two-phase region. This enables heating the recycle stream of s-CO<sub>2</sub> using the heat released during condensation of water in the flue gas mixture and thereby, addressing the issue of heat capacity mismatch between the recycle and flue gas stream to a large extent. The two-phase heat exchange process may require complicated recuperator designs, however, the gain in cycle efficiency would outweigh the engineering challenge in most cases. Besides, the PCHEs that are envisaged to be used with this cycle, are thought to be well equipped for handling multiphase, multifluid heat exchange processes.

The main challenge of modelling flue gas as a mixture in the present scope of work was due to the inability of the selected fluid database to directly provide mixture properties. Therefore, to get mixture thermodynamic properties, a mixing model had to be applied over the pure fluid properties obtained from CoolProp. For the sake of simplicity, an ideal mixture model was adopted and accordingly, it can be assumed that the properties of each component of the mixture are not affected by the presence of other components and the only effect of mixing is the dissolution of one component into the other. The impact of adopting an ideal mixture assumption is discussed in a more detailed manner in the subsequent sections of this chapter.

- Effect of turbine cooling:

The performance of a thermal power cycle is substantially affected by turbine cooling. This is because the coolant used is usually a fraction of the working fluid bled from the last stage of the compressor, before the heat addition process. This process of bleeding high-pressure coolant from the compressor, on one hand, reduces the efficiency of the cycle since a part of the compressed flow is not heated to maximum cycle temperature and thus, cannot produce the same amount of specific work output as the rest of the flow. Also, turbine blade cooling induces mixing losses which reduces the efficiency of the expansion process. On the other hand, turbine cooling allows a higher combustor outlet/turbine inlet temperature which reduces the overall exergy loss in the combustion process and also, increases the specific work of the expansion process, thereby, effecting an improvement in the net cycle performance. The overall result of these opposing effects of turbine cooling is the presence of an optimal range of TIT within which the cycle efficiency maximizes. Therefore, modelling the turbine cooling process is necessary to be able to analyse this variation in cycle thermodynamic characteristics.

#### **4. Assumptions and hypothesis:**

List of Assumptions: The thermodynamic model was developed with the following underlying assumptions and as such the validity of the results obtained by using it are subject to these underlying assumptions being true/applicable.

1. Compression and expansions are assumed to be adiabatic processes of specified isentropic efficiency.
2. Unwanted heat loss to surrounding at any point in the cycle is not considered in this model.
3. Pressure loss due to piping/connectors between various components is not considered.
4. A simple turbine cooling model is assumed under which the total cooling flow is split into two equal parts. One part is added at the inlet of the turbine while the second part is added at the outlet of the turbine. Turbine coolant flow requirement is calculated assuming the blades are cooled using film cooling technique.

5. Fuel and oxygen are stored and available in a pre-compressed state on the plant site and can be directly used for combustion. The energy required to compress/pre-heat them to combustor inlet conditions is ignored at this stage.

List of Hypotheses: In addition to the aforementioned assumptions, some hypotheses are made during the model development process which have to be checked/validated during model validation step. If all hypotheses are found to be valid, the analysis can proceed while invalid hypothesis, if any, have to be updated appropriately and hence lead to an iteration in the model development process.

1. Treating the flue gas as pure component ( $\text{CO}_2$ ) in the thermodynamic analysis will not result in substantial deviation in estimated performance – This hypothesis did not hold when tested and therefore, the base thermodynamic model was updated to include the effect of flue gas mixture.
2. Flue gas can be modelled using an ideal mixture model – The results obtained from ideal mixture model were compared with those obtained from two other specialized EoS designed for modelling  $\text{CO}_2/\text{H}_2\text{O}$  mixtures namely, GERG-2008 as implemented in REFPROP and PCP-SAFT as implemented in FluidProp. The observed deviation in estimated properties was small enough to be acceptable in the present study. A more nuanced discussion outlining the full details of this analysis is included in section 4.4.1.2 of this chapter.
3. Flue gas can be considered to be a binary mixture of water and carbon dioxide – The minor species produced during combustion are ignored while conducting the thermodynamic evaluation assuming their concentration in FG mixture is negligible. This hypothesis was tested by conducting combustion analysis and was found to be true. The details of this analysis are covered in the sixth chapter.

## 5. Sub-models:

At this point in the modelling process, the conceptual design for the thermodynamic model is almost ready. However, to keep the coding process manageable and the code itself more comprehensible, it was opted to code each of the processes listed in the previous step individually, in separate process modules that can be run sequentially and exchange data with a central memory block. This modular approach of coding can be seen in the software architecture diagram that is shown in Fig. 19 where, different process modules have been clearly marked.

## 6. Equations & calculation routine:

This section is structured such that the set of relevant equations & calculation routine are listed per module for better clarity. From an overall perspective, since the purpose of this model is to get initial estimates of the thermodynamic performance of the proposed cycle under static on-design conditions, it mainly involves iteratively solving sets of algebraic mass and energy balance equations. Therefore, even though the model will be required to handle a large volume of data in each simulation, the underlying calculations in themselves are quite simple. The implemented set of equations in each module is as follows.

### Initial calculations

Using the user defined values for pressure drop across various components and pressure at turbine inlet and outlet, pressure throughout the cycle can be evaluated. This is the first set of calculations included in the model.

### Compressor module

Given that pressure and temperature parameters at compressor inlet and the isentropic efficiency of compression are known, one can use the definition of isentropic efficiency to determine the thermodynamic state at the outlet of the compressor. The basic process followed for all compression process evaluations is explained using Calculation Routine #1.

#### Calculation Routine #1

Steps	Known parameter	Evaluated parameters
Step #1	Pressure and temperature at compressor inlet	Enthalpy and entropy at compressor inlet (CoolProp)
Step #2	Pressure and entropy at compressor outlet under isentropic compression condition	Enthalpy and temperature at compressor outlet (CoolProp)
Step #3	Isentropic efficiency, enthalpy at inlet and ideal enthalpy at outlet	Actual enthalpy at outlet
Step #4	Actual enthalpy and pressure outlet of compressor	All other thermodynamic states required (CoolProp)

Isentropic efficiency of compressor is defined by equation (1);

$$\eta_{is,comp} = \frac{h_{is,out} - h_{inlet}}{h_{out} - h_{inlet}} \quad \dots(1)$$

### Recuperator module

After the compression process parameters are determined, the recuperation process can be evaluated. The model requires the user to input conditions at hot side inlet of the recuperator while, the evaluation of compression process determines the parameters at cold inlet of the recuperator. Knowing the conditions at inlet of hot and cold end of the recuperator, and also, the effectiveness of the recuperator, the heat exchange process can be evaluated. It should be noted that, although this is the essence of the calculation routine in the recuperator module, it is a rather simplistic view of the same.

Firstly, the recuperation process maybe taking place in two steps [LTR and HTR] depending on the split ratio opted by the user. This requires the process mentioned above to be iterative where the model starts with a guess value for the temperature at hot inlet of LTR and evaluates the conditions at cold outlet of the LTR. Having assumed the temperature at hot inlet of LTR (= temperature at hot outlet of HTR) the heat released by flue gases in the HTR is known. This information can be used to evaluate the parameters at cold outlet of the HTR. At this point, the physicality/soundness of the obtained state at cold outlet of HTR is examined and the observed HTR effectiveness is calculated. If both conditions are satisfied, the guess value of temperature at LTR hot inlet is accepted or else the process iterates with an updated value.

Another aspect that makes the evaluation process tricky is the fact that, the hot side of the recuperator is a mixture of carbon dioxide and water. The first challenge this presents is CoolProp is not yet designed to handle mixtures very well and therefore, the mixing laws have to be applied on thermodynamic properties of pure carbon dioxide and water (which are obtained from CoolProp at their respective partial pressures in the flue gas mixture). Secondly, in this flue gas mixture, water is a condensable component and the heat exchange process enters the two-phase zone at some point within the heat exchanger (HEX). These factors require another iterative process to estimate the necessary fluid state on the hot side of the recuperator.

On the whole, the evaluation of recuperator is a nested loop of two iterative calculation routines and is briefly explained in Calculation Routine #2.

## Calculation Routine #2

Steps	Known parameter	Evaluated parameters
Step #1	LTR hot side inlet pressure, temperature (guessed value) and mixture composition at HTR hot side inlet	Check for any condensation and evaluate the enthalpy at LTR hot side inlet
Step #2	LTR hot side inlet conditions and cold side inlet temperature, and LTR effectiveness	Evaluate the maximum possible heat transfer and actual heat transfer in LTR
Step #3	Actual heat transfer in LTR and cold side inlet parameter	LTR cold side outlet parameter by heat balance across the heat exchanger
Step #4	LTR cold side outlet conditions, flow split ratio and condition of flow bypassing the LTR	Condition at inlet of HTR cold side by considering adiabatic mixing of the two streams
Step #5	Inlet and outlet (guessed value) conditions of HTR Hot side; HTR cold side inlet conditions	Evaluate maximum possible heat transfer in HTR, and heat dumped by hot side in the HTR
Step #6	Given the heat exchange in HTR, and condition at inlet of HTR cold side	Evaluate the values at outlet of HTR cold side
Step #7	Conditions at HTR cold side outlet	Check if values make physical sense, compare the resulting HTR effectiveness with the user defined HTR effectiveness
Step #8	If the value at HTR cold side outlet is acceptable	Complete the recuperation evaluation by finding the values at LTR hot side outlet.
	If the value at HTR cold side outlet is not acceptable	Update the assumed temperature at LTR hot side inlet and repeat the process till acceptable values are obtained

During mixture evaluation, a simple mixing model is used in conjunction with Dalton's law of partial pressures. The most important parameter in the calculation explained above is mixture enthalpy. This was evaluated using the steps shown in Calculation Routine #3.

## Calculation Routine #3

Steps	Known parameter	Evaluated parameters
Step #1	Mixture composition and pressure at any given point	Partial pressure of individual components
Step #2	Partial pressure and temperature at any given point	Enthalpies of pure component (CoolProp)
Step #3	Ideal mixture assumption	Enthalpy of mixture

Mixture enthalpy is defined by equation (2);

$$h_{mix} \left[ \frac{J}{kg} \right] = \sum y_i * h_i^* \left[ \frac{J}{kg} \right] \quad \dots(2)$$

$y_i$  = mass fraction of  $i^{\text{th}}$  component

$h_i^*$  = Specific enthalpy of  $i^{\text{th}}$  component at its partial pressure and mixture temperature

## Expansion module

For the expansion process, the user defines the FG parameters at inlet of the recuperator and also selects a turbine cooling model. Using this information, the model calculates turbine outlet temperature [TOT] and turbine outlet pressure [TOP]. The calculations for the expansion process are similar to that described for compression process, with only difference being these are now done iteratively. There are two reasons for this change. First, the model only knows the outlet conditions for the expansion process leaving two unknown variables in equation (3) (i.e. inlet enthalpy and ideal outlet enthalpy). Secondly, since we are dealing with a mixture and CoolProp cannot handle mixture data directly, the model is required to evaluate the properties of constituent components separately and then apply a mixing model

on this data. This makes the process, a nested loop of two iterative calculations. The process is briefly explained in Calculation Routine #4.

#### Calculation Routine #4

Steps	Known parameter	Evaluated parameters
Step #1	Inlet pressure & temperature at recuperator inlet, cooling model	Evaluate the turbine outlet parameters
Step #2	Turbine outlet parameters, turbine inlet pressure and mixture compositions. Assume arbitrary value for TIT	Evaluate corresponding values for mixture enthalpy and entropy at inlet of turbine
Step #3	Parameters at turbine inlet	Evaluate turbine outlet parameters under isentropic expansion assumption (iteratively)
Step #4	Enthalpy at turbine outlet, (and current values of) turbine inlet and ideal turbine outlet	Evaluate the resulting isentropic efficiency of the process. Compare with user defined value of efficiency
Step #5	If the two values are close enough (set tolerance limit)	Proceed with calculations
	If the value is not within tolerance limit	Update the guess value of TIT and repeat the process

Isentropic efficiency of expansion process is defined by equation (3);

$$\eta_{is,exp} = \frac{h_{inlet} - h_{out}}{h_{inlet} - h_{is,out}} \quad \dots(3)$$

Mixture properties are evaluated by equation (4) & (5);

$$h_{mix} = \sum y_i * h_i^* \quad \dots(4)$$

$$s_{mix} = \sum y_i * s_i^* - n * R * \sum x_i * \ln x_i \quad \dots(5)$$

$y_i$  = mass fraction of  $i^{\text{th}}$  component;  $x_i$  = mole fraction of  $i^{\text{th}}$  component

$h_i^*$  = enthalpy of  $i^{\text{th}}$  component calculated at mixture temperature and its partial pressure

$s_i^*$  = entropy of  $i^{\text{th}}$  component calculated at mixture temperature and its partial pressure

$n$  = total number of moles in the mixture;  $R$  = universal gas constant

#### Combustor module

In case of evaluation of the combustion process, several parameters at inlet and outlet are already known. From the recuperator module the pressure and temperature of the pure CO<sub>2</sub> stream is known, while from the turbine module the pressure and temperature of the flue gas mixture is known. However, the outlet parameters are based on arbitrarily initialized values of FG mixture composition at the recuperator inlet, which at the start of the calculation loop is different from the composition that would exist due to combustion. The main module that controls the whole calculation process is tasked with the function of converging the deviation between these values of mixture composition within acceptable level as set by the user. The calculation in the combustor module is a simple energy balance equation, to find the fuel burn with the knowledge of the conditions at combustor inlet and outlet. The required fuel flow rate is evaluated by solving equation (6) for the combustor;

$$\Delta H_{combustor} = LHV_{H_2} * \eta_{combustion} * \dot{m}_f \quad \dots(6)$$

In this equation  $H$  is the enthalpy in joules,  $\dot{m}_f$  is the required fuel flow rate, and  $\eta_{combustion}$  is the efficiency of the combustion process. Since the fuel flow rate affects the composition of the FG mixture at combustor outlet, equation (6) has to be solved using an iterative method.

### Cooling flow module

Once all the four main processes complete one iteration, the model runs the module to update the cooling flow requirement of the turbine. Depending on the options selected by the user (whether fixed or variable or no cooling flow), the model evaluates the new cooling flow rate required by the turbine (assuming film cooling is employed). In case when uncooled turbine is opted, this module is skipped. In case of fixed cooling flow option, the value of cooling flow remains the same as fixed by the user no matter the variation in turbine inlet temperature. Lastly, if the user has opted for variable cooling flow rate, the cooling model is adopted from [52]. In this turbine cooling model, the cooling flow requirement is defined as per the equation (7) and (8);

$$\dot{m}_c = \mu_c * \dot{m}_{GT} * \left( \frac{\Phi}{\Phi_\infty - \Phi} \right)^\beta \quad \dots(7)$$

$$\Phi = \frac{COT - T_b}{COT - T_c} \quad \dots(8)$$

The terms in the equations are briefly explained.  $\dot{m}_c$  &  $\dot{m}_{GT}$  are the mass flow rate of cooling flow and main flow.  $\mu_c$  is a coolant flow rate correction factor that represents the combined effect of the surface area of the cooled blade surface, the cross-sectional area of gas flow, and the correction factor for thermal barrier coating. Since the purpose of this thermodynamic model is only to get a first estimate of s-CO<sub>2</sub> cycle performance, the value suggested by the author [52] ( $\mu_c = 0.08$ ) is simply used. However, if a need to recalibrate this factor for more accurate prediction arises in future works, it should be noted that it is mainly a function of the Stanton number, flue gas – to – coolant specific heat ratio, and turbine blade row geometry and further literature may have to be review on this topic. The exponent  $\beta$  accounts for the type of cooling employed and its suggested value is  $\beta = 0.9$  for film cooling and  $\beta = 1.25$  for convective cooling. Lastly,  $\Phi$  represents the cooling effectiveness where,  $COT$  is the combustor outlet temperature,  $T_b$  is the maximum allowable blade metal temperature, and  $T_c$  is the temperature of coolant.  $\Phi_\infty$  is the asymptotic value of maximum cooling effectiveness that occurs when coolant flow rate is increased to an infinite value. Theoretically,  $\Phi_\infty = 1$  for film cooling and  $\Phi_\infty = 0.85$  for convective cooling, however, based on model calibration, Gülen [52] suggests  $\Phi_\infty = 0.9$ .

### **7. Software architecture**

Software architecture adopted for this model is shown in Fig. 19. The software consists of a nested convergence loops in which the inner loop is designed to calculate the performance of the cycle using the inputs received from the user at the start of the process, while the outer loop is used to set the net output of the model to desired value. The first loop is contained within the module called cycle evaluator which essentially runs the various process modules in a sequential manner until the error between the current and predicted flue gas composition at recuperator inlet is below the set tolerance level. Once this convergence is achieved, the process moves to the next module where the work output of the cycle is calculated. If this is within the set tolerance of the desired output set by the user, the code prepares the requested output file and if not, the cycle evaluator module is re-triggered with updated values of total mass flow in the cycle. All the processes have been designed such that all the necessary data interactions are strictly routed through the central memory block. The error used in the first convergence criterion is calculated based on the mole fraction of water at recuperator inlet (current value vs predicted future value) and the tolerance is set at 1E-3. The error used in the second convergence criterion is based on the predicted vs desired work output of the cycle and the tolerance for convergence is set at 1E-6.

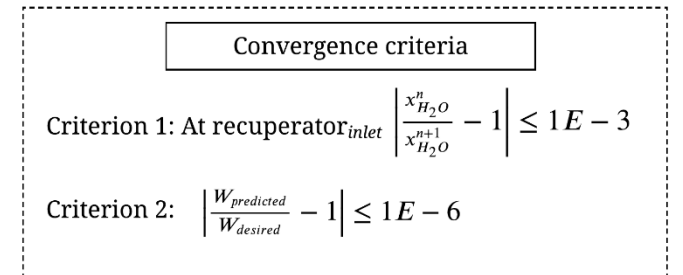
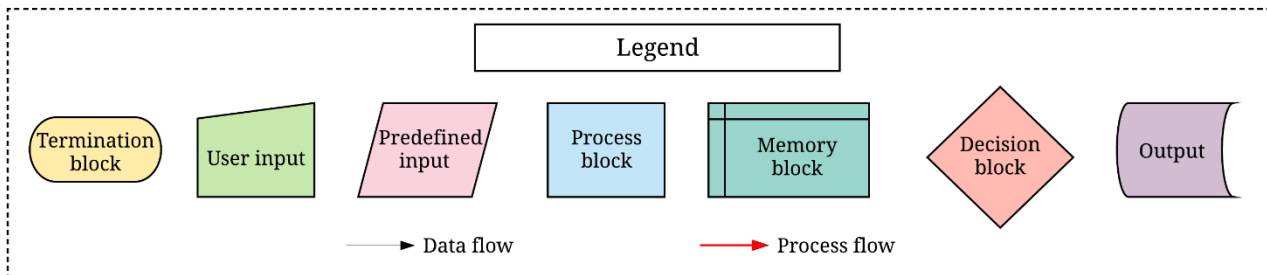
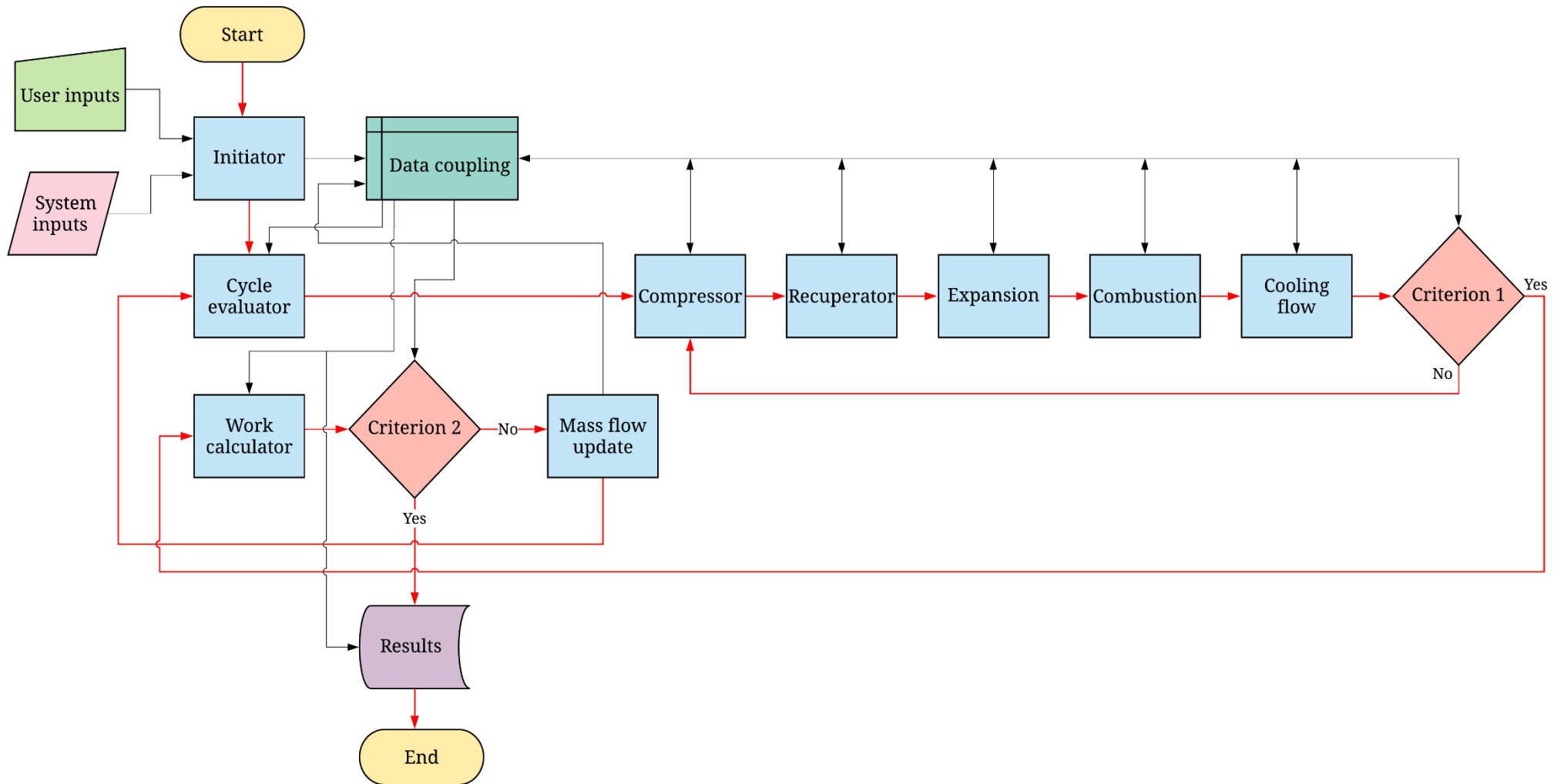


Fig. 19 Software architecture

## 8. Software Validation:

The last step in the model development process is running simulations using the code & testing the validity of the obtained results. Model validation includes a number of steps such as careful inspection of the results to check for logical and technical soundness, comparing the results with reference experimental data or cross-referencing the results obtained with data obtained from other sources that are widely accepted etc. In the current project, performance data from an Allam cycle based power plant is used for validation. NET Power LLC is developing a 50 MW<sub>th</sub> power plant in the US. This plant has received much attention since it is one of the first plants at this scale to be operated on s-CO<sub>2</sub> Brayton cycle. Therefore, the cycle performance data of this cycle is available in literature and has been numerically scrutinized by several researchers in the past. Most studies found good agreement between the numerically predicted performance and the performance data published by the developer. One such study done by Scaccabarozzi et. al. [53] provides detailed insights in performance analysis of this plant. Therefore, this data can be used to validate the results of the model developed in this study. In addition to this, some missing details about the proposed power cycle by NET Power LLC can be found in appendices of IEAGHG's report on oxy-combustion cycle [36] & [54]. Very detailed heat and mass balance diagrams and performance data sheets (as submitted by the developer) are included in this report. Although in order to use this data, the model had to be modified to some extent to accommodate natural gas as fuel in place of hydrogen, all other aspects remain the same. Thus, if the deviation between the estimated performance obtained from the model and the published performance data is within an acceptable range, the model will be considered validated. Model validation results are discussed in detail in the next section of this report.

### 4.4 Model Validation

#### 4.4.1 Validation of model hypotheses

The first step in validation process was to test the hypotheses made while model development. This section discusses the validation process of the first two hypotheses while the details pertaining to the third hypothesis on modelling of flue gas as a binary mixture of CO<sub>2</sub> and H<sub>2</sub>O is discussed in the sixth chapter of this report.

##### 4.4.1.1 Hypothesis #1: FG can be treated as a stream of pure CO<sub>2</sub> (Invalid)

As mentioned earlier, it was hypothesised at the start of model development process that since the flue gas mixture was expected to be 95% CO<sub>2</sub> – 5% H<sub>2</sub>O (mass basis), the thermodynamic properties of flue gas would be governed by CO<sub>2</sub> component. Therefore, the effect of flue gas mixture could be neglected, and flue gas could be modelled as a stream of pure CO<sub>2</sub>. To test this hypothesis, a simple simulation was designed wherein a high pressure CO<sub>2</sub> stream (at 304.67 bar pressure and 313.7 K) could exchange heat with the hot flue gas stream entering the recuperator at varying inlet temperature. This simulation was repeated twice with the only change being that the effect of mixture modelling was accounted in the first case while it was ignored in the second simulation. The result of this test is shown in Fig. 20. It can be clearly seen from these plots that ignoring the effect of mixture results in a large error in estimating the temperature of the high-pressure, recycle stream at the recuperator outlet. This difference arises because the moisture in the flue gas mixture has considerably higher heat capacity compared to the CO<sub>2</sub> and thus, enhances the heat transfer capacity of flue gas mixture. This simple test showed that ignoring effect of mixture while modelling the flue gas will grossly underestimate cycle performance and thus, the model hypothesis should be updated.

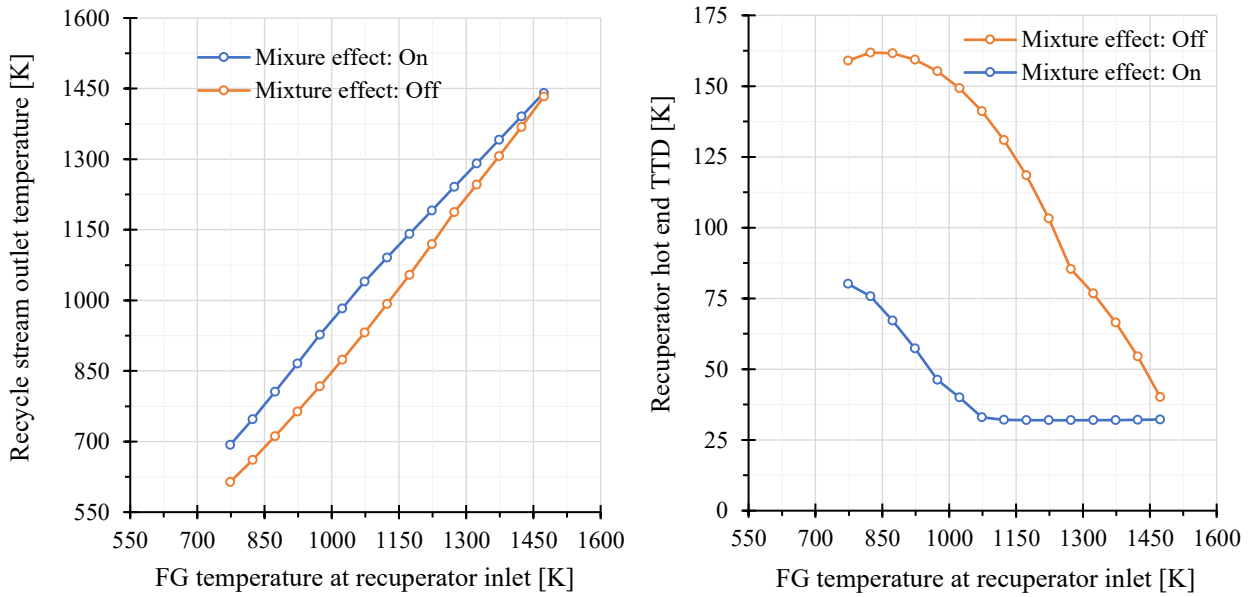


Fig. 20 Plot showing the effect of flue gas mixture on recuperator performance

#### 4.4.1.2 Hypothesis #2: FG can be modelled as an ideal mixture of CO<sub>2</sub>/H<sub>2</sub>O (Valid)

Using the previous simulation, it was established that the model should treat flue gas as a mixture to correctly estimate the cycle performance. However, the selected fluid property database (CoolProp) does not provide mixture properties. Therefore, mixing rules were defined that could be used to evaluate the properties of a mixture based on the properties of its constituent species. As mentioned earlier, a simple ideal mixture assumption was implemented for this purpose. This mixing model is mathematically represented by the equation (9) defining the value of an arbitrary thermodynamic property  $w$  in terms of pure component values of property,  $w_i^*$  and the change induced in it by mixing.

$$w_{mix} = \sum y_i * w_i^* + \Delta_{mix}w \quad \dots(9)$$

Note the thermodynamic property  $w$  considered in the above equation is assumed to be a mass specific value. If molar specific values are to be considered, the mass fractions ( $y_i$ ) under the summation changes to mole fractions ( $x_i$ ). The pure component property is evaluated at partial pressure of the  $i^{th}$  component and corresponding mixture temperature. The change in enthalpy, and volume upon mixing is assumed to be zero under ideal mixture assumptions and that in entropy is given by equation (10);

$$\Delta_{mix}v = 0; \Delta_{mix}h = 0 \text{ and } \Delta_{mix}s = -R \sum_{i=1}^C x_i \ln x_i \quad \dots(10)$$

Here  $\Delta_{mix}v$ ,  $\Delta_{mix}h$ ,  $\Delta_{mix}s$  are change caused by mixing in specific volume, specific enthalpy and specific entropy respectively.

Under ideal mixture model, it is assumed that the molecular behaviour of all the constituent species of the mixture remains unaffected by the presence of other species. This may be applicable to certain mixtures under very specific conditions (very low pressures/very high temperatures) but is not case for most mixtures. Both CO<sub>2</sub> and H<sub>2</sub>O are polar molecules and are very likely to affect each other's molecular behaviour. Therefore, it was deemed important to quantify the deviation caused by ideal mixture assumption in the thermodynamic evaluation.

Simulations depicting the thermodynamic processes of the power cycle were designed and analysed using different mixture models and the deviation in each case was noted. The other two mixture models used for comparison are GERG-2008 EoS(developed for modelling NG and other mixtures) implemented in REFPROP and the PCP-SAFT(developed for modelling FG mixtures in natural gas combustion) EoS implement in FluidProp. These are briefly discussed in the following subsections.

a. Effect of ideal mixture assumption on the recuperation process

A simple recuperation process was setup with the inlet and outlet parameters of the cold side (high-pressure recycle stream of pure CO<sub>2</sub>) kept at fixed values. In addition to this, flue gas parameters at hot side inlet of the recuperator were also fixed at a predefined condition. All these parameters were set to approximately represent the values encountered in the base case simulation of the proposed cycle. The flue gas condition at hot side outlet of the recuperator was estimated using the three mixture models, and the results were compared and analysed. The set of parameters fixed for this test are listed in Table 7a while the result of comparing the three mixture models is shown in Table 7b.

Table 7 Effect of mixture model on recuperator

Table 7a Recuperator parameters used in this analysis

Stream Parameter	Cold inlet	Cold outlet	Hot inlet	Hot outlet
Pressure [bar]	304.67	303.03	34.00	32.82
Temperature [K]	313.72	Case A: 1040.2	1073.15	Refer Table 7b
		Case B: 908.15		
Mass flow [kg/s]	130.01	130.01	143.25	
Molar composition: X <sub>CO2</sub>	100%	100%	89.64%	
Molar composition: X <sub>H2O</sub>	--	--	10.36%	

Table 7b Effect of mixture model on recuperator hot outlet parameters

Case	Mixture Model	CoolProp (+ Ideal mixture)	REFPROP [GERG]	PCP-SAFT EoS
Case A [Base case]	Temperature [K]	356.50	357.05	359.68
	Vapor mass flow [kg/s]	137.72	137.74	137.84
	Condensate mass flow [kg/s]	5.53	5.51	5.41
	Molar composition: X <sub>CO2</sub>	98.35%	98.31%	98.14%
	Molar composition: X <sub>H2O</sub>	1.65%	1.69%	1.86%
	Equivalent Cp = Δh/ΔT [J/kg.K]	1312.69	1313.69	1318.54
	Deviation in Cp estimation [%]	Base value	-0.0765%	-0.4453%

Case	Mixture Model	CoolProp (+ Ideal mixture)	REFPROP [GERG]	PCP-SAFT EoS
Case B [Non-condensing case]	Temperature [K]	416.76	420.72	426.35
	Vapor mass flow [kg/s]	143.25	143.25	143.25
	Condensate mass flow [kg/s]	0.00	0.00	0.00
	Molar composition: $X_{CO_2}$	89.64%	89.64%	89.64%
	Molar composition: $X_{H_2O}$	10.36%	10.36%	10.36%
	Equivalent $C_p = \Delta h/\Delta T$ [J/kg.K]	1196.95	1204.21	1214.68
	<b>Deviation in <math>C_p</math> estimation [%]</b>	<b>Base value</b>	<b>-0.6061%</b>	<b>-1.4813%</b>

As can be seen from Table 7b, the FG temperature at outlet of recuperator predicted by all the mixture models is very similar in Case A (where there is two phase heat exchange involved). However, a larger deviation in temperature prediction is seen in Case B when there is no condensation taking place. Since the cold side parameters in all three cases are kept constant, the overall heat transfer happening in each case is the same. Using the values of specific enthalpy change and the temperature drop occurring across the recuperator, an equivalent value of overall heat capacity defined as  $(\Delta h/\Delta T)$  is calculated. The deviation seen in this heat capacity is highlighted in the table. The deviation is calculated using following equation (11).

$$Deviation = 1 - \frac{Property_{ref\ model\ [i.e.\ REFPROP\ or\ PCP\ SAFT]}}{Property_{Coolprop\ based\ model}} \quad \dots(11)$$

From the results shown in Table 7b, it can be observed that the absolute deviation increases from Case A to Case B (condensing vs non-condensing case). This was probed further by evaluating the specific heat profile of the mixture as function of its temperature using the three models. The data showing variation in specific heat capacity of the mixture and deviation in its estimation as a function of mixture temperature is plotted in Fig. 21.

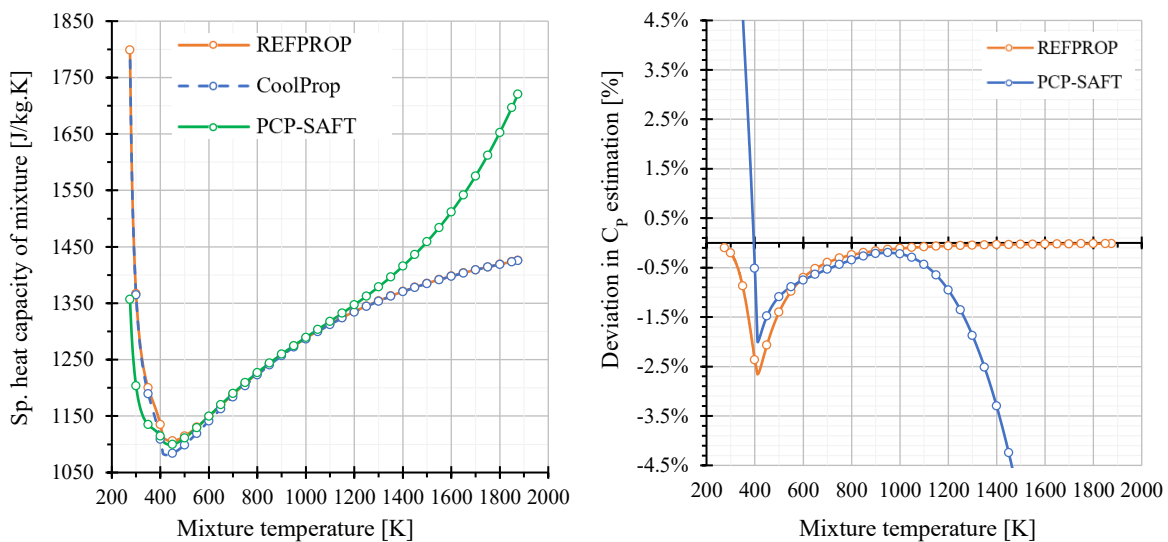


Fig. 21 Specific heat capacity of flue gas mixture at 34 bar estimated using different models

The increase in deviation from condensing to non-condensing case of heat transfer process can be explained by noting the following two points. Firstly, in the temperature range in which the recuperator, in the present example, operates [300 – 1100 K], both reference models predict higher heat capacities (represented by negative deviation) and the deviation in prediction increases as the mixture approaches its dew point (~411 K). Below this temperature the trend changes direction and the absolute value of deviation starts decreasing. The values predicted by PCP-SAFT show a very rapid change with the deviation becoming positive below ~400K, which shows that CoolProp based model predicts higher heat capacities below this temperature. This trend when viewed together with the fact that below the dew point temperature, the actual value of mixture heat capacity can be substantially higher, explains the behaviour seen in Table 7b.

In Case B, the FG mixture always stays above its dew point temperature and therefore, given that CoolProp predicts lower heat capacities in this region, the temperature drop seen when using CoolProp based mixture model is higher than that seen in the other two models. In Case A, i.e. two phase heat exchange process, this deviation will begin to minimize since the CoolProp based model will predict mixture cooling at slower rate relative to the reference models. The deviation seen between REFPROP and CoolProp based mixture models always stays negative which suggests that the former will always predict slightly higher FG outlet temperature. This is not the case when PCP-SAFT is considered. For temperatures below 400K, it predicts heat capacities that are lower than those evaluated using CoolProp and ideal mixture assumption. Therefore, it is possible that PCP-SAFT may predict a lower FG outlet temperature depending on the amount of the heat transfer required.

The key takeaway point from this analysis of the recuperation process is that, as far as the heat transfer capacity of the FG mixture is higher than the recycle stream (as was the case in this simulation), the small variation in estimation of FG temperature between different mixture models will not affect the cycle performance. This is because the impact of choice of mixture models will mainly be seen in the FG temperature at outlet of recuperator/inlet of heat rejection process which does not directly impact cycle efficiency. In cases where the cold stream has a higher heat transfer capacity, CoolProp based model is expected to underestimate the recycle stream temperature at combustor inlet. The quantification of actual range of uncertainty was not pursued mainly because the deviation observed in FG heat capacity estimation was small (< 2%) and was therefore, deemed acceptable at this stage of initial investigation.

b. Effect of ideal mixture assumption on the combustion and expansion process

Like in the case of recuperation process, the effect of mixture model on the combustion and expansion process was studied by performing simulations on a simplified case. For analysis of the combustion process, the combustor inlet and outlet parameters were fixed, and fuel burn required to achieve the desired outlet temperature was evaluated using the three mixture models. The specific parameter used for this simulation and the results obtained are tabulated in Table 8.

For studying the effect of mixture model on the expansion process, parameters at turbine inlet and isentropic efficiency of expansion were held constant and the three models were used to determine the conditions at outlet of the turbine. The difference was seen in terms of turbine outlet temperature and the specific expansion work generated in each case. These values are tabulated in Table 9. The equation used for calculating deviation in fuel burn and specific work of expansion is consistent with the previous definition.

Table 8 Effect of mixture model on combustor performance

Cycle Parameter	CoolProp	REFPROP [GERG]	PCP-SAFT
Combustor inlet temperature [K]	1040.2 [Held constant for this analysis]		
Combustor outlet temperature [K]	1452.33 [Held constant for this analysis]		
Combustor inlet pressure [bar]	303.03 [Held constant for this analysis]		
Combustor outlet pressure [bar]	300 [Held constant for this analysis]		
Mass flow at combustor inlet [kg/s]	130.01 [Held constant for this analysis]		
Mass flow at combustor outlet [kg/s]	136.48	136.49	136.57
Mixture composition at combustor outlet:			
$X_{CO_2}$	0.8916	0.8915	0.8903
$X_{H_2O}$	0.1084	0.1085	0.1097
Fuel burn [kg/s]	0.7188	0.7200	0.7287
<b>Deviation in fuel burn [%]</b>	<b>[Base value]</b>	<b>0.16%</b>	<b>1.38%</b>

Table 9 Effect of mixture model on turbine performance

Cycle Parameter	CoolProp	REFPROP [GERG]	PCP-SAFT
TIT [K]	1452.33 [Held constant for this analysis]		
Turbine inlet pressure [bar]	300 [Held constant for this analysis]		
Turbine outlet pressure [bar]	34 [Held constant for this analysis]		
Isentropic efficiency of turbine [%]	83% [Held constant for this analysis]		
Flue gas molar composition	CO <sub>2</sub> : 85% & H <sub>2</sub> O: 15% [Held constant for this analysis]		
Estimated TOT [K]	1110.99	1110.31	1113.52
Specific work of expansion [kJ/kg]	472.9324	474.5529	475.2039
<b>Deviation in specific work estimation [%]</b>	<b>Base value</b>	<b>- 0.343%</b>	<b>- 0.480%</b>

As can be seen from Table 8 and Table 9, the magnitude of deviation observed in fuel burn and the specific work of expansion are not very substantial. Both models predict higher fuel burn and higher specific work as can be expected after the previous discussion where it was shown that CoolProp tends to underestimate the heat capacity of the mixture. The overall effect on cycle performance in case of REFPROP mixture model would be negligible, since both these effects (increase in fuel burn and increase in specific work output) tend to nullify each other's impact on the overall cycle calculations. In case of PCP-SAFT, the deviation observed is slightly higher and therefore, it may reduce the net cycle efficiency by ~1% depending on the chosen cycle parameters, with the expected general trend being increased impact on overall efficiency with increasing TIT/TOT.

### c. Final comments on ideal mixture assumption

Based on the analysis presented in this section, the ideal mixture assumptions can be considered acceptable while performing preliminary thermodynamic evaluation of the s-CO<sub>2</sub> cycle. The deviations caused by choice of mixture model in the cycle calculations and component performance evaluation were found to be relatively small, especially in case of REFPROP based mixture model. PCP-SAFT EoS showed a larger deviation in mixture properties under certain operating conditions however, the effect on the cycle parameters and performance is not expected to be very large in most cases (variation in net cycle efficiency <  $\pm 2\%$ ). Having said this, it is important to take note that the mixture showed clear signs of deviation from ideal mixture behaviour. The plots in Fig. 22 show the comparison of variation in estimation of specific volume (thus, density) of the mixture between various models.

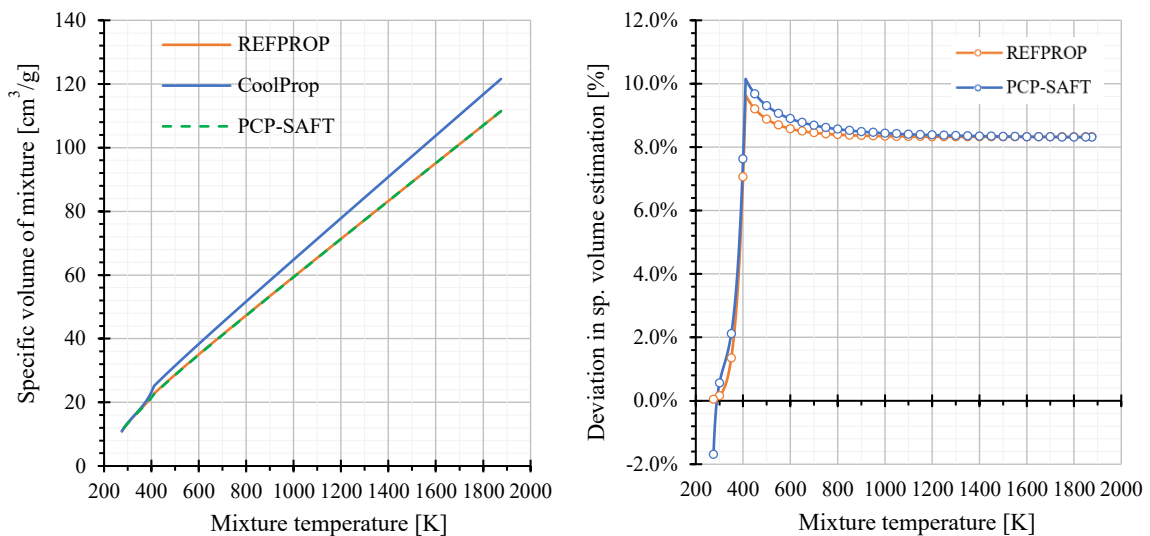


Fig. 22 Specific volume of flue gas mixture at 34 bar estimated using different mixture models

As can be seen the CoolProp based model overestimates the specific volume of the mixture consistently over the entire temperature range that is investigated. This deviation, although substantial (over  $\sim 8\%$ ), is not expected to affect calculations included in the present thermodynamic evaluation, since mixture specific volume/density is not explicitly used in the model. However, this large deviation (underestimation) in mixture density will surely affect the equipment design and sizing and therefore, ideal mixture assumption is not recommended while performing detailed design and sizing of power cycle components. Since, the effect of mixture model on cycle thermodynamics is not expected to be substantial and the component level design/sizing is not the objective of this study and, the hypothesis of considering flue gas as an ideal mixture of CO<sub>2</sub>/H<sub>2</sub>O is considered valid within the present scope of work.

#### 4.4.2 Model testing

After validating the hypotheses, the next step in model validation process is to validate the results obtained from the model. Since a novel concept of hydrogen based s-CO<sub>2</sub> power cycle is being proposed in this project, no reference data for validation was as such available. Because of this reason, it was decided to simulate the NET power cycle using this model and validate the results obtained against the published performance of the cycle. However, three modifications were required to be able to simulate the NET power cycle using the current model. These modifications are discussed in the following subsection.

#### 4.4.2.1 Required modifications

##### 1. Natural gas vs hydrogen as fuel

NET Power cycle has been proposed based on oxy-combustion of natural gas while the present model was developed to analyse cycle using hydrogen as fuel. Therefore, the code in the combustion module had to be update in order to be compatible with natural gas. The main change required in the code was to change the composition of combustion product from pure water to a mixture of water and carbon dioxide.

##### 2. Multi-fluid recuperator with WHR vs simple two fluid recuperator without WHR

NET Power cycle has been proposed with a multi-fluid regenerator that allows use of waste heat from other power plant components to improve heat integration at low temperature. It was found that this provision was not particularly important to be modelled in the present case mainly because of two reasons; a) No large source of waste heat was available for such use and b) the mass fraction of water in flue gas mixture when using H<sub>2</sub> as fuel is greater in comparison to cycle using NG and this inherently alleviates the heat integration problem to a large extent by increasing the heat transfer capacity of the hot stream. Developing a new multi-fluid recuperator model only for validation purpose was not an efficient solution. Hence, to be able to use the NET Power cycle data for validation, an assumption was made that the high pressure stream (recycled CO<sub>2</sub>) was supplemented with 62.03 MW of heat which is equal to the amount of waste heat that is recovered in NET power cycle. A portion of this heat is added to the CO<sub>2</sub> stream entering the combustor while the remaining part is added to the turbine coolant heater. This heat is distributed such that hot end TTD of ~20 K is obtained as is the case in the original cycle. In absence of this assumption, the cycle simulated in the thermodynamic model would become substantially different from NET Power cycle and cannot be compared for validation purposes. This makes this assumption an important caveat of this validation process.

##### 3. Natural gas compressor and Air separation units are not modelled.

NET Power cycle data includes naturel gas compressor and air separation unit (ASU) as plant auxiliaries. These are not required in the proposed power cycle since both hydrogen and oxygen are assumed to be available in pre-compressed state from the storage units. Therefore, the auxiliary load of these units is simply assumed to be equal to the value stated for NET Power cycle in [36 & 54].

#### 4.4.2.2 Comparison of estimated NET Power cycle performance with the reference data

With the knowledge of the assumptions and modifications made in the model to accommodate this test case, the estimated cycle performance can be compared with the reference available in literature. Fig. 23 shows the schematic layout of the NET Power cycle.

The compression process is a four stage intercooled vapor phase compression process followed by two stage pumping in centrifugal pumps. The density at the start of pumping process is maintained to be around 700 kg/m<sup>3</sup> at 26 °C (the intercooled temperature) corresponds to a pressure of about 80 bar. After the first stage of pumping, at pressures between 100-120 bar recycle stream is split in two parts. One of these streams is mixed with the oxidizer stream emerging from the ASU after which both streams are pumped to maximum cycle pressure in the second stage of pumping process. Turbine cooling flow is bled from the stream of pure CO<sub>2</sub> after final stage compression. These 3 (cold) streams then enter the recuperator for heating while the hot streams come from the turbine exhaust and air compressors in the

ASU. After recuperation, the oxidizer stream and the diluent stream are sent to combustor and emerge as the flue gas stream entering the turbine which is cooled using the previously extracted coolant stream. Table 10 shows the comparison of estimated cycle performance with reference data available in literature.

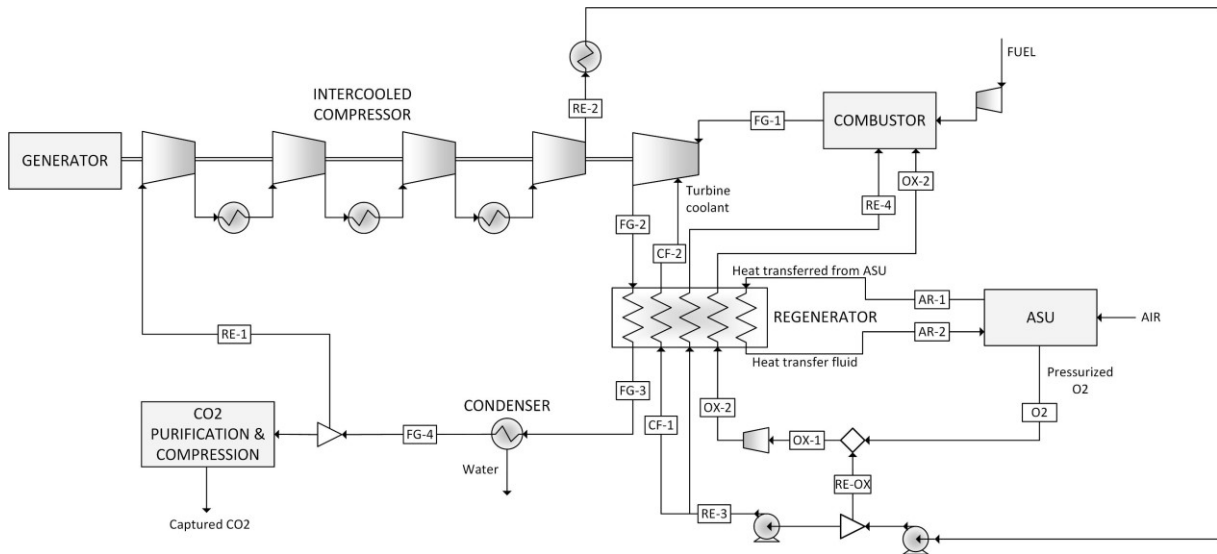


Fig. 23 Schematic representation of the proposed layout of NET Power cycle [53]

Table 10 Comparison of NET Power cycle performance parameters for model validation

	Unit	Results of [53]	Results of [54]	Results of this work	Deviation from [54]
Thermal energy of feedstock (LHV)	MW <sub>th</sub>	768.31	768.31	768.58	[*]
Turbine power output	MW <sub>e</sub>	622.42	631.95	613.85	-2.9%
Recycle flow compressors consumption	MW <sub>e</sub>	111.15	103.95	103.75	-0.2%
NG compressor	MW <sub>e</sub>	4.18	4.75	4.75	[*]
Air separation unit	MW <sub>e</sub>	85.54	85.45	85.45	[*]
Net electric power output	MW <sub>e</sub>	419.31	422.95	418.64	-1.0%
Net specific work <sup>4</sup>	kJ/kg	329.91	334.43	324.81	-2.9%
Net electric efficiency (LHV)	%	54.58	55.05	54.47	-1.1%
Turbine outlet temperature	°C	741.2	740	740	[*]
Recycle flow final temperature	°C	721.2	720	721.5	[*]
Cooling flow final temperature	°C	183	284	227.1	-20.0%
Flue gas to condenser temperature	°C	62.1	55	60.1	9.2%
Recycle flow to regenerator temperature	°C	54.2	50	53.3	6.6%
Turbine inlet flow rate	kg/s	1271	1264.7	1288.9	1.9%
Cooling flow rate	kg/s	99.4	145	104.2	-28.1%

<sup>4</sup> Net electric power output/turbine inlet mass flow rate.

	Unit	Results of [53]	Results of [54]	Results of this work	Deviation from [54]
Turbine outlet flow rate	kg/s	1370.4	1409.7	1428.6	1.3%
[*] Deviation measurement is not applicable since the values of these parameters are either assumed to be equal to that in base case [54] or are adjusted to match the base case [54].					

As can be seen from Table 10 most of the cycle parameters predicted by the model are in good agreement with the published performance related data of the NET Power cycle. Although the predicted cycle efficiency is ~1% lower than the published, it can still be considered a fairly decent estimate since the purpose of this model is to give first estimates of the novel power cycle concept and not its exact value. All parameters show deviation within an acceptable range, except for the parameter related to cooling flow calculations. The main cause of this deviation lies in the cooling flow model adopted in this code & two particular reasons are most likely to cause the observed deviation.

The first reason being that the turbine cooling model was originally developed and calibrated to be used with conventional gas turbines such that cooling flow estimation were in line with F-class turbines [52]. Since not enough data is published about s-CO<sub>2</sub> turbine design, the model could not be re-calibrated and the original model coefficients were implemented. This is most probably the underlying reason of variation in cooling flow requirement. However, as can be seen from Table 10, a deviation in cooling flow calculation was also seen in the NET Power cycle analysis done by Scaccabarozzi et. al. [53] and the trends in terms of the physics of the problem seems consistent.

The second reason, that can potentially cause variation in the performance estimation is the manner in which cooling flow is added to the main flow. In practice, cooling flow would be added at each of the cooled stages of the turbine. In this case, the cooling flow participates in the process of work production in all downstream stages while gradually cooling the main flow. To model this process, Scaccabarozzi et. al. [53] have used an improved versions of El-Masri's continuous expansion model which assumes (n+1) stage turbine with n being the number of cooled stages. However, this level of detail is not included in this model and a simpler approach of adding 50% of the total cooling flow at turbine inlet and turbine outlet was implemented. This simplification is bound to induce some finite error in the expansion process evaluation, and it can be expected that the model will predict slightly lower work output from the turbine as compared to base data, as seen from the data represented in Table 10.

Other than the cooling flow related calculations, the performance estimated by the thermodynamic model is generally in good agreement with reference data. Having said that, the deviation resulting from the turbine cooling model can be expected to be present in all the data extracted using this thermodynamic evaluation model. Albeit, since the main purpose of the model is to get only the initial estimates of cycle performance, the potential error induced by assuming a simple turbine cooling module was presumed to be acceptable. Therefore, the model can be considered validated and deemed fit for conducting preliminary thermodynamic cycle evaluation studies on the proposed internally fired, H<sub>2</sub>/O<sub>2</sub> fuelled s-CO<sub>2</sub> power cycle.

This concludes the model validation process and the model can now be used for thermodynamic analysis of the proposed H<sub>2</sub>/O<sub>2</sub> fuelled s-CO<sub>2</sub> power cycle, the details of which are discussed at length in the next chapter.

# Chapter 5

## Thermodynamic Analysis

### Overview

Thermodynamic evaluation of the proposed internally fired  $H_2/O_2$  fuelled  $s\text{-CO}_2$  power cycle is discussed in this chapter. The first section of the chapter briefly outlines the selection of the design point and the range of parameters over which the cycle will be analysed. The second section discusses the selection of the final configuration of the cycle that is proposed under this project. After selecting the design point and the final configuration, the effect of various parameters on the performance of the cycle was analysed. The third section of the chapter discusses the main findings of this parametric analysis. Although the parametric study proved to be useful in understanding the effect of individual cycle parameters on its overall performance, it did not give insights about the effects of coupling between cycle parameters like pressures and temperatures. Therefore, an additional analysis was set-up in which the performance of the cycle was simulated over a wide range of pressure and temperature. The data obtained in this analysis was used to develop a performance map of the proposed cycle. This aspect is further discussed in the fourth section of the chapter while the last section comprises of a summary of the key findings of this thermodynamic analysis.

### 5.1 Design point selection

The first step in the cycle evaluation process was to select the design point parameters that could be considered practical based on the information reviewed during literature survey phase of this project. The main objective of the project was to test the feasibility of this concept vis-à-vis the existing fuel-cell based systems. Therefore, while selecting the design point parameters, conservative values that could be implemented with the present level of technological progress were preferred over optimistic

values that relied on futuristic developments. The information collected during this process was not only useful for defining the design point parameters of the cycle, but it was also useful in defining the range over which these parameters could vary in the coming years. This was helpful while selecting the range of variation for the parametric analysis. The design point values and the range of variation of important cycle parameters that are studied under this chapter are listed in Table 11.

Table 11 List of parameters analysed during parametric study

Sr. No.	Cycle parameter	Unit	Design point value	Range of variation
1	Turbine inlet pressure [TIP]	bar	300.00	250 – 450
2	Turbine outlet pressure [TOP]	bar	34.00	20 – 95
3	Turbine outlet temperature [TOT]	K	1073.15	823.15 – 1223.15
4	Compressor inlet temperature	K	302.15	293.15 – 313.15
5	Recuperator pressure drop			
	a. LP side pressure drop ratio	[%]	1.75%*	0 – 10%
	b. HP side pressure drop ratio	[%]	0.27%*	0 – 10%
6	Isentropic efficiency of compression	[%]	80%	73 – 92%
7	Isentropic efficiency of expansion	[%]	83%	73 – 92%
8	Recuperator effectiveness	[%]	90%**	80 – 95%

\*Value selected to get the heat exchanger pressure drop mentioned in [54].

\*\*Value selected to set the hot end TTD and pinch point at 33K and 16.8K respectively.

## 5.2 Selection of final configuration of the proposed cycle

After selecting the design point parameter, a preliminary investigation was conducted for selecting the final the cycle configuration. The goal was to select the most suited configuration for the compression and expansion process and the logical justification for the final choice is explained in the following paragraphs.

### Selection of compression configuration

During literature survey, two possible variations of the simple compression process were identified, intercooled compression (IC) and split flow compression (SFC). These two options are depicted in the process flow diagrams shown in Fig. 24. Intercooling is a well-known technique to reduce the compressor work requirement and coupled with recuperation can give substantial boost in efficiency. SFC on the other is a special feature that is proposed with s-CO<sub>2</sub> to tackle the heat integration problems created by heat capacity mismatch between the cold recycle stream and the hot flue gas stream. The basic idea is to directly compress a small fraction of the of the flue gas without cooling it in the condenser. This results in a hot stream of recycled gas that can mixed with the remaining flow at the outlet of low temperature recuperator. The additional work required by the split flow compressor gets compensated by the reduction in heat input to the cycle. This compression configuration is often proposed with closed circuit, indirectly heated cycles since pure working fluid in these cycles are particularly prone to issue related to heat capacity mismatch. This compression configuration was initially found to be of interest in the current project to address the issues caused by heat capacity mismatch between the hot and cold line. However, during analysis it was found that for a directly fired cycle using hydrogen as the fuel, the flue gas post combustion has higher heat transfer capacity under

most operating condition. This makes the SFC configuration thermodynamically unsuitable since it will result in increased heat rejection and increased compressor work requirement reducing the net cycle efficiency quite substantially. To demonstrate this point, the net cycle efficiency obtained with split flow compressor (with a 4 staged intercooled main compressor) is compared with efficiency obtained with a 4 stage intercooled compression at design point is shown in Table 12. In case of split flow compression  $(1 - \text{FSR})$  represents the fraction of flow being compressed without being cooled in the condenser.

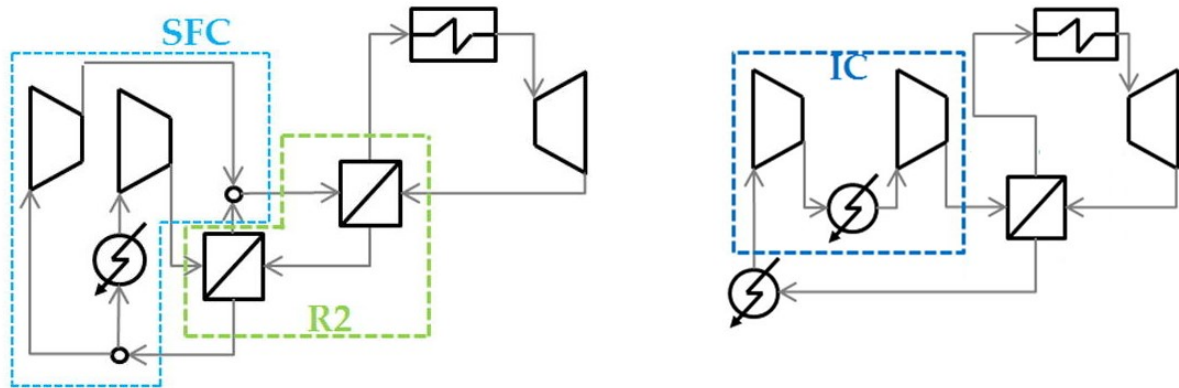


Fig. 24 Schematic representation of the SFC and IC configurations

Table 12 Net cycle efficiency obtained with SFC configuration and IC configuration at design point

Flow Split ratio (FSR) <sup>5</sup>	1	0.9	0.8	0.7	0.6	0.5	0.4
% flow through SFC	0%	10%	20%	30%	40%	50%	60%
Net cycle efficiency: SFC	57.96%	49.27%	41.86%	35.44%	29.84%	24.08%	18.33%
Net cycle efficiency: IC	57.96%						

As can be clearly seen from this data, use of SFC configuration was found have severely adverse impact on cycle efficiency due to worse integration in the recuperator. Therefore, option of using SFC has been ruled out from the present analysis and intercooled compression process is proposed.

#### Selection of expansion configuration

Like in the case of compression, two options were shortlisted during literature review for the expansion process, simple expansion and re-heated expansion. In theory, a re-heated expansion can relieve thermal stress in the hot section of the gas turbine by reducing the peak temperatures encountered in the cycle. This may lead to marginal saving in cooling flow requirement. In addition to this, it was initially thought that lower combustor temperature would help address the CO<sub>2</sub> dissociation occurring during combustion. Albeit, it was found on testing that none of these perceived benefits of the re-heated expansion process could be achieved in the proposed cycle (without substantial loss in cycle efficiency). It is true that re-heated expansion can in fact decrease TIT but results in a substantial loss in cycle efficiency. This is because the proposed s-CO<sub>2</sub> cycle is already quite constrained in terms of the TIT given the limitation imposed by recuperator design (discussed further in section 5.3.2) and the prevailing low pressure ratio of the cycle. Using re-heated expansion simply reduces the average temperature at which heat is added in the circuit which increases the cycle irreversibility and makes the process more inefficient. Secondly, the combustion analysis conducted for this cycle showed that the mole of fraction

<sup>5</sup> Flow split ratio is defined as the ratio of mass flow through main compressor to total compression mass flow.

of CO in this flue gas is quite low and therefore, it should not be a major concern for the proposed cycle (refer chapter 6 for more details). Lastly, reheated cycle was envisaged to have better part-load performance, however, since part-load performance analysis is not included in the present scope of study, this notion could not be verified. Overall, like SFC, no performance indicators were found that supported the choice of reheated expansion over simple expansion and therefore it was decided to rule it out from the present analysis. However, it may be interesting to study reheated configuration in future work when evaluating off-design and part-load performance of this cycle. Fig. 25 shows simplified schematics of intercooled reheated cycle (IC-RH) and intercooled simple expansion (IC-SE) cycle configurations.

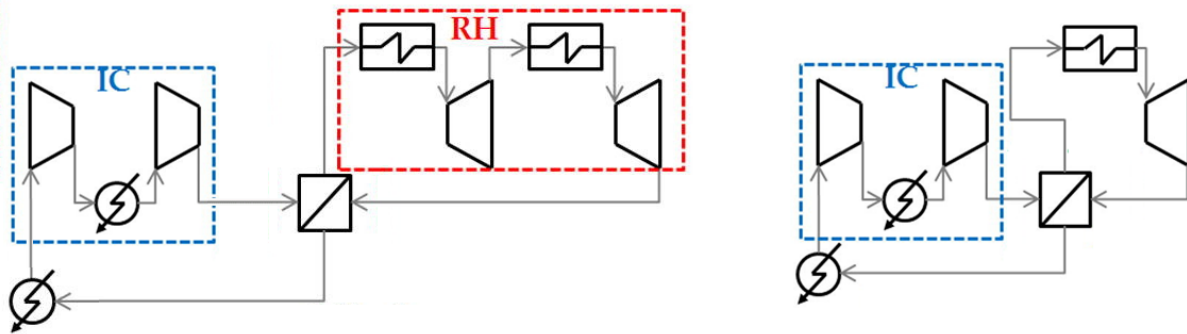


Fig. 25 Schematic representation of the IC-RH and IC-SE cycle configurations.

Table 13 Key cycle parameters of IC-RH vs IC-SE cycle configurations at design point.

Cycle parameter	IC-RH cycle	IC-SE cycle
Net cycle efficiency [%]	56.36%	57.96%
Net specific work output [kJ/kg]	364.25	365.55
Cooling flow fraction (as % of total compressed flow)	7.01%	4.95%
Other cycle parameters	IC-RH cycle	IC-SE cycle
Turbine inlet pressure [bar]	300	300
Turbine outlet pressure[bar]	34	34
Work output from expansion [MW]	63.39	63.34
Work input to compression [MW]	13.39	13.34
Thermal input in the combustor [MW]	88.72	86.26
Turbine inlet temperature [K]	1423.15	1452.33
Recuperator inlet temperature [K]	1073.15	1073.15
Combustor inlet temperature [K]	1043.1	1040.16
Condenser inlet temperature [K]	364.32	354.44
Turbine cooling flow temperature [K]	352.53	341.46
Sink temperature [K]	302.15	302.15
Reheated turbine inlet temperature [K]	1253.58	--
Main turbine 1 outlet temperature [K]	1202.45	--

As can be seen from the data shown in Table 13, there are no clear benefits in favour of the reheated configuration and therefore, it is ruled out from current analysis. However, it may have some operational advantage under part load condition and therefore, it recommended to analyse it further under future research work.

With this, the process of selecting the final cycle configuration is completed and it was found that *an s-CO<sub>2</sub> cycle with intercooled compression and simple expansion is the most suited configuration for the proposed application*. This choice is also supported by the fact that the NET power plant, which will be the first commercial implementation of the s-CO<sub>2</sub> power cycle, is also based on this fundamental cycle configuration. The layout of the proposed cycle is presented in the Fig. 26 along with its T-s chart representation drawn at the previously selected design point.

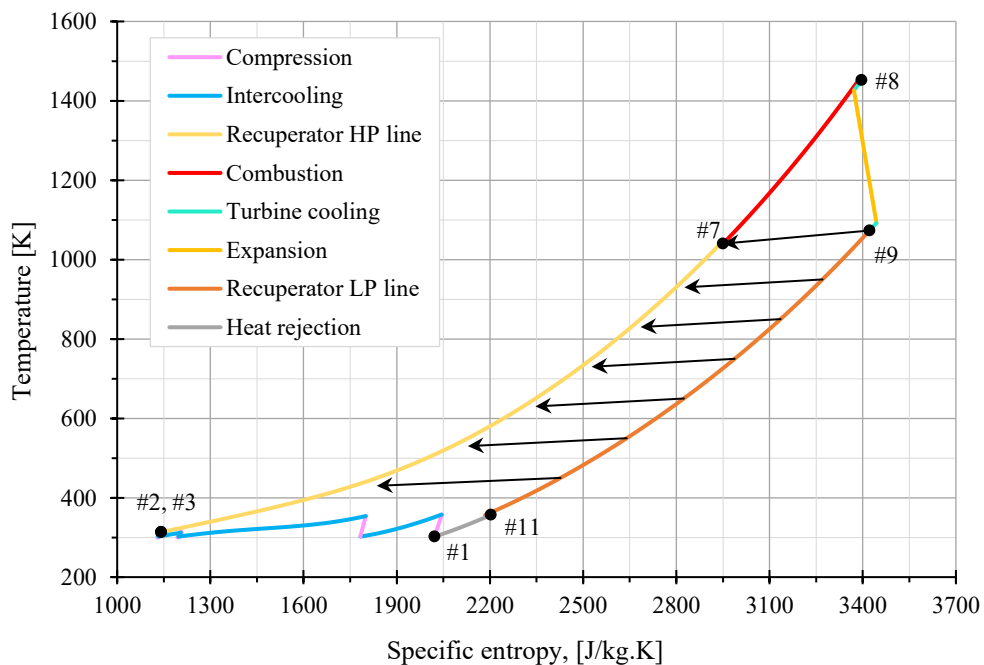
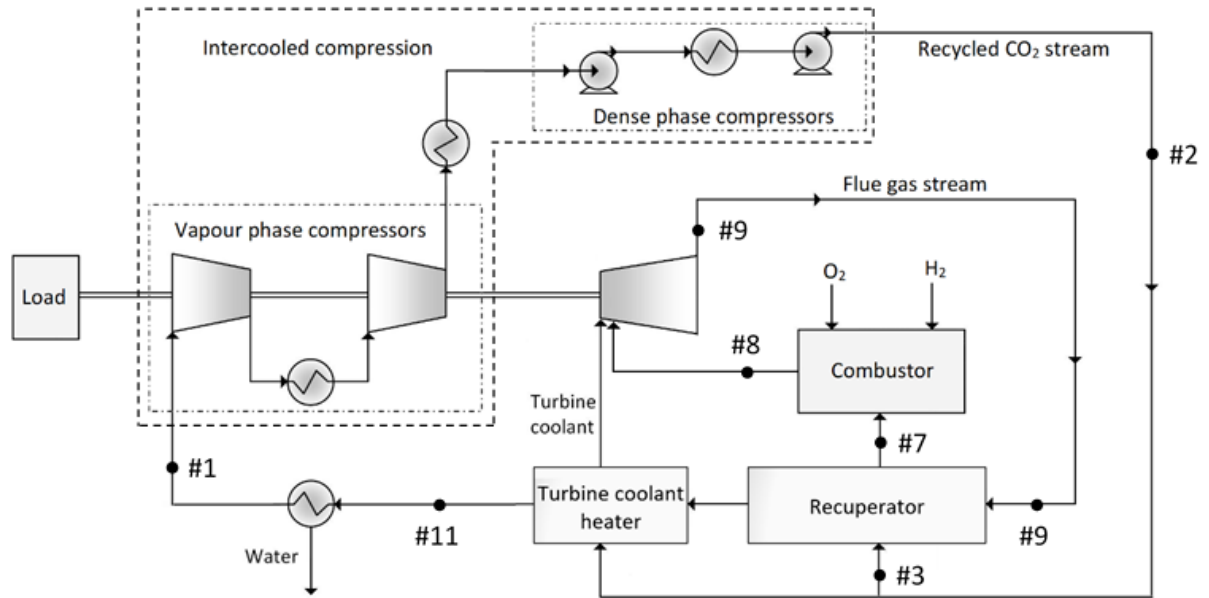


Fig. 26 Schematic layout and T-s chart representation of the proposed s-CO<sub>2</sub> power cycle

### 5.3 Parametric analysis

This section discusses the thermodynamic analysis of the proposed cycle at and around its design point. It should be noted that the model developed for this project is an on-design, static evaluation tool and therefore, any variation in the cycle parameter is treated as a new design point and not as an off-design condition. The effect of following design parameters will be analysed in this section.

1. Pressure related parameters
  - 1) Turbine inlet pressure
  - 2) Turbine outlet pressure
2. Temperature related parameters
  - 1) Turbine outlet temperature
  - 2) Compressor inlet temperature
3. HEX pressure drops
4. Isentropic efficiencies of compression and expansion
5. Recuperator performance
6. Turbine coolant heating

#### 5.3.1 Effect of pressure related parameters on cycle performance

The first parameter analysed under this study is the effect of selected cycle pressure. The typical pressure levels studied in the context of s-CO<sub>2</sub> cycles are often several times higher than the pressures at which conventional Brayton cycle is operated. The main reason for these high cycle pressure (coupled with a low cycle pressure ratio) is that critical pressure of carbon dioxide as mentioned earlier is ~73.8 bar. This pressure itself without any compression is about twice the typical pressure at which modern industrial gas turbines are operated. To operate the power cycle in a fully supercritical mode the lower pressure contour of the power cycle will have to be above this critical pressure. Such operation would severely limit cycle pressure ratio since material limitation would impose a maximum pressure limit on component design. Therefore, it is anticipated that future plants based on s-CO<sub>2</sub> Brayton cycles will instead be operated in transcritical mode. In addition to thermodynamics, limitation imposed by material operating limits will also play a large role in selecting operational parameters of these future power cycles.

##### 5.3.1.1 Effect of Turbine inlet pressure (TIP)

For the current analysis a wide of turbine inlet pressure (250 – 450 bar) is selected. Pressure approaching the upper limit of this range are considered mostly for the purpose of theoretical analysis of the cycle. However, operating turbines at inlet pressure of around 300-350 bar, although technically challenging, is not completely new for the power sector. Steam turbines in supercritical Rankine cycle based power plants have been long operated at comparable pressure levels, although their operating temperatures are comparatively lower. Allam cycle based NET Power plant is a promising step in the direction of addressing the design and engineering challenges of operating gas turbines such pressure levels. The combustor and turbine for this plant are developed by Toshiba and they demonstrate the technical feasibility of designing and operating at these components at these high pressure and temperature levels.

The simulation to analyse the effect of turbine inlet pressure was conducted keeping all other parameters are their base value. The result obtained for net cycle efficiency at different inlet pressures is reported in Fig. 27.

An increase in pressure at turbine inlet increases both the expansion pressure ratio (EPR) across the turbine and the temperature at its inlet (at constant TOT). This effect has a positive impact on cycle efficiency since heat addition and expansion processes at higher pressure and temperature lead to better utilisation of the thermal energy (lower exergy losses). On the other hand, with an increase in TIP, the compressor work requirement and the turbine cooling flow requirement also increase. Both these factors negatively affect the net cycle efficiency. Therefore, the overall trend seen was that an increase in TIP would initially improve the efficiency because the positive impact of increasing TIT outweighs the negative effects of increased compressor work and turbine cooling flow requirement. But as the TIP continues to increase further the gain in efficiency will start to diminish (as seen by gradual flattening of the efficiency curve), the trend will eventually reverse.

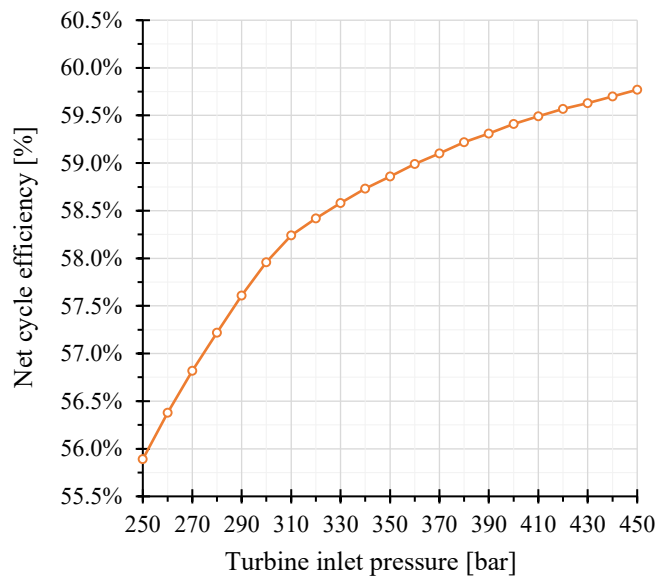


Fig. 27 Effect of varying turbine inlet pressure on cycle efficiency

### 5.3.1.2 Turbine OUTLET pressure (TOP)

After analysing the effect of TIP, the effect of varying TOP while holding all other parameters constant at their base value is studied in this section. The range of outlet pressures considered in this case (20 – 95 bar) is selected such that the thermodynamic behaviour of the s-CO<sub>2</sub> cycle can be studied when the compressor operates in transcritical (20-75 bar) as well as entirely supercritical mode (TOP > 75bar). The result obtained from this simulation is shown in Fig. 28. Unlike the monotonous trend seen in the previous case, the variation seen in cycle performance due to variation in TOP is more involved.

As TOP increases from its lowest value of 20 bar the expansion pressure ratio across the turbine decreases and causing a decrease in specific work output of the turbine. However, this is partly compensated by the decrease in compressor work requirement of the vapor compressors since an increase in TOP results in less work required to reach high density region. In addition to these two effects, a decrease in expansion pressure ratio decreases the maximum temperature in the cycle which reduces the specific heat input in the combustor and also results in a decrease in cooling flow requirement. These latter effects of decrease in TIT have a favourable impact on the performance while a decrease in net specific work output of the cycle has a negative effect on performance. The end result of these opposing effects is that as TOP increases from 20 bar, initially the efficiency of the cycle

marginally improves because the resulting savings outweighs the reduction in turbine output. However, the drop in turbine work output soon becomes the dominant effect and the efficiency then continues to decrease with further increase in TOP.

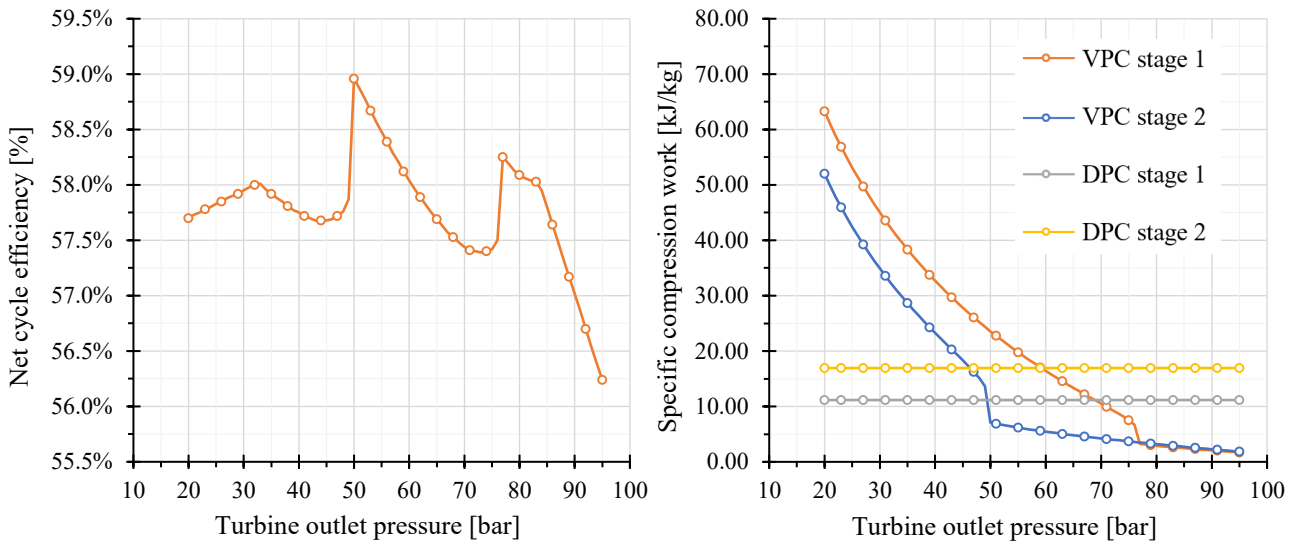


Fig. 28 Effect of varying turbine outlet pressure on cycle efficiency

In addition to this general behaviour of reducing efficiency, the simulation showed sharp rise in net cycle efficiency at two distinct values of TOP (50 bar and ~76 bar). These efficiency peaks are caused when the operation of the vapor phase compressors shifts from low-density vapor phase region to the high-density supercritical region. This can be seen by the change in specific compression work requirement shown in the Fig. 28 and also by the T-s diagrams depicting the compression process at two different TOPs shown in Fig. 29. As can be seen from these plots, the first peak (at TOP ~50 bar) corresponds to the point when VPC stage 2 starts operating in the supercritical region. The second peak at TOP of ~76 bar occurs because at this point all the compressors used in the cycle shift to the supercritical region and the cycle becomes fully supercritical.

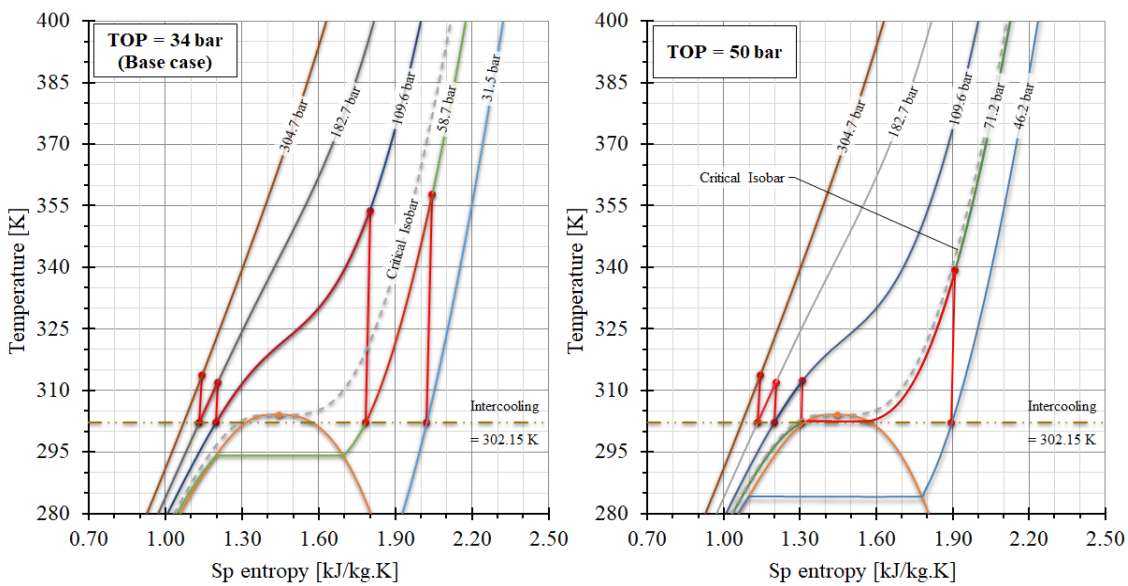


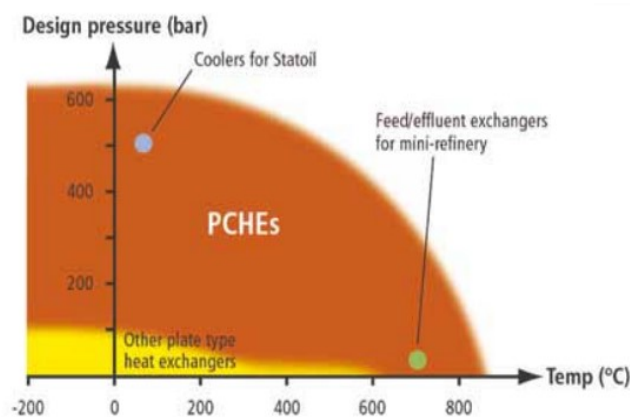
Fig. 29 T-s diagram of the compression process illustrating they effect of varying TOP

As can be seen from the first T-s diagram for TOP = 34 bar, the first two steps of the compression process that take place in the vapor region of carbon dioxide require considerably more work than the two dense phase compression steps. However, as TOP increases beyond 50bar, the compression process changes such that one of the compression stages that was initially operating in the vapor region shifts to supercritical region. This causes a step change in the compression work requirement resulting in the aforementioned spike in the net cycle efficiency.

It should be noted from the T-s chart that the dense phase compression process remains unaffected by choice of TOP since it depends only on the choice of a) recycle stream temperature at outlet of intercoolers (302.15 K in the present analysis, b) the density at inlet of dense phase compressors (800 kg/m<sup>3</sup>) and c) the number of steps selected to preform dense phase compression process.

### 5.3.2 Effect of temperature related parameters on cycle performance

In this section effect of cycle temperatures on the performance of the cycle is discussed. The selected temperature parameters are temperature at turbine outlet (TOT) and temperature at compressor inlet(s). Turbine outlet temperature is selected over its inlet temperature in this study because during the literature review of the s-CO<sub>2</sub> cycle it was found that its design is constrained by TOT/recuperator inlet as opposed to the conventional gas-turbine design which is constrained mostly by the highest of TIT possible. This mainly because of two reasons. The first reason is the limitation imposed by the operating limits of the recuperator. For an efficient operation of this recuperated cycle, it is necessary that the hot end TTD be as low as possible. This means that the recuperator will have to handle very hot flows at very high pressures. Current developments in material technology and manufacturing techniques of PCHEs impose a limit on the operating pressure/temperature. Typical operational envelope for PCHEs designed by Heatric (as published by the manufacture) is shown in the Fig. 30. Although, the values mentioned in this diagram are only indicative, it does show the limitation that heat exchanger design would impose on the selection of cycle parameters. As can be seen from this figure, the maximum temperature in the heat exchanger is severely limited as the design pressure increases.



Source: Technical brochure (2018) published by [Heatric](#)

Fig. 30 Design pressure & temperature capabilities of PCHE

The second factor that supports the choice of TOT over TIT as the design parameter is the fact that s-CO<sub>2</sub> cycles typically operate at lower pressure ratios compared to conventional Brayton cycle, which in turn limits the temperature ratio (T.R.) (T.R. < 1.5 in most cases). Therefore, even though high turbine

inlet pressure requirements may push the design envelop of contemporary gas turbines (and also combustors), the values so TIT (corresponding to allowable range of TOT) were found to be well within the range of operating temperature found in modern gas turbines. These two reasons show that TOT is a more constrained parameter while designing s-CO<sub>2</sub> power cycles. Therefore, TOT was selected over TIT as the design parameter.

### 5.3.2.1 Effect of turbine outlet temperature (TOT)

The effect of varying TOT on cycle performance keeping all other parameters at the base value is plotted in Fig. 31. The expansion pressure ratio in this analysis remains constant and therefore, the TIT is almost a linear function of TOT as can be seen in Fig. 31. The variation in cycle efficiency is mainly caused by the variation in cooling flow requirement and the recuperation process.

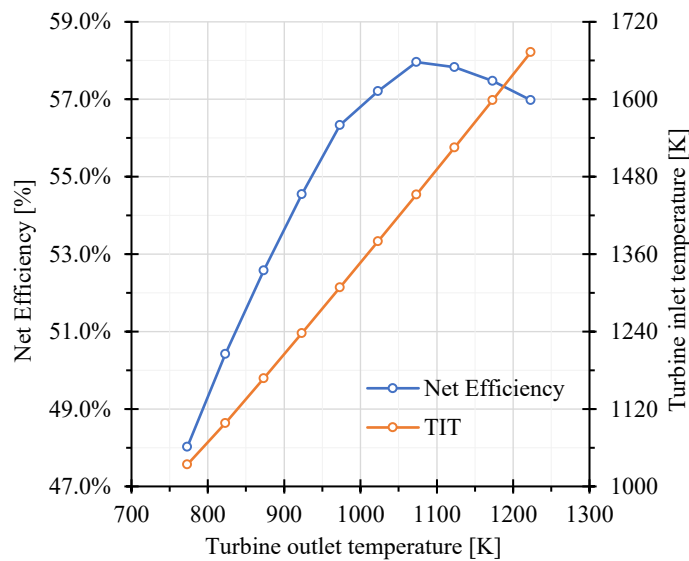


Fig. 31 Effect of varying turbine outlet temperature on cycle parameters

For TOT values smaller than 1073.15 K (design point TOT), the specific heat transfer capacity of the flue gases reduces, and combustor inlet temperature also reduces. Although because of the decreased TIT (corresponding to lower TOT), the specific heat added in the combustor decreases, the mass flow in the cycle has to increase to maintain a constant net output causing the overall fuel burn increase. In addition to this, a reduction in TIT reduces the cooling flow requirement, which leads to an increase in recycle flow through the recuperator resulting in further reduction of the combustor inlet temperature. The overall effect is that the thermal input required to generate desired power output increases thus decreasing the cycle efficiency.

On the other hand, at TOT higher than design point value, the specific heat transfer capacity of the flue gases increases causing an increase in the heat rejection from the cycle. Increased value of TIT (corresponding to higher TOT) causes the turbine cooling flow requirement to increase. This reduces the mass flow at the cold side of the recuperator which further leads to an increase in heat rejection in the cycle. This increased in heat rejection is thermodynamically responsible for reduced cycle efficiency at higher values of TOT (higher than design point TOT). The efficiency loss caused by higher heat rejection can be partly reduced by using the turbine cooling flow to absorb the spare thermal energy of the fuel gases and this effect is discussed further in section 5.3.5.

### 5.3.2.2 Effect of compressor inlet temperature

The other important temperature parameter required by the model is the temperature at compressor inlet which is also the minimum cycle temperature. However, the designer does not have much freedom while selecting it because, it is a function of the temperature of the sink available which is often dictated by the ambient temperature at project location. It is by exploiting this particular parameter that very high simple cycle efficiencies can be achieved if the option of using the cold energy from cryogenic fuels/oxidizer is available in the project. Fig. 32 shows the effect of compressor inlet temperature on key performance parameters.

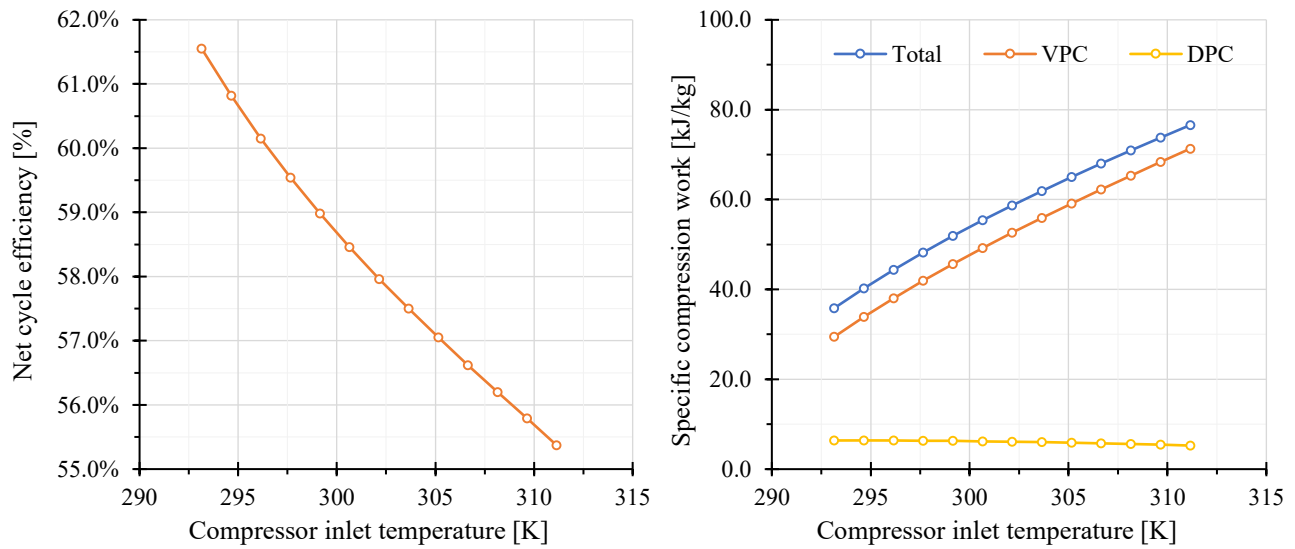


Fig. 32 Effect of varying compressor inlet temperature on cycle parameters

As would be expected during compression, a decrease in the inlet temperature results in reduction of the total work required and thus the observed trend in efficiency. Fig. 32 also shows the resulting variation in specific work requirement of the vapour phase and dense phase compressor. As can be seen, the increment in total compressor work requirement is solely caused by increase in VPC work requirement while the DPC work requirement marginally reduces. The variation seen in VPC work requirement (increase) is consistent with a typical compression process. However, the variation in DPC work requirement (a mild decrease) is caused by the design choice of holding the density at inlet of DPC constant. As the DPC inlet temperature increases, the pressure at start of dense phase compression process also increases thus reducing the work required to reach the final pressure of the cycle.

### 5.3.3 Effect of pressure drop on cycle performance

In this section the effect of high pressure (HP) and low pressure (LP) side pressure drop is analysed. In this analysis, even though the effect of pressure drop variation simulated by varying the pressure loss across the HP and LP side of the HEX, the observations made in this section apply to pressure drop occurring in HP/LP side components. Loss of efficiency due to pressure drops is a result of increase in compressor work requirement since any pressure loss occurring in the power cycle is finally compensated by the compressor (at constant TIP and TOP). The effect of pressure drop in the low and high pressure stream on the cycle efficiency is shown in Fig. 33. During this analysis, it was seen that LP side pressure drop has much larger effect on the cycle efficiency when compared to HP side pressure drop. This is clearly seen in the plot show in Fig. 33.

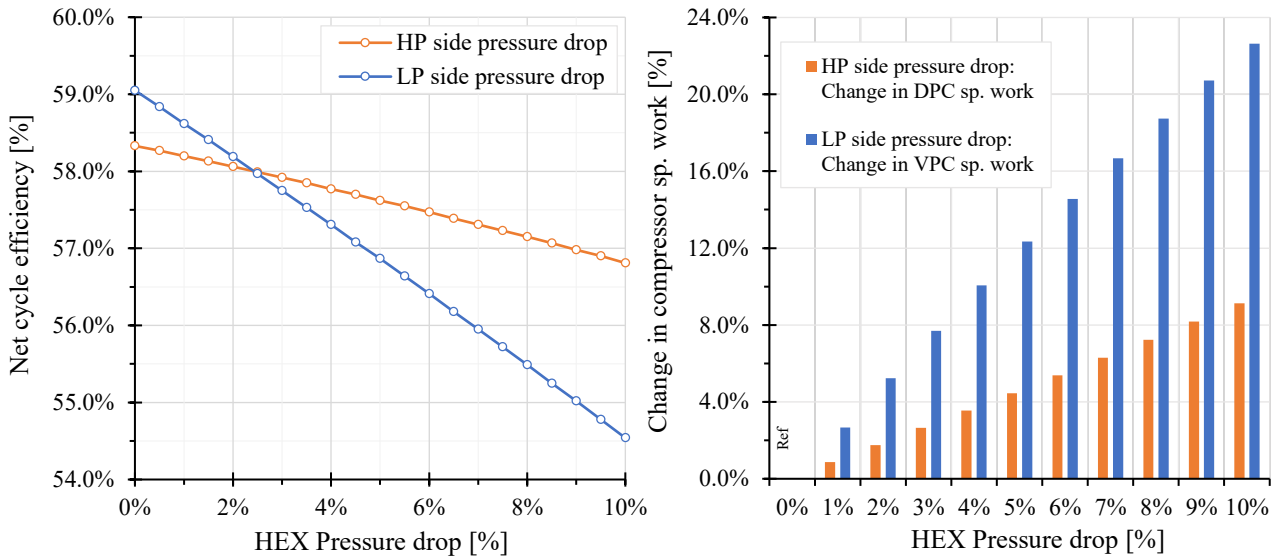


Fig. 33 Effect of pressure drop on cycle performance

The reason for this effect becomes clear when the compression process is analysed more closely. The final effect of any pressure loss on the LP side is a reduction of compressor inlet pressure while any pressure loss occurring on the HP side requires the compressor outlet pressure to increase (to keep TIP constant). Both these conditions cause an increase in compressor work requirement. However, since the conditions at inlet of DPC are only a function inlet temperature and selected fluid density, a change in pressure at the start of compression process (caused by LP side pressure drop) affects only the VPC while a change in final outlet pressure affects only the DPC. Since the specific work requirement of vapor phase compression is considerably larger than the dense phase pump, any loss of pressure on the LP side cause a large drop in efficiency. Variation in specific work requirement in the two cases is also shown in Fig. 33. It should be noted that the specific work requirement of DPC remains constant when LP side pressure drop is being studied and that of VPC is constant when HP side pressure drop is being studied.

### 5.3.4 Effect of isentropic efficiency of compression and expansion process

In this section the effect of varying the isentropic efficiency of compressor and turbine is discussed. The results obtained during this analysis are shown in Fig. 34. Net cycle efficiency is seen to be more sensitive to the reduction in turbine efficiency as compared to compressor efficiency. When the isentropic efficiency of the turbine is varied between 75–92%, the net cycle efficiency varies by ~8% points. In case of the compressor, the same variation in isentropic efficiency causes the net cycle efficiency to vary by only ~3%. This is trends is obtained because the change in specific work output of the turbine is much larger than the change in specific work input of the compressor caused by change in their respective isentropic efficiencies. Isentropic efficiency is defined as the ratio of actual work to ideal work for turbine and vice versa for compressor. Since all other cycle parameters remain constant ideal work of turbine and compressor also remain constant and the same reduction in isentropic efficiency will bring about the same percentage change in turbine and compressor work. However, because ideal work of turbine is much large than ideal work of compressor, the absolute change in turbine work is larger than the absolute change in compressor work. At net cycle level, this is reflected as the higher sensitivity to the isentropic efficiency of expansion as compared to that of the compression process. Similar reasoning is applicable when the overall sensitivity to the isentropic efficiency of VPC is

compared to the sensitivity to the isentropic efficiency of DPC. The specific work required by VPC is larger than that of DPC and thus has a larger effect on the net cycle efficiency.

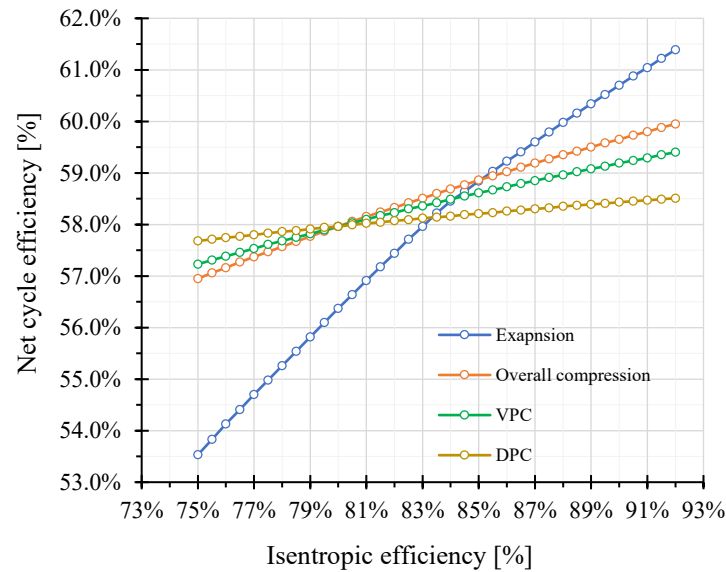


Fig. 34 Effect of varying isentropic efficiency of compression & expansion process

### 5.3.5 Effect of heating turbine coolant flow

In this section, the effect of using the turbine cooling flow as a sink for dumping spare thermal energy of flue gas after recuperation is analysed. During parametric study of the s-CO<sub>2</sub> cycle, it was found that except for some specific operating conditions (lower turbine outlet temperature &/or lower expansion pressure ratios), the terminal temperature difference at cold end of the recuperator was quite substantial (>25 K). This was indicative of the spare thermal energy in the flue gas that could not be recovered during recuperation process and thus would subsequently get rejected in the low temperature condenser. As TOT increases, the specific heat transfer capacity of flue gases increases while that of the recycled stream remains almost constant. This results in additional loss during heat rejection in the condenser at higher values of TOT. This heat loss can be partially reduced by using the turbine cooling flow to absorb extra heat. However, a hotter cooling flow produces two opposing effects on cycle efficiency because for a fixed TOT, an increase in coolant temperature reduces the combustor outlet temperature and increases the cooling flow requirement. The reduction in combustor outlet temperature results in reduction of specific heat input (via fuel combustion) to the cycle but also reduces the specific work output of the turbine (i.e. a reduction in the net specific work output of the cycle). The increase in cooling flow requirement leads to a marginal increase in the specific work requirement of the compression process causing the net specific work output of the cycle to decrease further. Therefore, the final variation in the net efficiency is dependent on the which of these two effects (reduction in specific heat input vs the reduction in net specific work output) is dominant at the selected TOT. The variation observed in key cycle parameters in plotted in Fig. 35 while the effects of the increase in cooling flow temperature on the cycle are illustrated on a representative T-s chart shown in Fig. 36.

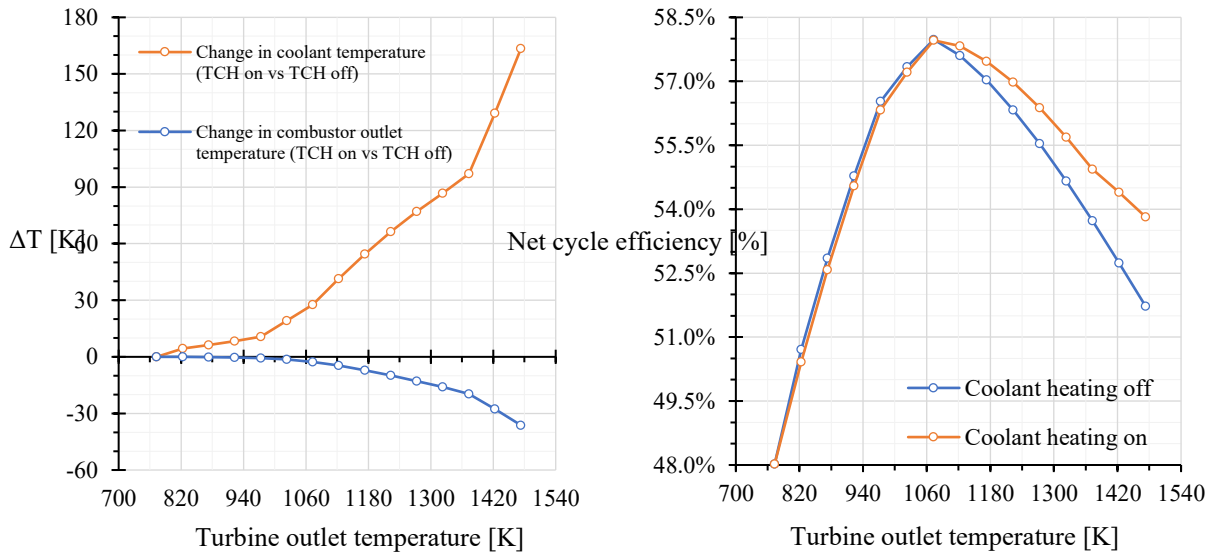


Fig. 35 Effect of heating the turbine cooling flow cycle parameters

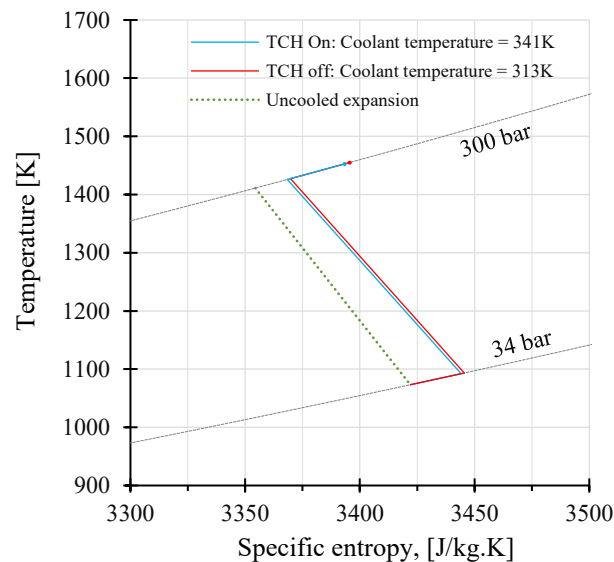


Fig. 36 T-s chart showing effect of coolant temperature on expansion process at design point TOT

As can be seen from Fig. 36, for a fixed TOT, the value of combustor outlet temperature depends on the degree of cooling induced by turbine coolant flow. The coolant at lower temperature produces stronger cooling effect and thus results in slightly higher combustor outlet temperature and specific work of expansion (or in other words, increase in turbine cooling flow temperature shifts the expansion curve towards lower temperatures along the isobars). Both the cases of expansion with turbine coolant heating on and off are shown alongside the expansion in an uncooled turbine. With an increase in TOT, the difference between coolant temperature increases and this shift in expansion curves also becomes more pronounced. The observed reduction in combustor outlet temperature was as much as  $\sim 40$  K which corresponds to substantial fuel saving (up to 4%) when compared to case where turbine coolant is not being used to absorb the spare thermal energy in the flue gas post recuperation. Reduction in combustor outlet temperature also results in marginal decrease in cooling flow requirement which partly offsets the increase in cooling flow fraction caused by higher coolant temperature. Overall, the effect of reduction in fuel burn tends to dominate the other effects and results in an increase in cycle efficiency.

Although this analysis generally shows the use of turbine coolant heating in positive light from cycle performance perspective, it should be noted that the highest benefits are reaped at very high values of TOT ( $> 1200$  K). Practical s-CO<sub>2</sub> cycles are unlikely to use such high TOT values in the near future due to the limitations imposed by the recuperator. At lower temperature, the gain in efficiency, if any, is only marginal and may not justify adding an extra HEX component to the cycle. Therefore, a case specific cost-benefit analysis may be required to comment on the feasibility of using turbine coolant heater.

### 5.3.6 Effect of recuperator effectiveness

The last parameter studied in this analysis is the effect of the recuperator effectiveness on the performance of the proposed cycle. The performance of the recuperator in the thermodynamic model is controlled by means of its effectiveness. Its value at the design point was selected such the resulting hot end TTD and the internal pinch point have conservatively high values of  $\sim 33$ K and  $\sim 16.8$ K. Since recuperator sizing is not pursued in this project, these two parameters are used to characterize the size of the HEX. Lower values of TTD and pinch point represents a better heat exchange process at the cost of overall size of the heat exchanger and vice versa. The plots shown in Fig. 37 represents the effect of varying the HEX effectiveness on the cycle performance.

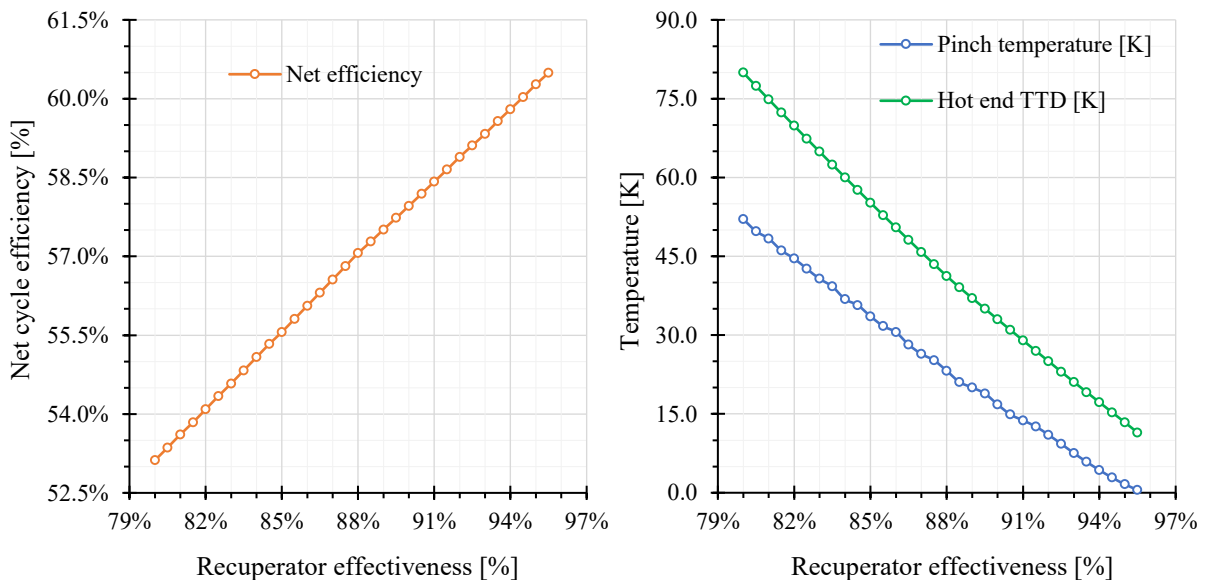


Fig. 37 Effect of varying isentropic efficiency of compressor and turbine

From Fig. 37 it can be seen as the recuperator effectiveness increases, the hot end temperature difference decreases. This results in an increase in the combustor inlet temperature and a decrease in the fuel burn; and thus, the net cycle efficiency improves almost linearly with effectiveness. However, as effectiveness increases, the pinch point temperature difference in the recuperator decreases and limits the maximum recuperator effectiveness that can be practically be achieved. As mentioned earlier, with increase in recuperator effectiveness, the cycle performance will increase but so will the size and cost of the recuperator. Thus, a detailed cost-benefit analysis maybe required on a case-to-case basis to select the optimum value of recuperator effectiveness (i.e. the recuperator TTD and the pinch temperature).

Fig. 38 shows the Q-T diagram of the heat exchanger at design point. As can be seen from this diagram, the total heat exchanged in the recuperator is  $\sim 135$  MW for a 50 MW power cycle that requires  $\sim 85$  MW of heat input from the combustion of fuel. While this fact in itself is not surprising knowing that the

proposed cycle is a highly recuperative cycle, it would be very interesting to study the effect of thermal inertia of the recuperator on part-load/transient performance of the cycle. Since modelling of transient effects and part-load performance is not a part of the present scope, this analysis is proposed as one of the recommendations for future work in this area.

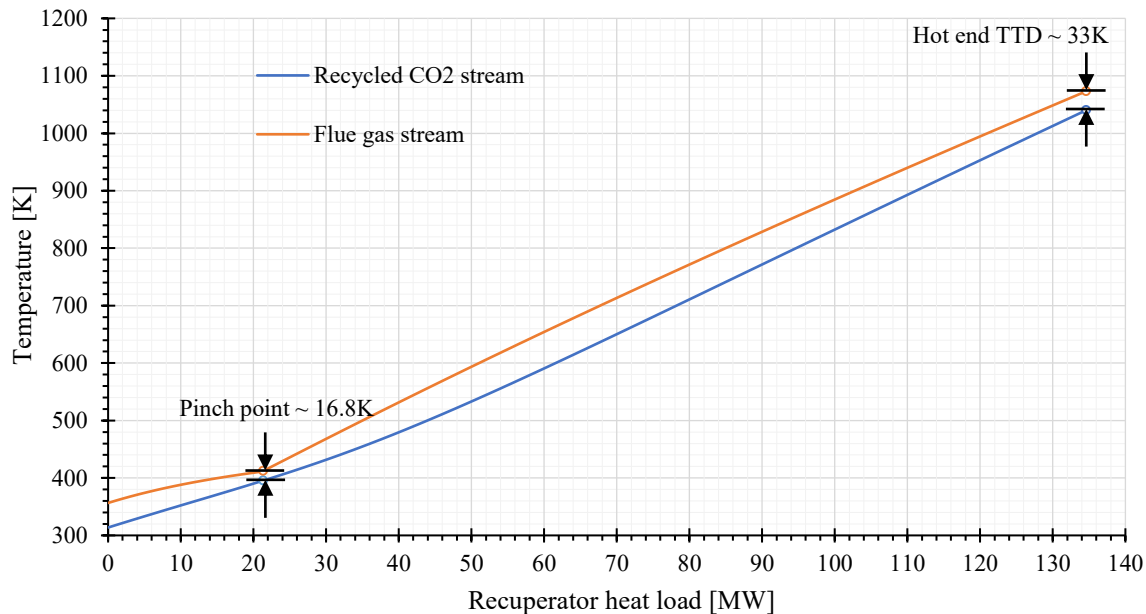


Fig. 38 Heat exchange process in the recuperator at design point

## 5.4 Performance Map

After analysing the effect of individual parameters on the cycle performance, this section explores the combined effect of some key cycle parameter. Of all the parameters evaluated in the previous section, cycle pressures and temperatures are most strongly coupled and are therefore, usually selected in pairs. This combined effect is analysed in this section where the pressure at turbine inlet and temperature at compressor inlet are held constant while the pressure and temperature at turbine outlet is varied. The decision of holding turbine inlet pressure and compressor inlet temperature constant was made because from a designer's perspective, the choice of these parameters will be very restricted by the mechanical design limitations and the prevailing ambient condition. Keeping the TIP (300 bar) and compressor inlet temperature (302.15K) fixed at design point values, the pressure and temperature at turbine outlet was varied and their effects on several cycle parameters were monitored. The variation of net cycle efficiency, the turbine inlet temperature and the pinch point temperature in the recuperator is plotted in the performance map shown in Fig. 39.

An important caveat that the reader should note while referring to this performance maps is that the level of details included in the present thermodynamic model is just enough to provide a first level estimate of the net cycle efficiency. The aim of this evaluation was to study the thermodynamic behaviour of the cycle and not to optimise its performance. Therefore, although the performance map shown in Fig. 39 cannot be used to predict the best efficiency of the cycle, it can be used as reference to select the base parameters/starting design point during optimisation studies of the proposed cycle in future research work.

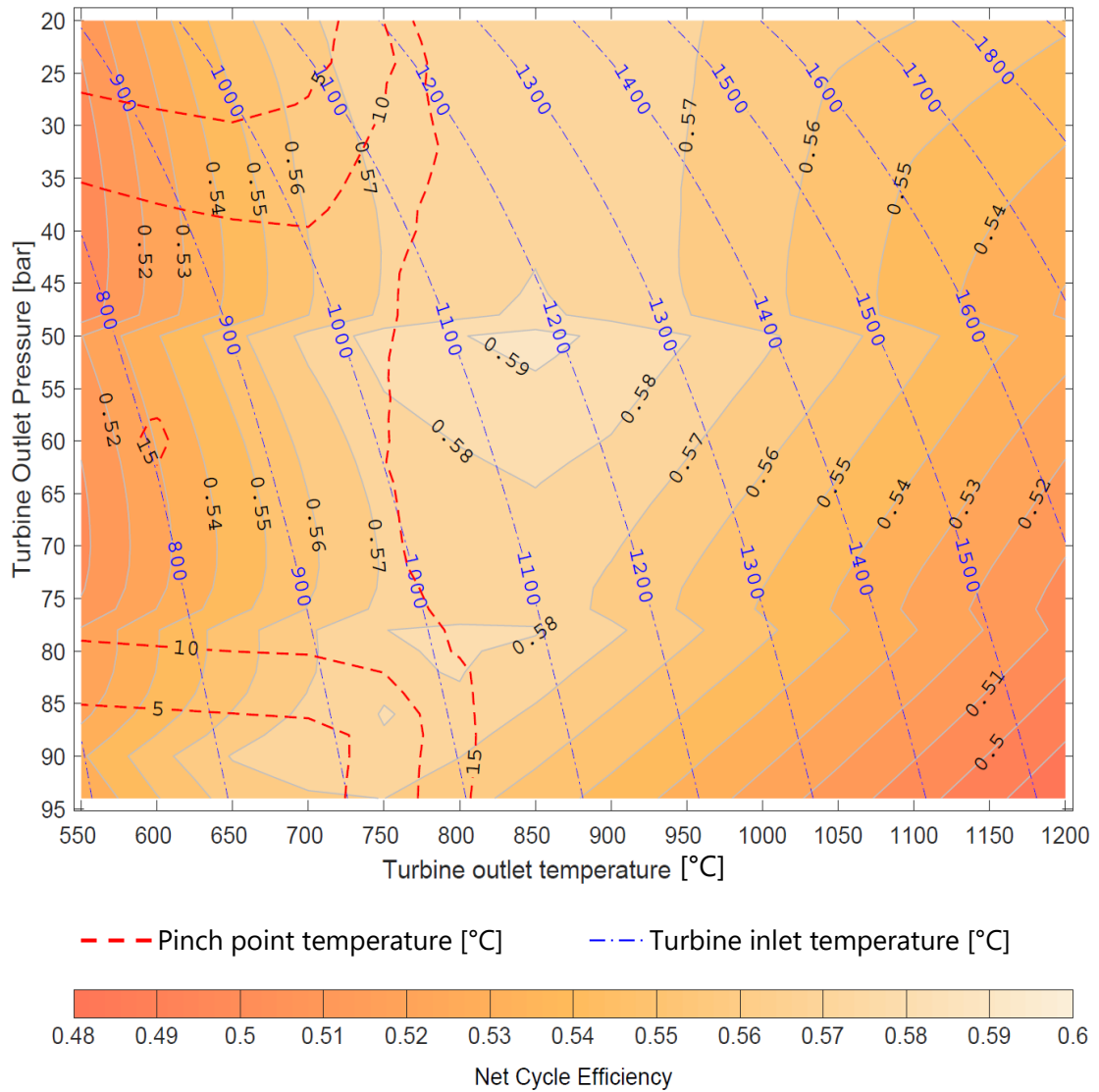


Fig. 39 Performance map

This concludes the thermodynamic evaluation of the proposed internally fired, H<sub>2</sub>/O<sub>2</sub> fuelled s-CO<sub>2</sub> power cycle.

## 5.5 Summary

In this section, key findings of the thermodynamic analysis are summarized.

1. The thermodynamic analysis begins with the selection of the design point for the cycle. The main consideration while selecting the base value for various cycle parameters was that, it should be practically feasible to implement the selected parameters with the current level of technology development. Optimistic values that rely on futuristic developments were avoided as far as possible.
2. After selecting the design point, the configuration of the s-CO<sub>2</sub> cycle was finalized. Different options for the compression and expansion process were available. Using an evaluation based elimination process, a cycle with an intercooled compression process and a simple expansion process was

selected as the final configuration for the power cycle proposed under this project. Details related to this selection process can be found in section 5.2 of this chapter.

3. After selecting the design point and the final configuration for the cycle, a parametric analysis was performed by varying the key design parameters of the cycle. The insight gained from this analysis is briefly outlined in the subsequent points.
4. The first design parameters to be analysed were pressure at the turbine inlet and outlet. The effect of varying TIP on cycle performance was consistent with that expected from a Brayton cycle. It was seen that the efficiency follows the variation in TIP.
5. When the TIP is increased while keeping all other parameters constant, the expansion pressure ratio across the turbine increases. This also causes an increase in TIT (since TOT is held constant), the overall effect being an increase in net cycle efficiency and the net specific work output of the cycle. Inversion of the efficiency curve was not seen within the investigated range of TIPs although, a gradual flattening of the efficiency curve was observed.
6. The general trend in variation of the cycle efficiency caused by varying TOP was consistent with the previous observations. As TOP was increased from its lowest value, the efficiency initially increases (marginally increase of less than 0.5%) and then continues to drop throughout the entire range of TOP. The exception to this trend was that a step change (increment) in the net efficiency was observed at two specific pressure levels. Further analysis revealed that this aberration in efficiency trend was caused when the operating point of the two vapour compressors used in the compression process shifted from the low-density vapour phase region to high-density supercritical region.
7. After analysing the effects of cycle pressure levels, key temperature parameters were analysed. It was found that the limitation imposed by the recuperator design requirements governed the choice of maximum cycle temperature. Therefore, it was opted to use TOT instead of the conventional choice of TIT as the cycle design parameter. The other temperature parameter used to define the cycle was the temperature at the inlet of the compressor(s). This parameter was selected because it is mainly restricted by the temperature of sink used for heat rejection/intercooler, which usually is a function of ambient temperature.
8. The analysis of the effect of TOT highlighted the peculiar behaviour of the s-CO<sub>2</sub> power cycle. Unlike conventional Brayton cycle, the efficiency of the s-CO<sub>2</sub> was found to peak at comparatively lower maximum cycle temperatures in the range of 1300 – 1600 K. This is rather low for a gas-turbine based cycle and is caused by several factors including lower expansion pressure ratios, the effect of turbine cooling, increased heat rejection in the condenser caused by deterioration in heat integration at higher flue gas temperature etc.
9. The efficiency trend caused by variation in compressor inlet temperature was consistent with the expected variation. A decrease in compressor inlet temperature resulted in an improvement in net cycle efficiency mainly caused by the decrease in compressor work requirement.
10. Thermodynamically, it is possible that reduction in compressor inlet temperature has an adverse effect on net cycle efficiency. This occurs when the increase in net specific work output of the cycle

due to the decrease in compressor inlet temperature is outweighed by increased heat requirement due to the decrease in compressor outlet temperature. However, this effect is not seen in the present analysis since the resulting additional heat requirement is fulfilled by recuperation.

11. Having analysed the effect of cycle pressures and temperature, the focus of the parametric analysis was shifted to investigate the effect of individual component performance on the overall cycle efficiency. The parameters studied under this included the LP/HP side pressure drop, isentropic efficiency of the compression and expansion, and the recuperator effectiveness.
12. While analysing the effect of pressure drop on the cycle efficiency, it was found that overall performance was more sensitive to pressure drops occurring on the LP side in comparison to HP side pressure drops. The reason for this effect was that any pressure drop on the LP side of the cycle is ultimately compensated by the VPC while pressure drops on HP side are compensated by DPC. The work requirement of VPC was substantially higher than that of DPC and therefore, it had a larger depreciation on the cycle efficiency. A 10% drop in pressure on the HP side resulted in ~1.5-1.6% drop in net cycle efficiency, while the same drop in LP side pressure would decrease the cycle efficiency by over 4.5%.
13. The next parameter analysed under this study was the isentropic efficiency of the expansion and compression process. In this case, the cycle efficiency was found to be highly sensitive to the isentropic efficiency of expansion. This behaviour is mainly caused by the fact that the specific output of the turbine is much larger than the specific work requirement of the compressor. Thus, a decrease in turbine efficiency will cause the net output to decrease by a larger magnitude when compared to the effect of compressor efficiency.
14. In addition to this, it was seen that the absolute sensitivity to turbine/compressor efficiency was much lower than in the case of conventional Brayton cycle, where for every 1% drop in turbine/compressor efficiency, the net efficiency depreciates by an equal amount. In case of s-CO<sub>2</sub> cycle, 1% drop in isentropic efficiency of the turbine causes ~0.5% drop in net cycle efficiency while 1% drop in compressor isentropic efficiency results in only 0.2% drop in net cycle efficiency.
15. This is very promising from the aspect of scalability of this cycle and based on these numbers it can be expected that the proposed s-CO<sub>2</sub> cycle will have better scaling characteristics in comparison to conventional gas turbine systems.
16. After this, the impact of recuperator effectiveness was analysed. The trend observed was quite monotonous with the net cycle efficiency increasing with increasing recuperator effectiveness. The sensitivity observed was of the same magnitude as that of turbine efficiency; with every 1% drop in recuperator effectiveness causing about a 0.5% drop in net cycle efficiency.
17. The key observation made during this analysis was that of the importance of the recuperation process. For a cycle with 50 MW output, energy added in the combustor by burning fuel was ~85 MW<sub>th</sub>, while that added in the recuperator was ~135-140 MW<sub>th</sub>. These values highlight the highly recuperative nature of the proposed s-CO<sub>2</sub> power cycle, while clearly emphasising the role of the recuperator in achieving the extremely high net cycle efficiencies (> 50%) observed under this thermodynamic analysis.

18. The last effect analysed under this parametric study was to assess the option of using turbine cooling flow to absorb spare thermal energy from the flue gases post the recuperation process and before heat rejection in the condenser. The analysis showed that using this technique, it would be possible to recover some efficiency lost due to deteriorating heat integration at higher TOTs. However, the benefit at practical values of TOT (800 – 1200K), if any, was marginal and it may not always justify the addition of an extra HEX to the cycle. Therefore, it was concluded that case-specific cost-benefit analysis would be needed to assess the feasibility of using turbine cooling flow to recover spare thermal energy from the flue gas mixture after the recuperation process.
19. Lastly, using the thermodynamic evaluation model, a performance map for the proposed cycle was developed. Although this map shows only the initial estimate of the cycle performance, it can be used as a reference while selecting the initial design point during future analyses of this power cycle.
20. With this, the thermodynamic evaluation of the proposed H<sub>2</sub>/O<sub>2</sub> fuelled s-CO<sub>2</sub> power cycle was completed and it was concluded that in the light of the understanding gained from this analysis, achieving high net cycle efficiencies (> 50%) should be generally feasible with the proposed cycle. In addition to this, this power cycle can be expected to have better scaling characteristics compared to conventional gas turbine power systems, although its performance under part-load conditions will have to be critically analysed before this can be stated with a high level of confidence.

# Chapter 6

## Combustion Analysis

### Overview

This chapter discusses the combustion analysis that was conducted in the last phase of the thesis. The first section outlines the basic framework of the combustion study by defining the key objectives and the methodology adopted during the analysis. The second section summarises the literature reviewed during this phase of the project. During this review several H<sub>2</sub>/O<sub>2</sub> combustion mechanisms were studied based on which four mechanisms considered suitable for simulating H<sub>2</sub>/O<sub>2</sub> combustion in high CO<sub>2</sub> environment are shortlisted. In addition to this, some important aspects of H<sub>2</sub>/O<sub>2</sub> combustion reactions are also described in this section. The third section contains the discussion related to finalisation of the combustion simulation package and the combustion mechanism to be used during this combustion analysis while the results of this analysis are reported in the fourth section of this chapter. The combustion analysis discussed in this chapter is concluded by providing a summary of the main findings of the analysis in the fifth and the last section of the chapter.

### 6.1 Framework of the proposed combustion analysis

During the thermodynamic evaluation of the proposed s-CO<sub>2</sub> cycle, all the processes of the cycle were simplified and treated as a mass and energy balance problem across different power cycle components. Although this method gives a decent first level estimation of the cycle performance, it veils all the intricacies of different thermodynamic processes involved in the power cycle. This is especially true for the combustion process, which really is an elaborate thermo-chemical equilibrium problem but gets reduced to a simple process of heat and mass addition instead. Therefore, the thermodynamic analysis

presented in the previous chapter falls short of providing any meaningful information required to understand the chemical kinetics involved in burning  $H_2/O_2$  mixture in s- $CO_2$  environment at elevated pressures and temperatures. Because of this limitation, a preliminary combustion analysis is included in the project with an overall goal of understanding the broad level chemical kinetic involved in combustion of  $H_2/O_2$  in an environment of s- $CO_2$ .

### 6.1.1 Objectives of the combustion analysis

Similar to the case of thermodynamic evaluation, the first task of this module was to set the specific objectives of this analysis and these are briefly defined in subsequent paragraphs.

#### **Objective #1 of the combustion analysis**

It was hypothesized during the thermodynamic evaluation that; *flue gas could be treated as a binary mixture of water and carbon dioxide* and testing this hypothesis is the first objective of this combustion analysis. This is envisaged to be achieved by simulating and studying the combustion of  $H_2/O_2$  mixture with s- $CO_2$  as the bath gas under conditions that closely represent typical a gas turbine combustor arrangement. The combustion parameters required during this evaluation will be calculated based on the design point parameters used during the thermodynamic evaluation.

#### **Objective #2 of the combustion analysis**

The second objective of this analysis is to gain preliminary understanding of the mechanisms involved in the combustion of  $H_2/O_2$  mixture in an s- $CO_2$  environment by analysing the effect of several combustion process parameters on the properties of flue gas generated during combustion. The design parameters included in this analysis are,

- 1) Combustor residence time
- 2) Combustor inlet pressure & temperature
- 3) Dilution rate
- 4) Equivalence ratio

The last two parameters are relevant in case of combustors that have reactant/diluent inlet ports at different location in the combustor and to some extent would represent a staged combustion system. Therefore, the model adopted for the parametric analysis will have a configuration suitable to simulate such a combustion process. More details are included in the following sections of this chapter.

### 6.1.2 Methodology adopted for combustion analysis

After defining specific objectives of the combustion analysis, the methodology required to achieve these objectives was selected. Since a detailed research related to  $H_2/O_2$  combustion was not included in the previous phase of literature review, the task in this module was to study relevant background literature available on this subject. In addition to getting general familiarity with various aspects of  $H_2/O_2$  combustion and the tools/software of combustion analysis, the main aim of this second literature review was to identify suitable chemical reaction mechanisms that could be used to simulate the combustion of  $H_2/O_2$  mixture in s- $CO_2$  environment. Several published mechanisms were reviewed during this selection process which gave valuable insights on the effects  $CO_2$  dilution can have on the kinetics of

the combustion reactions. These aspects are discussed in much greater detail in the second section of this chapter.

After having shortlisted suitable reaction mechanisms, two reactor networks were developed in ANSYS Chemkin Pro<sup>®</sup>, one each for the two objectives defined in the previous section. The main reason for using two different models to achieve the stated objectives was that the reactor network representing a gas turbine combustor is very complicated and the parameters used to control this network were highly interlinked. If such a network was to be used for a parametric study, it would be very difficult to isolate and study the effect of change in individual parameter on the combustion reaction. Therefore, it was decided that the optimum solution would be to analyse combustion at base case parameters in a reactor network representing an actual gas turbine combustor and to use a simplified reactor network for the parametric analysis. After developing the necessary combustion networks, the shortlisted combustion mechanisms were compared with a set of experimental data found during literature review, based on which the final mechanism to be used during this analysis was finalized. These aspects are described in the third section of the chapter.

The last phase of the combustion module consisted of simulating the combustion of H<sub>2</sub>/O<sub>2</sub> mixture using s-CO<sub>2</sub> as the diluent. Running the simulation at the base case parameters selected during thermodynamic evaluation, the flue gas composition was evaluated. This estimated composition was used to test the validity of the aforementioned hypothesis (which was found to hold true). After this validation, the second reactor network was used to analyse the effect of selected combustion parameters on the flue gas properties. The detailed results of this analysis are discussed in fourth section of this chapter.

## 6.2 Literature reviewed on H<sub>2</sub>/O<sub>2</sub> combustion

### 6.2.1 Existing research on hydrogen combustion

Hydrogen combustion has been an active area of research not only because it is the simplest fuel in terms of its chemistry but understanding its combustion chemistry is of key importance since it is a subset of combustion of all hydrocarbons and oxygenated hydrocarbon fuels studied for industrial application. Therefore, several studies have been conducted to investigate hydrogen combustion in a variety of conditions. This resulted in development of numerous reaction mechanisms in the last two decades to numerically model the chemical kinetics of hydrogen combustion. Since testing all these mechanisms was not practical under the current scope of the project, review papers comparing the performance of several of the recent hydrogen combustion mechanisms were relied on as the first level shortlisting criterion. The goal of studying these mechanisms was not limited to selection of the most suitable mechanism for simulation purposes but included a more general intent of getting insights on different combustion aspects such as the main rate determining reaction(s), the effect of CO<sub>2</sub> concentration on these reactions, whether or not the mechanisms are designed to account for such effects etc.

Olm et. al. [55] have analysed the performance of nineteen recent hydrogen combustion mechanisms and compared them with a large set of experimental data. In this study, they have not only ranked these mechanisms based on their overall performance but also identified specific strengths and weaknesses of several mechanisms in predicting different aspects of combustion process such as ignition delay time, species concentration (time profile in flow reactors and outlet concentration in jet stirred reactors (JSR)) and laminar flame velocity measurements. The mechanisms included in this study are listed in Table 14.

Table 14 Recent hydrogen combustion mechanisms compared by Olm et. al. [55]

#	Mechanism name	No. of species analysed (originally proposed)	No. of reactions analysed (originally proposed)	Average error function values <sup>6</sup>				
				A	B	C	D	E
1	<b><u>Kéromnès-2013</u></b>	12 (17)	33 (49)	<b><u>11.9</u></b>	3.0	13.3	<b><u>13.9</u></b>	<b><u>12.2</u></b>
2	NUIG-NGM-2010	11 (293)	21 (1593)	14.0	3.0	7.3	20.2	14.8
3	ÓConaire-2004	10	21	15.4	3.0	8.2	18.5	15.0
4	Konnov-2008	10	33	19.7	3.1	10.9	15.2	16.3
5	Li-2007	11 (21)	25 (93)	20.7	3.0	7.8	16.0	16.8
6	Hong-2011	10	31	14.5	3.0	8.1	28.5	17.9
7	Burke-2012	11	27	26.6	3.1	3.9	14.6	18.9
8	SaxenaWilliams-2006	11 (14)	21 (30)	23.8	3.0	28.3	16.5	20.5
9	Davis-2005	11 (14)	25 (38)	36.7	3.0	4.9	16.4	24.7
10	<b><u>Starik-2009</u></b>	12 (16)	26 (44)	37.4	3.4	<b><u>3.8</u></b>	24.4	27.7
11	USC-II-2007	10 (111)	28 (784)	36.2	3.0	4.7	26.1	27.7
12	CRECK-2012	11 (14)	21 (34)	15.2	2.9	21.4	56.9	29.1
13	SanDiego-2011	11 (50)	21 (244)	78.0	3.0	27.7	16.5	47.7
14	<b><u>GRI3.0-1999</u></b>	10 (53)	29 (325)	71.4	<b><u>2.4</u></b>	11.6	32.0	48.0
15	Sun-2007	11 (15)	32 (48)	97.9	3.1	25.4	26.7	61.0
16	Rasmussen-2008	10 (24)	30 (105)	197.1	3.0	17.8	35.4	113.1
17	Ahmed-2007	10 (246)	20 (1284)	257.9	3.1	3.9	20.7	137.4
18	Zsély-2005	10 (13)	32 (44)	544.3	3.2	15.6	26.0	284.5
19	Dagaut-2003	9 (132)	21 (922)	–	3.1	4.9	–	–

The best performing mechanisms in measurement of individual combustion characteristics are highlighted in the Table 14. As can be seen, the Kéromnès-2013 [56] mechanism is best at predicting the ignition delay time and laminar flame velocity, but does not do so well in predicting the flue gas composition. For calculating the outlet composition in a JSR, GRI Mech 3.0-1999 [57] outperforms all the mechanisms, while Starik – 2009 is best for predicting concentration time profiles in flow reactors. Several other studies [58, 59 & 60] showed similar results and ranked Kéromnès-2013 [56] and NUIG-NGM-2010 [61] (along with few other mechanisms namely, Li-2015, Konnov-2008 etc.) amongst the best performing mechanisms for modeling hydrogen combustion.

Research conducted while development of NET Power cycle combustor is another important work that was referred to during the literature review [62] and it was found that the designers of this combustor used NUIG-NGM-2010 [61] & GRI Mech 3.0-1999 [57] during the development process. Although the NET power cycle is based on oxy-combustion of natural gas, the operating conditions of the combustor in this cycle are expected to be very similar to that in the proposed H<sub>2</sub>/O<sub>2</sub> fuelled s-CO<sub>2</sub> power cycle. Therefore, the combustion mechanisms used during the development of NET power cycle combustor are included in this analysis as well.

### 6.2.2 Selection of combustion mechanisms

It was observed while studying the review papers comparing combustion mechanisms that, although these studies rank the analysed combustion mechanisms in order of their performance, the difference in

<sup>6</sup> The values of the average error function for all mechanisms are given for five cases: A: Ignition delay times, all diluents; B: JSR concentrations, all profiles; C: Flow reactor concentrations, all profile; D: Flame velocities, all diluents except He; E: Overall results, all diluents except He

performance of the top two or three mechanisms was quite less. Therefore, it was decided that instead of selecting the final mechanism solely based on recommendations made in literature, a selected number of mechanisms will first be tested under this module. The mechanisms selected for this analysis are listed below.

1. Kéromnès-2013 [56]
2. NUIG-NGM-2010 [61]
3. GRI Mech 3.0-1999 [57]
4. NUIG-SG-2017 [63]

The choice of shortlisting the first three mechanisms is entirely based on the findings of the literature study. Kéromnès-2013 & NUIG-NGM-2010 are included since these are amongst the best H<sub>2</sub>/syngas combustion mechanisms currently available. Inclusion of GRI Mech 3.0-1999 was motivated by the fact that Olm et. al. [55] showed it to be the best when it comes to predicting concentration of the product gases in JSRs. Therefore, it may prove to be useful, since analysing effect of combustion parameters on flue gas composition was one of the key objectives of this combustion analysis. The fourth and the last mechanism, NUIG-SG-2017, was added to this list because it is an updated version of the Kéromnès-2013 model which was improved by including several critical reactions based on new experimental and theoretical data.

It is envisaged to compare the performance of these four mechanisms vis-à-vis data from H<sub>2</sub>/O<sub>2</sub>/CO<sub>2</sub> combustion experiments during validation. Based on the result of this comparative analysis and the recommendations found in literature, the best performing mechanism will then be selected to study the combustion process of the proposed H<sub>2</sub>/O<sub>2</sub> fuelled s-CO<sub>2</sub> power cycle.

### 6.2.3 Important reactions in H<sub>2</sub>/O<sub>2</sub> combustion mechanisms

Hydrogen combustion reaction is an important subset of reaction mechanisms for hydrocarbon and oxygenated hydrocarbon fuel combustion. Therefore, a large amount of research effort has been dedicated to understanding the thermochemistry of hydrogen combustion. Several studies in this area have shown that reactivity of hydrogen is governed by the competition between the main branching reaction  $\dot{\text{H}} + \text{O}_2 \leftrightarrow \ddot{\text{O}} + \dot{\text{O}}\text{H}$  (R1) and the pressure dependent chain terminating reaction  $\dot{\text{H}} + \text{O}_2(+\text{M}) \leftrightarrow \text{H}\dot{\text{O}}_2(+\text{M})$  (R9). In addition to this, at high pressures the thermal decomposition of hydrogen peroxide (H<sub>2</sub>O<sub>2</sub>) via the pressure-dependent reaction  $\text{H}_2\text{O}_2(+\text{M}) \leftrightarrow \dot{\text{O}}\text{H} + \dot{\text{O}}\text{H}(+\text{M})$  (R15) becomes an important chain branching reaction<sup>7</sup>. Lastly, from high pressure reactivity point of view, the reaction between hydroperoxyl radical and fuel is also particularly important. This reaction is as follows  $\text{H}\dot{\text{O}}_2 + \text{H}_2 \leftrightarrow \text{H}_2\text{O}_2 + \dot{\text{H}}$ .

The dependence of hydrogen reactivity on these reactions is clearly seen from the sensitivity analysis [56] performed on Kéromnès-2013 mechanism (Fig. 40). The figure represents the effect of reaction rate constants on the ignition delay times calculated for a mixture of H<sub>2</sub>/O<sub>2</sub>/N<sub>2</sub>/Ar (molar composition: 1/1/1.88/1.88) over a wide range of operating pressure (1-100 atm at temperature of 1000 K) and a range of operating temperature (850-1200 K at pressure of 1 atm). The analysis was carried out by doubling

---

<sup>7</sup> The reaction numbering used in this section are kept constant throughout the report. For an instance, reaction R1 will refer to the main branching reaction ( $\dot{\text{H}} + \text{O}_2 \leftrightarrow \ddot{\text{O}} + \dot{\text{O}}\text{H}$ ) throughout the report.

and halving each reaction rate and measuring the corresponding ignition delay times  $\tau'$  and  $\tau''$ , respectively. The sensitivity coefficient  $\sigma$  is calculated using equation (12);

$$\sigma = \frac{\log\left(\frac{\tau'}{\tau''}\right)}{\log\left(\frac{2}{0.5}\right)} \quad \dots(12)$$

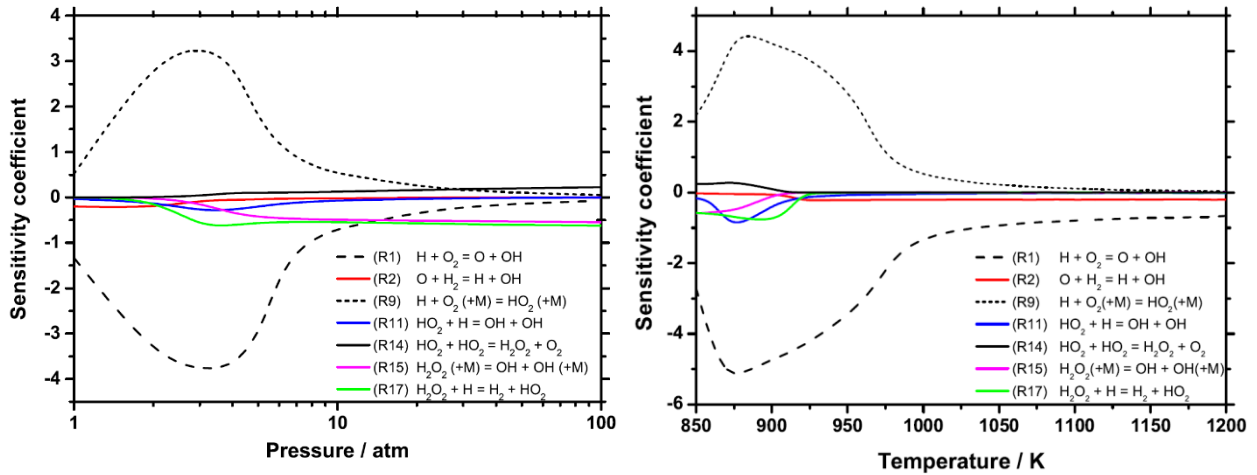


Fig. 40 Sensitivity analysis of ignition time delays as a function of pressure at 1000 K [56]

If the reactivity of the mixture increases upon doubling the rate constant and reduces when rate constant was halved, it would lead to  $\tau' < \tau''$  and  $\sigma < 1$ . In other words, the reactions with a negative sensitivity coefficient increase the reactivity in the mixture, while those with a positive sensitivity coefficient decrease the reactivity. The left plot (sensitivity with varying pressure) clearly shows the dominance of reactions R1 and R9 at low pressure condition and the increasing importance of the reactions R15 and R17 at higher pressures. The plot representing variation in sensitivity co-efficient at different temperatures shows that as temperature increases, the mixture reactivity is mainly governed by the main branching reaction. This analysis was done with a mixture of  $N_2$  and Ar as the bath gas and it would be quite interesting to see the effect of using  $CO_2$  on reactivity of hydrogen. Therefore, this topic was further pursued and is discussed in the following subsection.

#### 6.2.4 Effect of $CO_2$ dilution on kinetics of $H_2/O_2$ combustion

Studying the effects of high  $CO_2$  concentration during hydrogen combustion is of interest for wide ranging applications like syngas combustion, combustion with exhaust gas recirculation, etc. Many studies have found  $CO_2$  to have an inhibiting effect on hydrogen combustion reaction [64 & 65]. The common explanation found for this behaviour is that  $CO_2$  molecule has a higher third body collision efficiency as compared to nitrogen. Thus, at low temperatures, use of  $CO_2$  as diluent enhances the inhibiting effect of the main chain terminating reaction R9, over the main branching reaction R1. At higher temperatures, where the importance of reactions R9 partly diminishes,  $CO_2$  promotes the occurrence of binary reaction,  $CO_2 + \dot{H} \leftrightarrow C\dot{O} + \dot{O}H$ , which reduces the availability of hydrogen radicals, reducing the rate of main branching reaction R1.

The effect of  $CO_2$  dilution can be separated into two different phenomena. First, being a physical/thermal effect mainly caused by its higher heat capacity in comparison to nitrogen and argon, while the second being the kinetic effect that can be attributed to its higher third body collision efficiency. The thermal effect reduces the temperature rise post combustion (assuming the same combustor inlet temperature),

while the kinetic effect presents itself in form an increase in ignition delay. Although the two effects are inter-related, Sabia et. al.[65] in their analysis were able to demonstrate these effects separately by making some clever assumptions. First, they simulated  $H_2/O_2$  combustion using pure  $N_2$  and  $CO_2$  as diluents. These simulations were performed for the same combustion parameters, under the assumption of non-adiabatic condition with a global heat exchange coefficient equal to  $0.0015 \text{ cal/cm}^2\text{sK}$ . They used Polimi mechanism for this analysis. After comparing the results obtained,  $N_2$  was assigned the thermal properties of  $CO_2$  while maintaining its actual value of third body efficiency and ignoring the  $NO_x$  reactions from the Polimi mechanism. This allowed them to study only the thermal effect  $CO_2$  dilution. Subsequently, they assigned the third body collision efficiency of  $CO_2$  to  $N_2$  while maintaining the change in thermodynamic database made in the previous step. This allowed them to account for both thermal and kinetic effect (caused by third body reaction of  $CO_2$ ). The results of these simulations are shown in fig. 41.

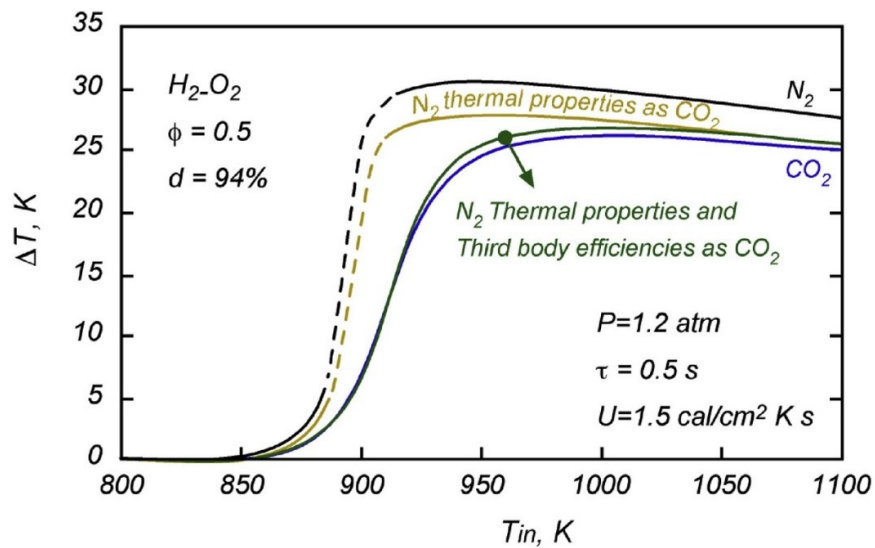


Fig. 41 Temperature profile changing with  $N_2$  thermodynamic and kinetic properties[65]

As can be seen in Fig. 41, black curve represents the case of using pure  $N_2$  as the diluent while the blue curve shows the case of pure  $CO_2$  as diluent. The olive-green curve represents the case when  $N_2$  was assigned the thermal properties of  $CO_2$  while the dark green curve shows the result of case when  $N_2$  was assigned both thermal and kinetic properties of  $CO_2$ . The dash part of the black curve shows the region of instability that is caused by a set of competing chemical reactions when using  $N_2$  as the diluent. The rightward shift (increase in ignition delay) of the blue and the dark green curve is indicative of the reduction in the mixture reactivity caused by  $CO_2$  dilution.

When nitrogen is assigned the thermal properties of  $CO_2$ , the temperature rise observed across the combustor is lower than that observed in case of  $N_2$  dilution. This trend is consistent with the expected behaviour of the mixture since the specific heat capacity of  $CO_2$  is higher than that of  $N_2$ . In addition to this effect, a slight decrease in mixture reactivity can also be observed from the rightward shift of the olive-green curve. These two observations clearly indicate that the thermal effect of  $CO_2$  dilution strongly affects the final temperature of combustion products while its influence on the mixture reactivity is quite small.

Similarly, when  $N_2$  is assigned both the thermal properties of  $CO_2$  and its third body collision efficiency, the resulting trend is similar to that seen in the case  $CO_2$  dilution. This shows that the reduced reactivity and increased ignition delay when using  $CO_2$  dilution are mainly caused by the kinetic effects of increase

in third body efficiency. As noted, the green and blue curves are very similar but not the same and the small deviation observed can be attributed to participation of CO<sub>2</sub> in the bimolecular reactions which cannot be accounted by simply assigning the properties of CO<sub>2</sub> to N<sub>2</sub>.

This concludes the discussion about the literature reviewed on H<sub>2</sub>/O<sub>2</sub> combustion. the key take-aways are as follows,

- Understanding the kinetics of hydrogen combustion is crucial not only for applications that directly use hydrogen as fuel, but for all cases where combustion analysis of any hydrocarbon fuels is involved.
- Four reaction mechanisms were shortlisted for further analysis during this literature review. These are Kéromnès-2013, NUIG-NGM-2010, GRI Mech 3.0-1999 & NUIG-SG-2017.
- It is envisaged to test these mechanisms against a set of experimental datapoint during model validation phase and select the mechanism that gives the most suitable results.
- After this, some key reactions that dictate the combustion characteristics of hydrogen were analysed. This was first done for a conventional case of H<sub>2</sub>/O<sub>2</sub>/N<sub>2</sub>/Ar mixture and later for case with CO<sub>2</sub> dilution.
- It was found during this analysis that CO<sub>2</sub> dilution causes two main effects on H<sub>2</sub>/O<sub>2</sub> combustion reaction. First, due to its higher heat capacity, CO<sub>2</sub> dilution results in lowering of the equilibrium mixture temperature (in comparison to N<sub>2</sub>/Ar case). Secondly, CO<sub>2</sub> also induces a kinetic effect by means of its higher third body collision efficiency that tends to decrease the reactivity of hydrogen and increase its ignition delay time.
- These findings are expected to be relevant from the combustion analysis perspective of the proposed H<sub>2</sub>/O<sub>2</sub> fuelled s-CO<sub>2</sub> power cycle.

## 6.3 Combustion model development

### 6.3.1 Selection of combustion simulation package

After a brief discussion on important aspects of hydrogen combustion, this section focusses on the combustion model development process. The first part of this process was to select the software that would be used for these simulations. Both Cantera and ANSYS Chemkin Pro<sup>®</sup> were available for use in this analysis. In terms of technical capabilities, both these software have fairly similar capabilities [66] except for the ease factor that Cantera offers while integrating it with other programs to run large sets of simulations. However, the advantage of using ANSYS Chemkin Pro<sup>®</sup> is that, unlike Cantera, all its capabilities are neatly organized by means of user-friendly GUIs that makes running combustion simulations a less daunting task for beginners.

At the start of the modelling process, both these packages were used to run test simulations on H<sub>2</sub>/O<sub>2</sub>/CO<sub>2</sub> mixture in simple one PSR network. The results from software were in good agreement and key findings from this exercise were, 1) It was very easy to setup standalone simulations and build complex reactor networks in ANSYS Chemkin Pro<sup>®</sup> although data post processing step required longer runtime in case of large datasets 2) It would be advantageous to use Cantera if the combustion model had to be integrated with the thermodynamic model and in cases where large set of conditions had to be simulated.

Based on the experience of running above mentioned test simulations, it was decided to build the current combustion model using ANSYS Chemkin Pro<sup>®</sup> mainly because of its user friendliness. Integrating the combustion model with the MATLAB based thermodynamic model is not envisaged under this project

and therefore, the choice of ANSYS Chemkin Pro<sup>®</sup> presents no real disadvantage. However, if at a later stage in this research the two models must be integrated, it would be preferable to switch the current combustion model to Cantera because of its higher integration capabilities and more efficient handling of a large number of simulations.

### 6.3.2 Selection of combustion mechanism

#### 6.3.2.1 Initial assessment of the shortlisted mechanisms

In this sub-section, the performance of the shortlisted mechanisms is compared at expected combustor operating pressure and temperature. Combustion process assuming a single Perfectly Stirred Reactor (PSR) and a reactant mixture of H<sub>2</sub> (10.29%), O<sub>2</sub> (5.14%) & CO<sub>2</sub> (84.57%) was analysed. The temperature and pressure in the combustor were assumed to be equal to the base case parameters of the thermodynamic analysis. The residence time was varied from 10 micro-seconds to 10 seconds. Result of this simulation was obtained in terms of the temperature and the flue gas composition at the outlet of the PSR. These results are presented in Fig. 42 and Fig. 43.

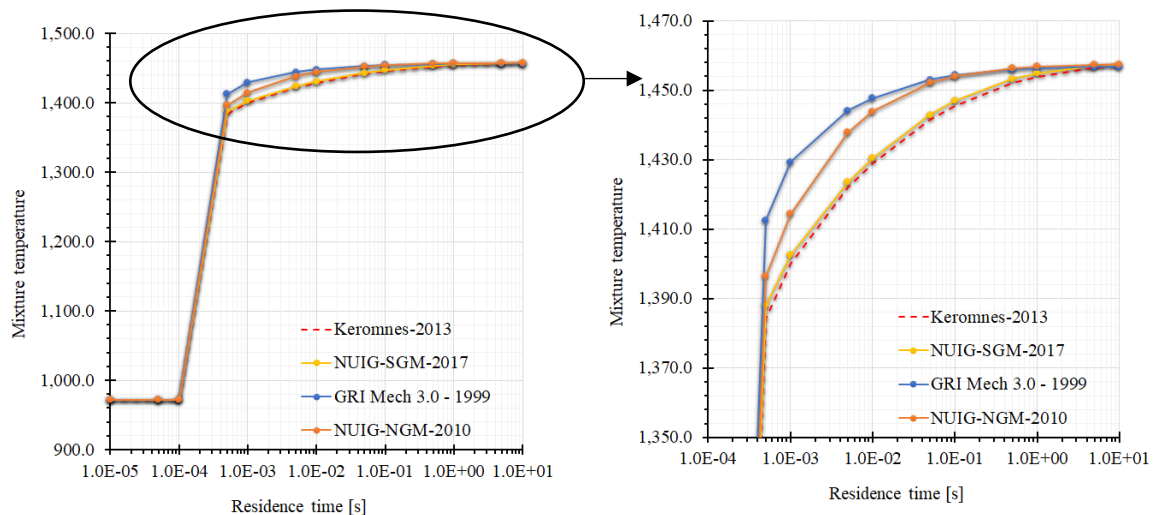


Fig. 42 Flue gas temperature at outlet of PSR predicted using shortlisted mechanisms

The following are the key points that can be observed based on this analysis.

1. Flue gas was predicted to be a mixture of same molecular species even though the overall number of species included in each mechanism varies drastically. It should be noted that all the species with molar concentrations smaller than 1E-9 or 1 ppb are ignored in this analysis.
2. The estimated FG temperature is plotted in Fig. 42. From this plot it can be said that for large enough residence times, all mechanisms tend to predict the same equilibrium temperature while this is not the case for shorter combustor residence times. It can be seen that the two reaction mechanisms optimized for natural gas combustion (GRI MECH 3.0 and NUIG-NGM-2010) tend to over predict mixture reactivity and result in faster temperature rise (also seen as faster reduction in H<sub>2</sub>/O<sub>2</sub> concentration). This observation is well supported by the previous discussion on effects of CO<sub>2</sub> dilution.

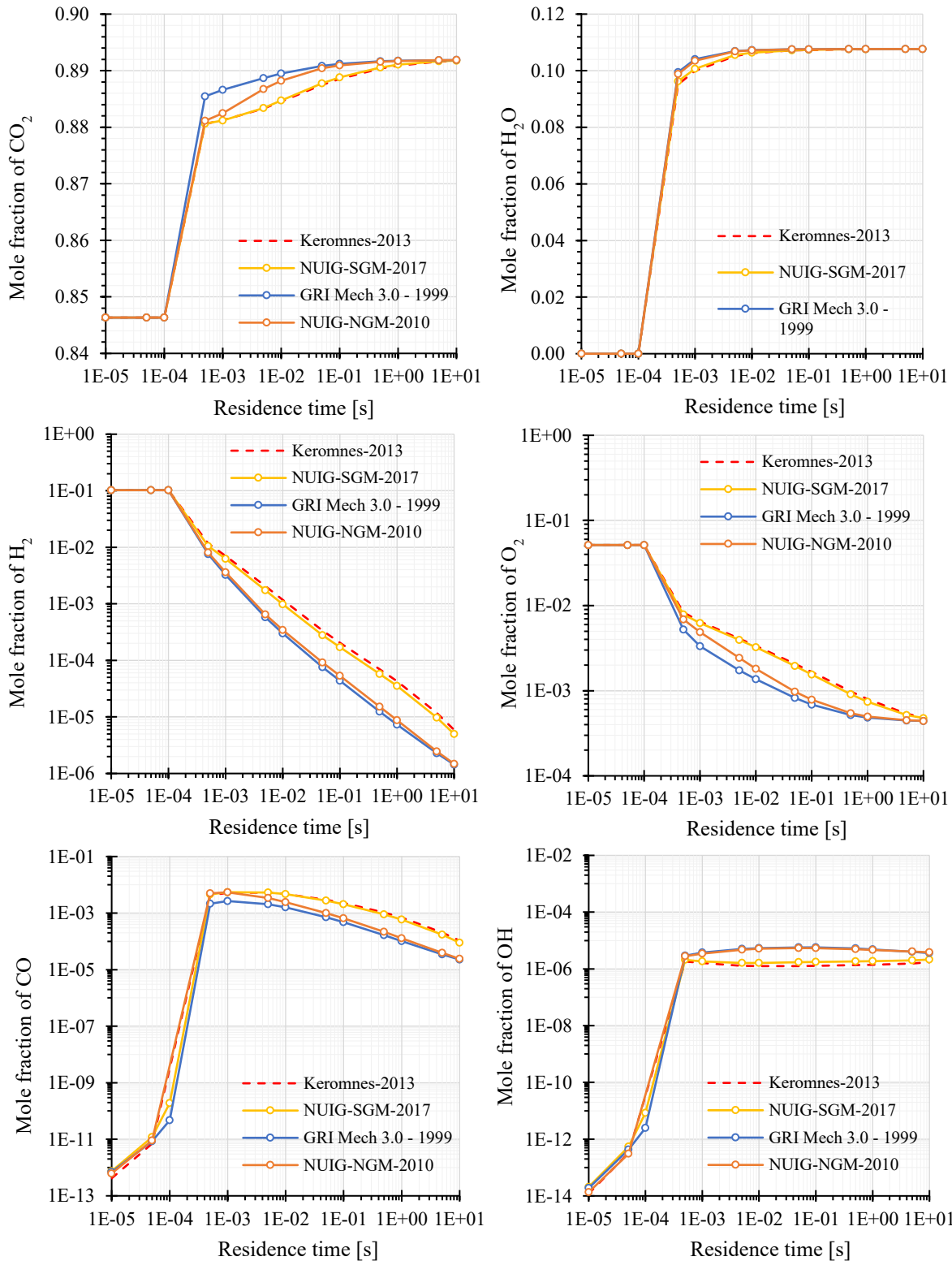


Fig. 43 Concentration of the main products of H<sub>2</sub>/O<sub>2</sub>/CO<sub>2</sub> combustion at 300bar & ~1450K

3. All the mechanisms account for the thermal effect of high concentration of CO<sub>2</sub> in the combustion process. This is evidently supported by the fact that all mechanisms predict similar flue gas temperatures at very long residence times. However, both the natural mechanisms seem to neglect the kinetic effects of CO<sub>2</sub> dilution and therefore, they overestimate the reactivity of

the mixture. A similar effect was demonstrated by Sabia et. al. [65] by assigning thermal properties of CO<sub>2</sub> to N<sub>2</sub> without changing its third body collision parameters. The result of this change showed a similar trend to the one seen in Fig. 41 (refer section 6.2.4 for more details)

4. The last point to be discussed is the grouping behaviour displayed by shortlisted mechanisms as seen in Fig. 43. It can clearly be seen that both the natural gas combustion mechanisms tend to predict very similar values, whereas the other two H<sub>2</sub>/syngas mechanisms also tend to estimate almost the same results. The cause of this behaviour is most likely rooted in the manner in which effect of CO<sub>2</sub> dilution is accounted in both these sets of reaction mechanism. The H<sub>2</sub>/syngas mechanisms (designed for combustion in high CO<sub>2</sub> environment) do seem to account for the kinetic effects of CO<sub>2</sub> dilution while the NG mechanisms seem to ignore this effect. In addition to this, the H<sub>2</sub>/syngas mechanisms included in this analysis are relatively new in comparison to the natural gas mechanisms. The reaction parameters such as rate co-efficient, etc., included in them are likely to be more accurate at predicting reaction behaviour in comparison with the other two mechanisms.
5. Therefore, as was found during literature review [55, 56–58], the two recent H<sub>2</sub>/syngas mechanisms may clearly have an edge in estimating parameters like ignition delay and mixture temperature, while not enough data is available at present to compare and comment on the quality of FG composition predictions made by these 2 sets of combustion mechanisms.

### 6.3.2.2 Comparison of the shortlisted mechanisms with experimental data

In this sub-section, the flue gas parameters predicted by combustion simulations using the shortlisted mechanisms are compared with actual experimental results. Experimental data from the study (Sabia et. al. [65]) analysing the combustion of H<sub>2</sub>/O<sub>2</sub> mixture in several bath gases, including CO<sub>2</sub>, will be used for this purpose. The dataset published by these authors includes the measured value of temperature rise and concentration of H<sub>2</sub>, O<sub>2</sub> and CO at exit of the reactor, tested at various mixture inlet temperatures. The experiments were conducted in a fused silica JSR having a volume of 113 cm<sup>3</sup>. The tests were done under lean conditions with the equivalence ratio held constant at  $\phi = 0.5$  with a dilution ratio of 94%. The inlet temperature of the mixture was varied between 800 – 1000 K while the pressure was held constant at 1.2 atm. The volumetric flow rate was adjusted such that the averaged residence time in the reactor was held at  $\tau = 0.5$  seconds. In this case,  $\tau$  is defined as the ratio of volumetric flow rate of the mixture and the reactor volume measured under non-reactive conditions. The experiment was known to be non-adiabatic and therefore, a heat exchange co-efficient approximating the heat loss in the set-up is defined by the author for each test case. In case of CO<sub>2</sub> dilution, the value of heat exchange co-efficient is assumed to be equal to 2.25 E-3 cal/cm<sup>2</sup>Ks. Having briefly outlined the experimental set-up used by Sabia et. al in their study, it is useful to discuss the simulation set-up that will be used. The simulation will be based on a single PSR operating under non-adiabatic conditions. Knowing the heat transfer co-efficient to be used, reactor surface area through which heat transfer takes place was required. Since there we no details about this in the experimental set-up, it was assumed that the JSR used in the experiment is was spherical in shape with a radius of 3 cm. Based on this assumption, the surface area of the reactor can be calculated and used while setting up the PSR. The mixture composition used in the experiment as well as the simulation is a pre-mixed mixture of H<sub>2</sub>/O<sub>2</sub>/CO<sub>2</sub> in the 3%/3%/94% by volume which is same as saying the mole fraction of H<sub>2</sub>/O<sub>2</sub>/CO<sub>2</sub> in the mixture is 0.03/0.03/0.94 respectively. The experimental data published by Sabia et.al. [65] is shown in Table 15.

Table 15 Experimental data used to compare the shortlisted combustion mechanisms [65]

$T_{inlet}$ [K]	$\Delta T$ [K]	H <sub>2</sub> concentration	O <sub>2</sub> concentration	CO concentration
868	0	3.000E-02	3.000E-02	0.000E+00
875	0	2.930E-02	3.000E-02	0.000E+00
887	0	2.930E-02	3.000E-02	0.000E+00
897	0	2.930E-02	3.000E-02	0.000E+00
905	0	2.930E-02	3.000E-02	0.000E+00
915	2	2.680E-02	2.906E-02	0.000E+00
915	2	2.647E-02	2.877E-02	0.000E+00
925	5	2.370E-02	2.655E-02	8.700E-05
934	8	2.081E-02	2.447E-02	1.530E-04
935	9	1.989E-02	2.530E-02	1.840E-04
940	10	1.721E-02	2.348E-02	2.630E-04
940	10	1.679E-02	2.280E-02	2.880E-04
959	16	1.327E-02	2.250E-02	4.400E-04
959	16	1.323E-02	2.227E-02	4.280E-04
970	16.2	1.106E-02	2.140E-02	5.510E-04
982	16	8.859E-03	2.015E-02	7.060E-04
982	16	8.867E-03	1.945E-02	6.900E-04
996	15.5	7.474E-03	1.974E-02	8.400E-04
996	15.5	7.715E-03	1.973E-02	7.300E-04
1005	15	6.530E-03	1.972E-02	8.920E-04
1005	15	6.770E-03	1.971E-02	8.510E-04
1014	15	5.768E-03	1.972E-02	9.480E-04
1014	15	5.689E-03	1.973E-02	9.820E-04

The plots shown in Fig. 44 compare the experimentally measured values of temperature rise, H<sub>2</sub>, O<sub>2</sub> and CO concentrations with the values predicted by simulation using the four shortlisted mechanisms. Looking at first plot showing the temperature rise across the reactor the trend seen in experimental data is slightly different from one seen in simulated data. In case of experimental data, the temperature rises quickly over a shorter range of inlet temperatures when compared to simulated data. There could be several factors causing this deviation, the key ones in decreasing order of probability are error in simulated data due to use of approximate heat transfer coefficient, error introduced in experimental data set during temperature measurement, varying inlet temperature of the mixture etc. However, the flue gas temperature appears to be stabilizing in the same range for both experimental and simulated data therefore, the results can be considered acceptable for the current investigation.

The interesting point to note here is that the grouping observed in previous analysis and shown in Fig. 43 can again be seen in the plots of Fig. 44, albeit it is not as prominent as in the previous analysis. The deviation between the mechanisms optimized for NG/air mixtures (NUIG-NGM-2010 and GRI Mech 3.0) and those optimized for H<sub>2</sub>/syngas combustion (NUIG-SG-2017 and K eromn es -2013) could be lower in the present case mainly because of the lower system pressure. As was discussed in section 6.2.4, the inhibiting effects of CO<sub>2</sub> by means of increased third body collision efficiency is more pronounced at higher pressure and thus, the deviation between the two sets of mechanisms was more in the previous analysis.

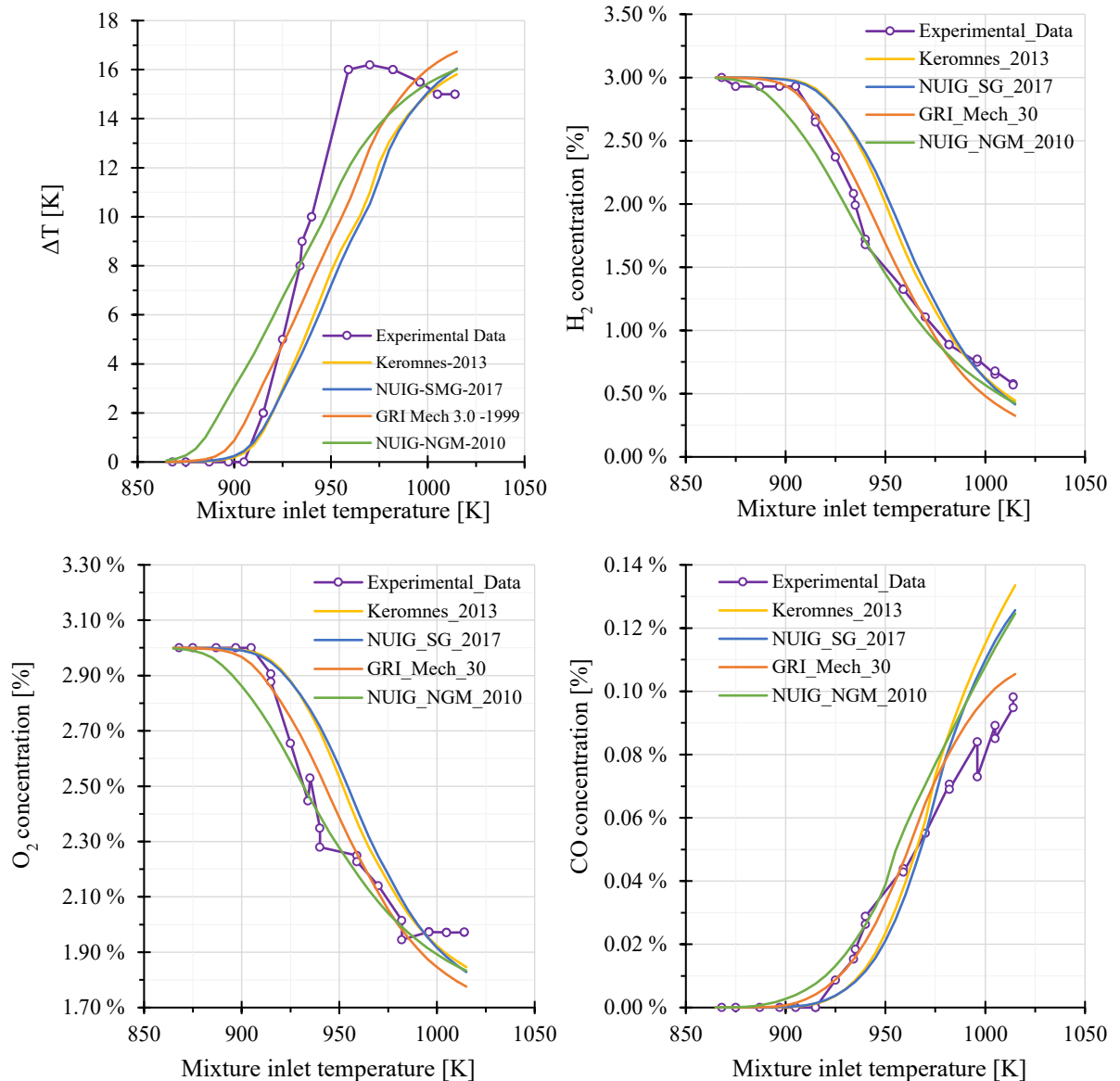


Fig. 44 Experimental data [65] vis-à-vis simulated results from shortlisted mechanisms

Another important observation related to the temperature rise plot is that both K eromn es -2013 and its updated version NUIG-SGM-2017 seem better at predicting the mixture inlet temperature at which temperature rise across the reactor occurs, in other words, these mechanisms tend to better model the ignition delay. This is in line with the findings of the studies mentioned in section 6.2, including the one by Olm et. al. [55], which had ranked K eromn es-2013 as the best available  $H_2/O_2$  combustion mechanism, to model ignition delays and laminar flame velocities. The results of this analysis tend to align with this observation.

In addition to this, the trends seen in mixture concentration profiles are also consistent with the rankings of the of Olm et. al. study [55], where GRI Mech 3.0 was ranked as the best mechanism to model JSR concentration profiles. GRI 3.0 most closely matches the species concentration profiles that are experimentally observed. The specialized  $H_2$ /syngas mechanisms tend to underestimate the mixture reactivity as evidenced by the higher concentration of  $H_2/O_2$  in the flue gas mixture. In case of predicting

CO concentration, only GRI 3.0 shows resemblance to the trend seen in the experimental data while all other mechanisms tend to overestimate the CO levels for mixture inlet temperature over 1000K.

### 6.3.2.3 Final choice of the combustion mechanism

Overall, the analysis conducted for the selection of combustion mechanism leads to a split conclusion. On one hand, GRI Mech 3.0 evidently outperforms other shortlisted mechanisms in predicting the mixture composition at lower operating pressures. This trend is also supported by findings from the literature reviewed on this topic. However, in absence of experimental data at higher operating pressure, its suitability for simulating  $H_2/O_2/CO_2$  combustion in high-pressure applications cannot be verified. To add to this predicament, there is data (refer discussion related to Fig. 42 and Fig. 43) that indicates it GRI Mech 3.0 (and other natural gas combustion mechanisms in general) may overestimate the reactivity of hydrogen at higher operating pressures.

The  $H_2$ /syngas combustion mechanisms, on the other hand, are designed and optimized to be used in combustion application which typically operate in high  $CO_2$  concentration environment. Therefore, these were found to be better at predicting combustions parameters like the ignition delay and the flue gas temperature. In both previous analyses, however, Kéromnès-2013 and NUIG-SGM-2017 showed the tendency to estimate higher CO levels during combustion in comparison to those predicted by the other two NG combustion mechanisms. Although this may not be desirable in other combustion studies, in the scope of the present investigation this tendency to overestimate CO is not necessarily a bad thing. If anything, the estimates obtained using the  $H_2$ /syngas mechanisms can be treated as the conservative, higher-end values of expected CO levels in flue gas at combustor outlet. Since one of the objectives of this combustion analysis is to validate the hypothesis that flue gas can be treated as binary mixture of  $CO_2$  &  $H_2O$ , it is rather preferable to consider the conservative values of minor species and change the hypothesis to include more species in the flue gas mixture if it fails upon scrutiny than to consider the lower and optimistic estimate of values of the minor species concentration and moving ahead with an erroneous hypothesis.

Therefore, in light of all these considerations, it is decided to not opt for GRI 3.0 mechanism and to use a specialized  $H_2$ /syngas mechanism instead. From amongst the two specialized  $H_2$ /syngas mechanisms analysed, it was decided to use Kéromnès-2013 since it has been around for a few years now and widely regarded as the best mechanism for modelling  $H_2$  combustion systems. NUIG-SG-2017, although is technically an update of Kéromnès-2013, it is a relatively new mechanism and has not yet been studied and tested as widely as Kéromnès-2013. Apart from this, the difference observed between these mechanisms was not substantial and thus, it was decided to opt for the more published and referred mechanism over its updated but relatively new version.

## 6.4 Combustion Studies

After finalizing the combustion simulation package and reaction mechanism to be used, the simulations required for achieving the objectives of this modules could be performed. These simulations are divided into two parts. The first set of simulations study the combustion process at the design point selected during the thermodynamic evaluation. In this, a combustor flow arrangement similar to a typical gas turbine is adopted. Combustion simulations are performed using the Kéromnès-2013 mechanism and the results obtained are evaluated to test the validity of the hypothesis made while developing the thermodynamic model. The second part of this analysis is related to the parametric study of the combustion process that was discussed in the beginning of this chapter.

### 6.4.1 Design point combustion analysis

The combustor inlet parameters for this simulation are selected based on the thermodynamic evaluation of the proposed cycle at the selected design point and are listed in Table 16. In addition to this, a typical gas turbine combustor flow arrangement is assumed where part of the diluent enters the combustor in the primary combustion zone while the remaining diluent flow is added in the dilution zone. This is pictorially represented in Fig. 45. It should be noted that the flow ratios shown in Fig. 45 are arbitrarily selected to keep the maximum temperature in the combustor below 1800K.

Table 16 Combustor inlet parameters at design point

Flow Stream	Pressure [bar]	Temperature [K]	Mass Flow rate [kg/s]	Flow fraction [%]
H <sub>2</sub> stream at primary inlet	303.03	298.15	0.7189	100%
O <sub>2</sub> stream at primary inlet	303.03	298.15	5.7511	100%
CO <sub>2</sub> stream at primary inlet	303.03	1040.2	50%	
CO <sub>2</sub> stream at secondary inlet	303.03	1040.2	65.005	50%

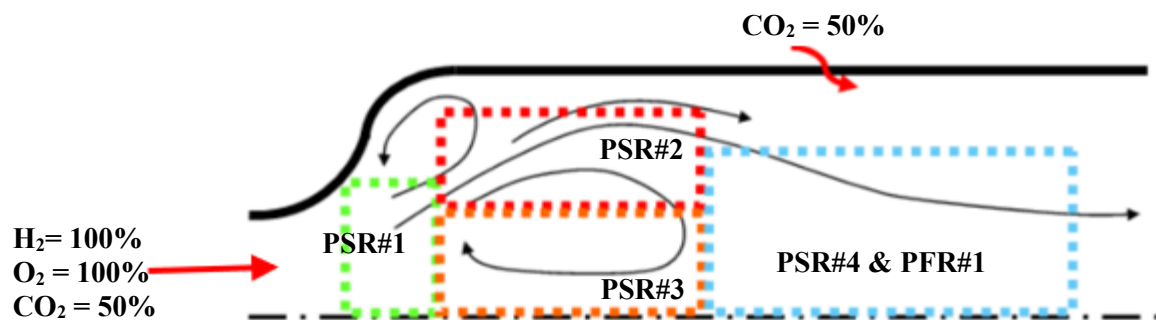


Fig. 45 Flow distribution (shown as % of total flow) in the base case of combustion simulation

After assuming the combustor configuration, it was converted to reactor network in ANSYS Chemkin Pro<sup>®</sup>. The gas turbine combustor network included in user manual of this simulation package was adopted with necessary modifications. The reactor network designed to represent this combustor flow arrangement is shown in Fig. 46. The first 3 PSRs together represent the primary ignition zone while PSR#4 and PFR#1 represent the secondary zone of the combustor.

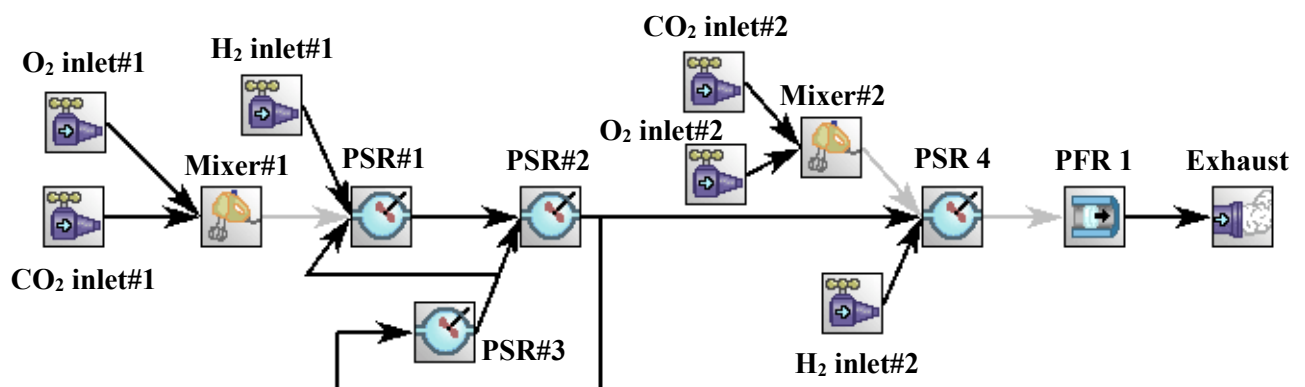


Fig. 46 Reactor network used for design point combustion analysis

Along with flow parameters, a few other reactor settings are assumed in this simulation. Given that the residence time in industrial gas turbine combustor is typically between 10-40 ms, the total residence time assumed in the present simulation was ~35 ms. This is split across different reactors as shown in the Table 17 below. The residence time in PFR reactor is indirectly set by varying its length and cross section area. The length of combustor selected (arbitrarily) in this case is 30 cm with a cross section area of 0.2 m<sup>2</sup>. The overall dimensions of the combustor can be put in perspective by assuming an annular cross section and a combustor height of ~15 cm, the outer radius of the combustor can be calculated to be ~30 cm. In addition to this, flue gas recycling was set-up such that, 20% of gases in the flame zone are recycled back to recirculation zone while 80% is sent to dilution zone. Gases entering the recirculation zone are split further in two equal parts and sent to mixing zone and flame zone, respectively.

Table 17 Reactor parameters used during base case simulation.

Name of Reactor	Pressure [bar]	Initialisation Temperature [K]	Residence time [ms]
PSR#1: Mixing Zone	303.03	1000	0.25
PSR#2: Flame Zone	303.03	1700	1.50
PSR#3: Recirculation Zone	303.03	1700	1.50
PSR#4: Dilution Zone	303.03	1460	0.25
PFR#1: Post-flame zone	303.03	1495	~30.5

Having set the necessary parameters of the combustion model, combustion process at design point was simulated. It was found that the flue gas temperature predicted by the combustion model (1458.43K) is in very good agreement with the temperature estimated during thermodynamic evaluation (1457.28K) based on heat and mass balance. The important minor species in FG mixture (molar concentration > 1.E-6 at outlet of combustor) are O<sub>2</sub>, CO, H<sub>2</sub> and OH<sup>8</sup>. This simulation proves that the minor molecular species with largest concentration that can potentially affect the properties of the flue gas mixture are the unburnt reactants and CO. The results of this simulation are plotted in Fig. 47 and Fig. 48.

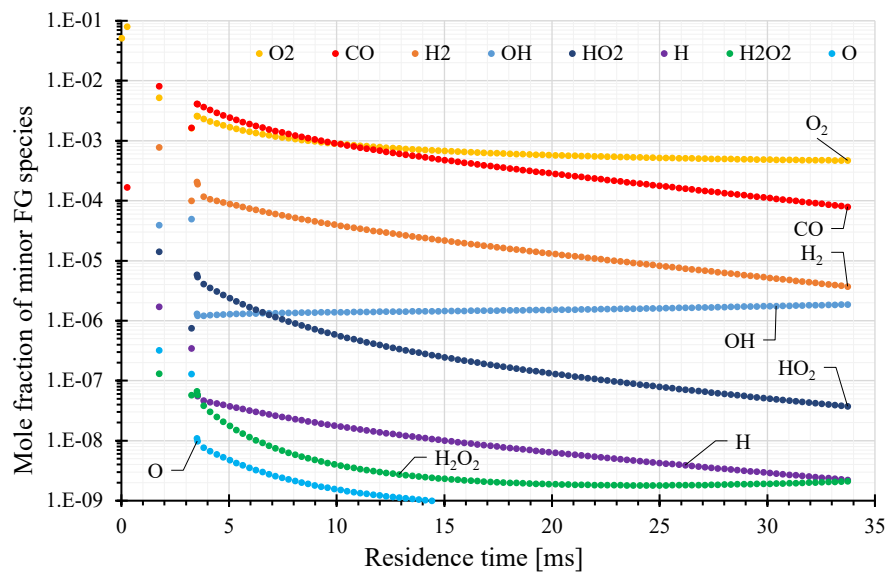


Fig. 47 Evolution of flue gas mixture composition during combustion

<sup>8</sup> All species with concentration larger than 1 ppm are considered except for OH since the selected database does not support calculation of thermodynamic properties of radical species.

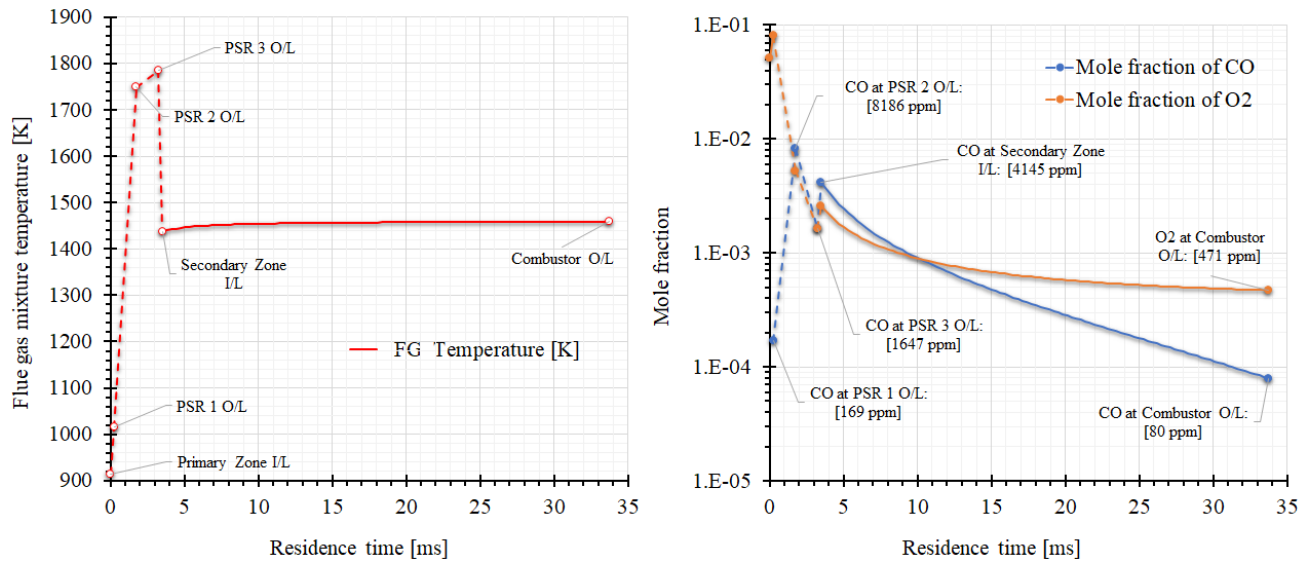


Fig. 48 Temperature profile and evolution of O<sub>2</sub>/CO concentration profile at design point

After calculating the flue gas composition at design point, effect of minor species on mixture property was analysed. Four cases are considered in the calculation. The first case takes into account the complete flue gas composition obtained from the simulation. The second case accounts for the major species plus the unburnt reactants but ignores the CO concentration in the flue gas. The third case represents the hypothesis made in the model and considers flue gas as a binary mixture of CO<sub>2</sub> and H<sub>2</sub>O. The fourth case where flue gas is treated as pure CO<sub>2</sub> is included mainly to highlight the error this assumption would induce in the calculations. The result of this analysis is presented in Table 18.

Table 18 Estimation of deviation in flue gas properties caused by ignoring minor species.

	Case 1	Case 2	Case 3	Case 4
Flue gas temperature [K]	1458.43			
Flue gas pressure [bar]	300			
Major species	CO <sub>2</sub> [89.1786%] H <sub>2</sub> O [10.7658%]	CO <sub>2</sub> [89.1858%] H <sub>2</sub> O [10.7666%]	CO <sub>2</sub> [89.2282%] H <sub>2</sub> O [10.7718%]	CO <sub>2</sub> [100%]
Minor species considered	O <sub>2</sub> [471.37 ppm] H <sub>2</sub> [3.74 ppm] CO [79.74 ppm]	O <sub>2</sub> [471.51 ppm] H <sub>2</sub> [3.74 ppm]	[--]	[--]
Sp. heat capacity [J/kg. K]	1404.9750	1404.9827	1405.0742	1344.014
Deviation [%]	Base value	5.47 E-04 %	7.06 E-03 %	-4.34%

As can be seen from Table 18, the hypothesis that flue gas can be treated as a binary mixture of CO<sub>2</sub> and H<sub>2</sub>O is valid since the observed deviation caused by this presumption is negligible (case 3). The deviation seen in case 4 (when flue gas is treated as pure CO<sub>2</sub>) highlights the need of modeling the flue gas as a mixture, in absence of which large errors can be expected in the cycle calculations. It is also interesting to see that the deviation caused by ignoring the unburnt reactants (and CO) in case 3 is an order or magnitude larger than the deviation caused by just ignoring the CO in the flue gases in case 2.

From this it can be said that, ignoring unburnt reactants (i.e. assuming complete combustion) results in a larger deviation in flue gas properties than that caused by neglecting the CO component. Having said that, the overall deviation in either case is quite small ( $\ll 1\%$ ) and therefore, both, the assumption of complete combustion and the hypothesis of FG being a binary mixture, can be considered to be valid.

#### 6.4.2 Parametric study

The base case simulation of the combustion model creates a reference point for the expected behaviour of an  $H_2/O_2$  combustion process diluted by s- $CO_2$ . From this simulation it was identified that, amongst all the intermediate products of combustion, CO and OH are the only major contaminants in the flue gas post combustion. To get a better insight into the combustion process, a parametric study was conducted to see the effects of 1) residence time 2) combustor inlet pressure and temperature 3) dilution rate and 4) equivalence ratio. The reactor network representing the gas turbine combustor was not very suitable for this analysis since it would need controlling a large number of reactor network variables causing 1) the simulation to become complicated and more prone to errors 2) make the simulation outcome dependent on all those variable settings making it that much harder to isolate and identify the effect of the parameter of interest. Therefore, it was decided to perform this analysis using a simple reactor network consisting of only two PSR each with its independent supply of fuel, oxidizer, and diluent to adjust the flow rates as needed. This decision greatly reduced the complexity of setting up the parametric study. The reactor network used for parametric study is shown in Fig. 49. In addition to this, given that carbon monoxide was found to be the most abundant minor product of combustion in the flue gas mixture (not counting unburnt  $O_2$ ), only the plots tracking evolution of CO concentration and the temperature profile under different conditions are included in this section. However, other species were also monitored to keep note of deviant behaviour and this is included in the discussion as and when needed.

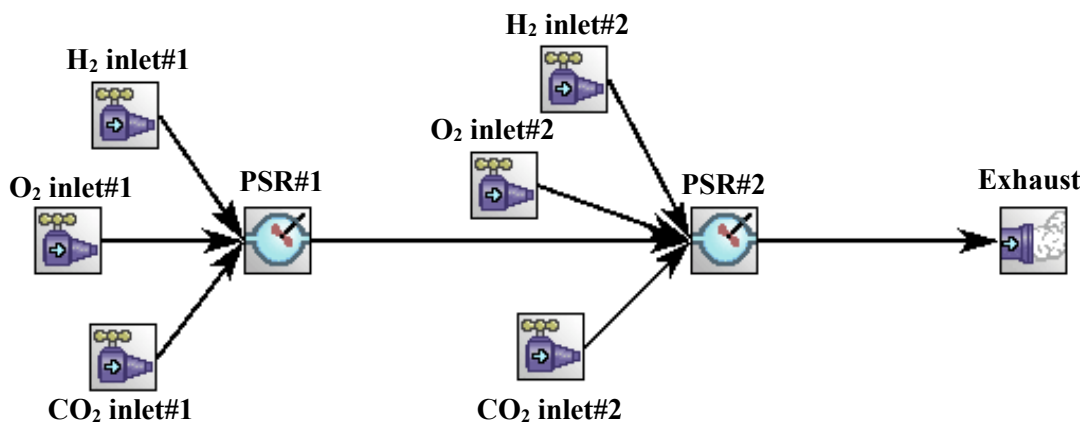


Fig. 49 Reactor network used for parametric study of the combustion process

In the following subsections, the effect of each of the five parameters listed above are discussed. All parameters are kept constant at values reported in the previous section (as in base case scenario) except for the one parameter which is being studied. Residence time, unless specified otherwise, is split equally between the two PSRs. Lastly, it is useful to take note of the interpretation of the terms  $CO_2$  dilution rate and equivalence ratio in the present context. Since the total flow of  $H_2/O_2/CO_2$  is fixed, both these terms pertain to the first PSR. Any flow that remains is added in the second combustor. Therefore, both dilution rate and equivalence ratio of the second PSR always stays the same i.e. 100% and  $\phi_{PSR2} = 1$  respectively. Equations (13) and (14) define both these terms for PSR#1.

$$\text{Dilution rate in PSR\#1} = \frac{\text{CO}_2 \text{ added in PSR 1}}{\text{Total flow of CO}_2} \quad \dots(13)$$

$$\text{Equivalence ratio, } \phi = \phi_{\text{PSR}_1} = \frac{\left(\frac{\dot{m}_{\text{O}_2}}{\dot{m}_{\text{H}_2}}\right)_{\text{stoichiometric}}}{\left(\frac{\dot{m}_{\text{O}_2}}{\dot{m}_{\text{H}_2}}\right)_{\text{PSR}_1}} = \frac{8}{\left(\frac{\dot{m}_{\text{O}_2}}{\dot{m}_{\text{H}_2}}\right)_{\text{PSR}_1}} \quad \dots(14)$$

### 6.4.2.1 Effect of combustor residence time

The effect of variation of combustor residence time is an integral part of this analysis and will be studied in collaboration with all other listed parameter as well. Albeit the main effects of residence time variation are discussed in this section.

The first point to consider is the relevance of residence time parameter in the context of combustor design. Combustion reactions require a very long time to reach equilibrium, however, designing for such long residence time usually requires an impractically large combustor, making it unfeasible. Another problem associated with systems having long residence time is high NO<sub>x</sub> emission, although this is not a concern in the present context since the project is proposed based on oxy-combustion of hydrogen in CO<sub>2</sub> environment – making NO<sub>x</sub> emission irrelevant. However, this is one of the biggest predicaments while designing air based combustion systems, since other unwanted products of combustion like CO and UHC reduce when using long residence time and higher combustor operating temperature, while NO<sub>x</sub> tends to increase in these conditions. Therefore, understanding the fundamental mechanisms of combustion and the behaviour of the species involved in combustion reactions under varying operating conditions is critical for designing modern combustors required to meet with stringent emission norms.

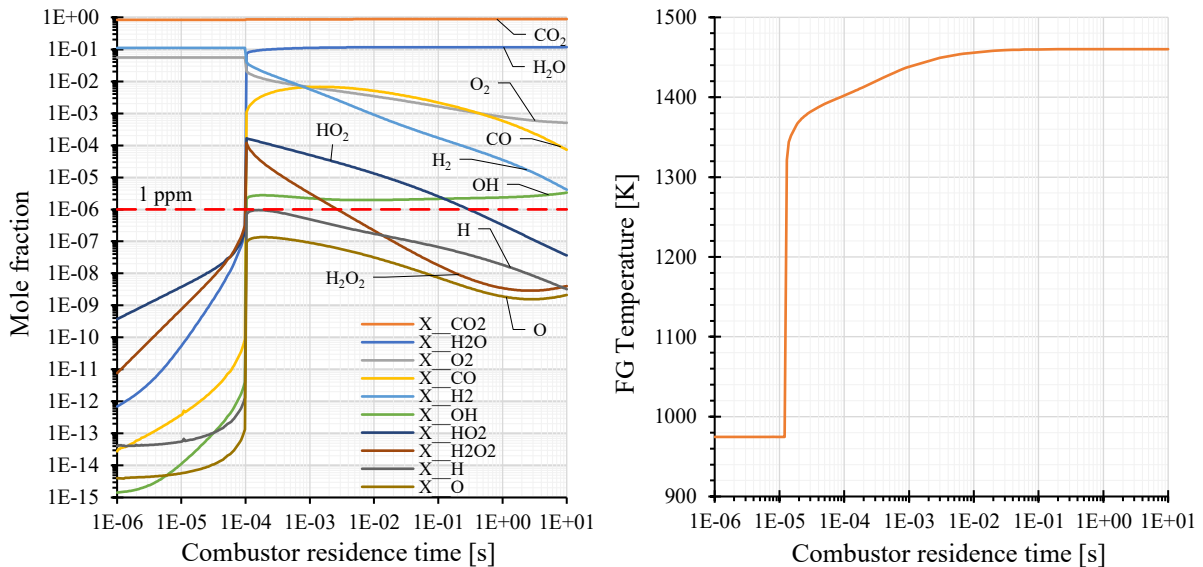


Fig. 50 Effect of combustor residence time on the flue gas properties

The effect on varying residence time on flue gas properties in a combustor is shown in Fig. 50. The first graph shows variation of species concentration at the combustor outlet under different residence time ranging from 1 $\mu$ s – 10seconds. To give sense of scale, for the flow parameters of the base case simulation, a combustor with ~12 m<sup>3</sup> of volume would be required to provide a residence time of 10

seconds. This is just too large to be feasible for most applications (similar to proposed configuration). And even with such a large residence time, the concentration profiles of many species still seem to be evolving. Fortunately, most of these species have a negligible concentration and therefore, it does not matter if all reactions do not reach equilibrium condition in the combustor. Hence, combustors are usually designed such that, the concentration of the most important minor products are reduced to sufficiently low values before the flue gas leaves the combustor. Like the molar concentration of species, flue gas takes exceedingly long residence time to reach their equilibrium temperature. This is partly seen in the second plot in Fig. 50 where the exit temperature of flue gas appears to end as an asymptote.

### 6.4.2.2 Effect of combustor operating pressure

The effect of operating pressure on the combustion is studied by varying the pressure in the range from 250 bar to 450 bar. Dilution rate and equivalence ratio in PSR#1 are dilution rate = 50% and  $\phi = 1$ . The results of these simulations are shown in Fig. 51.

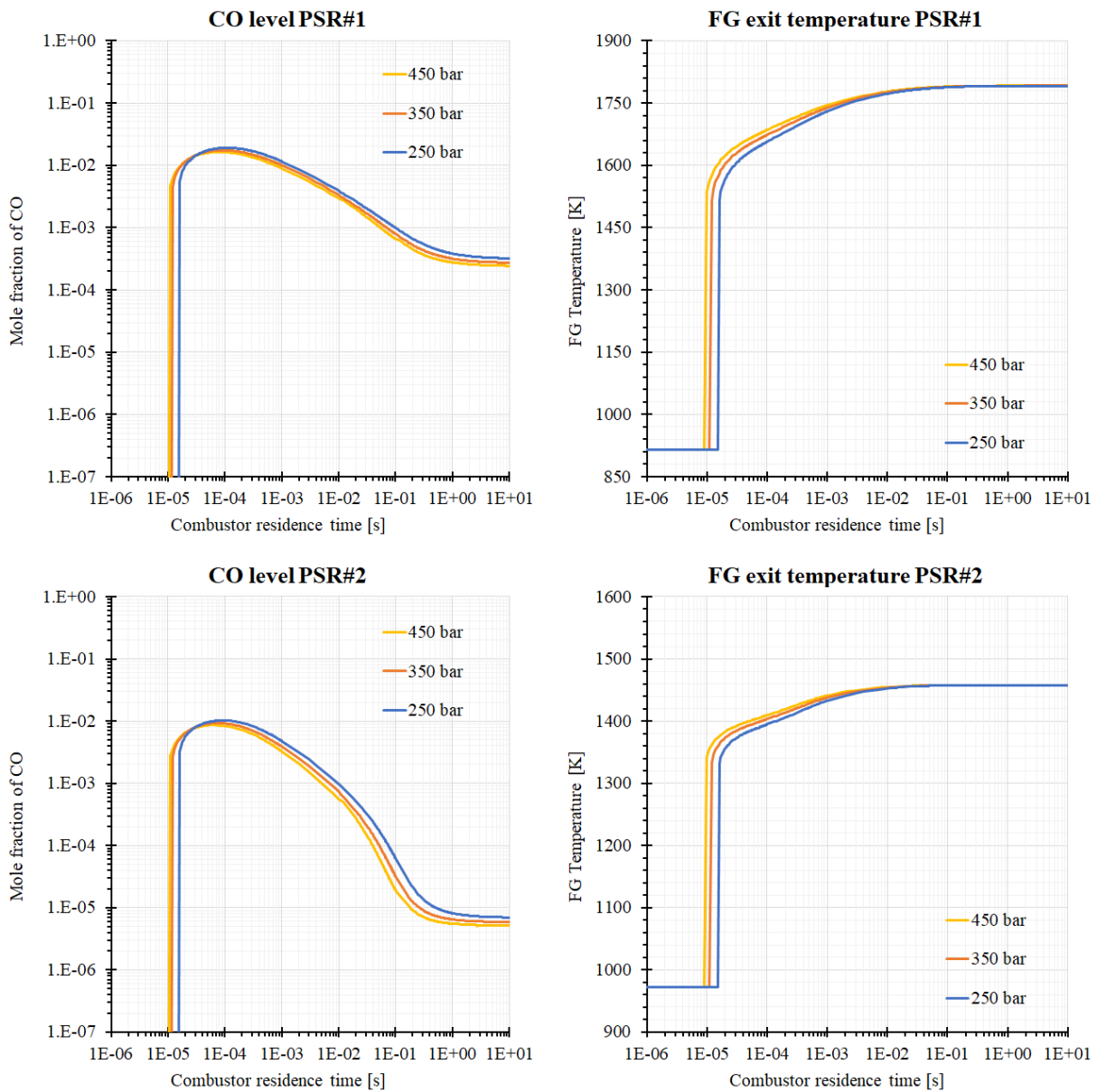


Fig. 51 Effect of combustor inlet pressure on the flue gas properties

Increasing the pressure of a gaseous chemical reaction in generally enhances the rate of reaction since the molecular interactions (collisions) increase with pressure. This effect can be clearly observed in the plots shown in fig. 51. The decrease in ignition delay and time required to achieve chemical equilibrium (stabilized flue gas properties) are indicative of the increased mixture reactivity at higher pressures. The other visible effect of increase in combustion pressure is the fact that CO levels in the combustor reduces with increase in combustion pressure. This is an expected trend given that in the current combustion set-up, CO is mainly formed either by means of direct dissociation of CO<sub>2</sub> or by bimolecular reactions of CO<sub>2</sub> with the H/O/OH radicals. The concentration of these radicals is also ultimately dependent on the dissociation of fuel and oxidizer molecules. An increase in pressure, in general, discourages the dissociation reactions – a trend that is consistent with the behaviour predicted by Le Chatelier's principle. This finally results in an overall decrease in CO level with increase in combustion pressure causing the trends seen in the plots in Fig. 51.

Having said that, the important point to note from these plots is that, from a practical point of view, combustion aspects such as the variation in flue gas property with change in combustion pressure is not expected to be large enough to influence the choice of the operating pressure of the combustor. Instead the mechanical aspects of the combustor design are likely to dominate this choice during the design process.

#### 6.4.2.3 Effect of combustor operating temperature

The combustor inlet temperature is an indirect function the temperature of the CO<sub>2</sub> stream because both fuel and oxidizer are assumed to be available at constant temperature (ambient temperature) and requisite pressure. Therefore, to analyse the effect of inlet temperature, the incoming temperature of diluent stream is set at 1273.15K, 773.15K & 1043.15K – the highest, the lowest and the base value considered in thermodynamic model. As in the previous case, the dilution rate and equivalence ratio in PSR#1 are dilution rate = 50% and  $\phi = 1$  while the combustor pressure is set at 303.03 bar. The resulting variation in flue gas profile is reported in Fig. 52.

The effect of varying inlet temperature of mixture on its reactivity is much stronger than the effect of varying its inlet pressure. As can be the seen from the plots in Fig. 52, the time required for the combustion initiation (characterized by the spike in flue gas temperature) increases substantially when the inlet temperature of the mixture is reduced. In case of the highest mixture temperature analysed (achieved when temperature of CO<sub>2</sub> stream at combustor inlet is 1273.15K), the residence time at which the initial temperature rise occurs was about  $\sim 5\mu\text{s}$  while it was over  $\sim 100\mu\text{s}$  in case of the lowest mixture temperature analysed. In case of hydrogen combustion, the reactivity at lower temperatures is mainly controlled by the balance between the main branching reaction  $\dot{\text{H}} + \text{O}_2 \leftrightarrow \dot{\text{O}} + \dot{\text{O}}\text{H}$  (R1) and the chain terminating reaction  $\dot{\text{H}} + \text{O}_2(+\text{M}) \leftrightarrow \text{H}\dot{\text{O}}_2(+\text{M})$  (R9). However, as the temperature increases, the balance between these two reactions starts favouring reaction R1 which causes the reactivity of the mixture to increase rapidly. Hence, the trends observed in the flue gas temperature profile.

An increase in mixture inlet temperature causes the flue gas temperature to increase as well, which in turn, increases the rate of constant of the CO<sub>2</sub> dissociation reaction. The sub-mechanism modelling CO reactions during combustion is an important rate determining factor in H<sub>2</sub>/O<sub>2</sub>/CO<sub>2</sub> combustion and therefore, CO formation/consumption is an integral step of the combustion process. Higher temperature in the combustor promotes/enhances both the CO forming and CO consuming set of reactions. Therefore, based on the CO concentration profile shown in Fig. 52 one can observe that, not only the peak CO level but also the rate of CO oxidation (characterized by the rapid decrease in CO level) after reaching the peak is higher in case of the higher mixture inlet temperature.

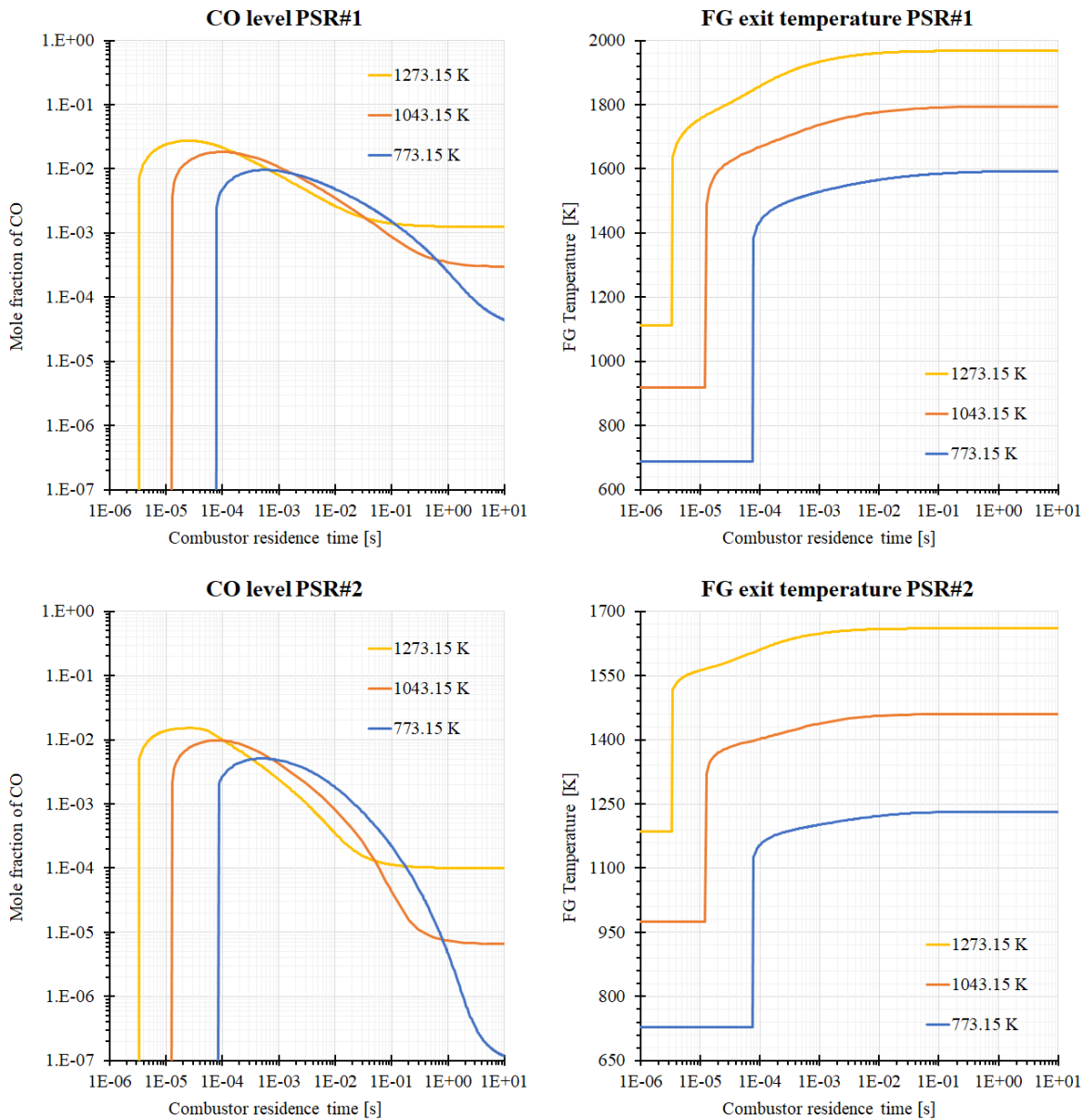


Fig. 52 Effect of combustor inlet temperature on the flue gas properties

#### 6.4.2.4 Effect of CO<sub>2</sub> dilution rate

The dilution rate in the combustor is controlled by varying the flow rate of CO<sub>2</sub> entering PSR#1 through CO<sub>2</sub> inlet#1 shown in Fig. 53. This directly affects two main combustor parameters, 1) the temperature of reacting mixture 2) Initial concentration of CO<sub>2</sub> in the reactant mixture. The first effect is seen as the downward shift of the temperature curves (pre-ignition) in the Fig. 53 while the second effect can be deduced from rising temperature levels (post-ignitions) and the leftwards shift of the temperature curve, in the combustion chamber. Both these effects are phenomenologically discussed in this section.

The CO<sub>2</sub> stream causes two thermal/physical effects in the reactant mixture. Firstly, it heats up the fuel/oxidizer mixture from its ambient temperature and secondly, it dilutes the mixture which increases the heat absorbing capacity of the mixture. Hence, when the flow rate of CO<sub>2</sub> in the first reactor is reduced, the temperature of the reactant mixture under non-reactive condition starts to drop and this is

seen by the downward shift of the temperature curves in PSR#1. But this also leads a reduction in the overall amount of the mixture available to absorb the heat release during combustion. This results in a larger peak in the local temperature in PSR#1 post ignition.

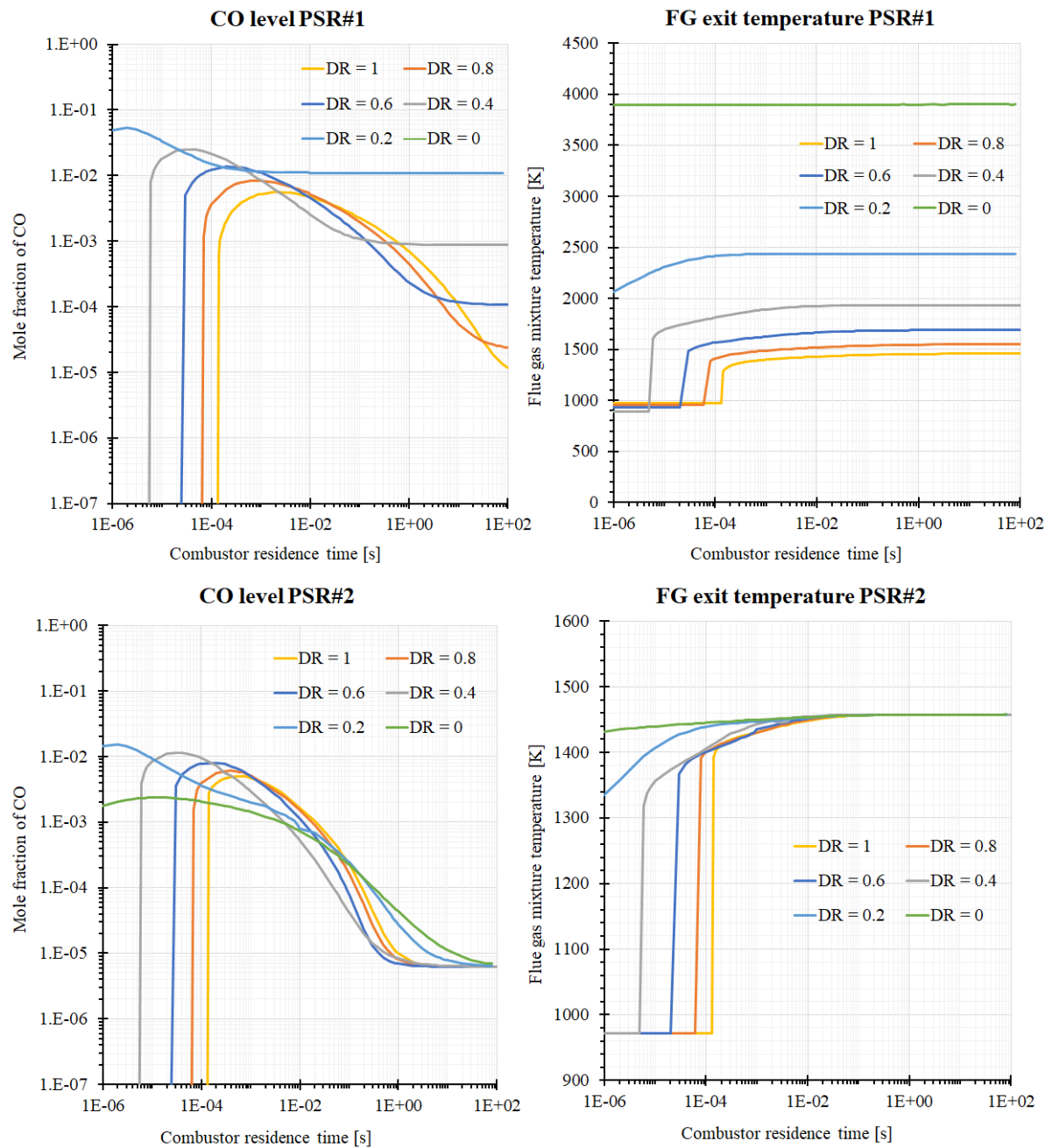


Fig. 53 Effect of dilution rate on the flue gas properties

In addition to these two physical effects, CO<sub>2</sub> dilution level must also affect the kinetics the combustion reactions. This is because the trend observed in this case – a decrease in mixture temperature caused by a decrease in CO<sub>2</sub> flow rate in PSR#1, decreases the ignition delay (time at which the initial temperature spike is observed) – is contradictory to the trend observed while studying the effect of mixture inlet temperature. The main difference in these two cases is that, in the previous case, the mixture composition remained constant while the inlet temperature was reduced and in the present case both mixture temperature and CO<sub>2</sub> dilution decreases. This behaviour quantitatively demonstrates the effect of CO<sub>2</sub>

dilution previously discussed in section 6.2.4, key points of which are repeated here for better clarity. CO<sub>2</sub> induces an inhibiting effect on H<sub>2</sub>/O<sub>2</sub> combustion. It not only enhances the rate of the main chain terminating reaction (R9), but also actively participate in bimolecular reactions reducing the concentration of H radicals and in turn slowing the rate of the main branching reaction (R1). Therefore, a decrease in CO<sub>2</sub> concentration leads to an increase in mixture reactivity characterized by the leftward shift of the temperature curves (i.e. a reduction in ignition delay).

After analysing the trends seen in flue gas temperature curves, the trends observed in CO formation are discussed. As the temperature increases, rate of all chemical reactions generally increases due to increased molecular activity and the equilibrium in case of reversible reactions is governed by how fast the rate of forward reaction changes relative the reverse reaction. In case of reactions involving CO, the rate of CO producing reaction increases at a faster rate as compared to its reverse reaction (i.e. CO oxidation reactions). This does not necessarily change the direction of the net reaction; however, it does increase the CO concentration that the mixture can support at equilibrium. Thus, one can notice the CO curves in PSR#1 stabilize at higher CO concentration as the dilution rate decreases (local temperature increases). This tendency of increase in equilibrium CO concentration is applicable even to the previous analysis related to mixture inlet temperature and can be observed in fig. 52 as well.

The variations seen in PSR#2 are not as prominent as the trends seen in PSR#1. This is simply because the flue gas mixture leaving PSR#1 is diluted with the remaining amount of CO<sub>2</sub>  $[(1 - D.R) * \dot{m}_{total,CO_2}]$ . FG temperature in all cases stabilizes at the same final value as would be expected since the heat release in all cases is more or less constant and the variation in flue gas composition is not large enough to affect its bulk thermal properties. Hence, thermal balance dictates this case and causes the final temperature to practically be the same. Also, under pre-ignition conditions, temperature in all cases must be almost equal since entire flow rate reactant/diluent was now introduced in the combustion chamber.

Flue gas composition on the other hand, does see some variation in concentration of minor species as an effect of changing dilution rate<sup>9</sup>. This is because the final concentration of minor species and time required to reach equilibrium are both functions of the prevailing flue gas condition at the inlet of PSR#2. As the rate of dilution decreases, the peak CO level formed increases but also the rate at which it is re-oxidized increases. This generates an interesting trend that can be observed in the Fig. 53. As the combustor residence time increases, the choice of optimum dilution rate (one that results in lowest CO level at PSR#2 outlet) shifts towards higher values. For practical combustor systems, residence time will vary from few milliseconds to tens of milliseconds. In this range of residence time, the optimum dilution rate (for this particular reactor network) ranges between 0.4 and 0.6. It is important to take note of the fact that the reactor network used in this analysis does not consider flue gas recirculation and no temperature limitation in the combustor is imposed. If the effect of flue gas recirculation was accounted, it will tend to promote oxidation of CO formed during combustion and thereby pushing the optimum value of dilution rate towards a higher range (>0.6). If a maximum temperature limit is imposed during the combustor design, the optimum dilution rate tends to increase as the value of maximum allowable temperature is decreased (with the lowest possible temperature occurring at dilution rate =1).

---

<sup>9</sup> Variation is only seen when limited residence times are considered. At exceedingly long residence time (>10s), the flue composition eventually stabilizes to almost the same values.

### 6.4.2.5 Effect of varying the equivalence ratio

Similarly, the effect of varying the PSR#1 equivalence ratio ( $\phi_1$ ), was analysed and the resulting plots are shown in Fig. 54. The value used in base case simulation is  $\phi_1 = 1$  and this is varied to show results for case of rich combustion  $\phi_1 = 1.4$  and a case of lean combustion  $\phi_1 = 0.6$ . In all three cases the dilution rate was held constant at value of 50% as in the base case simulation. The equivalence ratio was varied, either by limiting the flow of oxygen in PSR#1 (rich condition) or by limiting the flow rate of hydrogen in PSR#1 (lean condition).

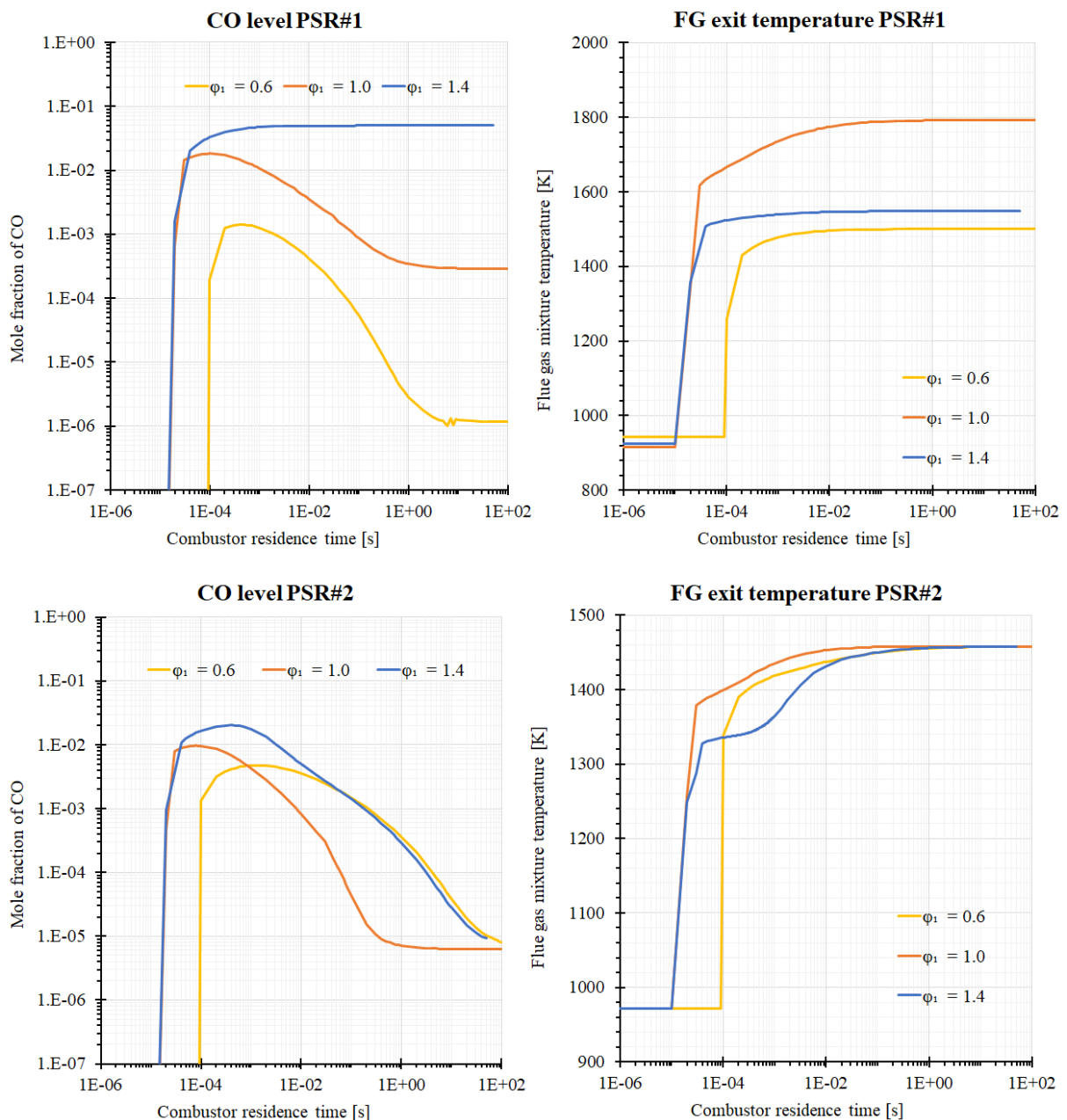


Fig. 54 Effect of equivalence ratio on the flue gas properties

Since both the reactants enter the system at an ambient temperature ( $\sim 298.15\text{K}$ ), a reduction in flow rate of either reactant cause the mixture temperature to slightly increase. This can be seen by an upward shift in temperature curves under non-reactive conditions. The upward shift in lean curve is more than that in

the rich curve simply because of higher heat capacity of hydrogen. Therefore, when less hydrogen is added in lean cases, less cooling of diluent stream is observed if compared with the rich case where oxygen flow is reduced. Changing the equivalence ratio in PSR#1 in turn changes the H<sub>2</sub>/O<sub>2</sub>/CO<sub>2</sub> concentration in the mixture as reported in Table 19.

Table 19 Mixture composition at different equivalence ratios

	H <sub>2</sub>	O <sub>2</sub>	CO <sub>2</sub>
$\phi = 0.6$	11.44%	9.61%	78.96%
$\phi = 1.0$	17.71%	8.93%	73.36%
$\phi = 1.4$	18.18%	6.54%	75.28%

Based on data in Table 19 and the temperature plot of Fig. 54, it can be said that mixture reactivity is more sensitive when combustion occurs under lean conditions. This observation can logically be justified when seen in context of discussion in section 6.2.4. Increase or decrease in hydrogen concentration will produce a likewise effect on rate of reaction since it is the main promoter of combustion reactions, whereas, an increase or decrease in CO<sub>2</sub> concentration will produce an inverse effect since it acts as the inhibitor. Under lean conditions, H<sub>2</sub> concentration decreases & CO<sub>2</sub> concentration increases, and both these changes tend to reduce the reactivity. This explains the rightward shift of the temperature curve (increased ignition delay) in the lean case. In case of rich combustion, not only the effect of change in H<sub>2</sub> & CO<sub>2</sub> concentration will tend to have an opposite effect on mixture reactivity but also the magnitude of the change observed is quite small when compared to the lean burning case. Therefore, no discernible change in ignition time is seen in the temperature plot of Fig. 54. Another visible change is the reduction in flue gas mixture temperature in PSR#1 post ignition (compared to the stoichiometric case). This trend is consistent with the general behaviour of combustion reaction occurring at non-stoichiometric conditions. When PSR#1 operates under non-stoichiometric condition, FG enters PSR#2 at temperature lower than its equilibrium temperature. In case of lean combustion, as more fuel is added in the second PSR combustion reactions continue and the flue gas is heated further. In case of rich combustion in PSR#1, addition of oxygen promotes completion of oxidation of exiting unburnt fuel and CO (much like syngas combustion) which leads to heating of the products gases entering PSR#2.

Having discussed the evolution in flue gas temperature, variation of CO concentration in combustors operating at different equivalence ratios can be discussed. The first noticeable difference between the three operating conditions is large variation in CO levels in PSR#1. When going from lean to stoichiometric to rich operating condition, the CO concentration in the product gases in PSR#1 increases at least by a factor of 10 (for  $T_{res} > 10ms$ ). The cause of this trend lies in the following behaviour of reactions responsible for CO formation. CO is mainly formed in two ways 1) by dissociation of CO<sub>2</sub> or 2) when CO<sub>2</sub> participates in bimolecular reactions. The temperature in these cases is not sufficiently high for CO<sub>2</sub> dissociation to be the main cause of CO production and therefore, it must be produced via the bimolecular reaction path. CO<sub>2</sub> reacts with all three radicals commonly formed during H<sub>2</sub>/O<sub>2</sub> combustion i.e. H/O/OH resulting in formation of CO and other radical/products. The concentration of these radicals is likely to be far more under rich conditions since the reactions are taking place in an oxygen starved environment and therefore, the rate of CO production is likely to be higher in case of rich condition. Thus, the tendency of CO formation will be the highest in rich condition.

Another noticeable difference between rich and lean (and stoichiometric) case is that after reaching the peak concentration, CO tends re-oxidize as the residence time increases in the latter two cases. However,

under rich conditions, the reactions are oxygen starved and the CO formed during combustion reactions cannot be re-oxidized and tends to persist in the FG mixture. This is the reason that CO concentration in PSR#1 under rich conditions tends to stabilize around its highest value instead of undergoing re-oxidation. Reburning of CO does happen in the second PSR when more oxygen is added to the mixture but as can be expected, the time required to reach this the final equilibrium level is far more than in stoichiometric case. This is also true for CO formed when PSR#1 is operating under lean conditions because, unlike in rich (and stoichiometric) case where PSR#2 mainly just re-oxidizes CO already present in FG, as more fuel is added in PSR#2 in lean case and new CO continues to be formed before getting oxidized to the final equilibrium value. This effect can be deduced from the plot shown in Fig. 54 although it is not very evident since the plot only reports values at PSR exit and not its temporal evolution.

## 6.5 Summary

A preliminary analysis of combustion of H<sub>2</sub>/O<sub>2</sub> mixture in s-CO<sub>2</sub> environment was presented in this chapter. The key findings of this investigation are briefly summarised in this section.

1. H<sub>2</sub>/O<sub>2</sub> combustion in s-CO<sub>2</sub> environment fundamentally differs from its combustion in N<sub>2</sub>/Ar environment because CO<sub>2</sub> has a higher a) specific heat capacity b) third body collision efficiency.
2. At the same dilution level, final flue gas temperature and the mixture reactivity will be lower in the case when CO<sub>2</sub> is used as the bath gas.
3. H<sub>2</sub> combustion is a subset of all hydrocarbon fuels and therefore, understanding its reaction mechanism is considered immensely important from scientific as well as industrial perspective. Because of this reason, there is a long-standing interest in studying combustion chemistry of H<sub>2</sub> and several reaction mechanisms have been proposed over the years to numerically model its behaviour.
4. Since it was not practical to test many of these mechanisms under this project, four mechanisms were shortlisted based on the information reviewed during literature survey.
5. A suitable simulation package had to be selected for this module and the choice of using either Cantera or ANSYS Chemkin Pro<sup>®</sup> was available. Each software was tested, and it was found that while Cantera was superior for handling large simulations and for integration with other applications, ANSYS Chemkin Pro<sup>®</sup> was user friendly and was more suitable for studying reaction mechanisms. In terms of the simulation outcomes, both these packages gave comparable results.
6. Since it was not envisaged to integrate the combustion model with the thermodynamic model under this project, it was decided to opt for ANSYS Chemkin Pro<sup>®</sup>.
7. Once the simulation package was selected, the performance of the shortlisted reaction mechanisms was compared under two different operating pressure levels. The first of these tests were performed at combustor pressure level of ~300 bar which is in the expected range of operating pressure of the proposed s-CO<sub>2</sub> cycle. However, experimental data for comparison was not available at such high pressure and therefore, a second test was performed at a lower pressure of ~1.2 bar at which experimental data was found during literature review.

8. The high pressure test revealed that reaction mechanisms that are designed/optimized for natural gas combustion tends to overestimate mixture reactivity when used to simulate H<sub>2</sub>/syngas combustion. The main reason for this tendency is most likely due to the difference in the way these mechanisms account for effects of CO<sub>2</sub> dilution. Similar effect was seen in low pressure test, but the difference was not as prominent as in the high pressure case since the effects of CO<sub>2</sub> dilution increase with increase in pressure.
9. In addition to this, the H<sub>2</sub>/syngas mechanisms considered in this study are comparatively newer than the natural gas combustion mechanisms and therefore, they also benefit from the recent (and more accurate) experimental measurements.
10. Based on the findings of these two tests, Kéromnès-2013 was selected for use in the present combustion analysis. More details related this choice can be found in section 6.3.2.
11. Having selected the combustion simulation package and a suitable reaction mechanism, simulations to analyse H<sub>2</sub>/O<sub>2</sub> combustion process with s-CO<sub>2</sub> dilution at very high pressure were performed. These simulations were split in two parts such that each addressed a specific objective of this combustion module.
12. The first simulation was performed at design point selected during the thermodynamic evaluation. The goal of this simulation was to test the modeling hypothesis where the flue gas was considered to be a binary mixture of CO<sub>2</sub> and H<sub>2</sub>O.
13. The results of this simulation proved the hypothesis to be valid. The deviation caused by this approximation in estimating heat capacity of the flue gas at combustor outlet was found to less than 0.001%.
14. The next set of combustion simulation focused on the parametric study of the combustion process under which the effects of combustion parameters (namely, residence time, combustor inlet pressure/temperature, dilution rate and equivalence ratio) were analysed.
15. Multiple simulations were performed while individually varying these parameters. Only the overall effect of these parameters is concisely mentioned in this summary. A detailed analysis can be found in section 6.4.2
16. With increasing residence time in the combustor, the concentration of minor species in flue gases tends to reduce to their equilibrium concentration levels which were found to be generally very small (the largest minor product of combustion was found to be CO with concentration < 10 ppm at equilibrium).
17. Both combustor operating pressure and inlet temperature were found to have a noticeable effect on combustion. Increase in combustion pressure was found to have a positive impact on mixture reactivity while reducing the CO level in the combustor. Equilibrium mixture temperature and CO concentration was found to be more or less comparable under different operating pressure however, the time required to reach these values was seen to decrease with an increase in pressure.
18. The effect of varying the mixture inlet temperature on the reactivity of the mixture was similar to that observed in the case of varying the mixture inlet pressure. However, unlike the previous case,

the equilibrium values of temperature and CO concentration were found to be different. The increase in flue gas temperature post combustion is consistent with the expected logical outcome of increasing mixture inlet temperature. Meanwhile, an interesting trend was observed in the variation of CO concentration in the combustor. Both the peak level of CO produced during combustion and its equilibrium value increased with increasing mixture inlet temperature however the rate at which it converges to its final values was also substantially increased. This was clearly indicative of higher mixture reactivity.

19. After this the effect of varying the mixture dilution rate was analysed. The trends observed were mainly caused due to variation in thermal and kinetic effects of CO<sub>2</sub> dilution. It was seen that flue gas temperature exiting the combustor would practically remain unaffected, but the concentration of minor species may be affected by the choice of dilution rate. The optimum rate of dilution was found to be a function of maximum allowable temperature in the combustor and the selected residence time.
20. For residence times typically used in industrial gas turbine applications, i.e., 10-50ms and maximum combustor temperature limited to about ~1800 K, the optimal range of dilution rate was found to be 60 – 80%. This range shifts towards higher values as the residence time increases and the maximum allowable temperature in the combustor decreases. At purely theoretical and exceedingly long residence times (> 10 seconds), all the cases tend to converge to similar values of exit temperature and flue gas composition.
21. Lastly, the effect of equivalence ratio in a presumed case of a two stage combustion was analysed. It was found that injecting fuel/oxidizer at stoichiometric ratio (with the necessary amount of diluent to control flue gas temperature with desired limits) gave the best result in terms of the time required to achieve the converged values of flue gas temperature and minor species concentration. When using lean conditions in the first stage of combustion, additional fuel has to be added in the second stage (since total fuel flow rate should be constant) and burning of this fuel causes additional generation of minor species that require longer residence times to reach their final value. Under rich condition, lack of oxygen leads to formation of higher level of minor species in the first combustor which then have to be oxidized in the second combustor and thus this process also requires more time to stabilize the final mixture composition.
22. On the contrary, when all the fuel and oxidizer is added in the first stage of combustor, production of minor species occurs mainly in the first stage itself and the second stage serves as the stabilisation zone where the minor species get converted to the main products of combustion i.e. CO<sub>2</sub> and H<sub>2</sub>O in this case. Therefore, combustion under stoichiometric condition requires the least amount of time to reach equilibrium.



# Chapter 7

## Conclusions & Recommendations

### Overview

This chapter presents the final conclusions of the work conducted during this thesis project. The first section of the chapter provides a brief summary of the key findings of each phase of this project. Following this, all the research questions defined at the start of the project are briefly answered in the second section of this chapter. Recommendations for future research work in this topic are outlined in the third section of this chapter.

### 7.1 Project summary

In this section, discussion pertaining to the research work presented in this report is brought to a logical conclusion. First, the main findings from each phase of this work are outlined in the following paragraphs.

Based on a review of trends in the existing energy market, the main challenges that are delaying the transition of current energy markets to a more sustainable low-carbon model were identified. Amongst these challenges, the key issue that requires urgent attention is the technical difficulty of integrating a large share of VRES into the existing energy grids, that are designed around a reliable generation model. This topic was further explored, and it was found that seasonal energy storage is a vital technology that is needed to support a large share of low-carbon renewables (>40%) in the energy grid. This further motivated a review of the energy storage technologies, which resulted in the identification of hydrogen based integration of VRES in the energy grid as one of the only viable long-term solution that can ensure decarbonisation of future global economy.

After this, various aspects of hydrogen technology were briefly reviewed, and it was found that there are several broad ranging challenges & developmental issues with hydrogen technologies that are yet to be addressed. One of these issues was identified in the P2G2P application, where a technology gap exists between the available solutions based on fuel cells and conventional gas turbines for converting green hydrogen back to power. This was selected as the main area of focus for the current project and the aim was to address this technology gap by proposing a novel H<sub>2</sub> combustion based thermal power cycle that could give efficiencies comparable to fuel-cell systems whilst having the operational characteristics of a conventional gas turbine. Many advanced power cycles were reviewed to fill this role and it was found that the s-CO<sub>2</sub> Brayton cycle was most suitable for this application.

Subsequently, existing literature on the s-CO<sub>2</sub> power cycle was thoroughly reviewed and several configurations of this cycle were shortlisted. These configurations included various thermodynamics variations like, intercooled compression, split flow compression with multistage recuperation and reheating, in addition to the simple configuration of a recuperated Brayton cycle. A thermodynamic analysis of these configurations was performed using the model developed under this project and an intercooled recuperated s-CO<sub>2</sub> power cycle was proposed as the final configuration. Using the same model, a parametric study was performed to gain insights on the effect of design parameters on the performance of the proposed cycle. The detailed results of this analysis can be found in section 5.3 of this report. Also, a performance map for the proposed cycle was developed using the model that can be used as a reference to select the starting point of design during future work in this area. The most important findings of the thermodynamic analysis are summarized in section 5.5.

In addition to thermodynamic analysis, a preliminary combustion study was also done in this project to understand the behaviour of the process of combusting H<sub>2</sub>/O<sub>2</sub> mixture in an s-CO<sub>2</sub> environment at elevated pressure levels. One of the main objectives of this analysis was to determine whether or not the combustion process affects the macroscopic thermodynamic performance of the cycle. It was found that the variation in flue gas mixture due to the combustion process was not large enough to cause a change in the thermodynamic performance of the cycle. Similar to the previous case of thermodynamic analysis, a parametric analysis to study the effects of design parameters on the combustion process was conducted. The details of this analysis can be found in section 6.4.2. The most important findings of the combustion analysis are summarized in section 6.5.

This completes the analysis of the proposed H<sub>2</sub>/O<sub>2</sub> fuelled s-CO<sub>2</sub> power cycle performed in this project. From an overall perspective, the proposed cycle was found to be a technologically feasible alternative to the existing hydrogen-based power generation solutions. It can be expected to deliver net cycle efficiencies comparable to fuel-cell based systems, while having overall operational characteristics similar to those of gas-turbine based solutions. Also, it is inherently a zero-emission cycle which makes it the perfect choice for the power plants of the future.

## 7.2 Conclusions

In this section, all the research questions defined in section 1.3 are briefly answered based on the findings of this analysis.

**RSQ#1. What are the main design constraints that restrict the operating envelope of the proposed cycle? In terms of cycle pressures and temperatures, what is the operating envelope and the design point?**

- 1.1 The main design constraints identified during this analysis in decreasing order of criticality are as follows; a) Maximum pressure and temperature limitation imposed by the recuperator b) Mechanical design limitations imposed by the hot section of s-CO<sub>2</sub> gas turbine (combustor & first few stages of the turbine)
- 1.2 The recuperator design requirement is expected to impose the most severe limitations on the operating envelope of the proposed cycle.
- 1.3 The maximum pressure in the proposed cycle is expected to be less than 350 bar while the temperature of flue gas at recuperator inlet at this pressure is expected to be less than 900 – 950 K.
- 1.4 As the maximum pressure in the cycle reduces, the allowable flue gas temperature at recuperator inlet will increase. At maximum cycle pressure of 250 bar, the flue gas temperature at recuperator inlet is expected to be less than 1050 – 1100 K.
- 1.5 The corresponding range of (optimum) maximum cycle temperature is found to be between 1150 – 1350 K.
- 1.6 The following values were selected as the design point in the present analysis.
  - a. Turbine inlet pressure = 300 bar
  - b. Turbine outlet pressure = 34 bar
  - c. Turbine outlet temperature = 1073.15 K
  - d. Compressor inlet temperature = 302.15 K

**RSQ#2. What configurations of the s-CO<sub>2</sub> power cycle are relevant in the context of the proposed application? What is the final configuration selected for this internally fired H<sub>2</sub>/O<sub>2</sub> fuelled s-CO<sub>2</sub> power cycle?**

- 2.1 Based on the initial qualitative review of several s-CO<sub>2</sub> cycle variations, it was found that high efficiency configuration of this cycle often included intercooled compression, split flow compression with two stage recuperation, and reheated expansion on top of the simple recuperated cycle.
- 2.2 Therefore, these features were included in the thermodynamic model and analysed during the configuration selection process.
- 2.3 The final configuration of the s-CO<sub>2</sub> cycle proposed in this project, is an intercooled recuperated cycle with a simple expansion process. This choice was made based the comparison of the net cycle efficiency that could be achieved with different cycle configurations.
- 2.4 It was seen that both the split flow compression with two stage recuperation, and reheated expansion configurations resulted in a decrease in the net cycle efficiency and were therefore, found to be unsuitable for the proposed application.

**RSQ#3. What is the variation seen in the overall cycle performance within the imposed operating envelope? How is the cycle performance affected by variation in the critical design parameters?**

- 3.1 Parametric analysis shows that the net efficiency of the proposed cycle varies between 50-60%, with the efficiency at the design point being 57.9%.
- 3.2 The critical design parameters studied are cycle pressures (at turbine inlet and outlet), cycle temperatures (at turbine outlet and compressor inlet), LP and HP side pressure drops, isentropic efficiency of compression and expansion, and recuperator effectiveness.

- 3.3 Out of all the design parameters, the net cycle efficiency was found to be most sensitive to turbine outlet temperature, LP side pressure drops, isentropic efficiency of the turbine and lastly, to the performance of the recuperator.
- 3.4 As mentioned previously, turbine outlet temperature is expected to be a critical parameter during the detailed design of the proposed cycle. Disregarding the inherent pressure limitation imposed by choice of maximum temperature in the HEX, the net cycle efficiency was found to vary between 48-58% when the turbine outlet temperature was varied from a conservative value of 823.15 K to an optimistic value of 1223.15 K with the optimum turbine outlet temperature lying between 1050-1100 K.
- 3.5 From a detailed design perspective, one of the key design objectives should be to minimize LP side pressure loss in the cycle, since pressure loss on LP side is twice as penalizing as pressure loss on the HP side. A 10% pressure drop on the LP side of HEX was found to decrease net cycle efficiency by ~4.5% whereas, the same pressure drop on HP side of the HEX decreased the net cycle efficiency by <2%.
- 3.6 Similarly, improving isentropic efficiency of the turbine should be given precedence over improving the isentropic efficiency of the compressor, since its influence on the net cycle efficiency is over twice as much as that of the compressor. 1% drop in isentropic efficiency of the turbine costs almost ~0.5% drop in net cycle efficiency, while the same drop in compressor efficiency results in only ~0.18% drop in net cycle efficiency.
- 3.7 Lastly, given that the proposed cycle is a highly recuperative cycle, achieving a high effectiveness in the recuperator is the key to achieving high net cycle efficiencies. HEX effectiveness has a drastic impact on its size and thus, the cost of the HEX. Therefore, a cost-benefit analysis is recommended before selecting the desired value of recuperator effectiveness.

**RSQ#4. What is the feasibility of the combustion of H<sub>2</sub>/O<sub>2</sub> mixture in an s-CO<sub>2</sub> environment at elevated pressure levels? Can the proposed power cycle be categorised as a zero-emission cycle?**

- 4.1 Based on the findings of a preliminary combustion analysis, it can be concluded that the combustion of H<sub>2</sub>/O<sub>2</sub> mixture in an s-CO<sub>2</sub> environment is feasible.
- 4.2 No signs of combustion instability were observed in the trends obtained during this analysis.
- 4.3 The combustion analysis also showed that flue gas is mainly a mixture of CO<sub>2</sub> and H<sub>2</sub>O with trace amounts of minor species like CO and unburnt H<sub>2</sub>/O<sub>2</sub>.
- 4.4 Formation of no other unwanted combustion products was predicted during this analysis and therefore, this cycle can be considered as a zero-emission cycle.

**RSQ#5. What is the effect of varying combustion parameters like residence time, combustor inlet temperature and pressure, and relative concentration of the fuel/oxidizer/diluent species etc., on the kinetics of the combustion reactions? Is the thermodynamic performance of the cycle substantially affected by the composition of flue gas generated during combustion?**

- 5.1 During the combustion analysis it was found that the minor species concentration can be reduced to sufficiently low levels (tens of ppm) by using combustor residence times typically seen in industrial gas turbines (tens of milliseconds).
- 5.2 The general trend observed during the combustion analysis was that mixture reactivity tends to increase with an increase in the operating temperature and pressure of the combustor.
- 5.3 The final concentration of minor species in the flue gas post combustion was found to increase with increasing mixture inlet temperature and decrease with increasing mixture inlet pressure.

- 5.4 However, the effect of inlet pressure on the combustion process was not found to be large enough to drive the choice of operating pressure of the cycle during detailed design and it is expected that mechanical design considerations will be the key factor influencing this choice.
- 5.5 On the other hand, the inlet temperature has a large effect on the exit temperature of the flue gas and thus its composition, and therefore, it should be given due consideration along with the mechanical design requirement of the combustor while selecting the combustor operating temperature.
- 5.6 Studying the effect of the relative concentration of the fuel/oxidizer on the combustion process showed that stoichiometric combustion gave the best results in terms of flue gas mixture composition (lowest concentration of minor species at any selected residence time).
- 5.7 The optimum rate of dilution was found to be function of the maximum allowable temperature and the selected residence time in the combustor. For residence times typically used in industrial gas turbine applications, i.e., 10-50ms and maximum combustor temperature limited to about ~1800 K, the optimal range of dilution rate was found to be 0.6-0.8 and this range shifts towards higher values as the residence time increases and the maximum allowable temperature in the combustor decreases.
- 5.8 The combustion analysis showed that the concentration of minor products of combustion and of unburnt fuel and oxidizer was small enough to be neglected during thermodynamic evaluation.
- 5.9 Therefore, it was concluded that as far as the effect of the major products i.e., H<sub>2</sub>O and CO<sub>2</sub> are accounted, the thermodynamic performance of the cycle is not affected by the composition of flue gas generated during the combustion process.

**RSQ#6. Based on the thermodynamic and combustion analysis, what can be predicted about the operating characteristics of the proposed s-CO<sub>2</sub> power cycle? How does it compare with existing hydrogen-based power generation technologies?**

- 6.1 The net efficiencies obtained with the proposed s-CO<sub>2</sub> cycle within the operating envelope considered in this analysis ranged from 50-60% and therefore, is comparable with that of fuel-cell based solutions.
- 6.2 Analysis of other aspects of this cycle, such as its performance under transient and part-load conditions (load following capabilities), effect of component sizing on performance, lifetime of cycle components, etc., was not included in the scope of this project. Therefore, these aspects can be compared only qualitatively based on the expected trends. Further analysis is required to gain detailed insights into these aspects.
- 6.3 Poor load following capability was one of the drawbacks of fuel-cell based systems. From the present analysis, it can be expected that because of the thermal inertia of the recuperator, the proposed cycle will have transient characteristics lying somewhere between an open cycle gas turbine and a combine cycle gas turbine power plant.
- 6.4 Studying the effect of using s-CO<sub>2</sub> as the working fluid on the lifecycle of the power plant components is an active area of research. The operating life is expected to be better than fuel-cell (PEMFC/SOFC) based systems and not substantially different from comparable conventional gas turbine based systems.
- 6.5 The trends observed in this analysis suggests that the proposed cycle will have good scaling characteristics, possibly even better than that of conventional gas turbines, as it is expected to suffer lower efficiency loss when scaled-down to smaller power output levels (10-50MWe).

**RSQ#7. What can be concluded about the technical feasibility of the proposed H<sub>2</sub>/O<sub>2</sub> fuelled s-CO<sub>2</sub> power cycle concept? Should more research effort be dedicated in future towards developing this concept?**

- 7.1 Based on this preliminary analysis, the proposed power cycle concept can be considered a technologically feasible alternative to the existing hydrogen-based power generation systems.
- 7.2 Net cycle efficiencies in the targeted range of 50-60% can be achieved with this concept.
- 7.3 This is exceptionally high performance for a combustion based thermal power cycle and therefore, it is proposed that this concept should be developed further. The next steps in the future development of the concept are outlined in section 7.2.

### **7.3 Recommendations for future work**

The recommendations for further development of the proposed concept are listed below.

#### **7.3.1 Improvements proposed in the current model**

- 1. Update the thermodynamic model to replace the ideal mixture assumption and include capability simulating real mixture behaviour.
- 2. Update the recuperator model to include the capability of handling multi-fluid heat exchange processes.
- 3. Improve the turbine cooling flow rate estimation by recalibrating/updating cooling flow model.
- 4. Update the expansion model to include turbine cooling during the expansion process and remove the assumption in the current model that adds 50% of the coolant flow at inlet and outlet of turbine.
- 5. Build a combustion model in Cantera and integrate it with the present thermodynamic model.

#### **7.3.2 Additional research**

- 1. Investigate the performance of the proposed cycle under part-load and transient operating conditions to get insights on the load-following characteristics
- 2. Detailed design and performance analysis of individual components especially recuperator, combustor and s-CO<sub>2</sub> turbines.
- 3. This project was solely focused on assessing the technical viability of the proposed concept. However, energy market, above all else, is driven by economic drivers. Therefore, to truly assess the viability of the proposed concept, a detailed analysis of the economic aspect is recommended. In addition to analysing the economics of the proposed concept in the context of proposed application, such a study should probe other wider aspects as well, like other potential applications of the proposed cycle, synergies that can be created with other upcoming hydrogen and VRES technologies to further market suitability etc. To make the proposed H<sub>2</sub>/O<sub>2</sub> fuelled s-CO<sub>2</sub> power cycle more deployable, its technical development will have to be in sync with requirements of the contemporary energy markets.

# Bibliography

1. Jouzel, J., Masson-Delmotte, V., Cattani, O., Dreyfus, G., Falourd, S., Hoffmann, G., ... Wolff, E. W. (2007). *Orbital and millennial antarctic climate variability over the past 800,000 years*. *Science*, 317(5839), 793–796. <https://doi.org/10.1126/science.1141038>
2. IPBES (2019). *Summary for policymakers of the global assessment report on biodiversity and ecosystem services of the Intergovernmental Science-Policy Platform on Biodiversity and Ecosystem Services*. IPBES secretariat, Bonn, Germany. 56 pages. <https://doi.org/10.5281/zenodo.3553579>
3. IEA (2019). *Global Energy & CO<sub>2</sub> Status Report 2019*. IEA, Paris [https://www.iea.org/reports/global-energy-and-CO<sub>2</sub>-status-report-2019](https://www.iea.org/reports/global-energy-and-CO2-status-report-2019)
4. Intergovernmental Panel on Climate Change. (2014). *Anthropogenic and Natural Radiative Forcing*. In *Climate Change 2013 – The Physical Science Basis: Working Group I Contribution to the Fifth Assessment Report of the Intergovernmental Panel on Climate Change* (pp. 659-740). Cambridge: Cambridge University Press. <https://doi.org/10.1017/CBO9781107415324.018>
5. IRENA (2018). *Hydrogen from renewable power: Technology outlook for the energy transition*. International Renewable Energy Agency, Abu Dhabi. ISBN 978-92-9260-077-8. <https://www.irena.org/publications/2018/Sep/Hydrogen-from-renewable-power>
6. IEA (2019). *Electricity Information: Overview (2019 edition)*. IEA, Paris. ISBN 978-92-64-98635-0. [https://webstore.iea.org/download/direct/2563?fileName=Electricity\\_Information\\_2019\\_Overview.pdf](https://webstore.iea.org/download/direct/2563?fileName=Electricity_Information_2019_Overview.pdf)
7. DLR Institute of Combustion Technology (2015). *Electrical efficiency of several power plant concepts with respect to power output* [Digital image]. DLR Institute of Combustion Technology. Retrieved August 12, 2020, from <http://www.bio-hypp.eu/system/>
8. IEA (2019). *World Energy Outlook 2019*. IEA, Paris ISBN: 978-92-64-97300-8. <https://www.iea.org/reports/world-energy-outlook-2019>
9. Goodwin, D. G., Moffat, H. K., & Speth, R. L. (2009). *Cantera: An object-oriented software toolkit for chemical kinetics, thermodynamics, and transport processes*. Caltech, Pasadena, CA. <https://www.cantera.org>
10. ANSYS Chemkin-Pro 15112, Reaction Design: San Diego, 2011. <https://www.ansys.com/products/fluids/ansys-chemkin-pro>
11. Bell, I. H., Wronski, J., Quoilin, S., & Lemort, V. (2014). *Pure and pseudo-pure fluid thermophysical property evaluation and the open-source thermophysical property library coolprop*. *Industrial and Engineering Chemistry Research*, 53(6), 2498-2508. <https://doi.org/10.1021/ie4033999>

12. Allam, R. J., Palmer, M., & Brown, G. W., Jr. (Dec. 3, 2013). *U.S. Patent No. US 8,596,075 B2*. Washington, DC: U.S. Patent and Trademark Office  
<https://patents.google.com/patent/US8596075B2/en>
13. IEA (2019). *Electricity Information: Overview (2019 edition)*. IEA, Paris  
[https://webstore.iea.org/download/direct/2563?fileName=Electricity\\_Information\\_2019\\_Overview.pdf](https://webstore.iea.org/download/direct/2563?fileName=Electricity_Information_2019_Overview.pdf)
14. IEA (2019). *World Energy Outlook 2019*. IEA, Paris <https://www.iea.org/reports/world-energy-outlook-2019>
15. IRENA (2015). *Renewable Energy Statistics 2015*. The International Renewable Energy Agency, Abu Dhabi. <https://www.irena.org/publications/2015/Jun/Renewable-Energy-Capacity-Statistics-2015>
16. IRENA (2020). *Renewable Energy Statistics 2020*. The International Renewable Energy Agency, Abu Dhabi. <https://www.irena.org/publications/2020/Jul/Renewable-energy-statistics-2020>
17. IEA (2018). *Renewables 2018*, IEA, Paris <https://www.iea.org/reports/renewables-2018>
18. McPherson, M., Johnson, N., & Strubegger, M. (2018). *The role of electricity storage and hydrogen technologies in enabling global low-carbon energy transitions*. *Applied Energy*, 216, 649-661.  
<https://doi.org/10.1016/j.apenergy.2018.02.110>
19. Millet, P., & Grigoriev, S. (2013). *Chapter 2 - Water Electrolysis Technologies*. In L. M. Gandía, G. Arzamendi, & P. M. Diéguez (Eds.), *Renewable Hydrogen Technologies* (pp. 19–41).  
<https://doi.org/https://doi.org/10.1016/B978-0-444-56352-1.00002-7>
20. IEA (2020). *Will system integration of renewables be a major challenge by 2023?*, IEA, Paris.  
<https://www.iea.org/articles/will-system-integration-of-renewables-be-a-major-challenge-by-2023>
21. IEA(2017). *Selected countries by integration phase and share of VRE, 2017*, IEA, Paris.  
<https://www.iea.org/data-and-statistics/charts/selected-countries-by-integration-phase-and-share-of-vre-2017>
22. S. Mueller, F. de Sisternes, E. Patriarca, A. Portellano, A. Goeritz, J.D. Moller, J. Peter, H. Holttinen. International Energy Agency. (2014). *The power of transformation: Wind, sun and the economics of flexible power systems*. IEA. <https://webstore.iea.org/the-power-of-transformation>
23. Mararakanye, N., & Bekker, B. (2019). *Renewable energy integration impacts within the context of generator type, penetration level and grid characteristics*. *Renewable and Sustainable Energy Reviews*, 108, 441-451. <https://doi.org/10.1016/j.rser.2019.03.045>
24. Sinsel, S. R., Riemke, R. L., & Hoffmann, V. H. (2019). *Challenges and solution technologies for the integration of variable renewable energy sources—a review*. *Renewable Energy*.  
<https://doi.org/10.1016/j.renene.2019.06.147>
25. Dave, K. (2019). *Feasibility Analysis of Internally Fired s-CO<sub>2</sub> Cycle for Energy Transition Literature Study – AE 4020*. Unpublished manuscript, Delft University of Technology, Netherlands.

26. IEA (2019). *The Future of Hydrogen*, IEA, Paris. <https://www.iea.org/reports/the-future-of-hydrogen>
27. IRENA (2019). *Future of wind: Deployment, investment, technology, grid integration and socio-economic aspects (A Global Energy Transformation paper)*, International Renewable Energy Agency, Abu Dhabi. <https://www.irena.org/publications/2019/Oct/Future-of-wind>
28. IRENA (2019). *Future of Solar Photovoltaic: Deployment, investment, technology, grid integration and socio-economic aspects (A Global Energy Transformation: paper)*, International Renewable Energy Agency, Abu Dhabi. <https://www.irena.org/publications/2019/Nov/Future-of-Solar-Photovoltaic>
29. Khalilpour, K. R. (2018). *Polygeneration with polystorage: For chemical and energy hubs* (pp. 1-565) <https://doi.org/10.1016/C2016-0-04711-3>
30. IRENA (2018). *Hydrogen from renewable power: Technology outlook for the energy transition*. International Renewable Energy Agency, Abu Dhabi. ISBN 978-92-9260-077-8. <https://www.irena.org/publications/2018/Sep/Hydrogen-from-renewable-power>
31. World Energy Council (2019). *World Energy Issues Monitor 2019*. World Energy Council, London. <https://www.worldenergy.org/assets/downloads/1.-World-Energy-Issues-Monitor-2019-Interactive-Full-Report.pdf>
32. Balestrino C. (2017). *SGT-A45 TR mobile unit* [Fact sheet]. Siemens AG. <https://assets.new.siemens.com/siemens/assets/api/uuid:02bba73c787fea1cd9add157d1a0babec899faa7/566-180083-factsheet-sgt-a45-online.pdf>
33. FuelCell Energy, (2017). *Sure Source 1500*. FuelCell Energy, Danbury, Connecticut. <https://www.fuelcellenergy.com/wp-content/uploads/2017/02/Product-Spec-SureSource-1500.pdf>
34. Weidner, E., Ortiz Cebolla, R. and Davies, J., *Global deployment of large capacity stationary fuel cells – Drivers of, and barriers to, stationary fuel cell deployment*. EUR 29693 EN, Publications Office of the European Union, Luxembourg, 2019, ISBN 978-92-76-00841-5, <https://doi.org/10.2760/372263JRC115923>.
35. U. S. Department of Energy (2015). *Quadrennial Technology Review 2015*. Retrieved from <http://energy.gov/quadrennial-technology-review-2015>
36. IEAGHG, 2015. *Oxy-combustion turbine power plants*, Report 2015/5, August 2015, IEAGHG, Cheltenham, UK, available at link [http://ieaghg.org/docs/General\\_Docs/Reports/2015-05.pdf](http://ieaghg.org/docs/General_Docs/Reports/2015-05.pdf).
37. Vaclav Dostal, Pavel Hejzlar & Michael J. Driscoll (2006). *The Supercritical Carbon Dioxide Power Cycle: Comparison to Other Advanced Power Cycles*. Nuclear Technology, 154:3, 283-301. <https://doi.org/10.13182/NT06-A3734>
38. Ferrari, N., Mancuso, L., Davison, J., Chiesa, P., Martelli, E., & Romano, M. C. (2017). *Oxy-turbine for Power Plant with CO<sub>2</sub> capture*. Energy Procedia, 114, 471-480. <https://doi.org/10.1016/j.egypro.2017.03.1189>

39. Bae, S. J., Ahn, Y., Lee, J., & Lee, J. I. (2014). *Various supercritical carbon dioxide cycle layouts study for molten carbonate fuel-cell application*. Journal of Power Sources, 270, 608-618. <https://doi.org/10.1016/j.jpowsour.2014.07.121>
40. Sanchez, D., de Escalona, J. M., Chacartegui, R., Munoz, A., & Sanchez, T. (2011). *A comparison between molten carbonate fuel-cells based hybrid systems using air and supercritical carbon dioxide Brayton cycles with state of the art technology*. Journal of Power Sources, 196(9), 4347-4354. <https://doi.org/10.1016/j.jpowsour.2010.09.091>
41. Angelino, G. (July 1, 1968). *Carbon Dioxide Condensation Cycles for Power Production*. ASME. J. Eng. Power. July 1968; 90(3): 287–295. <https://doi.org/10.1115/1.3609190>
42. Angelino, G. (1969, March). *Real gas effects in carbon dioxide cycles*. ASME 1969 gas turbine conference and products show (pp. V001T01A071-V001T01A071). American Society of Mechanical Engineers. <https://doi.org/10.1115/69-GT-102>
43. Feher, E. G. (1968). *The supercritical thermodynamic power cycle*. Energy conversion, 8(2), 85-90. [https://doi.org/10.1016/0013-7480\(68\)90105-8](https://doi.org/10.1016/0013-7480(68)90105-8)
44. Feher, E. G. (1968). *Investigation of supercritical (Feher) cycle*. Astropower Laboratory, Missile & Space Systems Division.
45. Yantovski, E. I., Zvagolsky, K. N., & Gavrilenko, V. A. (1995). *The COOPERATE-demo power cycle*. Energy Conversion and Management, 36(6-9), 861-864 [https://doi.org/10.1016/0196-8904\(95\)00139-5](https://doi.org/10.1016/0196-8904(95)00139-5)
46. Mathieu, P., & Nihart, R. (1998). *Zero emission MATIANT cycle*. Paper presented at the American Society of Mechanical Engineers (Paper), (GT) <https://doi.org/10.1115/98-gt-383>
47. Dostal, V., Driscoll, M. J., & Hejzlar, P. (2004). *A supercritical carbon dioxide cycle for next generation nuclear reactors* (Doctoral dissertation). Massachusetts Institute of Technology, Department of Nuclear Engineering.
48. Allam, R. J., Palmer, M. R., Brown Jr, G. W., Fetvedt, J., Freed, D., Nomoto, H., ... & Jones Jr, C. (2013). *High efficiency and low cost of electricity generation from fossil fuels while eliminating atmospheric emissions, including carbon dioxide*. Energy Procedia, 37, 1135-1149. <https://doi.org/10.1016/j.egypro.2013.05.211>
49. Crespi, F., Gavagnin, G., Sánchez, D., & Martínez, G. S. (2017). *Supercritical carbon dioxide cycles for power generation: A review*. Applied Energy, 195, 152-183. <https://doi.org/10.1016/j.apenergy.2017.02.048>
50. R. Span and W. Wagner. *A New Equation of State for Carbon Dioxide Covering the Fluid Region from the Triple Point Temperature to 1100 K at Pressures up to 800 MPa*. Journal of Physical and Chemical Reference Data, 25:1509–1596, 1996. <https://doi.org/10.1063/1.555991>
51. Wagner, W., & Pruß, A. (2002). *The IAPWS formulation 1995 for the thermodynamic properties of ordinary water substance for general and scientific use*. Journal of Physical and Chemical Reference Data, 31(2), 387-535. doi:10.1063/1.1461829. <https://doi.org/10.1063/1.1461829>

52. Gülen, S. C. (2010). *A Simple Parametric Model for the Analysis of Cooled Gas Turbines*. ASME. J. Eng. Gas Turbines Power. January 2011; 133(1): 011801. <https://doi.org/10.1115/1.4001829>
53. Scaccabarozzi, R., Gatti, M., & Martelli, E. (2016). *Thermodynamic analysis and numerical optimisation of the NET Power oxy-combustion cycle*. Applied Energy, 178, 505-526. <https://doi.org/10.1016/j.apenergy.2016.06.060>
54. Ferrari, N., Mancuso, L., Davison, J., Chiesa, P., Martelli, E., & Romano, M. C. (2017). *Oxy-turbine for Power Plant with CO<sub>2</sub> capture*. Energy Procedia, 114, 471-480. <https://doi.org/10.1016/j.egypro.2017.03.1189>
55. Olm, C., Zsély, I. G., Pálvölgyi, R., Varga, T., Nagy, T., Curran, H. J., & Turányi, T. (2014). *Comparison of the performance of several recent hydrogen combustion mechanisms*. Combustion and Flame, 161(9), 2219-2234. <https://doi.org/10.1016/j.combustflame.2014.03.006>
56. Kéromnès, A., Metcalfe, W. K., Heufer, K. A., Donohoe, N., Das, A. K., Sung, C. J., ... & Krejci, M. C. (2013). *An experimental and detailed chemical kinetic modeling study of hydrogen and syngas mixture oxidation at elevated pressures*. Combustion and Flame, 160(6), 995-1011. <https://doi.org/10.1016/j.combustflame.2013.01.001>
57. Gregory P. Smith, David M. Golden, Michael Frenklach, Nigel W. Moriarty, Boris Eiteneer, Mikhail Goldenberg, C. Thomas Bowman, Ronald K. Hanson, Soonho Song, William C. Gardiner, Jr., Vitali V. Lissianski, and Zhiwei Qin. [http://www.me.berkeley.edu/gri\\_mech/](http://www.me.berkeley.edu/gri_mech/)
58. Varga, T., Olm, C., Nagy, T., Zsély, I. G., Valkó, É., Pálvölgyi, R., ... & Turányi, T. (2016). *Development of a joint hydrogen and syngas combustion mechanism based on an optimisation approach*. International journal of chemical kinetics, 48(8), 407-422. <https://doi.org/10.1002/kin.21006>
59. Alekseev, V. A., Christensen, M., & Konnov, A. A. (2015). *The effect of temperature on the adiabatic burning velocities of diluted hydrogen flames: a kinetic study using an updated mechanism*. Combustion and flame, 162(5), 1884-1898. <https://doi.org/10.1016/j.combustflame.2014.12.009>
60. Olm, C., Zsély, I. G., Varga, T., Curran, H. J., & Turányi, T. (2015). *Comparison of the performance of several recent syngas combustion mechanisms*. Combustion and Flame, 162(5), 1793-1812. <https://doi.org/10.1016/j.combustflame.2014.12.001>
61. Healy, D., Kalitan, D. M., Aul, C. J., Petersen, E. L., Bourque, G., & Curran, H. J. (2010). *Oxidation of C1–C5 alkane quaternary natural gas mixtures at high pressures*. Energy & Fuels, 24(3), 1521-1528. <https://doi.org/10.1021/ef9011005>
62. Iwai, Y., Itoh, M., Morisawa, Y., Suzuki, S., Cusano, D., & Harris, M. (2015, June). *Development approach to the combustor of gas turbine for oxy-fuel, supercritical CO<sub>2</sub> cycle*. In Turbo Expo: Power for Land, Sea, and Air (Vol. 56802, p. V009T36A013). American Society of Mechanical Engineers. <https://doi.org/10.1115/GT2015-43160>

63. Zhang, Y., Mathieu, O., Petersen, E. L., Bourque, G., & Curran, H. J. (2017). *Assessing the predictions of a NO<sub>x</sub> kinetic mechanism on recent hydrogen and syngas experimental data*. *Combustion and Flame*, 182, 122-141. <https://doi.org/10.1016/j.combustflame.2017.03.019>
64. Zhang, J., Mi, J., Li, P., Wang, F., & Dally, B. B. (2015). *Moderate or intense low-oxygen dilution combustion of methane diluted by CO<sub>2</sub> and N<sub>2</sub>*. *Energy & Fuels*, 29(7), 4576-4585. <https://doi.org/10.1021/acs.energyfuels.5b00511>
65. Sabia, P., & de Joannon, M. (2020). *On H<sub>2</sub>-O<sub>2</sub> oxidation in several bath gases*. *International Journal of Hydrogen Energy*, 45(15), 8151-8167. <https://doi.org/10.1016/j.ijhydene.2020.01.134>
66. Langer, R., Cuoci, A., Cai, L., Burke, U., Olm, C., Curran, H., ... & Pitsch, H. (2018). *A comparison of numerical frameworks for modelling homogenous reactors and Laminar flames*. In *Joint Meeting: The German and Italian Sections of the Combustion Institute-41st Meeting ASICI* (pp. 9-14). ITA. <https://re.public.polimi.it/handle/11311/1126409#.XwhMRSgzaXI>
67. Aneke, M., & Wang, M. (2016). *Energy storage technologies and real life applications – A state of the art review*. *Applied Energy*, 179, 350-377. <https://doi.org/10.1016/j.apenergy.2016.06.097>